Transport Canada
Development

Transports Canada
Développement

TP 6910E

Validation and Testing of the Tank-Car Thermal Analysis Program (TNKCAR)

Summary Report

Prepared for
Transportation
Development Centre

Transport Canada

MARCH 1985

Canada

CA1
DTC 845
85
V17S
c.2

TP 6910E

VALIDATION AND TESTING OF THE TANK-CAR THERMAL ANALYSIS PROGRAM (TNKCAR)

SUMMARY REPORT

Library and Information Centre /
Centre de Documentation (CDLA)
RECEIVED - REÇU LE
[illegible] 1986
Transport Canada | Transports Canada

Prepared For:

TRANSPORTATION DEVELOPMENT CENTRE
TRANSPORT CANADA

Prepared By:

DAVIS ENGINEERING LIMITED
CONSULTING ENGINEERS
OTTAWA, ONTARIO

DE File No: C83-29

MARCH 1985

THE CONTENTS OF THIS REPORT REFLECT
THE VIEWS OF THE CONTRACTOR AND NOT
NECESSARILY THE OFFICIAL VIEWS OR
POLICIES OF THE TRANSPORTATION
DEVELOPMENT CENTRE

REPORT DOCUMENTATION FORM

1. Transport Canada Report No.
TP 6910E

2. TDC Project No.
4917/4918

3. Recipient's Catalogue No.

4. Title and Subtitle
Validation and Testing of the Tank-Car Thermal Analysis Program (TNKCAR) - Summary Report

5. Report Date
March, 1985

6. Performing Organization Report No.
C83-29

7. Author(s)
A.M. Birk

8. Transport Canada File No.
D1465-302-6-5

9. Performing Organization Name and Address
Davis Engineering Limited
1260 Old Innes Road
Ottawa, Ontario
K1B 3V3

10. DSS File No.
11SD. T8200-2-2575

11. DSS or Transport Canada Contract No.
0SD83-00086

12. Sponsoring Agency Name and Address
Transportation Development Centre (TDC)
Complexe Guy Favreau, West Tower
200 Dorchester Blvd. W., Suite 601
Montreal, Quebec H2Z 1X4

13. Type of Report and Period Covered
Technical

14. Sponsoring Agency Code
4917/4918

15. Supplementary Notes

16. TDC Project Officer
D.W. Dibble

17. Abstract

A computer model of a rail tank-car exposed to external fire impingement (engulfing fire or torch fire) has been developed, tested and validated. The computer model is capable of simulating the response of a full sized or fifth scale tank, and can predict tank pressure, wall temperatures, lading temperatures, relief fire ignition. The computer model can account for a wide range of tank orientations, tank fill conditions and tank thermal protection (insulation, radiation shielding, fusible plugs, Explosafe).

The report presents the results of program sensitivity analyses, and program validation using avalable tank-car fire test data. A number of simulations of thermally protected tanks (including Explosafe) are also presented.

18. Key Words
Rail tank-car, Explosafe, thermal computer model

19. Distribution Statement
A limited number of copies are available from the sponsoring agency

20. Security Classification (of this report)
un-classified

21. Security Classification (of this page)
un-classified

22. No. of Pages
74

23. Price

TDC CDT 79-005

FORMULE DE DOCUMENTATION POUR RAPPORT

1. N° du rapport Transports Canada TP 6910E	2. N° de l'étude — CDT 4917/4918	3. N° de catalogue du destinataire

4. Titre et sous-titre Validation and Testing of the Tank-Car Thermal Analysis Program (TNKCAR) - Summary Report	5. Date du rapport mars 1985 6. N° du rapport de l'organisme exécutant C83-29
7. Auteur(s) A.M. Birk	8. N° de dossier Transports Canada D1465-302-6-5
9. Nom et adresse de l'organisme exécutant Davis Engineering Ltd. 1260 Old Innes Road Ottawa, Ontario K1B 3V3	10. N° de dossier — ASC 11SD. T8200-2-2575 11. N° de contrat — ASC ou Transports Canada 0SD83-00086
12. Nom et adresse de l'organisme parrain Centre de développement des transports (CDT) Complexe Guy Favreau, tour ouest 200 o., boul. Dorchester, Suite 601 Montréal, Qué. H2Z 1X4	13. Genre de rapport et période visée technique 14. Code de l'organisme parrain 4917/4918
15. Remarques additionnelles	16. Agent de projet — CDT D.W. Dibble

17. Résumé

Ce rapport rend compte de l'étude et de la validation d'un modèle de simulation par ordinateur figurant le comportement d'un wagon-citerne sous l'action de flammes extérieures: incendie enveloppant our flammes à effet torche. Ce modèle permet de simuler le comportement d'un wagon-citerne en vraie grandeur ou à l'échelle 1/5, prenant en compte les facteurs suivants: pressions intérieures, température des parois et de la cargaison, débit d'écoulement par les soupapes de sûreté, niveau de remplissage et tenue des parois, dont il indique l'évolution dans le temps à partir de la mise à feu. Il permet en outre de grandes variations dans les conditions de remplissage, l'orientation et les types de protection thermique à l'intérieur du récipient: isolation, écran anti-rayonnement, tampons fusibles, système Explosafe.

Le rapport rend compte également des résultats de l'analyse de sensibilité et de validation des programmes, utilisant les données tirées d'essais antérieurs. Il décrit en outre des simulation faites sur des wagons-citernes protégés de diverse façons, y compris le système Explosafe.

18. Mots-clés Wagon-citerne, Explosafe, modèle mathématique, simulation thermique	19. Diffusion Le CDT dispose d'un nombre limité d'exemplaires.

20. Classification de sécurité (de ce rapport) non-classifié	21. Classification de sécurité (de cette page) non-classifiée	22. Nombre de pages 74	23. Prix

TABLE OF CONTENTS

PAGE

1.0 INTRODUCTION 1
1.1 Project Background 1
1.2 Technical Background 1
1.3 Objectives 3
1.4 Summary 4

2.0 VALIDATION 7
2.1 Validation Method 7
2.2 Available Data 7
2.3 Validation Results 8

3.0 PROGRAM SENSITIVITY ANALYSIS 20
3.1 Time Step Sensitivity 20

4.0 EXAMPLE SIMULATIONS 38
4.1 Insulated Tank 38
4.2 Tank with Fusible Plugs 44
4.3 Explosafe Equipped Tank 55

5.0 FUTURE WORK 68
5.1 Overall Model Weaknesses 68
5.2 Recommended Model Modification 70

6.0 CONCLUSIONS 72

REFERENCES 74

LIST OF TABLES

1-1 System Confirguration Considered in Tankcar 2

LIST OF FIGURES

FIGURE		PAGE
2-1	Predicted Tank Pressure and Measured Tank Pressure for Enigma Test (from Reference 4))	10
2-2	Predicted Wall Temperatures and Measured Wall Temperatures from Enigma Test (from Reference 4))	11
2-3	Predicted Liquid Level and Measured Measured Liquid Level for Enigma Test (from Reference 4))	12
2-4	Predicted Tank Wall Stresses and Material Strength for Enigma Test (from Reference 4))	13
2-5	Predicted Tank Pressure and Measured Tank Pressure for Nova Test (from Reference 4))	15
2-6	Predicted Wall Temperatures and Measured Wall Temperatures from Nova Test (from Reference 4))	16
2-7	Predicted Liquid Level and Measured Liquid Level for Nova Test (from Reference 4))	17
2-8	Predicted Tank Wall Stresses and Material Strength for Nova Test (from Reference 4))	18
3-1	Predicted Tank Pressure for Unprotected Tank from Program Runs Using Different Time Steps	22
3-2	Predicted Wall Temperatures for Unprotected Tank from Program Runs Using Different Time Steps	23
3-3	Predicted Liquid Level for Unprotected Tank from Program Runs Using Different Time Steps	24
3-4	Predicted Tank Wall Stresses and Material Strength for Unprotected Tank from Runs Using Different Time Steps	25
3-5	Predicted Tank Pressure for Insulated Tank (With Steel Jacket) from Program Runs Using Different Time Steps	27
3-6	Predicted Wall Temperatures for Insulated Tank (With Steel Jacket) from Program Runs Using Different Time Steps	28

LIST OF FIGURES (Cont'd)

FIGURE PAGE

3-7 Predicted Liquid Level for Insulated Tank (With Steel Jacket) from Program Runs Using Different Time Steps 29
3-8 Predicted Tank Wall Stresses and Material Strength for Insulated Tank (With Steel Jacket) from Program Runs Using Different Time Steps 30
3-9 Predicted Tank Pressure for Insulated Tank (No Steel Jacket) from Program Runs Using Different Time Steps 33
3-10 Predicted Wall Temperatures for Insulated Tank (No Steel Jacket) from Program Runs Using Different Time Steps 34
3-11 Predicted Liquid Level for Insulated Tank (No Steel Jacket) from Program Runs Using Different Time Steps 35
3-12 Predicted Tank Wall Stresses and Material Strength for Insulated Tank (No Steel Jacket) from Program Runs Using Different Time Steps 36

4-1 Predicted Tank Pressure for Insulated Tanks with Different Thicknesses of Insulation, Exposed to an Engulfing Fire 39
4-2 Predicted Tank Wall Temperatures for Insulated Tanks with Different Thicknesses Insulation, Exposed to an Engulfing Fire 40
4-3 Predicted Liquid Level for Insulated Tanks with Different Thicknesses of Insulation, Exposed to an Engulfing Fire 41
4-4 Predicted Tank Wall Stresses and Tank Wall Material Strengths for Insulated Tanks with Different Thicknesses of Insulation, Exposed to an Engulfing Fire 42
4-5 Predicted Tank Pressures for Tanks Equipped with Different Numbers of Fusible Plugs, Exposed to an Engulfing Fire 45
4-6 Predicted Tank Wall Temperatures for Tanks Equipped with Different Numbers of Fusible Plugs, Exposed to an Engulfing Fire 46
4-7 Predicted Liquid Level for Tanks Equipped with Different Numbers of Fusible Plugs, Exposed to an Engulfing Fire 47

LIST OF FIGURES (Cont'd)

FIGURE		PAGE
4-8	Predicted Tank Wall Stresses and Tank Wall Material Strengths for Tanks Equipped with Different Numbers of Fusible Plugs, Exposed to an Engulfing Fire	48
4-9	Predicted Tank Pressures for Tanks Equipped with Fusible Plugs with Different Melting Temperatures, Exposed to an Engulfing Fire ..	49
4-10	Predicted Tank Wall Temperatures for Tanks Equipped with Fusible Plugs with Different Melting Temperatures, Exposed to an Engulfing Fire	50
4-11	Predicted Liquid Level for Tanks Equipped with Fusible Plugs with Different Melting Temperatures, Exposed to an Engulfing Fire ..	51
4-12	Predicted Tank Wall Stresses and Tank Wall Material Strengths for Tanks Equipped with Different Numbers of Fusible Plugs, Exposed to an Engulfing Fire	52
4-13	Predicted Tank Pressures for Tanks Equipped with Explosafe of Different Annular Thicknesses, Exposed to an Engulfing Fire ...	56
4-14	Predicted Tank Wall Temperatures for Tanks Equipped with Explosafe of Different Annular Thicknesses, Exposed to an Engulfing Fire ...	58
4-15	Predicted Liquid Level for Tanks Equipped with Explosafe of Different Annular Thicknesses, Exposed to an Engulfing Fire ...	59
4-16	Predicted Tank Wall Stresses and Tank Wall Material Strengths for Tanks Equipped with Explosafe of Different Annular Thicknesses, Exposed to an Engulfing Fire	60
4-17	Predicted Tank Pressures for Tanks Equipped with Explosafe of Different Orientation, Exposed to an Engulfing Fire	62
4-18	Predicted Tank Wall Temperatures for Tanks Equipped with Explosafe of Different Orientations, Exposed to Engulfing Fire	64
4-19	Predicted Liquid Level for Tanks Equipped with Explosafe of Different Orientations, Exposed to an Engulfing Fire	65
4-20	Predicted Tank Wall Stresses and Tank Wall Material Strengths for Tanks Equipped with Explosafe of Different Orientations, Exposed to an Engulfing Fire	66

1.0 INTRODUCTION

This report summarizes the work conducted in Phases III and IV of the Tank-Car Thermal computer Model Project, DSS Contract No. OSD-00086. The work in these phases primarily involved a model validation, a program sensitivity analysis, and the generation of example model simulations.

This report does not include technical details of the methods used in the Tank-Car Model. For such details, the reader is directed to Reference (1).

1.1 PROJECT BACKGROUND

As already mentioned, this report summarizes the results of Phases III and IV of the Tank-Car Thermal Computer Model Project (TCTCMP). The overall project was organized into four phases as follows:

Phase I : Model Formulation
Phase II : Model Development
Phase III: Model Validation
Phase IV : Model Simulations

This project was part of the Tank Car Explosion Protection Program (TCEPP). The overall objective of the TCEPP is, "to develop a technique of protecting rail, road and marine tankers carrying LPG, from the dangers of thermally induced ruptures and explosions".

The original intended use of the Tank-Car Thermal Computer Model was to analyze the results of partial scale experimental test programs conducted to understand the role of Explosafe[1] in protecting tank-cars from accidental fire impingement.

The model was also to be used to identify preferred design alternatives of the Explosafe explosion suppression system for full-sized rail tank-cars, and to compare the performance of these systems with conventional protection systems.

1.2 TECHNICAL BACKGROUND

The technical details behind the TCTCM are presented in Reference (1). This section will present a brief overview of the TCTCM and its capabilities.

---

[1] Explosafe Division, Vulcan Industrial Packaging ...

The TCTCM is a digital computer based model capable of simulating the response of a rail tank-car and its lading, to the conditions of external fire impingement (engulfing fire or 2-dimensional torch). The program is written in the FORTRAN IV programing language, and is presently running on a PDP 11/23 mini computer under the RT-11 operating system, and on the DEC VAX 11/780 under the VMS operating system.

The two-dimensional capabilities of the TCTCM have been validated (2) by comparing predictions with experimentally obtained data from previously conducted full and fifth-scale fire tests (3,4).

The model can consider several system configurations such as a rolled or pitched attitude of the tank, different fire conditions, different thermal protection schemes, and different ladings. Table 1-1 summarizes the various system configurations which can be considered by the program.

LADING	THERMAL PROTECTION	TANK ORIENTATIONS	FIRE CONDITIONS
propane n-butane n-pentane propylene	thermal insulation (three types) (with/without steel jacket) thermal radiation shielding special pressure relief devices (ie. fusible plugs) 'Explosafe'	variable roll angle variable pitch angle (pseudo 3-D)	engulfing fire 2-D torch fire

TABLE 1-1 SYSTEM CONFIGURATIONS CONSIDERED IN TANKCAR

The TCTCM is capable of predicting tank pressure, tank wall temperatures, relief valve flow rates, tank fill condition, tank wall stresses and tank wall failure, all as functions of time from fire ignition. The TCTCM is also capable of simulating the effects of a variety of thermal protection devices such as thermal insulation (with/without steel jacket, with/without thermally induced degradation), thermal radiation shielding, special pressure relief devices (fusible plugs or temperature sensitive valves), and 'Explosafe'. The model can consider a large number of different tank/lading/fire configurations.

The overall tank-car model is made up from a series of sub-models which represent the various processes taking place in and around the tank. These sub-models represent the following processes,

i) flame to tank heat transfer,
ii) heat transfer through the tank wall and associated coverings,
iii) interior surface heat transfer,
iv) pressure relief device operating characteristics,
v) thermodynamic properties of the lading,
vi) thermodynamic process taking place within the tank, and,
vii) wall stresses and material properties.

The TCTCM consists of a main program and a series of subroutines. The main program controls some of the I/O, initializes the variables and matrices, and controls the subroutine calling sequence. The subroutines contain the various process sub-models.

1.3 OBJECTIVES

The objectives of Phases III and IV of the Tank-Car Thermal Computer Model Project were as follows:

i) Validate the Tank-car Thermal Computer Model (TCTCM) using data available from fire tests and laboratory tests,

ii) Perform a sensitivity analysis on the TCTCM to establish the effects of input variables on the model predictive capabilities,

iii) Perform Simulations on a variety of thermal protection systems, including Explosafe, to investigate the performance of these systems when critical parameters are varied, and

iv) If the assessment of the Explosafe thermal protection system is satisfactory, determine the most effective design configuration of Explosafe for use in full-sized rail tank-cars.

All of the above mentioned project objectives have been achieved.

1.4 SUMMARY

As stated above, all of the project objectives have been achieved. The tank-car model has been validated with available fire test data. A sensitivity analysis has been performed to determine the effects of varying important inputs, and a number of simulations have been performed to show the predicted performance of different thermal protection schemes, including Explosafe.

The TCTCM validation has included data from a number of tests including full and partial scale pool fire tests and some torch fire tests. The results of the validation show that the TCTCM is quite accurate at predicting tank pressure, liquid level and wall temperatures. However, the TCTCM did not accurately predict the time to failure in all cases. This, of course, stems from the fact that tank failure is determined by material properties and these are usually statistically based with some degree of variation from tank to tank. In addition, valve performance also plays a key role in tank failure because of its effect on the rate at which the tank is emptied, and tank-car relief valves are also known to have significant variations from nominal performance characteristics.

In addition to the validation resulting from the comparison of model simulations with fire test data, a major model assumption has been validated with the results of an indoor fire test conducted to simulate the effects of a burning relief valve flare on a tank which is already engulfed in fire. Details of this test are presented in Reference (5). The test results support the assumption that the burning relief valve flare has little or no effect on the tank-car when it is already engulfed in fire. This assumption played a major role in the development of the fire heat transfer sub-model.

The sensitivity analyses showed that the TCTCM is a very flexible tool and its numerical operations remain stable and accurate for a wide range of input. However, users should beware of those inputs that can result in program instabilities and inaccuracies in the simulation results. As expected, the model simulations are extremely sensitive to the external boundary conditions, namely, the fire temperatures and radiating properties. The simulation results are also extremely sensitive to the valve operating characteristics because these effect the liquid level which dictates how the wall temperatures increase.

The example simulations that were performed show that a number of thermal protection schemes can prolong the life of a tank-car when in an engulfing fire or torch fire environment. Some methods increase the tanks survivability by slowing the heating process to maintain lower tank pressures and wall temperatures, others reduce the tank pressure by venting the lading more rapidly, and some act to reduce the wall temperatures in the vapour space by increasing the heat transfer from the tank inner surface in these areas.

The methods which reduce the heat flow to the tank usually involve a thermal insulating layer or radiation shielding, or both. Under the ideal conditions of the simulations, these systems proved to be extremely effective at protecting the tank-car. The only apparent drawback of these methods is that they prolong the time where a nearly full tank remains exposed to fire. A full tank is potentially a bigger bomb.

An example of a system which vents the lading more rapidly involves fusible plugs. These devices work by opening orifices through which the lading can pass. When the fusible plug temperature exceeds some critical value it causes a metallic core to melt and open a flow orifice. Fusible plugs do not affect the heat transfer rate significantly but work by reducing the internal pressure (lower than is possible by a standard relief valve) and by venting the tank contents as rapidly as possible. The advantage of such systems is their ability to empty the tank and thereby remove the explosive charge. However, the disadvantage of these systems is that once a fusible plug is opened it cannot be easily closed, and if the fire is quenched the tank will continue to vent the hazardous material into the atmosphere.

The internal protection scheme considered in this study involves the material known as Explosafe. The simulations performed for Explosafe equipped tank-cars show, as expected, that the Explosafe acts by increasing the heat transfer coefficient on the inner surface of the tank wall which is in contact with vapour. This increase in heat flux in these areas results in lower wall temperatures in the vapour space and thereby increases the survivability of a tank. However, this increase in heat flux also results in a slightly higher peak tank pressure which somewhat offsets the positive effects of the reduced wall temperatures.

Of all of the systems considered in the simulations, thermal insulation appears to be the most effective means of thermal protection. Thermal insulation covered with steel jacket is recommended because the steel jacket acts as a radiation shield. Fusible plugs also appear to be effective devices for protecting a tank-car. If the problem associated with the non-reversible nature of fusible plugs can be overcome with a temperature sensitive valve, such devices might be considered as back-up measures to thermal insulation. The Explosafe material did not, based on the simulations conducted, prove to be as effective as thermal insulation or fusible plugs.

The results of the validation, sensitivity analyses, and simulation activities have identified some weaknesses with the overal thermal model. These weaknesses are associated with the thermodynamic process model, the interior surface heat transfer model and the relief valve flow analyses. Future development of the TCTCM should concentrate on these areas.

2.0 VALIDATION

This chapter presents some example results from the program validation. For further examples of validation results, the reader is directed to Reference (2).

2.1 VALIDATION METHOD

The model outputs have been condensed into four summary plots which present the most significant information. The four summary plots are:

- pressure vs. time
- wall temperature vs. time
- liquid level vs. time
- wall stress and strength vs. time.

These four plots were chosen because they present data in a way that is similar to that used in the presentation of the fifth and full-scale fire test results. The overall model validation involved the comparison of the four summary plots with experimentally obtained data.

For the purposes of the validation, the model inputs, such as tank initial fill, lading initial temperature, relief valve size, etc., were chosen to match, as closely as possible, the actual test conditions which existed for a given data set. In some cases where this data was not recorded, some judgement was used to approximate these boundary conditions.

2.2 AVAILABLE DATA

For the purposes of validating the tank-car model, data is required which accurately describes an entire fire event, from start to finish (tank rupture or empty). Therefore, this data must include, as a minimum, the following information:

- tank initial conditions (fill level, lading type, equilibrium temperature and internal pressure).

- tank wall temperatures at various circumferential locations, during the test.

- lading temperatures at various locations in the liquid and vapour (preferably at different vertical locations), during the test.

- tank internal pressure, during the test.

- tank dimensions (length, diameter, wall thickness) and,

- relief valve size and operating range.

To obtain the desired data, a literature search was conducted. The scope of the literature search was confined to data relating to the response of rail tank-cars, or pressure vessels, exposed to external fire impingement.

The most useful data obtained so far has been that from fifth-scale tests conducted in Canada (4), full and fifth-scale engulfing fire tests and torch fire tests conducted in the U.S. (3, 6, 7, 8, 9, 10), and some smaller scale tests conducted in the UK (11) and the FRG (12).

Of this very useful data only the results from the Canadian and U.S. tests have been used directly in the validation of the model. Although the tests conducted in the UK and FRG were highly successful, the tank scales and the extent of the instrumentation resulted in data that was not easily reproducible by the tank-car model.

Futher details of the test data used in the validation process can be found in Reference (2).

2.3 VALIDATION RESULTS

This section presents some example comparisons between model simulations and the fire test data discussed in the previous section. Validation runs were performed for two of the TDC fifth-scale tests, for the AAR-RPI full-scale tests, for three of the AAR-RPI fifth- scale fire tests, and for some of the AAR-RPI torch fire tests.

Of all of these validation runs, only two examples are presented in the following sections; the TDC Enigma test of an unprotected fifth scale tank, and the TDC Nova test of an Explosafe equipped fifth scale tank. The results from the other validation runs can be found in Reference (2).

The Enigma data was chosen because it represents a baseline case of an unprotected tank. The Nova data was chosen because the Explosafe Configuration used in this case (annular configuration) is considered to be the most practical from the standpoints of wall contact maintainability and cost effectiveness (this configuration does not fill the tank as did the other configurations considered in the TDC fifth-scale tests).

The following sections present the model predictions plotted along with fire test data.

Enigma Case

The tank-car model was used to predict the response of a fifth-scale unprotected tank exposed to an engulfing fire. The simulation was performed with boundary conditions which represented the actual fire conditions as closely as possible. The results of the simulation are presented in Figures 2-1 to 2-4 along with the actual measured data from the fire test.

Figure 2-1 presents the predicted tank pressure along with the measured pressures from the fire test. As can be seen from the Figure, the predictions are in good agreement with the test results. The initial pressurization rate prior to relief valve action is in excellent agreement with the tests results. The length of the cycling period and the pressure rise during continuous venting is also well predicted. The predictions depart from the measured results after the peak pressure has been reached. The measured pressure drops more rapidly than the predicted values prior to tank failure at approximately 7½ minutes into the test.

Figure 2-2 presents the predicted wall temperatures along with the measured wall temperatures for three different wall locations. As can be seen from the figure, the predictions are in very good agreement with the fire test results. The temperature rise rates and the break times are in good agreement with the test results. The wall temperature in the liquid wetted regions is in excellent agreement with the measured data.

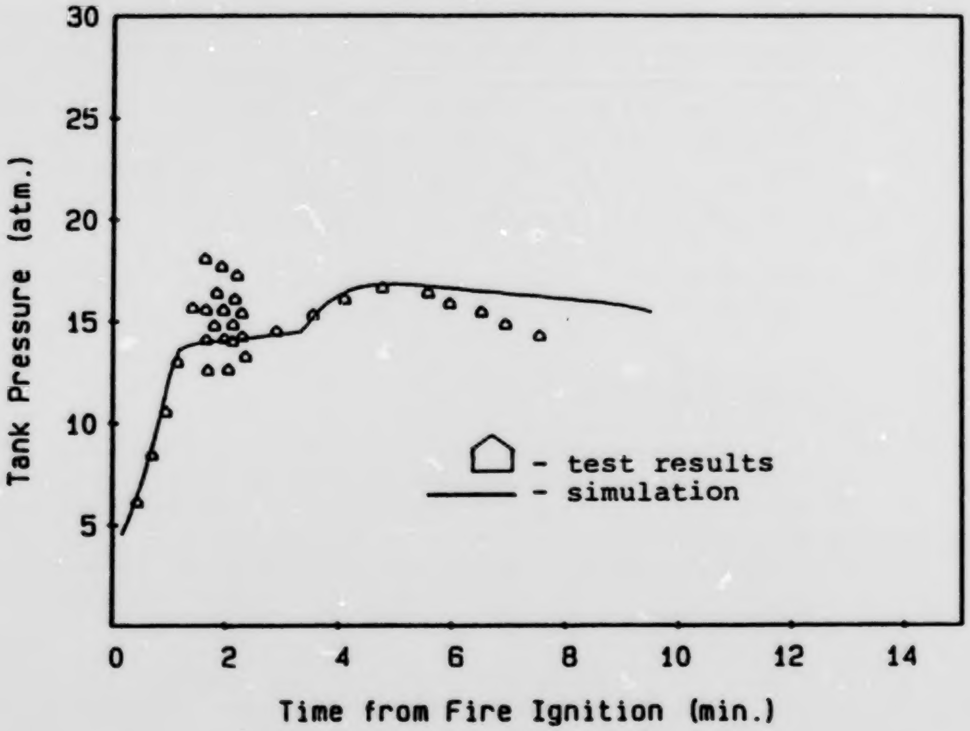

FIGURE 2-1 PREDICTED TANK PRESSURE AND MEASURED TANK PRESSURE FOR ENIGMA TEST (from Reference (4))

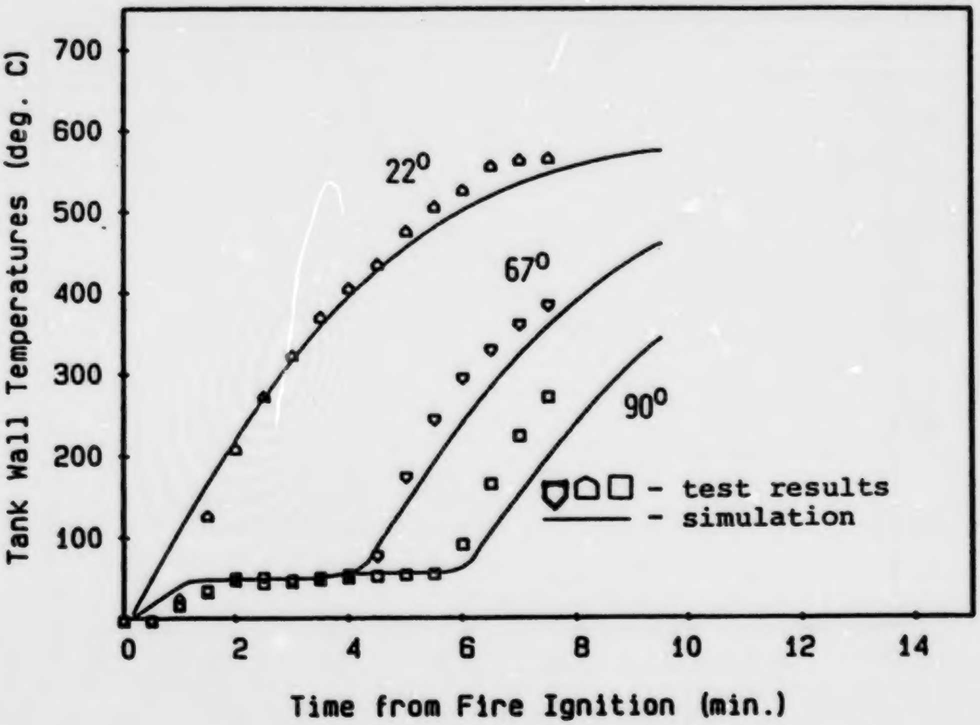

FIGURE 2-2 PREDICTED WALL TEMPERATURES AND MEASURED WALL TEMPERATURES FROM ENIGMA TEST (from Reference (4))

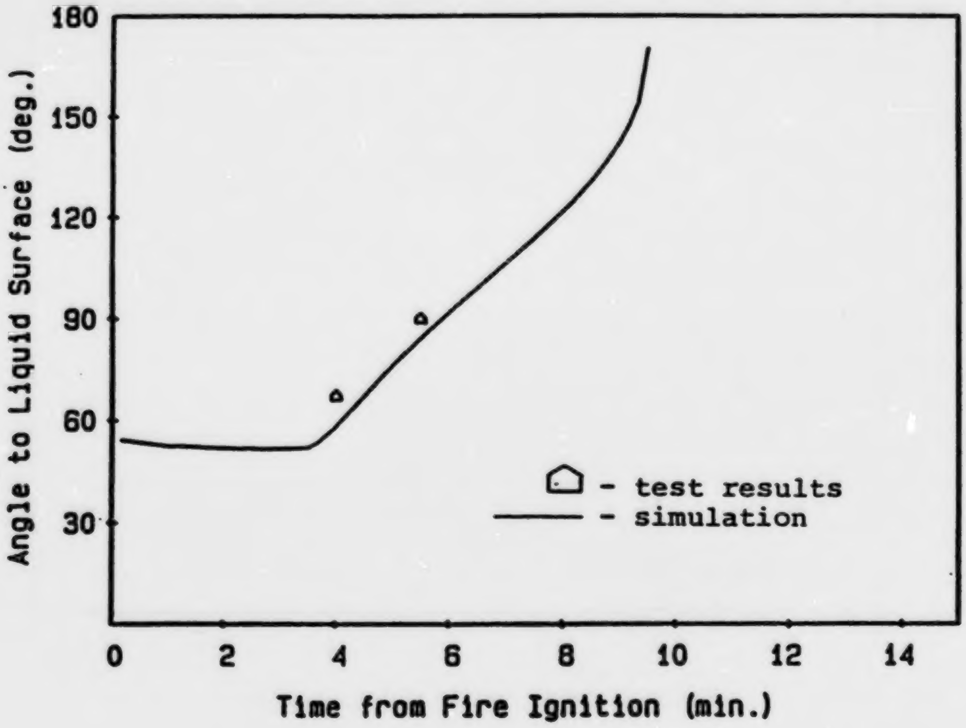

FIGURE 2-3 PREDICTED LIQUID LEVEL AND MEASURED LIQUID LEVEL FOR ENIGMA TEST (from Reference (4))

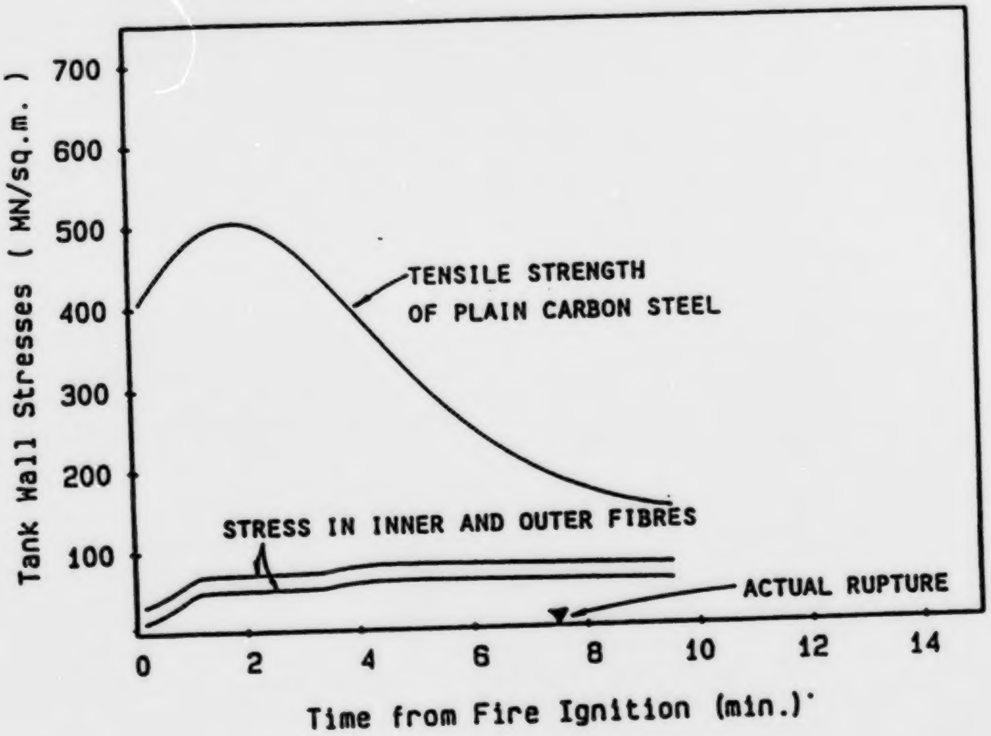

FIGURE 2-4 PREDICTED TANK WALL STRESSES AND MATERIAL STRENGTH FOR ENIGMA TEST (from Reference (4))

Figure 2-3 presents the predicted liquid level along with liquid level estimates from the actual fire tests. As can be seen from the Figure, the predictions are in good agreement with the limited data available from the fire tests. The model predictions slightly underpredict the rate at which the tank empties. This inaccuracy in the prediction of the liquid level could explain the departure of the predicted tank pressure from the actual measured tank pressure.

Figure 2-4 presents the predicted wall stresses and material properties for the Enigma test. The only data point from the fire tests shown on this figure is the actual time of failure of the tank at approximately 7½ minutes into the fire.

The figure shows the predicted tensile strength of the tank wall as a function of time from fire ignition. This tensile strength is of course a function of the wall temperature. The tensile strength shown is for the location on the tank wall where the maximum temperature is reached (at top-dead-centre).

The wall stresses at the inner and outer fibres of the tank wall are also shown. The maximum stresses occur at the inner fibres of the tank. The difference in the stress between the inner and outer fibres of the wall are due to the thermal gradient in the radial direction. Failure is indicated when the tensile strength of the wall drops below the stress levels in the wall. This, of course, is the maximum normal stress theory of failure.

As can be seen from the figure, tank failure is not predicted. This disagrees with actual observations from the fire test. The disagreement between the predictions and the actual test observations could be caused by a number of factors such as poor welds, or unpredicted hot spots in the tank wall.

Nova Case

The tank-car model was used to predict the response of a fifth-scale tank-car protected with material known as Explosafe. As in the unprotected tank case considered earlier, Nova was exposed to an engulfing fire environment. The simulation was performed with boundary conditions which represented the actual fire conditions as closely as possible. The results of the simulation are presented in Figure 2-5 to 2-8 along with the actual measured data from the fire tests.

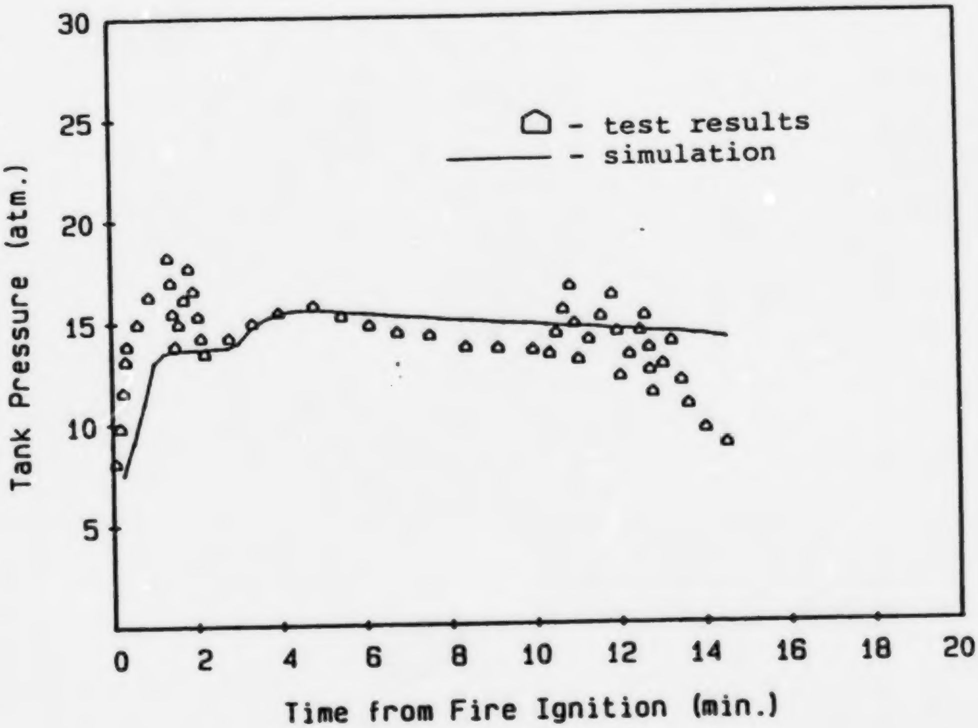

FIGURE 2-5 PREDICTED TANK PRESSURE AND MEASURED TANK PRESSURE FOR NOVA TEST (from Reference (4))

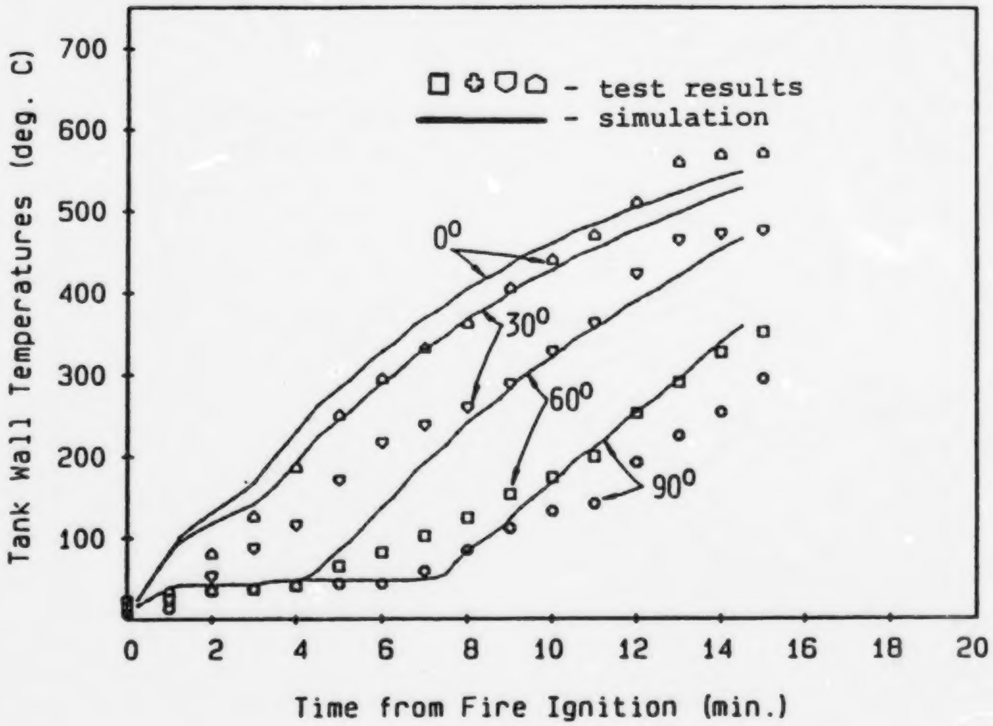

FIGURE 2-6 PREDICTED WALL TEMPERATURES AND MEASURED WALL TEMPERATURES FROM NOVA TEST (from Reference (4))

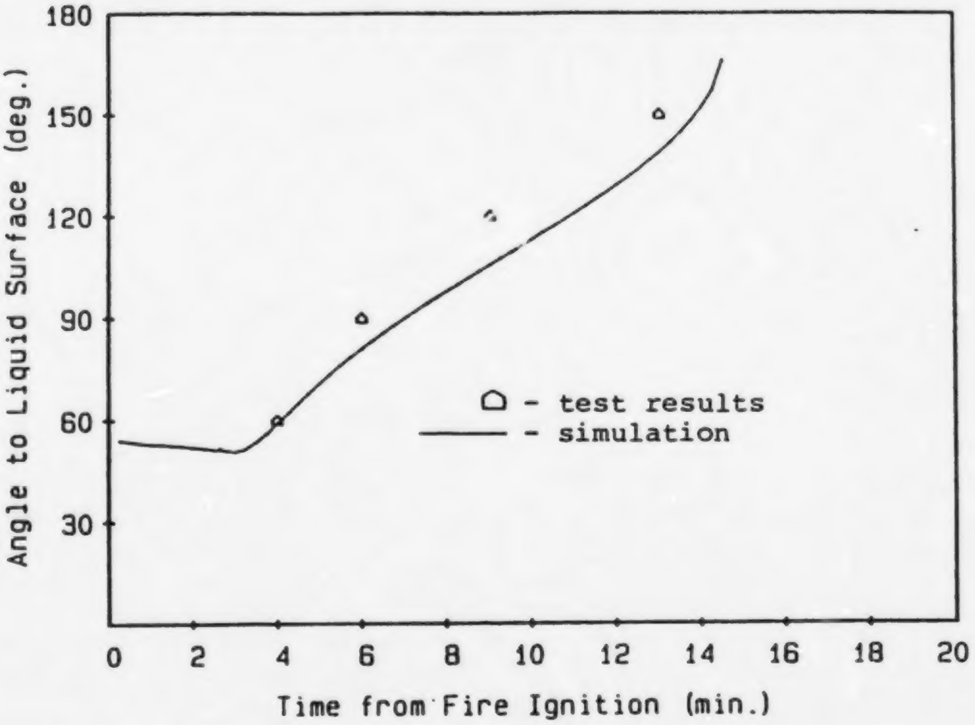

FIGURE 2-7 PREDICTED LIQUID LEVEL AND MEASURED LIQUID LEVEL FOR NOVA TEST (from Reference (4))

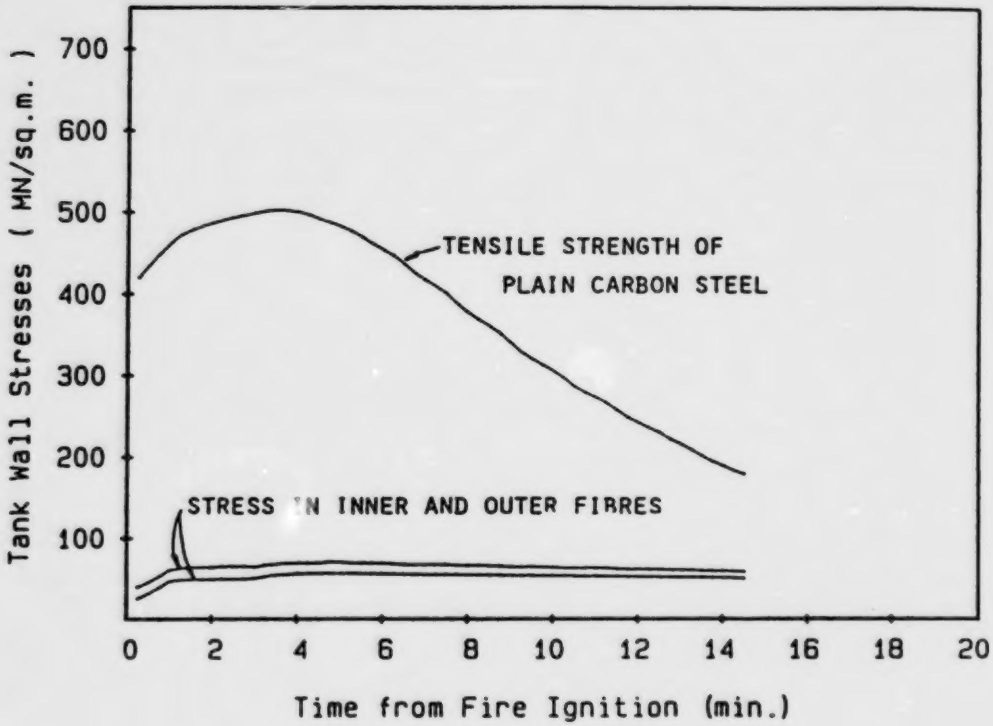

FIGURE 2-8 PREDICTED TANK WALL STRESSES AND MATERIAL STRENGTH FOR NOVA TEST (from Reference (4))

Figure 2-5 presents the predicted tank pressure along with the measured pressure from the fire test. As can be seen from the figure, the predictions are in good agreement with the test results. There is some disagreement in the initial pressurization rate prior to the relief valve cycling period, however, the length of the valve cycling period is well predicted. The tank pressurization during continuous venting is also well predicted up to the time where the peak tank pressure for continuous venting is reached. As in the Enigma case, the tank pressure drops more rapidly than predicted by the model.

Figure 2-6 presents the predicted wall temperatures along with measured wall temperatures, from the actual fire test. As can be seen from the figure, the actual wall temperature predictions are not in good agreement for the different locations indicated. However, the rates at which the temperatures increase at the different locations (slopes of the different curves) are well predicted by the tank-car model. A possible explanation for this disagreement, may be that the heat transfer coefficient within a tank filled with Explosafe may vary more dramatically than predicted by the model. This, of course, requires further experimental investigation. Generally speaking, the model is capable of predicting the trends associated with the wall temperatures and is also capable of predicting the range of temperatures expected in the tank wall.

Figure 2-7 presents the predicted and experimentally obtained liquid levels. As with the Enigma case, the tank-car model underestimates the rate at which the tank empties. This may explain why the wall temperatures were not well predicted. Possible reasons for the departure in the prediction of the liquid level are, an underprediction in the rate of venting, an error in the internal surface heat transfer coefficients, or an error in the fire heat transfer.

Figure 2-8 presents the predicted wall stresses and the material properties for the Nova test case. As can be seen from the figure, the model predicts that the tank will not fail, in agreement with the fire test results.

In summary, the model predictions are in fair agreement with the results of the Nova fire test. There is some disagreement in the prediction of the liquid level, and this may have been the cause for the differences between the predicted and the measured wall temperatures.

3.0 PROGRAM SENSITIVITY ANALYSIS

This section presents some example results from program runs conducted to test the sensitivity of the model to variations in key inputs.

The overall sensitivity analysis considered numerous inputs, including:

- time step size
- fire, temperatures and radiating properties
- tank roll angle
- tank pitch angle
- lading type

The results of the sensitivity analysis is presented in detail for the above cases, in Reference (2). The following section presents the results of the time step sensitivity analysis as an example.

The results are presented using the four summary plots; pressure vs. time, wall temperature vs. time, liquid level vs. time and wall stress conditions vs. time.

3.1 TIME STEP SENSITIVITY

The choice of the time step used in the program plays a key role in the model predictions. The size of the time step affects both the accuracy of the model predictions and the stability of the model solutions.

The time step sensitivity will be illustrated with two examples. The first is a simulation of an unprotected tank-car and it will be seen that the variation in time step has a small affect on the prediction of tank failure. However, in this particular case there are no stability problems. The second example, is a simulation of a tank with externally applied thermal insulation. It will be seen that increasing the time step in this particular case results in program instabilities and eventual model failure.

In both examples the time steps were increased while all other run parameters were kept constant. The results of the runs are presented in plots which present the tank pressure, wall temperature, liquid level and wall stresses as functions of time from fire ignition.

Unprotected Tank

This series of runs involved the simulation of a full-scale unprotected (except for standard size relief valve) tank-car filled to 95% capacity with propane at 25°C. In all the simulations the tank was exposed to an engulfing pool fire.

In total five time steps were considered, .5 sec, 1 sec., 5 sec., 10 sec., and 30 sec. The results from these runs are presented in Figures 3-1 to 3-4. As will be seen from these figures, there is very little difference between the .5 second and the 1 second runs and therefore it can been assumed that these time steps give accurate predictions. This was the basis for choosing a one second time step for all the validation runs which were performed.

Figure 3-1 presents the predicted tank pressure for the different time step runs. As can be seen from the figure the different time steps have very little effect on the pressure predictions other than a shifting along the time axis. This is due to the fact that the large time steps caused the initial heat up period to be poorly represented. The rapid thermal response in the first moments of the fire requires small integration intervals, i.e., small time steps. As can be seen from the figure the length of the valve cycling period is not affected by the time step size. The peak tank pressure is also unaffected by the time step choice.

Figure 3-2 presents the predicted tank wall temperatures for the different time step cases considered. As with the pressure predictions, the only effect that is seen is a slight shifting along the time axis. The peak wall temperatures are unaffected by the choice of the time step as is the length of time between temperature breaks. The slight shift along the time axis is again due to the poor representation of the initial heating period.

Figure 3-3 presents the predicted liquid level for the different time step cases considered. Again the only apparent affect is a slight shifting along the time axis. The actual slopes of the different curves are identical.

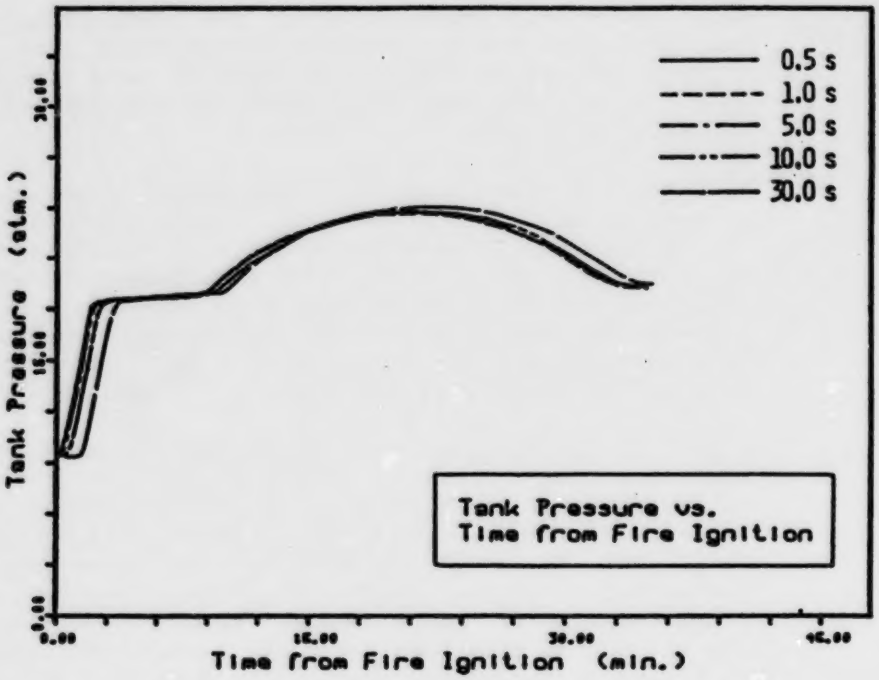

FIGURE 3-1 PREDICTED TANK PRESSURE FOR UNPROTECTED TANK FROM PROGRAM RUNS USING DIFFERENT TIME STEPS

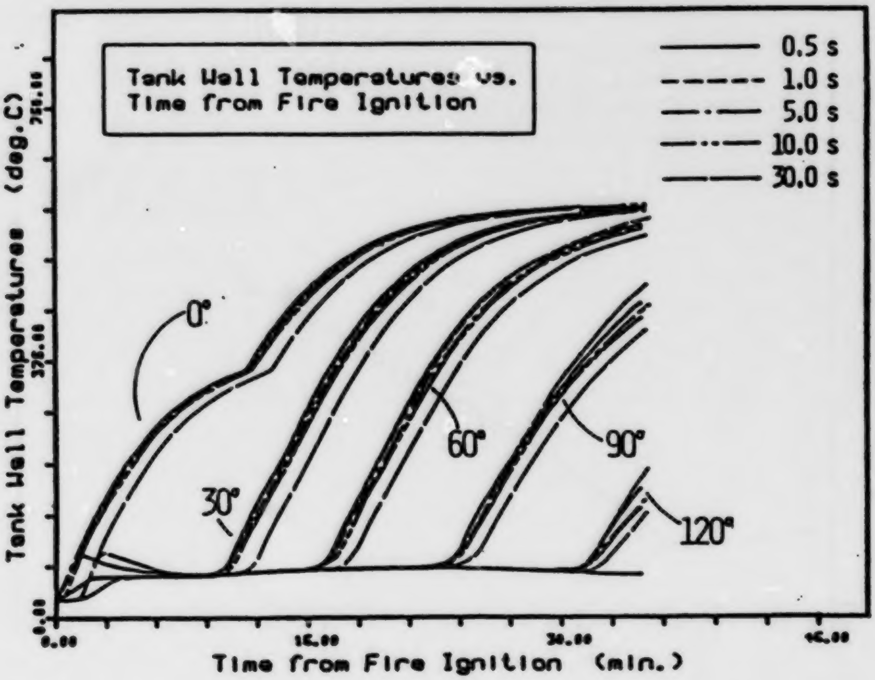

FIGURE 3-2 PREDICTED WALL TEMPERATURES FOR UNPROTECTED TANK PROGRAM RUNS USING DIFFERENT TIME STEPS

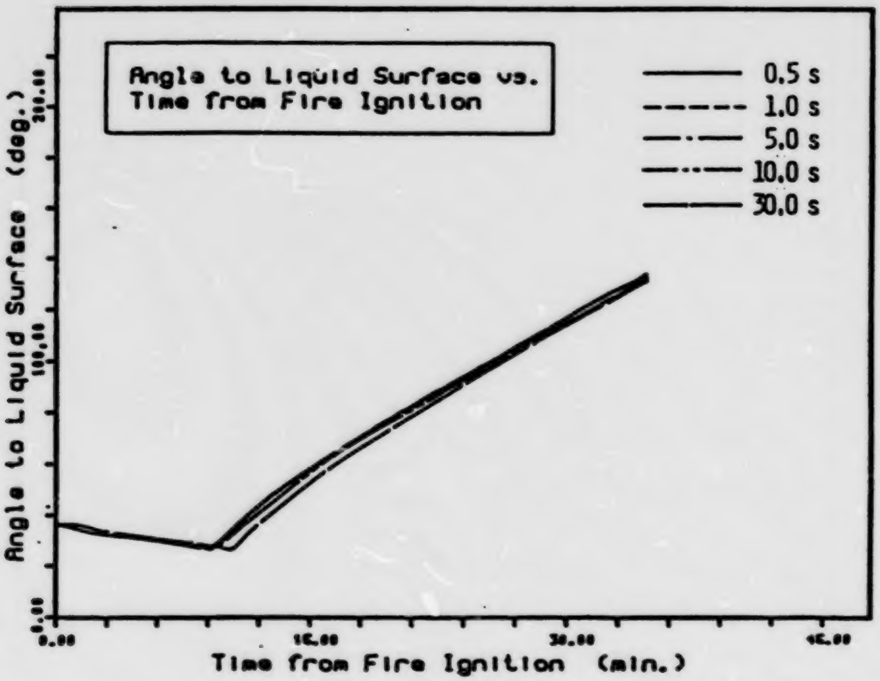

FIGURE 3-3 PREDICTED LIQUID LEVEL FOR UNPROTECTED TANK FROM PROGRAM RUNS USING DIFFERENT TIME STEPS

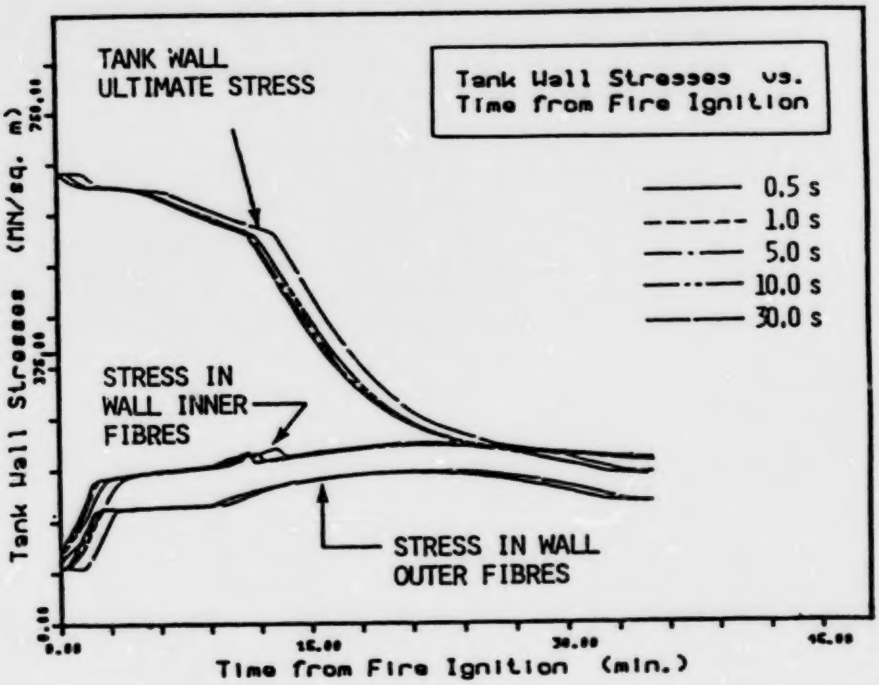

FIGURE 3-4 PREDICTED TANK WALL STRESSES AND MATERIAL STRENGTH FOR UNPROTECTED TANK FROM PROGRAM RUNS USING DIFFERENT TIME STEPS

Figure 3-4 presents the predicted tank wall stresses and tank wall material strengths. As with all the plots, the only apparent effect is a slight shifting along the time axis. This shifting however, affects the time to failure predictions. The error in the prediction of the time to tank failure is directly related to the degree of shifting along the time axis of all the prediction results. However, the total time shift is only approximately 3 minutes for the 30 second time step case. This is not considered to be a large error.

In summary, the results indicate that the Tank Car model is relatively insensitive to changes in time step, up to approximately 30 seconds, for the specific case of an unprotected tank-car. It is recommended therefore that time steps of less than 30 seconds be used for all simulations of unprotected tanks. It is believed that a time step of 1 second gives accurate results.

Insulated Tank

This series of runs involved the simulation of a full-scale thermally insulated tank (with standard size relief valve) filled to 95% capacity with propane at 25°C. The tank was exposed to an engulfing pool fire. In the simulation, it was assumed that the thermal insulation consisted of 6.4 mm thick layer of material with thermal and mechanical properties similar to those of asbestos. Both steel jacketed and unjacketed cases were considered because the calculation procedure changes when steel jacket is added. As will be seen from the following results, the model sensitivity to variations of time step size are significantly affected by the steel jacket. This is because the steel jacket analysis has a stabilizing effect on the overall calculations.

The results are presented for both jacketed and unjacketed cases using time steps of 1, 5, 10 and 30 seconds. The results for the jacketed insulation case are presented in Figures 3-5 to 3-8. The results for the unjacketed case are presented in Figures 3-9 to 3-12.

Case 1; Jacketed Insulation (Figures 3-5 to 3-8)

Figure 3-5 presents the predicted tank pressures as a function of time from fire ignition. As can be seen from this figure the pressure prediction is not significantly

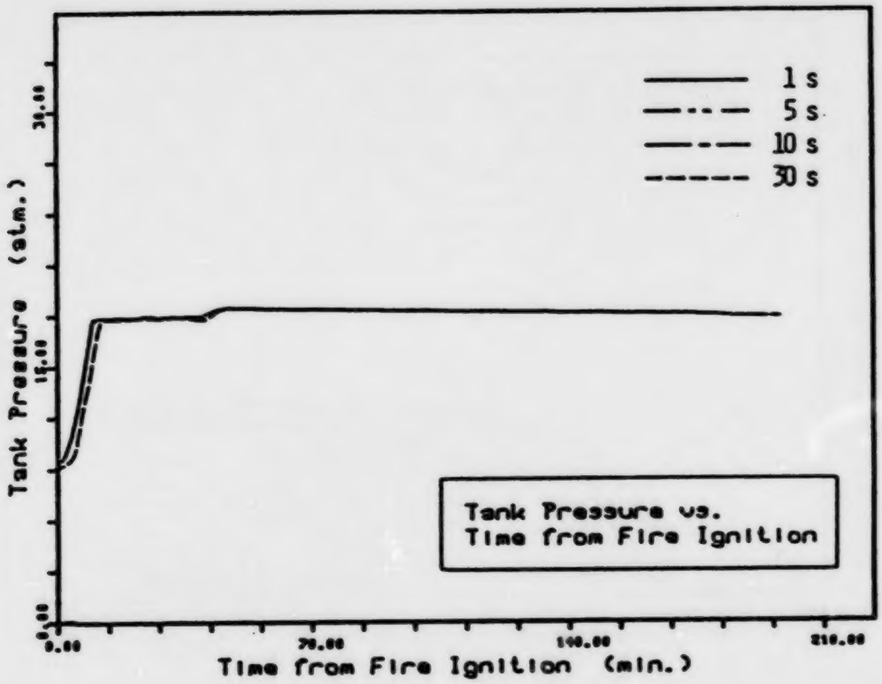

FIGURE 3-5 PREDICTED TANK PRESSURE FOR INSULATED TANK (WITH STEEL JACKET) FROM PROGRAM RUNS USING DIFFERENT TIME STEPS

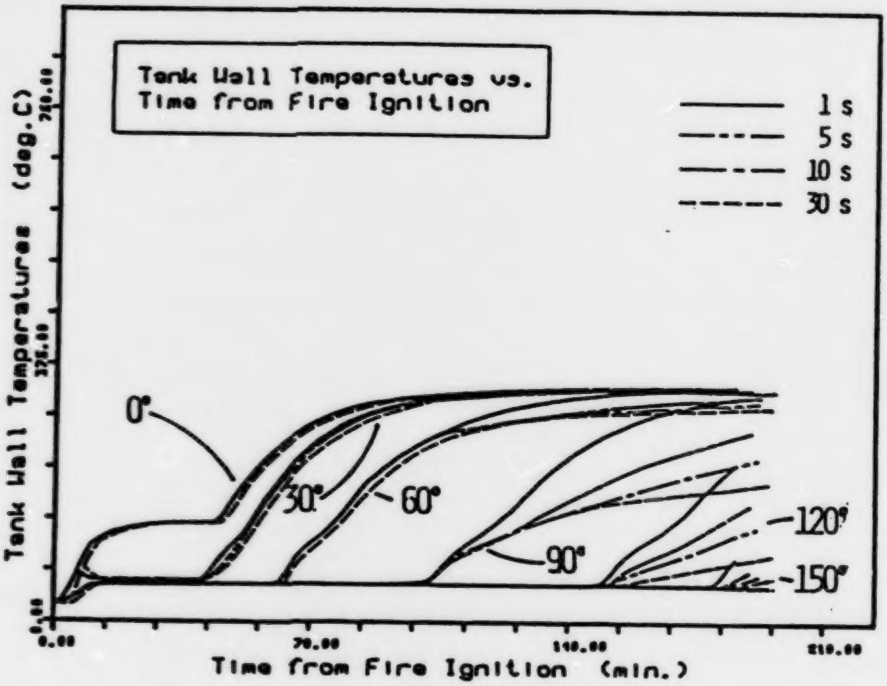

FIGURE 3-6 PREDICTED WALL TEMPERATURES FOR INSULATED TANK (WITH STEEL JACKET) FROM PROGRAM RUNS USING DIFFERENT TIME STEPS

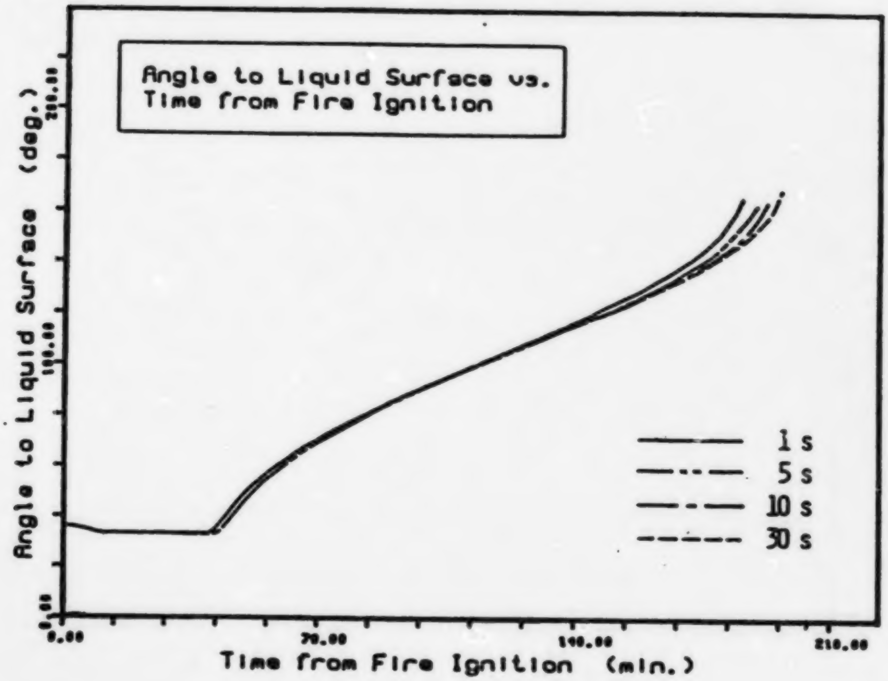

FIGURE 3-7 PREDICTED LIQUID LEVEL FOR INSULATED TANK (WITH STEEL JACKET) FROM PROGRAM RUNS USING DIFFERENT TIME STEPS

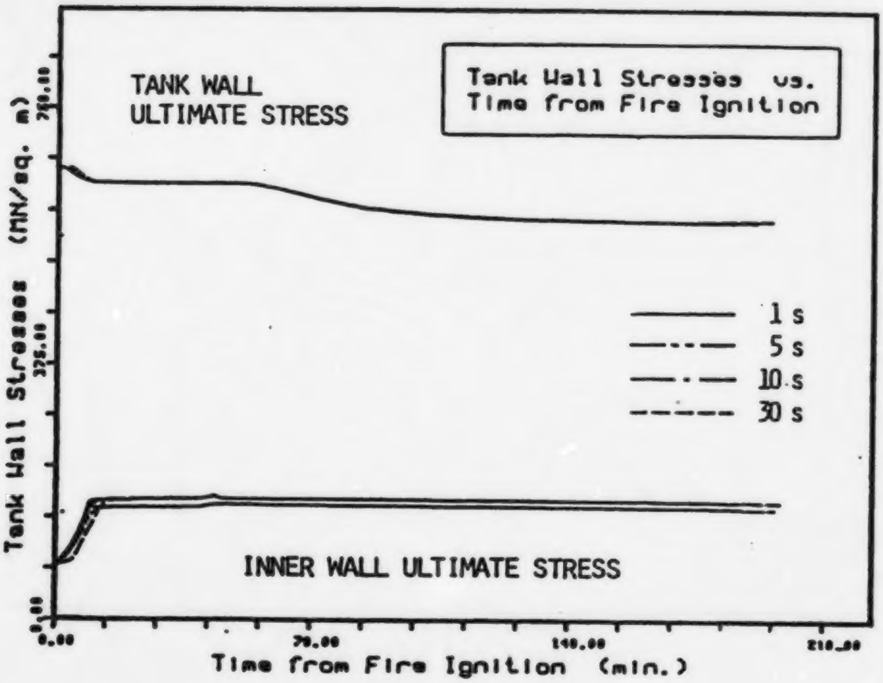

FIGURE 3-8 PREDICTED TANK WALL STRESSES AND MATERIAL STRENGTH FOR INSULATED TANK (WITH STEEL JACKET) FROM PROGRAM RUNS USING DIFFERENT TIME STEPS

affected by the variations of the time step. The only apparent effect is a slight shifting of the predicted response along the time axis. As with the case of an unprotected tank this shifting effect is caused by integration errors during the initial rapid heating of the tank/lading system. These inaccuracies however, have no affect on the overall peak pressure. This shifting along the time axis also has no effect on the length of the valve cycling period.

Figure 3-6 presents the predicted wall temperatures for the insulated and jacketed tank for the different time steps considered. Once again, the model predictions are shifted along the time axis as the time step size is increased. In addition, the predicted wall temperatures, especially at locations around the side of the tank, are significantly effected as the time step is increased. As the time step is increased the wall temperatures are reduced from those predicted using small (1 second) time steps. This deviation is due to a build up of integration error over the rather long real time duration of the simulation. This kind of build up of integration errors is not seen clearly with an unprotected tank case because the real time duration is much shorter for an unpredicted tank period. For the case of an unprotected tank, the real time duration may be approximately 30 or 40 minutes. Whereas, in the case of a thermally insulated tank, the real time duration may be as high as 300 to 400 minutes. This increase in the length of real time allows integration errors to build up until the point where they are very significant. This inaccuracy, however, does not affect the wall temperatures near the top of the tank significantly and since these are the peak temperatures which dictate the time to tank failure the actual prediction of failure is not significantly affected by this buildup of integration errors.

Figure 3-7 presents the model predictions for the liquid level. The plots again show a slight shifting of the predicted liquid level along the time axis. Additional to the shifting effect of the increased time step, the location of the liquid level deviates more and more as time goes on because of integration errors which build up. This error tends to keep the liquid level higher in the tank and this translates into the wall temperature prediction errors discussed earlier. The integration error is caused by the fact that over a time interval the relief valve mass flow is assumed to be constant.

Figure 3-8 presents the predicted tank stress conditions for the case of thermally protected tank with steel jacket. As can be seen from the Figure the only apparent affect of the different time steps is a very slight shifting along the time axis for the highest time steps chosen. However, the actual wall stresses and material strengths are not significantly affected by the different time steps chosen.

The wall material strength is directly related to the peak wall temperature. In the case of a tank-car exposed to engulfing pool fire the peak wall temperature will occur at the top-dead-centre of the tank. It was shown earlier that the peak wall temperature at top-dead-centre was not significantly effected by integration errors. Therefore, different time steps appear to have little or no effect on the material strength. The tank wall stresses are of course dictated by the tank internal pressure and a temperature gradient through the tank wall. Neither of these are significantly effected by changes in the time step, and therefore, there is no significant change in the predicted wall stresses. These effects combine to give no significant change in the prediction of time to failure.

In summary, the results indicate that variations in the size of the program time step for the specific case of an insulated tank with steel jacket exposed to an engulfing pool fire have little or no effect on the prediction of time to failure. However, variations in the time step can have a significant effect on the prediction of wall temperatures. Therefore, it is recommended that for such cases the time step be kept below five seconds. If however, it is not important to accurately predict the wall temperatures, time steps can be increased to a limit of approximately 30 seconds.

Case 2: Insulation without Steel Jacket (Figures 3-9 to 3-12)

This series of simulations involved an insulated tank with the same thermal barrier as described in the previous case, however, there was no steel jacket present. This case was considered in the sensitivity analysis because it is known that the analysis used to represent the steel jacket has a stabilizing effect on the calculation of wall temperatures.

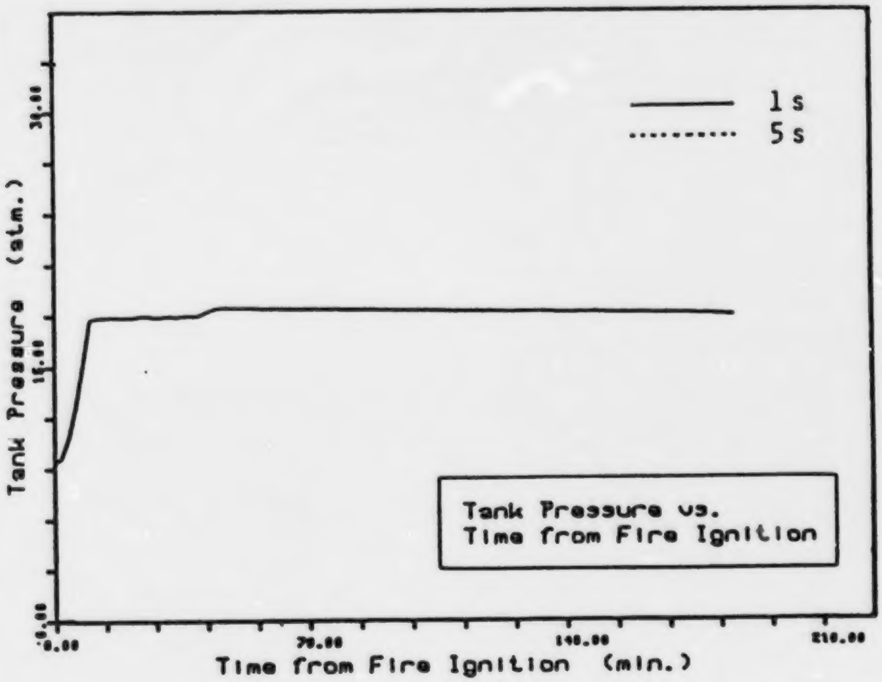

FIGURE 3-9 PREDICTED TANK PRESSURE FOR INSULATED TANK (NO STEEL JACKET) FROM PROGRAM RUNS USING DIFFERENT TIME STEPS

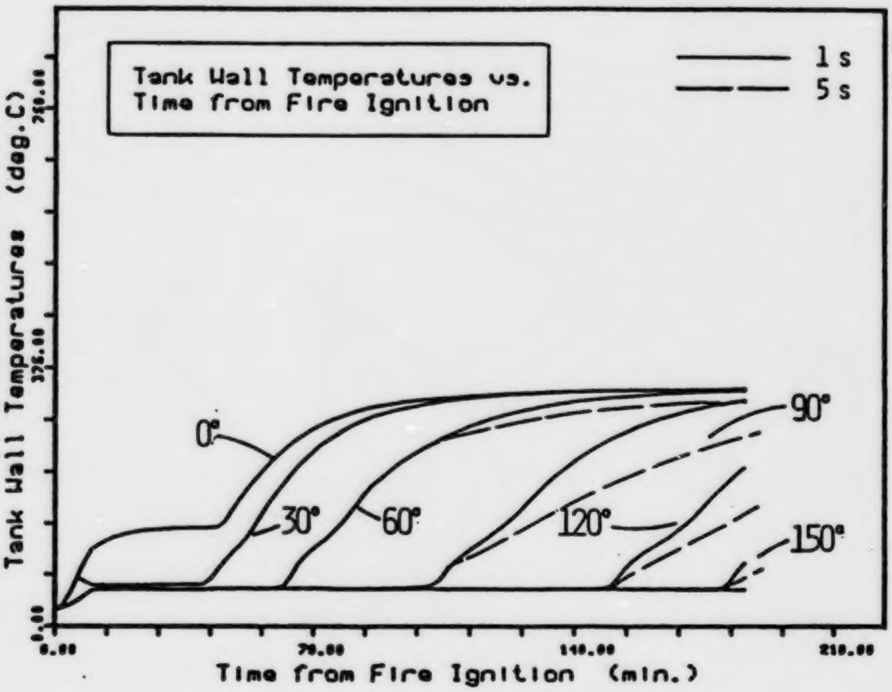

FIGURE 3-10 PREDICTED WALL TEMPERATURES FOR INSULATED TANK (NO STEEL JACKET) FROM PROGRAM RUNS USING DIFFERENT TIME STEPS

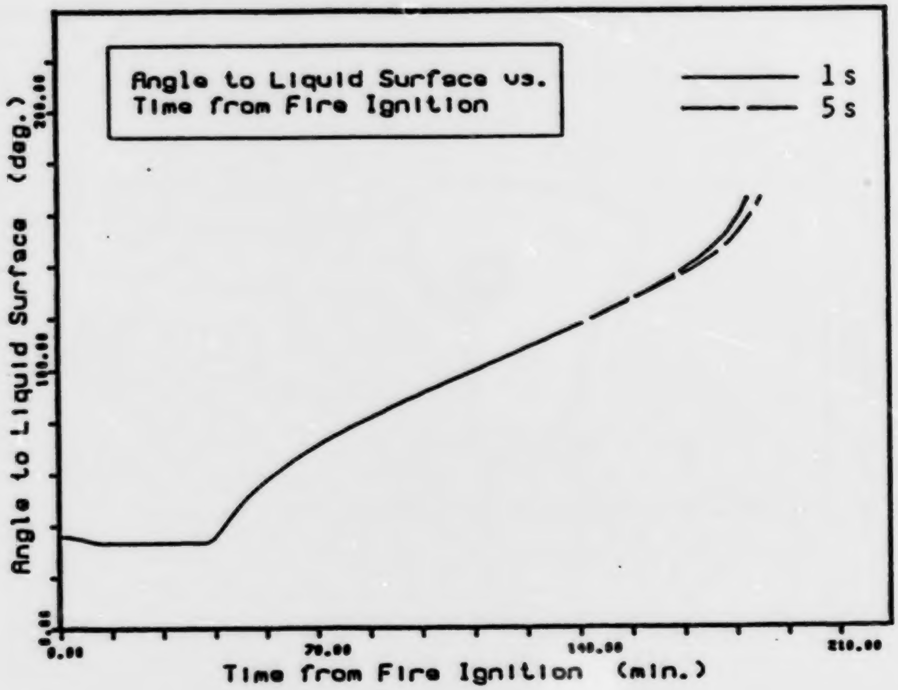

FIGURE 3-11 PREDICTED LIQUID LEVEL FOR INSULATED TANK (NO STEEL JACKET) FROM PROGRAM RUNS USING DIFFERENT TIME STEPS

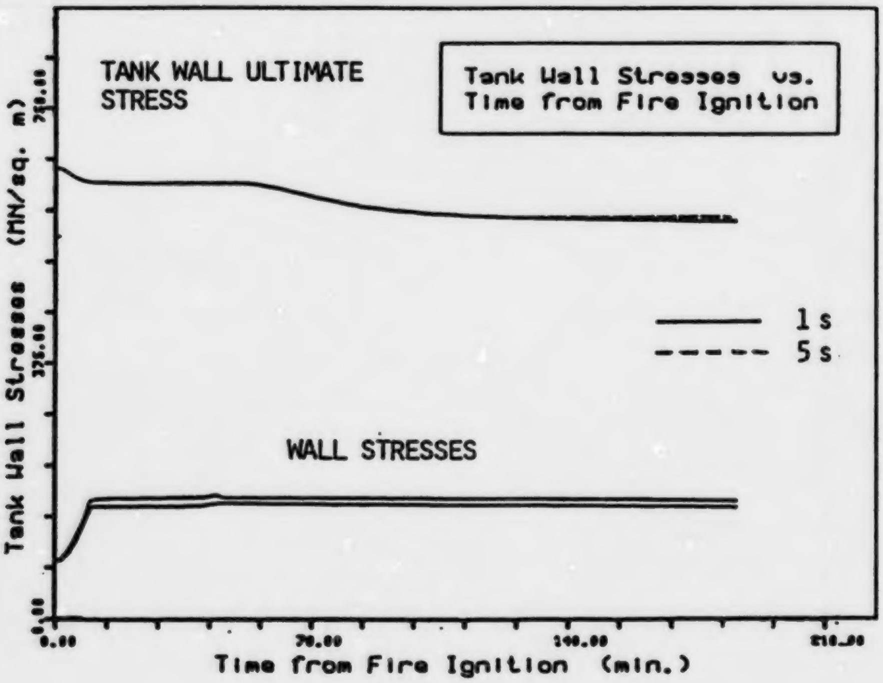

FIGURE 3-12 PREDICTED TANK WALL STRESSES AND MATERIAL STRENGTH FOR INSULATED TANK (NO STEEL JACKET) FROM PROGRAM RUNS USING DIFFERENT TIME STEPS

Figures 3-9 to 3-12 present the results of the simulations. Time steps of 1, 5, 10 and 30 seconds were considered. The results shown in the figures include only the results from the 1 and 5 second time step runs. The results from the other runs (ie. 10 and 30 second time step) are not plotted because those runs terminated very early in the simulations because of instabilities in the numerical solutions.

The results that are presented in Figures 3-9 to 3-12 for the 1 and 5 second time step cases are very nearly identical to those shown in the case of the an insulated tank with steel jacket. This is an indication that the predictions for 1 and 5 second time steps for this case are accurate. It is expected that from a thermal standpoint the presence of the steel jacket does not affect the temperatures in the insulation and tank wall as long as the insulation stays in contact with the steel jacket. If the insulation shrinks away from the steel jacket then the jacket will act as a radiation shield, an additional resistance to the flow of heat to the tank.

The cases with the 10 and 30 second time steps terminated early in the simulations because of instabilities in the calculation of the wall and insulation temperatures. The instabilities were caused by the large time steps.

In summary, when a simulation is to take place involving a tank-car with thermal protection, without a steel jacket the time step should be kept below 5 seconds. If the time step is increased above this the program solutions will become unstable and the program run will terminate.

4.0 EXAMPLE SIMULATIONS

This section presents results of a number of model simulations of tanks with different thermal protection schemes. Three basic systems were considered, insulated tanks, tank-cars with fusible plugs, and tank-cars equipped with Explosafe. A number of simulations were performed for each thermal protection system so that their performance could be predicted for different configurations of the thermal protection scheme.

Each simulation started with the same initial conditions, that is, initial temperature = 25°C, and initial fill = 95% of the tank capacity. In all cases the lading is pure propane, and the tank is assumed to be equipped with a standard size relief valve. All of the cases to be presented involved a tank fully engulfed in fire.

As before, the model predictions are presented using the four basic summary plots, pressure vs. time, wall temperature vs. time, liquid level vs. time and wall stresses vs. time.

4.1 INSULATED TANK

This section presents the results of a number of simulations involving a full-scale tank-car equipped with thermal insulation. Three simulations were performed with the tanks equipped with different thicknesses of thermal insulation with properties similar to that of asbestos. In all cases the insulation was assumed to be covered by a steel jacket.

The different simulations were performed to show the effects of thickening the thermal insulating layer on a tank-car. Figures 4-1 to 4-4 show the predicted response of the tank equipped with the different thicknesses of thermal insulation.

Figure 4-1 presents the predicted tank pressure for the different cases considered. As can be seen from the figure, the simulation for the tank with the thinnest insulating cover had the most rapid pressurization rate. This initial rapid pressurization rate was followed by a relatively short valve cycling period and then a rapid increase in the tank pressure during continuous venting.

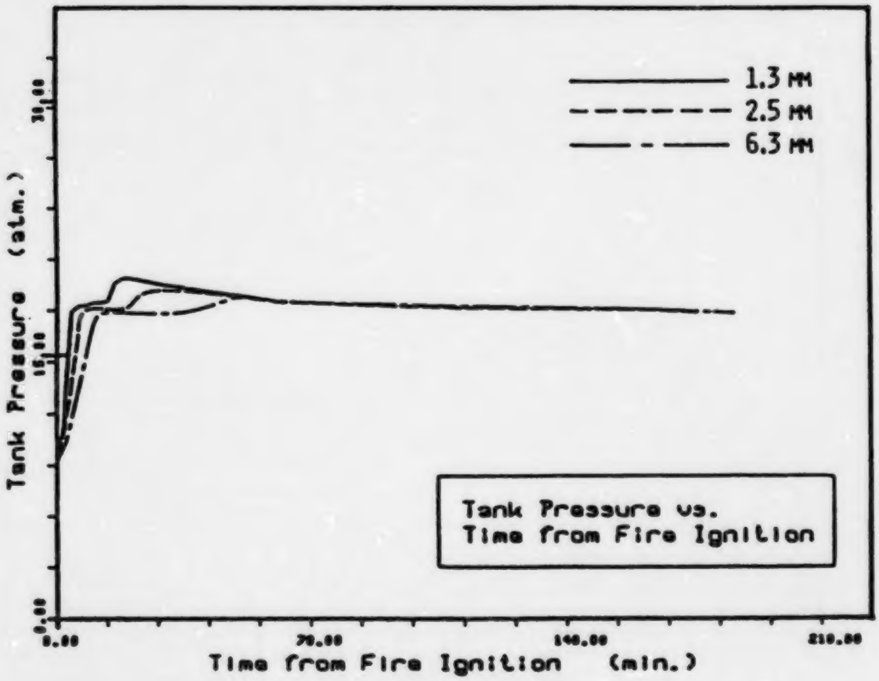

FIGURE 4-1 PREDICTED TANK PRESSURES FOR INSULATED TANKS WITH DIFFERENT THICKNESSES OF INSULATION, EXPOSED TO AN ENGULFING FIRE

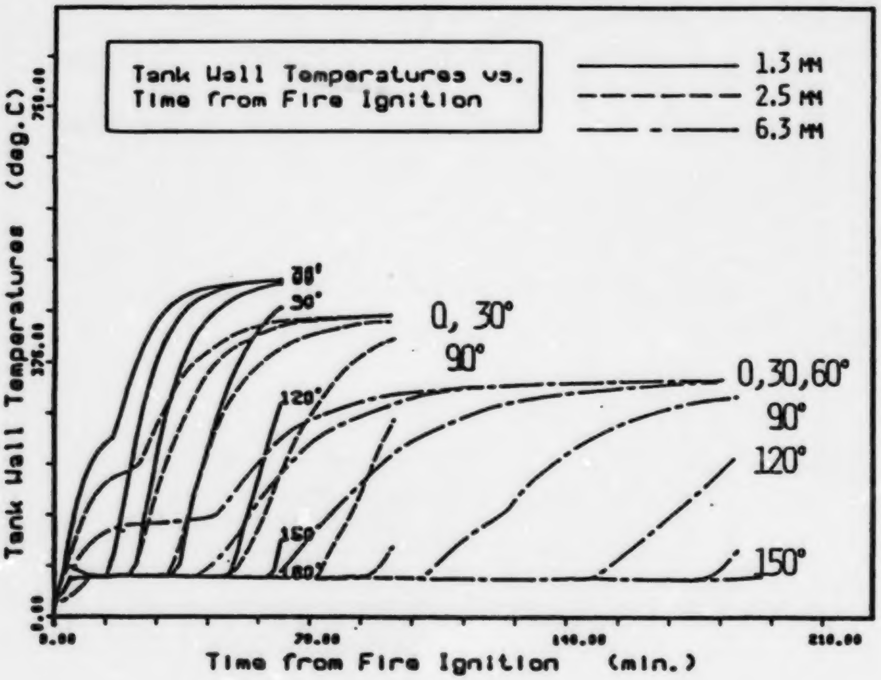

FIGURE 4-2 PREDICTED TANK WALL TEMPERATURES FOR INSULATED TANKS WITH DIFFERENT THICKNESSES OF INSULATION, EXPOSED TO AN ENGULFING FIRE

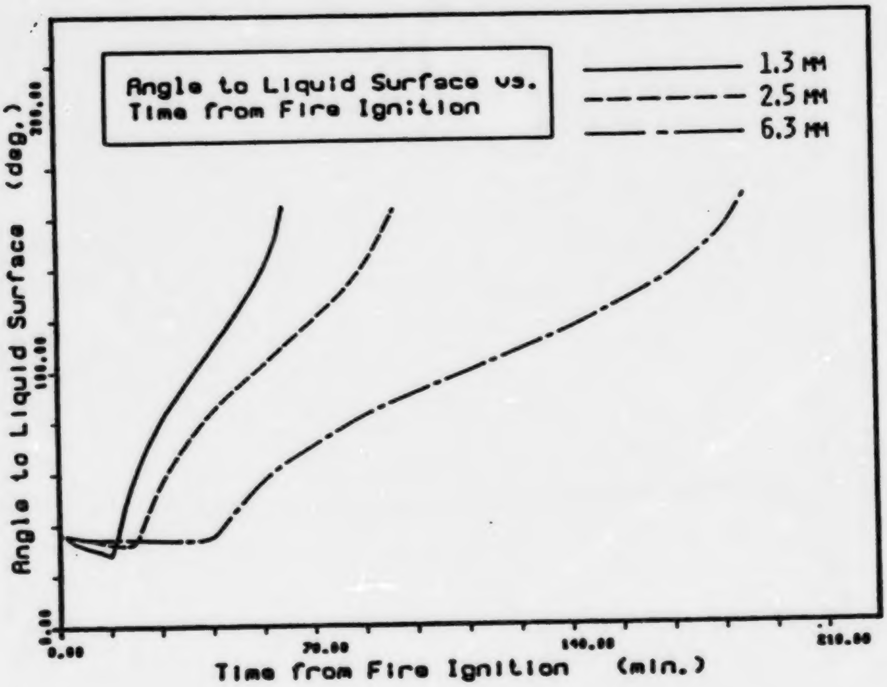

FIGURE 4-3 PREDICTED LIQUID LEVEL OF INSULATED TANKS WITH DIFFERENT THICKNESSES OF INSULATION, EXPOSED TO AN ENGULFING FIRE

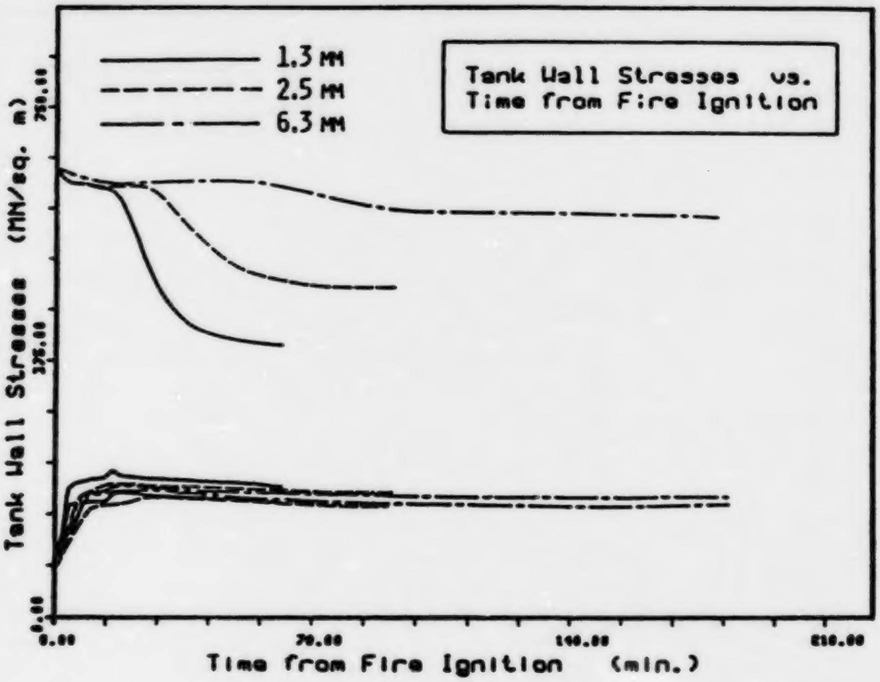

FIGURE 4-4 PREDICTED TANK WALL STRESSES AND TANK WALL MATERIAL STRENGTHS FOR INSULATED TANKS WITH DIFFERENT THICKNESSES OF INSULATION, EXPOSED TO AN ENGULFING FIRE

As can be seen from the figure, the valve cycling periods increase in duration as the thickness of the insulation is increased. The increased thickness of insulation also had the effect of reducing the tank peak pressure.

Figure 4-2 presents the predicted wall temperatures for the different cases considered. As can be seen from the figure, the thickness of the insulation layer has a significant effect on the predicted wall temperatures. As the insulation thickness is increased, the peak wall temperatures are decreased, as expected. It appears from the figure, that if the insulation thickness is doubled, the time scale of the simulation also doubles, approximately. In other words, the time during which the tank remains partially full of lading is increased as the insulation layer thickness is increased.

Figure 4-3 presents the predicted liquid level for the different cases considered. As can be seen from the figure, the simulation involving the thickest layer of insulation resulted in the longest time to empty. This, of course, is due to the fact that the rate at which the lading is vented through the relief valve is determined by the total heat input to the tank lading. By increasing the thickness of the insulating layer, the total heat input to the tank lading is reduced and this results in a lower venting rate.

Figure 4-4 presents the predicted wall stresses and tank material strengths for the different cases considered. As can be seen from the figure, none of the cases considered came close to rupturing. For the case with the thickest thermal insulation cover, there was very little loss of material strength due to high temperature degradation. However, the case with the thinnest insulation layer does show significant loss in material strength at the locations of the peak wall temperatures. The predicted wall stresses show that as the insulation layer is increased the difference between the stresses in the inner and outer fibres of the tank wall is decreased. This is, of course, due to the fact that the differences in the stresses of the inner and outer wall fibres is due to the thermal gradient through the wall, and this thermal gradient is of course reduced as the heat flux is reduced.

In summary, the simulations clearly shown that the thickness of the thermal insulation layer has a significant effect on the thermal response of the tank-car.

4.2 TANK WITH FUSIBLE PLUGS

The simulations about to be presented involve full-scale tanks equipped with fusible plug devices. Fusible plugs are devices consisting of an orifice plugged by a low melting temperature material. If the temperature of the device exceeds some predetermined limit, the plug melts and is blown free thereby opening the orifice so that the tank lading can be vented. In other words, a fusible plug is a temperature sensitive relief valve. The disadvantage of such devices is that they cannot be closed once they have been opened.

Two different sets of simulations were performed to show the sensitivity in the performance of fusible plugs to different plug numbers and melting temperatures. Figures 4-5 to 4-8 show the predicted response of a tank equipped with four, eight, or twelve 51 mm diameter plugs that melt out at 430°C. Figures 4-9 to 4-12 show predicted results for a full-scale tank equipped with four 51 mm diameter plugs that melt out at temperatures of 205, 315 and 430°C. In all cases the fusible plugs have been located at the tank top-dead-centre and the tank is level and upright. No attempt was made to locate the plugs to account for all possible tank orientations (i.e., plugs should be located so that some always remain above the liquid level no matter how the tank is oriented. This is necessary because the plugs will only melt out if they are above the liquid level).

Case #1 Different Numbers of Fusible Plugs:

Figure 4-5 presents the predicted tank pressure for the different cases considered. As can be clearly seen from the figure, the tank response prior to the opening of the fusible plugs is identical to that of an unprotected tank-car. However, once the fusible plugs come into play, the tank pressure histories differ. As is indicated in the figure, increasing the number fusible plugs increases the rate at which the tank pressure drops. It seems that there is not a great advantage to increasing the number of fusible plugs above 8.

Figure 4-6 presents the predicted tank wall temperatures for the different cases considered. As can be seen from the figure, the presence of fusible plugs has no effect up

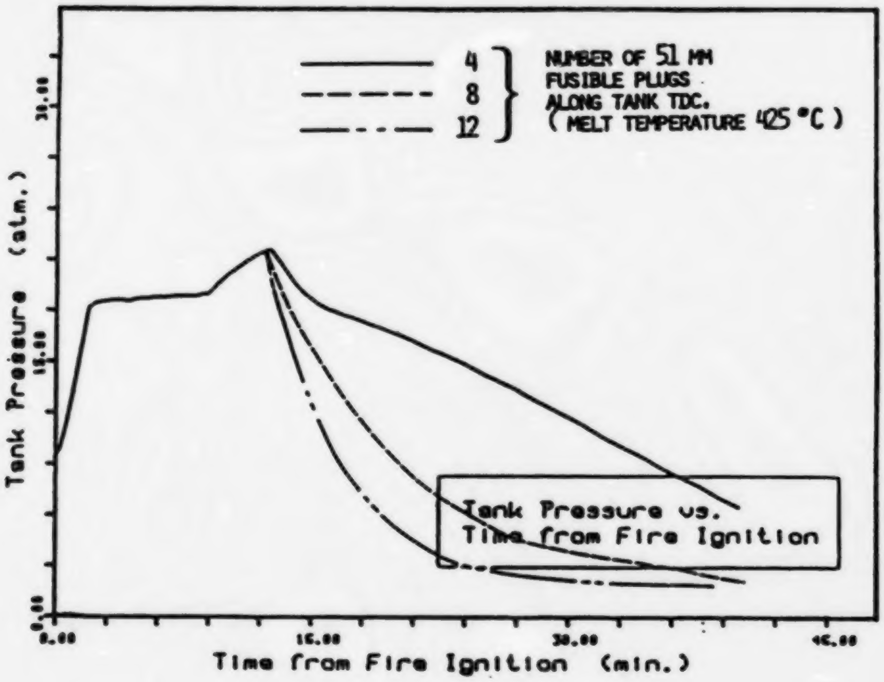

FIGURE 4-5 PREDICTED TANK PRESSURES FOR TANKS EQUIPPED WITH DIFFERENT NUMBERS OF FUSIBLE PLUGS, EXPOSED TO AN ENGULFING FIRE

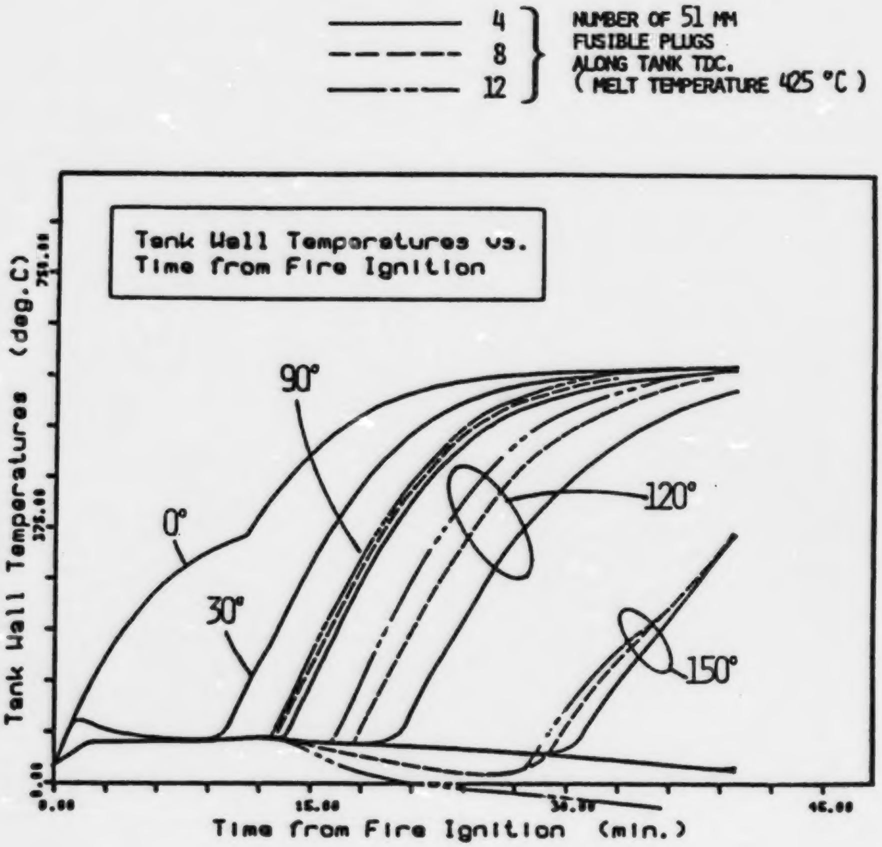

FIGURE 4-6 PREDICTED TANK WALL TEMPERATURES FOR TANKS EQUIPPED WITH DIFFERENT NUMBERS OF FUSIBLE PLUGS, EXPOSED TO AN ENGULFING FIRE

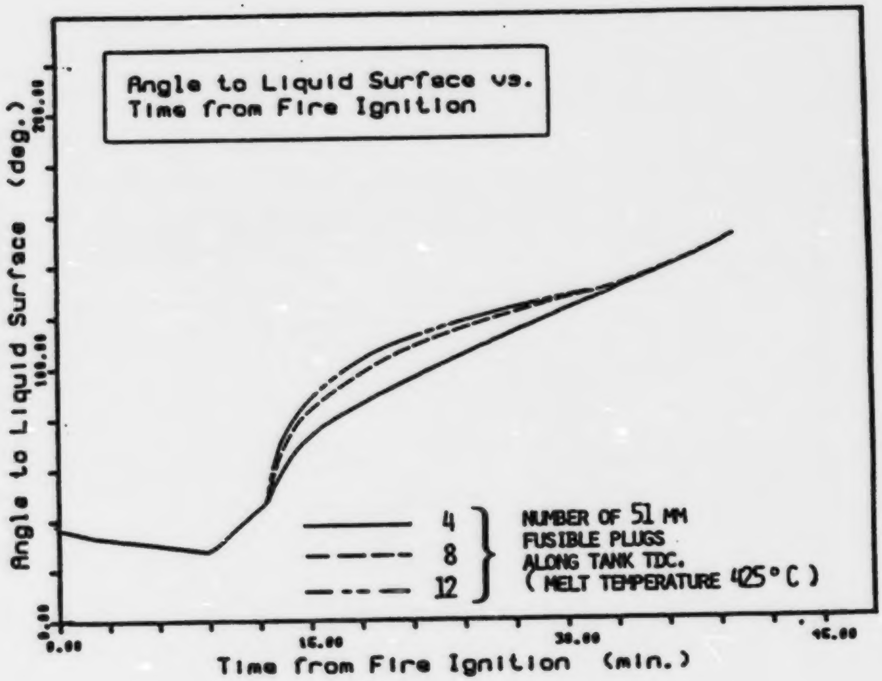

FIGURE 4-7 PREDICTED LIQUID LEVEL OF TANKS EQUIPPED WITH DIFFERENT NUMBERS OF FUSIBLE PLUGS, EXPOSED TO AN ENGULFING FIRE

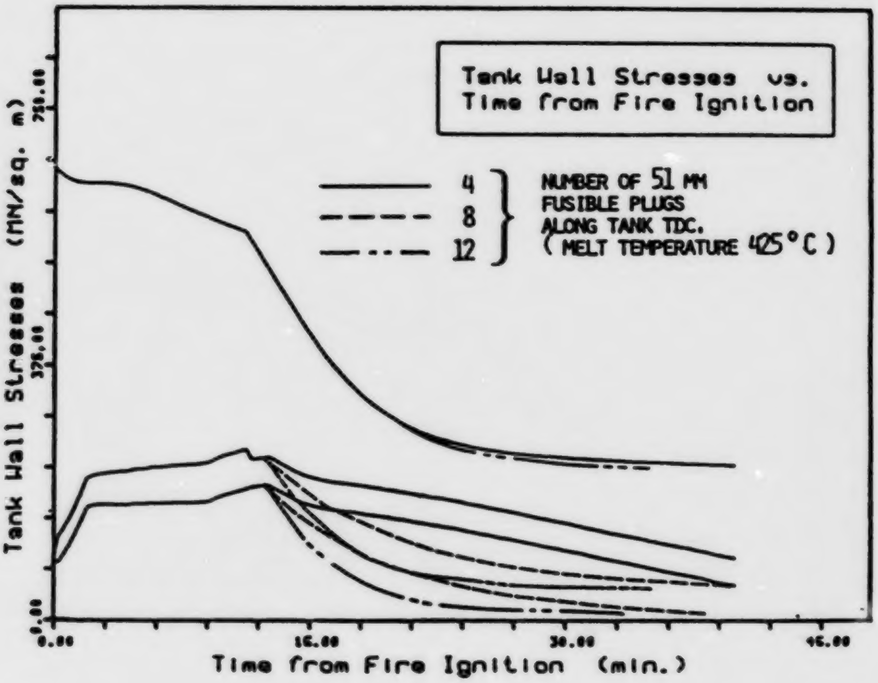

FIGURE 4-8 PREDICTED TANK WALL STRESSES AND TANK WALL MATERIAL STRENGTHS FOR TANKS EQUIPPED WITH DIFFERENT NUMBERS OF FUSIBLE PLUGS, EXPOSED TO AN ENGULFING FIRE

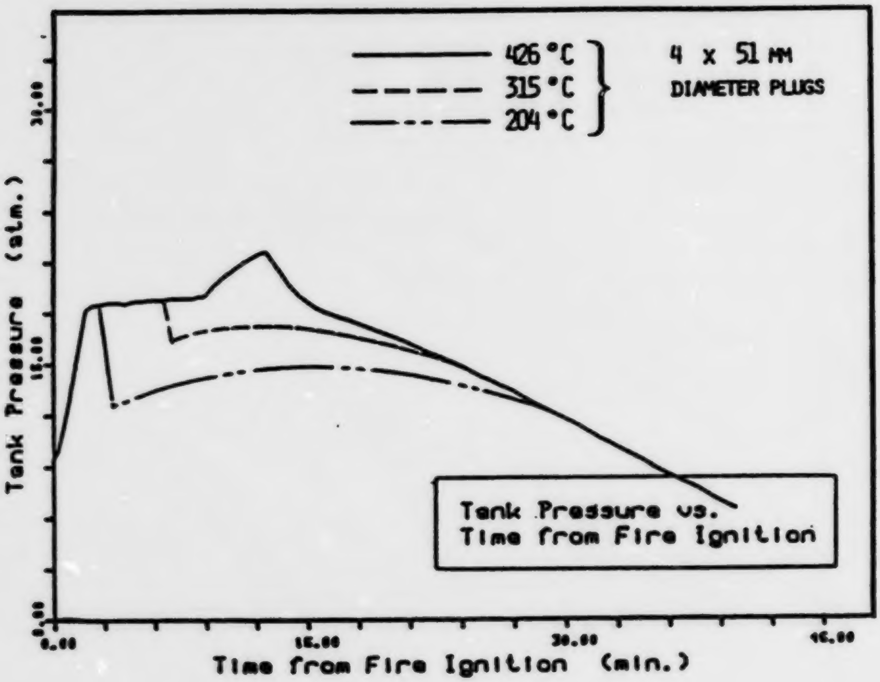

FIGURE 4-9 PREDICTED TANK PRESSURES FOR TANKS EQUIPPED WITH FUSIBLE PLUGS WITH DIFFERENT MELTING TEMPERATURES, EXPOSED TO AN ENGULFING FIRE

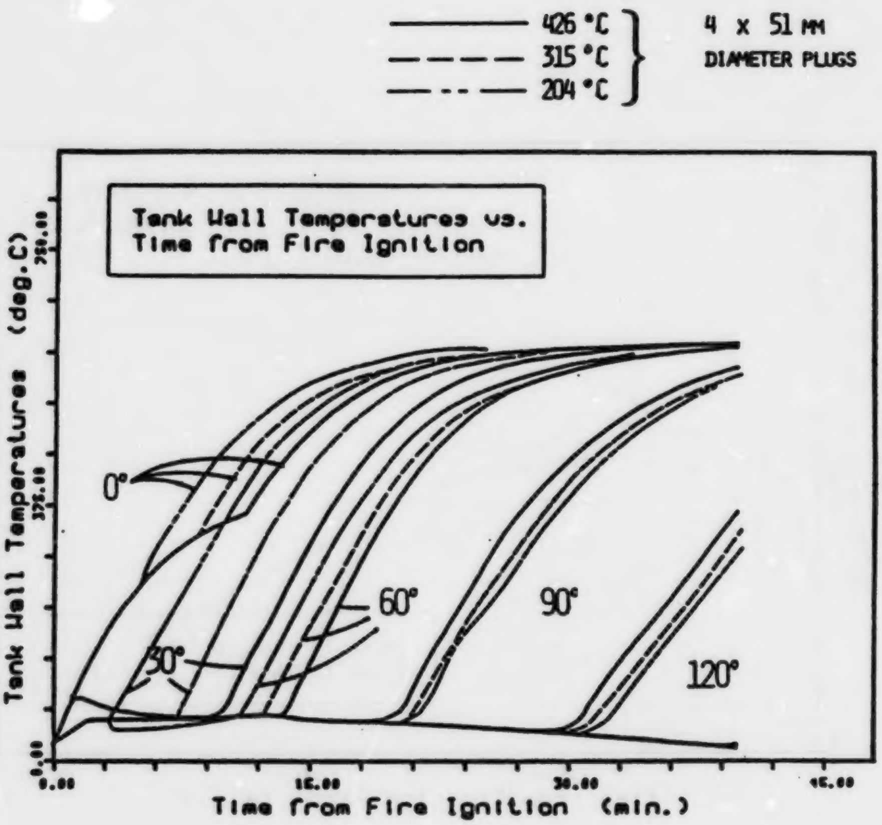

FIGURE 4-10 PREDICTED TANK WALL TEMPERATURES FOR TANKS EQUIPPED WITH FUSIBLE PLUGS WITH DIFFERENT MELTING TEMPERATURES, EXPOSED TO AN ENGULFING FIRE

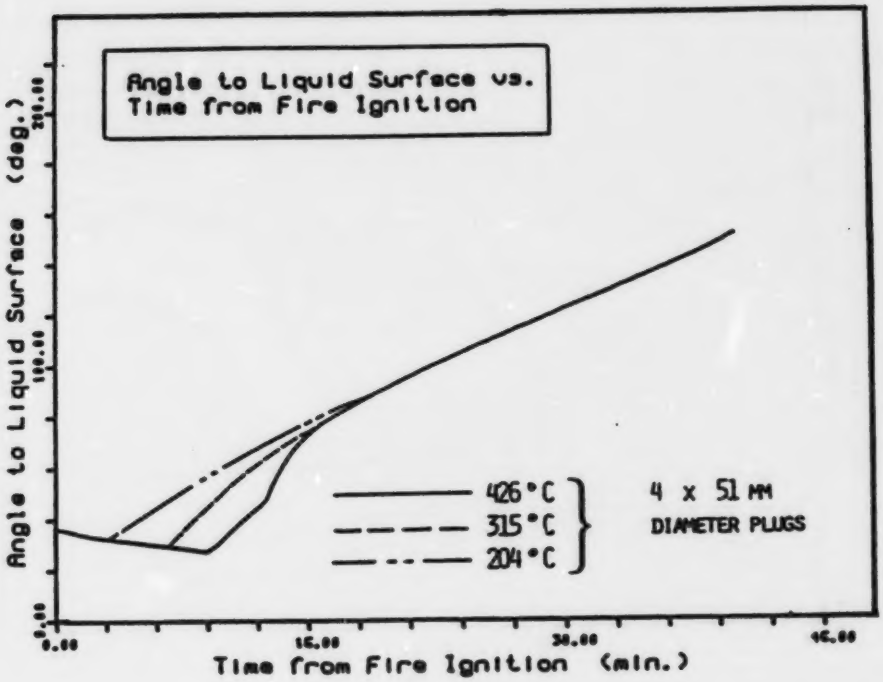

FIGURE 4-11 PREDICTED LIQUID LEVEL FOR TANKS EQUIPPED WITH FUSIBLE PLUGS WITH DIFFERENT MELTING TEMPERATURES, EXPOSED TO AN ENGULFING FIRE

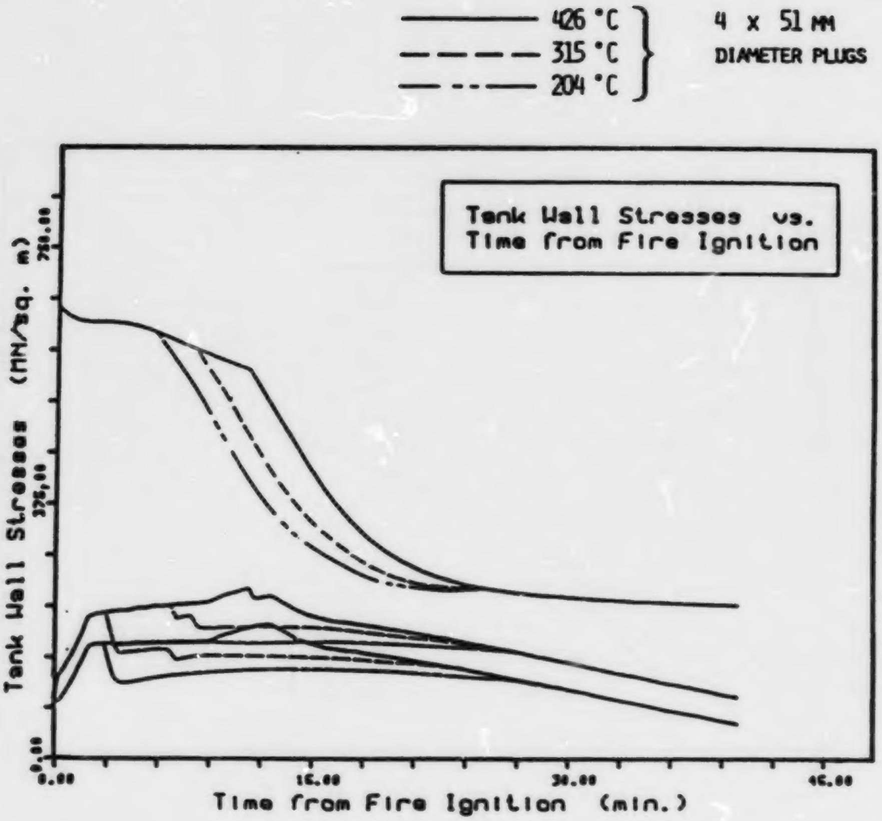

FIGURE 4-12 PREDICTED TANK WALL STRESSES AND TANK WALL MATERIAL STRENGTHS FOR TANKS EQUIPPED WITH DIFFERENT NUMBERS OF FUSIBLE PLUGS, EXPOSED TO AN ENGULFING FIRE

until the point where the fusible plugs melt. This was also seen in the previous figure that showed the predicted tank pressure. Once the fusible plugs melt and material is vented through the devices, the wall temperatures are affected because the lading is vented more rapidly to the atmosphere. This results in earlier break times for the temperatures near the bottom of the tank.

Figure 4-7 presents the predicted liquid level for the different cases considered. As can be seen from the figure, once the fusible plugs open there is a sudden increase in the rate at which the liquid level drops. However, the rate at which lading is vented from the tank eventually is reduced, and becomes almost identical to that for the case with the lowest number of fusible plugs. This can be explained as follows, as the tank pressure drops the rate at which lading is vented also drops. Therefore, by increasing the number of fusible plugs, one decreases the pressure at the same time one increases the total orifice area. The result of these two parameters being varied results in a cancelling out of the effectiveness of the fusible plugs. Therefore, this is another indication of the law of diminishing returns with regard to the number of fusible plugs used. It appears from the figure, that four fusible plugs are as good as twelve fusible plugs in terms of emptying the tank in a given period of time.

Figure 4-8 presents the predicted tank wall stresses and tank wall material strength for the different cases considered. As can be clearly seen from the figure, the fusible plugs have little effect on the material strength of the tank wall. This is because the peak tank wall temperatures are unaffected by the presence of the fusible plugs and it is these temperatures that determine the weakest point in the tank wall. The other two curves in the figure show the tank wall stresses at the inner and outer fibres of the tank wall. As can be clearly seen from the figure, the tank wall stresses are significantly reduced when the fusible plug is opened. This is because the tank pressure has been reduced and it is the tank pressure that is the determining factor in the tank wall stresses. Once again, the law of diminishing returns is clearly indicated in the predicted results. There seems to be little advantage in increasing the number of fusible plugs above 8.

Case #2 Fusible Plugs of Different Melting Temperatures:

Figure 4-9 presents the predicted tank pressures for the different cases considered. As can be clearly seen from the figure, the tank response up until the point where the fusible plugs open is identical to that of an unprotected tank-car. The cases where the plugs melt out at lower temperatures show rapid drops in the tank pressure when the fusible plugs open. As expected, the fusible plugs with the lowest melting temperatures come into play earliest. Eventually, the tank pressures for the three different cases become equal as can be seen from the figure.

Figure 4-10 presents the predicted tank wall temperatures for the different cases considered. As can be seen from the figure, the tank wall temperatures are significantly affected by the different melting temperatures of the fusible plugs. However, the fusible plugs do not affect the peak wall temperatures which affect the strength of the tank. The only apparent affect is a shifting of the temperature break times along the time axis.

Figure 4-11 presents the predicted liquid level for the different cases considered. As can be seen from the figure, the case with the lowest melting temperature plugs shows an earlier break in the rate at which the liquid level drops. However, as time goes on, the rate at which the liquid levels drop all become equal for the different cases considered. The ultimate time to empty does not appear to be affected by the melting temperature of the plugs. Therefore, there does not appear to be any advantage in reducing the melting temperature of the plugs. In fact, lower melting temperature plugs increase the risk of accidental or unwanted plug openings.

Figure 4-12 presents the predicted tank wall stresses and tank wall material strength for the different cases considered. As can be seen from the figure, there is actually a larger drop in the material strengths of the tank wall, for the lower melting temperature plugs. This is an unwanted side effect of the earlier fusible plug opening times for the lower melting temperature plugs. Because the lower melting temperature plugs open earlier, the time at which wall areas are exposed to vapour is earlier. The lower melting temperature plugs also result in an earlier drop in the tank wall stresses due to the drop in the tank pressure. However, eventually, the tank wall stresses for all the cases become equal.

In summary, there appears to be little advantage in reducing the melting temperature of fusible plugs. As mentioned earlier, there is actually a detrimental effect caused by lower melting temperatures because the risk of accidental or unwanted plug melting is increased for the lower temperature plugs. It appears, that a reasonably high melting temperature plug, with temperature limits based on tank material strengths is reasonable.

4.3 EXPLOSAFE EQUIPPED TANK

This section presents the results of a number of simulations involving a full-scale tank protected with the thermal protection system known as Explosafe. Two series of simulations were performed to show the effects of varying the installation of the material.

The first series of simulations consider the case where the annular thickness of the Explosafe material is varied for a fixed orientation of the material. The second series considered a fixed thickness, but the material orientation was varied. The orientation of the Explosafe is important because its thermal properties are anisotropic (they vary with direction). The thickness of the Explosafe is important from the standpoint of the thermal effectiveness of the installation, and of course the economics of the installation (the thicker the annular layer the higher the cost of the installation). The orientation of the Explosafe only effects the thermal effectiveness of the installation.

Case #1 The Effect of Varying the Annular Thickness

This series of simulations considered three different thicknesses of the Explosafe annulus - 51 mm, 102 mm, and 152 mm. The properties of the Explosafe were assumed to be identical to those used in the 1/5 scale tests conducted at Suffield. In all cases the Explosafe was oriented so that its highest thermal conductivity was parallel with the tank radius, and the second highest conductivity was oriented parallel with the circumference of the tank. This orientation is optimum if the Explosafe effect is caused by a fin effect, as it appears to be, based on simulations (see Case 2).

Figure 4-13 presents the predicted tank pressure for the different cases considered. As can be seen from the Figure, varying the annular thickness of the Explosafe material does not appear to effect the tank pressurization

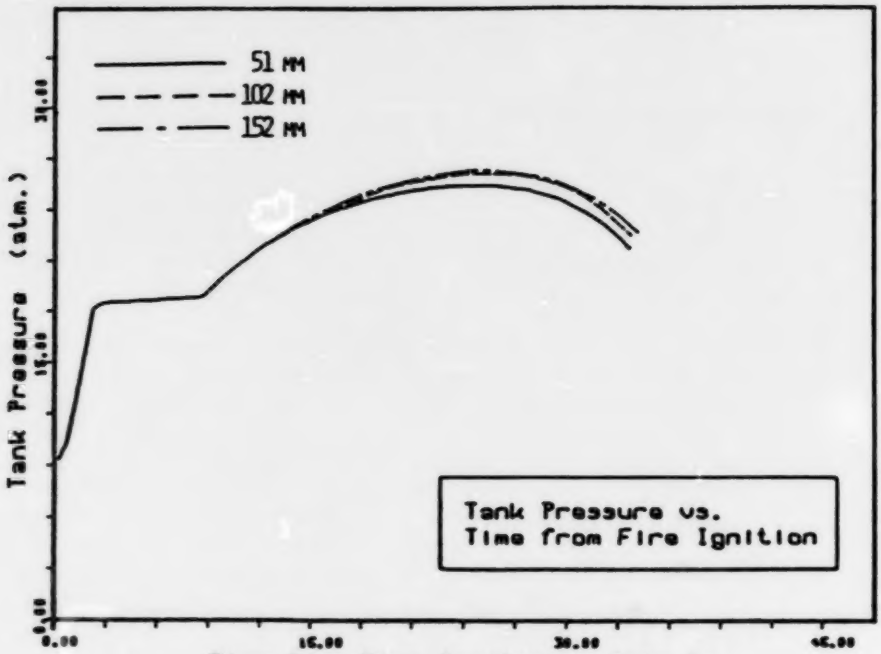

FIGURE 4-13 PREDICTED TANK PRESSURES FOR TANKS EQUIPPED WITH EXPLOSAFE OF DIFFERENT ANNULAR THICKNESSES, EXPOSED TO AN ENGULFING FIRE

significantly. Increasing the thickness increases the peak tank pressure slightly because of the fact that the Explosafe material will tend to increase the heat transfer from the inner surface of the tank wall. This, of course will increase the total heat flux to the lading, and hence the tank pressure increases.

Figure 4-14 presents the predicted tank wall temperatures for the different cases considered. As can be seen from the figure, the wall temperatures are affected by the variations in the annular thickness of the Explosafe. However, the effects on the wall temperatures are not large. As can be seen from the figure, there is little difference between the wall temperatures for the 102 mm and the 152 mm cases, and this indicates that there is little or no benefit to increase the thickness of the annulus above 102 mm.

Figure 4-15 presents the predicted liquid level for the different cases considered. Once again, it is clear from the figure that increasing the Explosafe thickness above 102 mm does not effect the response of the tank significantly.

Figure 4-16 presents the predicted tank wall stresses and material strengths for the different cases considered. In terms of tank wall stresses, the simulation results indicate that the wall stresses are actually increased by the thicker Explosafe because of the fact that the tank peak pressures are slightly higher for these cases. However, the tank wall material strengths (which are governed by the wall temperatures) are higher for the cases with the increased thickness of the Explosafe. The net result is that increasing the Explosafe thickness reduces the chance of thermally induced rupture of the tank wall. However, the benefits from increasing the Explosafe annulus from 102 mm to 152 mm are very small.

In summary, the simulation results indicate the increasing annular thickness of Explosafe above approximately 102 mm does not significantly increase the thermal effectiveness of the thermal protection system. From an economic standpoint, the optimum thickness of the Explosafe is the minimum thickness required for adequate thermal protection. Based on the simulations conducted, the practical limit in terms of effectiveness (the thickness beyond which incremental benefits are small) is approximately 102 mm. However, whether or not this thickness is actually adequate for the purposes of thermal

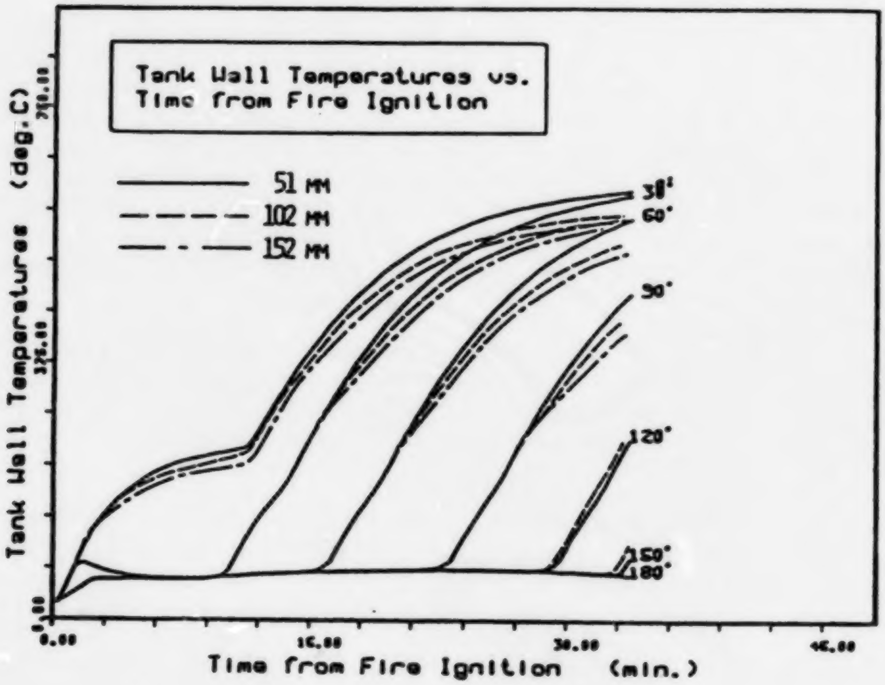

FIGURE 4-14 PREDICTED TANK WALL TEMPERATURES FOR TANKS EQUIPPED WITH EXPLOSAFE OF DIFFERENT ANNULAR THICKNESSES, EXPOSED TO AN ENGULFING FIRE

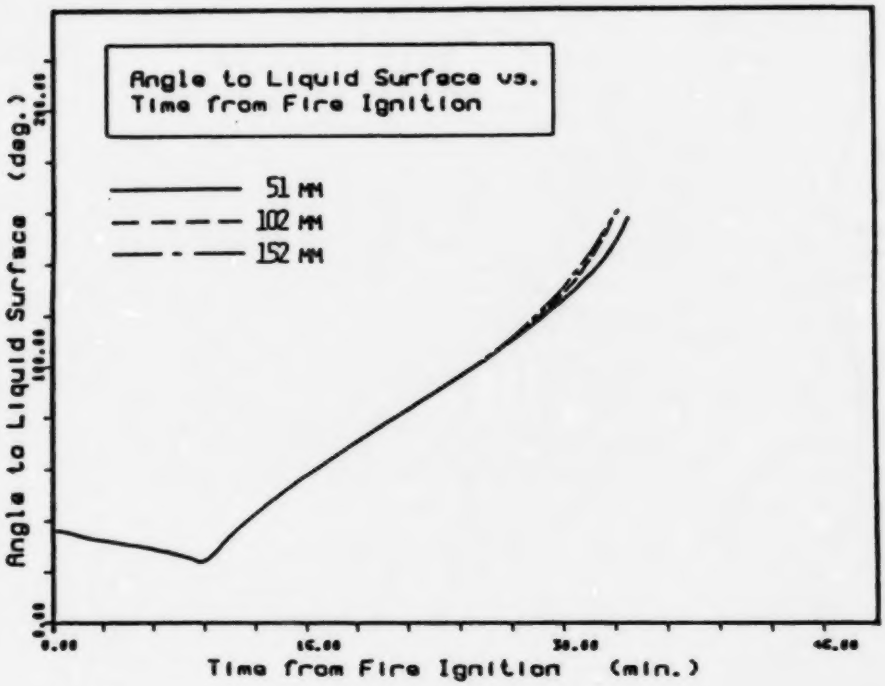

FIGURE 4-15 PREDICTED LIQUID LEVEL FOR TANKS EQUIPPED WITH EXPLOSAFE OF DIFFERENT ANNULAR THICKNESSES, EXPOSED TO AN ENGULFING FIRE

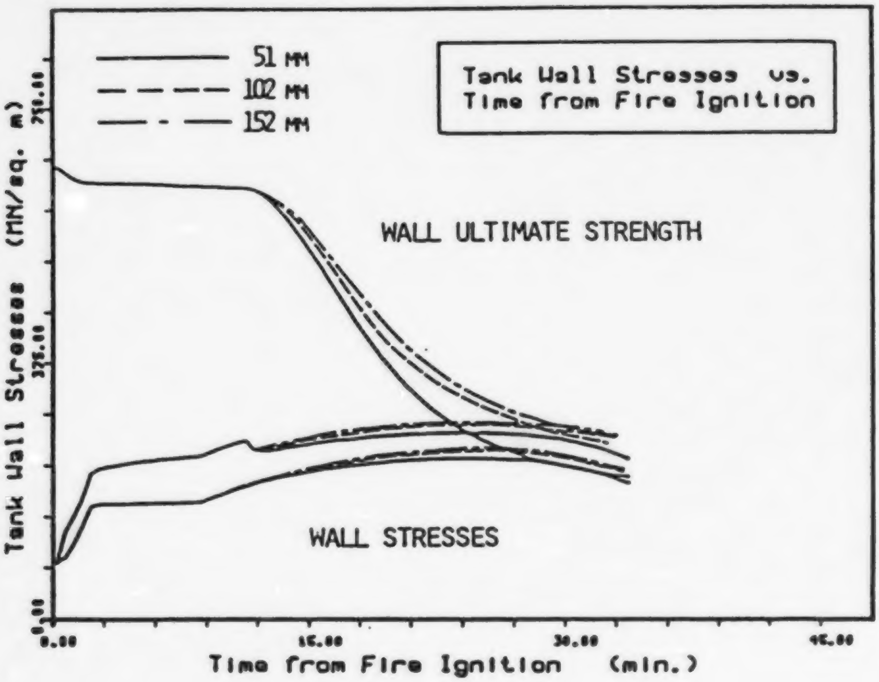

FIGURE 4-16 PREDICTED TANK WALL STRESSES AND TANK WALL MATERIAL STRENGTHS FOR TANKS EQUIPPED WITH EXPLOSAFE OF DIFFERENT ANNULAR THICKNESSES, EXPOSED TO AN ENGULFING FIRE

protection is another question. The simulations indicate that the tank ruptures, or at least comes very close to rupture, for all the Explosafe thicknesses considered.

Case #2 The Effects of Varying the Orientation

This series of simulations were performed to investigate the effect of varying the orientation of the Explosafe material. As mentioned above, the orientation of the Explosafe is important because of its anisotropic thermal properties.

In total, six different cases were considered. The following definitions of the three principal axes of the Explosafe were used.

Direction 1: axial direction of maximum thermal conductivity.

Direction 2: axial direction of intermediate thermal conductivity.

Direction 3: axial direction of minimum thermal conductivity.

The six simulations conducted are described as follows based on the above definitions of the principal axes:

Run A : 1 radial, 2 circumferential
Run B : 1 radial, 3 circumferential
Run C : 2 radial, 1 circumferential
Run D : 2 radial, 3 circumferential
Run E : 3 radial, 2 circumferential
Run F : 3 radial, 1 circumferential

The radial direction refers to the direction parallel to the tank radius, and the circumferential direction refers to the direction parallel to the tank circumference. Only two tank reference axes are considered because the tank-car model is 2-dimensional (i.e., no axial gradients are accounted for, and therefore the Explosafe orientation relative to the tank axis is irrelevant). In all cases the Explosafe annular thickness was set at 102 mm.

Figure 4-17 presents the predicted tank pressures for the different cases considered. As can be seen from the figure, the runs where the Explosafe is oriented with its maximum thermal conductivity parallel with the tank radius

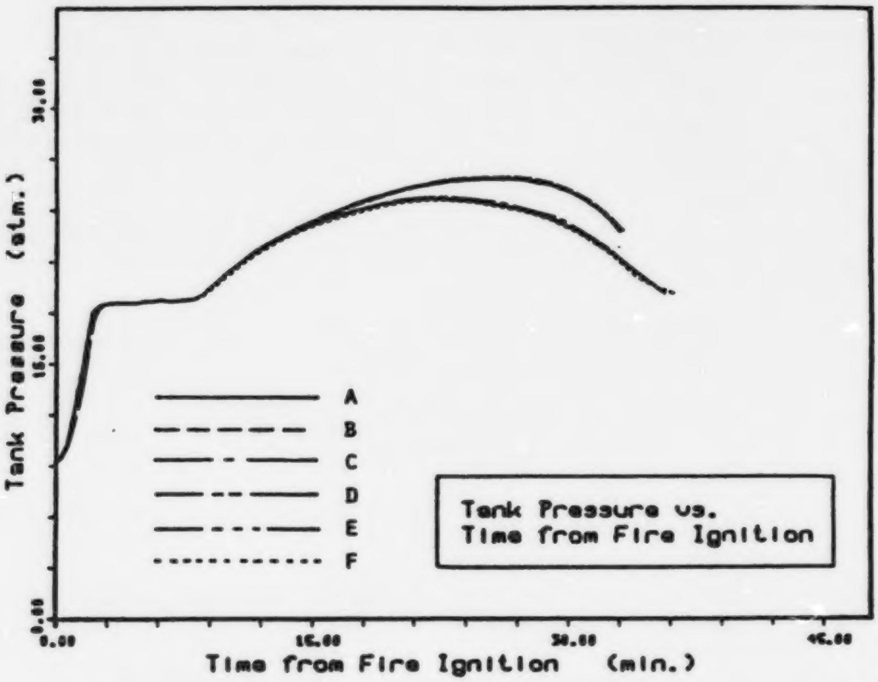

FIGURE 4-17 PREDICTED TANK PRESSURES FOR TANKS EQUIPPED WITH EXPLOSAFE OF DIFFERENT ORIENTATION, EXPOSED TO AN ENGULFING FIRE

resulted in the highest tank pressures. This indicates that the Explosafe is resulting in a higher heat transfer to the lading resulting in a higher tank pressure. All of the remaining cases resulted in lower tank pressures. It appears that there is very little difference between cases C, D, E and F.

Figure 4-18 presents the predicted tank wall temperatures for the different cases considered. As can be clearly seen from the Figure, cases A and B resulted in the lowest wall temperatures. Cases C, D, E and F resulted in significantly higher wall temperatures. Once again there appears to be very little difference between cases A and B and between cases C, D, E and F. The reason for the results as shown in Figure 4-18 are that the Explosafe is acting as a fin, i.e., the Explosafe is drawing the heat radially away from the wall into the lading. The Explosafe is not conducting the heat circumferentially away from the vapour wetted wall regions into the liquid lading.

Figure 4-19 presents the predicted liquid level for the different cases considered. As can be seen from the figure, the liquid dropped most rapidly for cases A and B because of the increased heat flux to the lading caused by the fin effect of the Explosafe.

Figure 4-20 presents the predicted tank wall stresses and material strengths for the different cases considered. As can be seen, the simulation results show that the Explosafe orientation has a significant effect on the predicted failure of the tank. For cases A and B the model predicts that the tank will narrowly escape failure, whereas the model predicts failure for the remaining cases. This clearly shows that the best orientation of the Explosafe is with the maximum thermal conductivity parallel to the tank radius.

In summary, the model simulations indicate that the best orientation for the Explosafe is with its maximum thermal conductivity parallel with the tank radius. It appears from the results that the orientations of the remaining axes are not significant. However, based on simple heat transfer considerations, it is believed that the minimum thermal conductivity axis should be parallel with the axis of the tank. When the maximum thermal conductivity is oriented in the radial direction, the tank experiences slightly higher peak pressures, and lower peak wall temperatures, with the net effect being a drop in the probability of tank rupture.

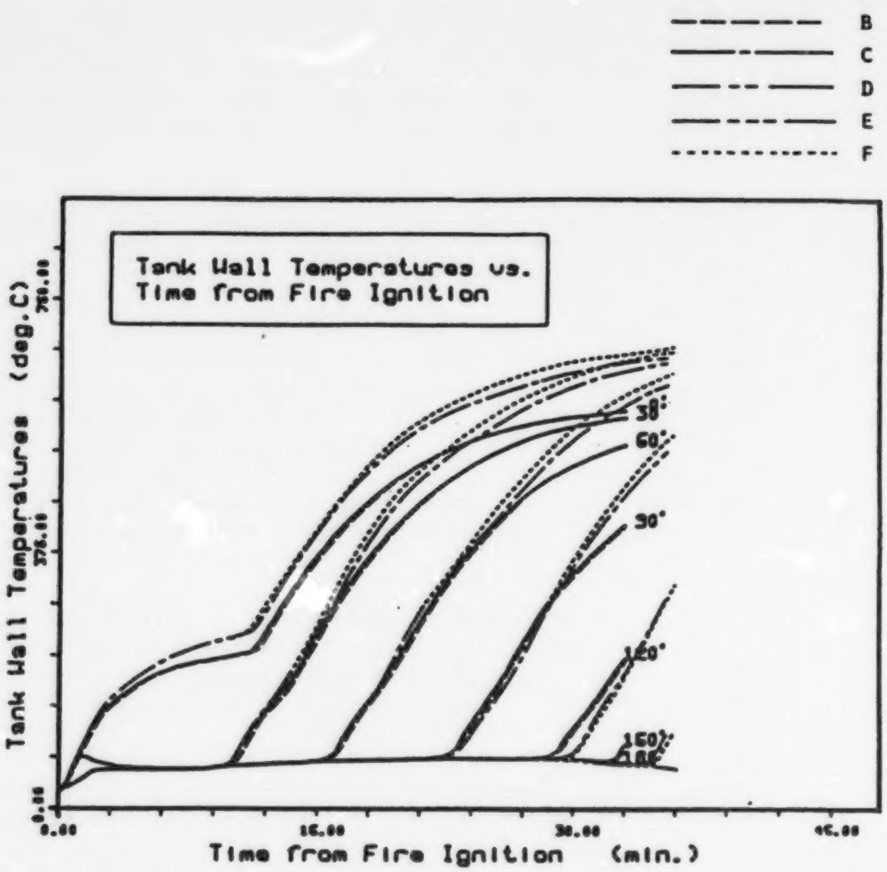

FIGURE 4-18 PREDICTED TANK WALL TEMPERATURES FOR TANKS EQUIPPED WITH EXPLOSAFE OF DIFFERENT ORIENTATIONS, EXPOSED TO AN ENGULFING FIRE

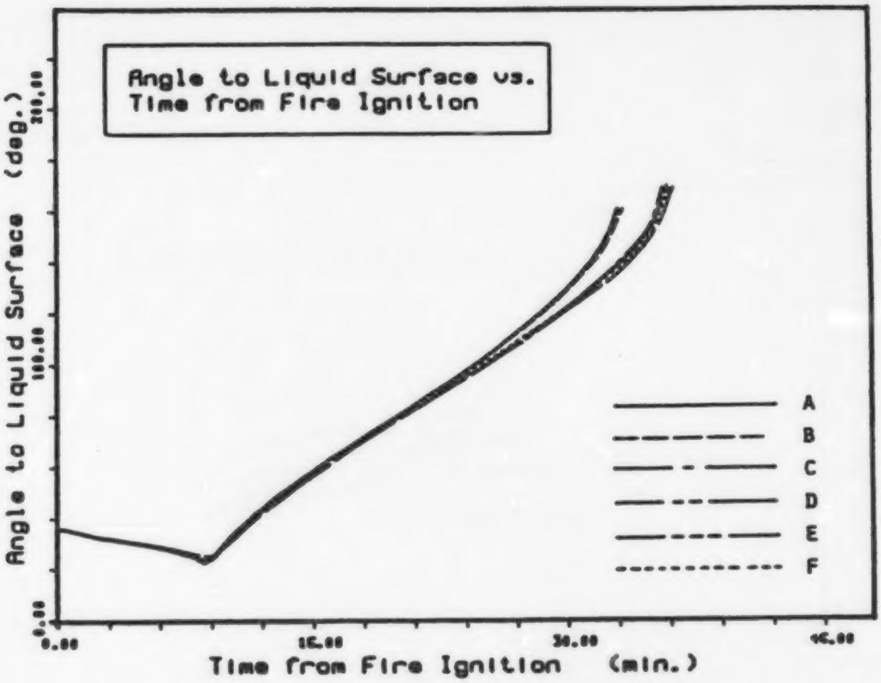

FIGURE 4-19 PREDICTED LIQUID LEVEL FOR TANKS EQUIPPED WITH EXPLOSAFE OF DIFFERENT ORIENTATIONS, EXPOSED TO AN ENGULFING FIRE

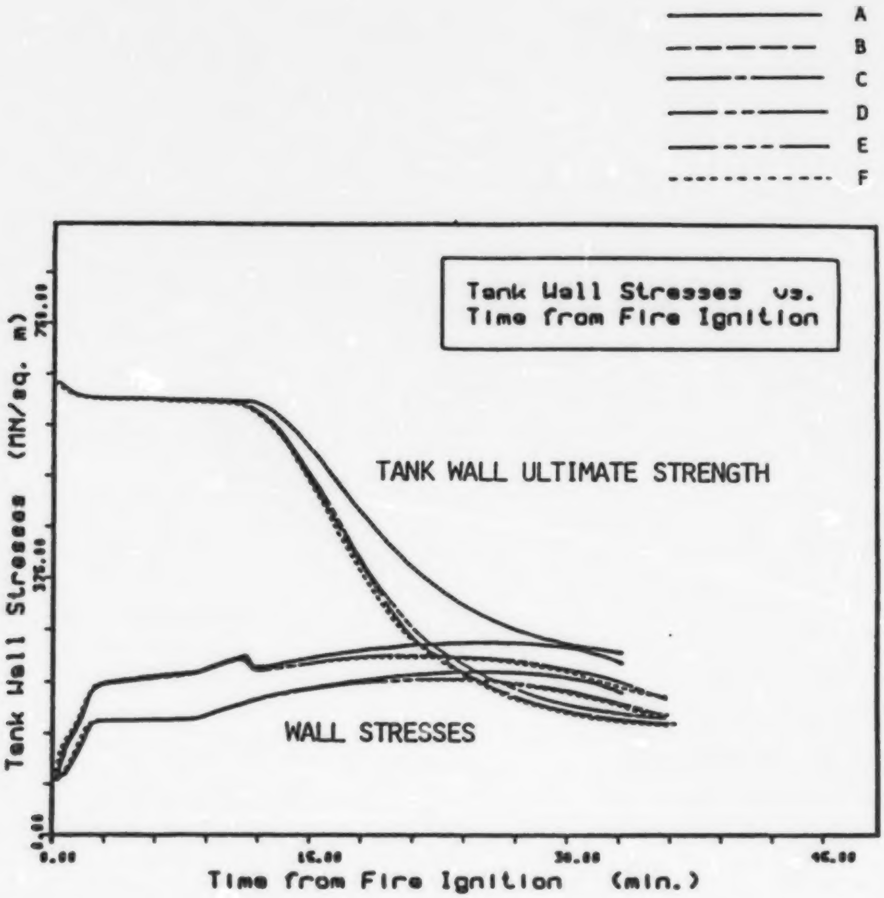

FIGURE 4-20 PREDICTED TANK WALL STRESSES AND TANK WALL MATERIAL STRENGTHS FOR TANKS EQUIPPED WITH EXPLOSAFE OF DIFFERENT ORIENTATIONS, EXPOSED TO AN ENGULFING FIRE

Based on the two cases considered, it appears that the most efficient Explosafe design would involve a 102 mm thick annulus of Explosafe with the material oriented with the maximum thermal conductivity parallel to the tank radius and the minimum thermal conductivity parallel with the axis of the tank. However, even with this thickness and orientation, the tank will come dangerously close to failure when exposed to an engulfing fire. Therefore, based on the results of simulations, Explosafe does not appear to be a viable thermal protection system when used without thermal insulation.

5.0 FUTURE WORK

A great deal of effort has gone into the development of the tank-car thermal analysis computer program. However, the tank-car model should still be considered as being a research tool, and not a packaged piece of software ready for release to the general engineering community. The tank-car model requires further refinement, enhancement, and validation. Further validation can only take place when new data is made available from fire tests.

The following sections highlite some possible future work related to the development of the tank-car model. First, the major model weaknesses are identified and briefly discussed, and recommended model modifications are listed. In addition, areas that require further data are highlited.

5.1 OVERALL MODEL WEAKNESSES

As stated earlier, the tank-car model consists of a number of sub-models which represent the various processes taking place in and around the tank-car. Presently, there are some weaknesses in the formulation of some of these sub-models. The most important weaknesses in the overall tank-car model are associated with the following:

1. The thermodynamic process sub-model,
2. The inner surface heat transfer sub-model,
3. The relief valve flow sub-model, and
4. The thermal insulation degradation sub-model.

The thermodynamic process model is weak because it relies on two empirical constants. It has been assumed, that these constants remain the same for all different tank-car scales and configurations. However, there is no data to support this conclusion other than the results of the validation to-date. Ideally, the thermodynamic process sub-model should be based entirely on the fundamentals of thermodynamics, and no empirical constants should have to be set. For the tank-car model to become a versatile design tool, further work is necessary on the thermodynamic process sub-model.

Presently, the inner surface heat transfer sub-model is based on rather simplistic correlations from experimentally obtained heat transfer data. Ideally, the internal surface heat transfer coefficients should be calculated from the basic governing equations. Several such analyses are available in the open literature, and only minor modification is required before they could be implemented in the tank-car model.

Presently, the relief valve flow analysis can only account for choked vapour flow through the relief valve, and frozen liquid flow through the relief valve. It is a distinct weakness that the model cannot account for two-phase flow through the relief valve. However, there does not exist at present an adequate analysis to represent all possible flow conditions through the relief valve. In addition, the present relief valve model is a simplistic, steady state model. Therefore the dynamic action of the valve is not accounted for. Temperature effects on the action of the relief valve (changing set pressures, etc.) are also not accounted for. Therefore, further work, both experimental and theoretical is necessary before a comprehensive relief valve flow analysis can be performed.

Finally, the remaining weakness in the program is the lack of data on the thermal degradation of available thermal insulations. The present tank-car model can account for thermal degradation of thermal insulating materials, however, data is needed on how these thermal insulating layers degrade, and how this degradation affects the insulation thickness, and the insulation thermal conductivity. As well, many thermal insulating materials such as intumescent paints provide transpiration cooling effects. These transpiration cooling effects should also be accounted for in the tank-car thermal analysis program.

The above mentioned program weakness do not render the existing tank-car model useless. As can be seen from the model validation of a previous section, the tank-car model is still quite accurate in predicting the thermal response of a tank-car exposed to either engulfing or torch-type fire environments. However, if the tank-car model is eventually to become a design tool for the general engineering community, these weaknesses should be studied further.

5.2 RECOMMENDED MODEL MODIFICATIONS

Of the model weaknesses discussed in the previous section, the most important are the thermodynamic process sub-model, and the relief valve flow analysis sub-model.

It is recommended that the tank-car model be modified to include a more comprehensive thermodynamic process model. However, it is anticipated that such a model would require considerable computer effort. Therefore, it is also recommended that the present thermodynamic process model remain in the overall tank-car program. At run time, the user would specify which thermodynamic sub-model is to be used, and therefore if a quick calculation is required the user would specify the existing thermodynamic process model. However, if a run is to be performed on a tank-car scale and configuration where no present data exists for validation, then one would be well advised to use the comprehensive thermodynamic model.

It is recommended that the relief valve flow analysis in the overall tank-car model be modified so that it can account for two-phase flow through the relief valve. This is extremely important, because the accurate prediction of venting rates is important for determining the liquid level in the tank, and hence the tank wall temperatures. It is essential, that the tank wall temperatures and the liquid level be known accurately so that the ultimate tank failure or time to empty can be predicted.

6.0 CONCLUSIONS

Based on the results of the model validation process, the following conclusions have been made:

1) Results of the validation show that the model is quite accurate at predicting the response of unprotected and protected tank-cars exposed to engulfing, and torch fire environments. A high degree of confidence can be used when modelling the following situations:

   - unprotected horizontal tanks (full or fifth-scale)
   - unprotected horizontal rolled tanks (full or fifth-scale)
   - insulated tanks (full or fifth-scale, using simple insulations only)
   - Explosafe equipped (using annular configurations only, fifth-scale)

2) The tank-car model's two-dimensional torch analysis can be compared directly to the U.S. DOT Transportation Test Center Torch Fire Test Facility.

Based on the results of the program sensitivity analysis the following conclusions can be made:

1) The tank-car model can be very sensitive to the time step used depending on the type of protection being simulated. For unprotected tanks the time step should be kept below 30 seconds. For insulated tanks incorporating steel jacket, the time step should be below 5 seconds. For all other tank-car protection scenarios, the time step should be kept below 5 seconds.

2) The model predictions for a tank-car thermal response are extremely sensitive to the fire conditions. This includes both the fire temperatures (pool fire or torch fire) and the fire radiating characteristics (effective flame emissivity)

Based on the results on the example simulations, the following conclusions can be made:

1) Thermal insulation appears to be an excellent thermal protection against accidental impingement as long as the thermal insulating layer is not damaged.

2) Fusible plugs (or temperature sensitive valves) also appeared to be effective means of reducing the risk of accidental ruptures of tanks.

3) Based on the simulations performed, Explosafe does not appear to be an effective thermal protection for full-size tank-cars. The Explosafe provides a very limited amount of thermal protection in the form of slightly reduced wall temperatures.

The results of the model validation, sensitivity analysis, and example simulations, show that the tank-car model is a powerful tool for predicting the thermal response of tank-cars to accidental fire impingement. However, there are still weaknesses with the overall model and these weaknesses should be studied. Most important areas requiring further examination are:

- The thermodynamic process sub-model, which is the most important sub-model used to predict the thermal response of the tank,
- The pressure relief valve submodel which is extremely important in accurately predicting the rate at which the lading is vented, and
- The thermal insulation sub-model which represents the thermal degradation of the thermal insulating layers.

REFERENCES

1) User Documentation for the Rail Tank-Car Thermal Analysis Program (TNKCAR), Davis Engineering, C83-29, March 1985.

2) Validation and Testing of the Tank-Car Thermal Analysis Program, Davis Engineering C83-29, March 1985.

3) Railroad Tank Car Safety Research and Test Project; Phase II Report on Full-Scale Fire Tests. AAR-RPI, RA-11-6-31, AAR-R-201, US6 AFI 17-75 ENG(BK).

4) Appleyard, R.D.; Testing and Evaluation of the Explosafe System as a Method of Controlling the Boiling Liquid Expanding Vapour Explosion, Transport Canada Report No. TP 2740, 1980.

5) Fire Test to Study the Significance of a Burning Relief Valve Flare from a Tank Car Engulfed in Fire, Davis Engineering, C83-29, March 1985.

6) Anderson, C. et al; Railroad Tank-Car Fire Test: Test #6, Ballistic Research Laboratories, US DOT FRA-OR&D 75-36, 1973.

7) Anderson, C. et al; Railroad Tank-Car Fire Test: Test #7, Ballistic Research Laboratories, US DOT FRA-OR&D 75-37, 1973.

8) Railroad Tank Car Safety Research and Test Project; Phase II Report on Analysis of 1/5 Scale Fire Tests, RPI-AAR, RA-11-5-26, US6 AFI 17-73 ENG(PF).

9) Railroad Tank Car Safety Research and Test Project; Phase II Report on Analysis of 1/5 Scale Fire Test Data, RPI-AAR, RA-11-2-14, US6 AFI 17-72 ENG(PF).

10) Anderson, C.E.; Rail Tank Car Safety by Fire Protection, 6th International Fire Protection Seminar, 1982.

11) Roberts, A.F., Cutler, D.P., Billinge, K.; Fire Engulfment Trials with LPG Tanks with a Range of Fire Protection Methods, Proc. 4th Int. Symposium on Loss Prevention and Safety Promotion in Process Industries, Vol. 3, Chem. Eng. Symposium Series, 1982.

12) Schulz-Forberg, B., Droste, B., Charlett, H.; Failure Mechanisms of Propane Tanks Under Thermal Stresses Including Fire Engulfment, Transport and Storage of LPG and LNG, pp. 295-305.

TP 6693E

VALIDATION AND TESTING OF THE TANK-CAR THERMAL ANALYSIS PROGRAM (TNKCAR)

Prepared For:

TRANSPORTATION DEVELOPMENT CENTRE
TRANSPORT CANADA

Prepared By:

DAVIS ENGINEERING LIMITED
CONSULTING ENGINEERS
OTTAWA, ONTARIO

DE File No: C83-29

Library and Information Centre /
Centre de Documentation (GSLA)
RECEIVED – REÇU LE
JAN 9 1986
Transport Canada / Transports Canada

MARCH 1985

THE CONTENTS OF THIS REPORT REFLECT THE VIEWS OF THE CONTRACTOR AND NOT NECESSARILY THE OFFICIAL VIEWS OR POLICIES OF THE TRANSPORTATION DEVELOPMENT CENTRE

REPORT DOCUMENTATION FORM

1. Transport Canada Report No. TP 6693E	2. TDC Project No. 4917/4918	3. Recipient's Catalogue No.

4. Title and Subtitle **Validation and Testing of the Rail Tank-Car Thermal Analysis Program (TNKCAR)**	5. Report Date March, 1985 6. Performing Organization Report No. C83-29
7. Author(s) A.M. Birk	8. Transport Canada File No D1465-302-6-5
9. Performing Organization Name and Address Davis Engineering Limited 1260 Old Innes Road Ottawa, Ontario K1B 3V3	10. DSS File No. 11SD.T8200-2-2575 11. DSS or Transport Canada Contract No OSD83-00086
12. Sponsoring Agency Name and Address Transportation Development Centre Complexe Guy Favreau, West Tower 200 Dorchester Blvd. W., Suite 601 Montreal, P.Q. H2Z 1X4	13. Type of Report and Period Covered Technical 14. Sponsoring Agency Code 4917/4918
15. Supplementary Notes	16 TDC Project Officer D.W. Dibble

17 Abstract

A computer model of a rail tank-car exposed to external fire impingement (engulfing fire or torch fire) has been developed, tested and validated. The computer model is capable of simulating the response of a full sized or fifth scale tank, and can predict tank pressure, wall temperatures, lading temperatures, relief valve flow rates, liquid level and tank failure, all as functions of time from fire ignition. The computer model can account for a wide range of tank orientations, tank fill conditions and tank thermal protection (insulation, radiation shielding, fusible plugs, Explosafe).

The report presents the results of program sensitivity analyses, and program validation using available tank-car fire test data. A number of simulations of thermally protected tanks (including Explosafe) are also presented.

18. Key Words Rail tank-car, Explosafe, thermal computer model	19. Distribution Statement A limited number of copies are available from the sponsoring agency

20. Security Classification (of this report) un-classified	21. Security Classification (of this page) un-classified	22. No. of Pages	23. Price - 289

TDC CDT 79-005

FORMULE DE DOCUMENTATION POUR RAPPORT

1. Nº du rapport Transports Canada

TP 6693E

2. Nº de l'étude — CDT

4917/4918

3. Nº de catalogue du destinataire

4. Titre et sous-titre

Validation and Testing of the Rail Tank-Car Thermal Analysis Program (TNKCAR)

5. Date du rapport

mars 1985

6. Nº du rapport de l'organisme exécutant

C83-29

7. Auteur(s)

A.M. Birk

8. Nº de dossier Transports Canada

D1465-302-6-5

9. Nom et adresse de l'organisme exécutant

Davis Engineering Ltd.
1260 Old Innes Road
Ottawa, Ontario
K1B 3V3

10 Nº de dossier — ASC

11SD.T8200-2-2575

11. Nº de contrat — ASC ou Transports Canada

OSD83-00086

12. Nom et adresse de l'organisme parrain

Centre de développement des transports (CDT)
Complexe Guy Favreau, tour ouest
200 o., boul. Dorchester, Suite 601
Montréal, Qué H2Z 1X4

13 Genre de rapport et période visée

technique

14 Code de l'organisme parrain

4917/4918

15. Remarques additionnelles

16 Agent de projet — CDT

D.W. Dibble

17 Resume

Ce rapport rend compte de l'étude et de la validation d'un modèle de simulation par ordinateur figurant le comportement d'un wagon-citerne sous l'action de flammes extérieures : incendie enveloppant ou flammes à effet torche. Ce modèle permet de simuler le comportement d'un wagon-citerne en vraie grandeur ou à l'échelle 1/5, prenant en compte les facteurs suivants : pressions intérieures, température des parois et de la cargaison, débit d'écoulement par les soupapes de sûreté, niveau de remplissage et tenue des parois, dont il indique l'évolution dans le temps à partir de la mise à feu. Il permet en outre de grandes variations dans les conditions de remplissage, l'orientation et les types de protection thermique à l'intérieur du récipient : isolation, écran anti-rayonnement, tampons fusibles, système Explosafe.

Le rapport rend compte également des résultats de l'analyse de sensibilité et de validation des programmes, utilisant les données tirées d'essais antérieurs. Il décrit en outre des simulations faites sur des wagons-citernes protégés de diverse façons, y compris le système Explosafe.

18 Mots-clés

Wagon-citerne, Explosafe, modèle mathématique, simulation thermique

19. Diffusion

Le CDT dispose d'un nombre limité d'exemplaires.

20 Classification de securité (de ce rapport)

non-classifié

21 Classification de securité (de cette page)

non-classifiée

22 Nombre de pages

23. Prix

– 289

CDT TDC 79-005

TABLE OF CONTENTS

Page

1.0 INTRODUCTION 1
- 1.1 Project Background 1
- 1.2 Technical Background 2
- 1.3 Objectives 4
- 1.4 Summary 5

2.0 VALIDATION 8
- 2.1 Validation Method 8
- 2.2 Available Data 9
  - 2.2.1 TDC Tests 10
  - 2.2.2 AAR - RPI Tests 42
    - 2.2.2.1 Full-Scale Tests 43
    - 2.2.2.2 One Fifth Scale Tests 63
- 2.3 Validation Results 86
  - 2.3.1 Simulations of TDC Tests 86
    - 2.3.1.1 Enigma 89
    - 2.3.1.2 Nova 94
  - 2.3.2 AAR - RPI Tests 100
    - 2.3.2.1 RAX-201 100
    - 2.3.2.2 RAX-202 107
    - 2.3.2.3 Test # 3 114
    - 2.3.2.4 Test # 6 120
    - 2.3.2.5 Test # 7 127
    - 2.3.2.6 Torch Fire Tests 133

3.0 PROGRAM SENSITIVITY ANALYSIS 138
- 3.1 Time Step Sensitivity 138
  - 3.1.1 Unprotected Tank 139
  - 3.1.2 Insulated Tank 144
- 3.2 Fire Condition Sensitivity 157
  - 3.2.1 Pool Fire Temperature Sensitivity 157
  - 3.2.2 Pool Fire Absorption Coefficient Sensitivity 162
  - 3.2.3 Torch Fire Temperature Sensitivity 167
  - 3.2.4 Torch Fire Application Angle Sensitivity 177
- 3.3 Tank Roll Sensitivity 193
- 3.4 Tank Pitch Sensitivity 199

TABLE OF CONTENTS (Cont'd)

Page

3.4.1 Variation in Pitch Angle 200
3.4.2 Variations in Location of Test Section 210
3.5 Lading Type Sensitivity 219

4.0 EXAMPLE SIMULATIONS 235
4.1 Insulated Tank 235
4.2 Tank with Fusible Plugs 241
4.3 Explosafe Equipped Tank 253

5.0 FUTURE WORK 266
5.1 Overall Model Weaknesses 266
5.2 Recommended Model Modification 268

6.0 CONCLUSIONS 269

REFERENCES 271

LIST OF FIGURES (Cont'd)

FIGURE PAGE

2-20 Measured Tank Inner Wall Temperatures (right side) from 'Enigma' Test (from Reference (3)) 37
2-21 Measured Tank Inner Wall Temperatures (left side) from 'Engima' Test (from Reference (3)) 38
2-22 Measured Lading Temperatures from 'Enigma' Test (from Reference (3)) 39
2-23 Key to Thermocouple Locations in 'Enigma' Test (from Reference (3)) 40
2-24 Measured Tank Pressure from AAR-RPI Test #8 (from Reference (2)) 46
2-25 Measured Lading Temperatures for AAR-RPI Test #8 (from Reference (2)) 48
2-26 Key to Thermocouple Locations for AAR-RPI Test #8 (from Reference (2)) 49
2-27 Measured Wall Temperatures from AAR-RPI Test #8 (from Reference (2)) 51
2-28 Measured Wall Temperatures from AAR-RPI Test #8 (from Reference (2)) 52
2-29 Measured Tank Pressure from AAR-RPI Test #9 (from Reference (2)) 55
2-30 Measured Lading Temperatures for AAR-RPI Test #9 (from Reference (2)) 57
2-31 Key to Thermocouple Locations for AAR-RPI Test #9 58
2-32 Measured Wall Temperatures from AAR-RPI Test #9 (from Reference (2)) 59
2-33 Measured Wall Temperatures from AAR-RPI Test #9 (from Reference (2)) 61
2-34 Estimated Liquid Level from AAR-RPI Test #9 (from Reference (2)) 62
2-35 Measured Tank Pressure from AAR-RPI Test #3 (from Reference (6)) 65
2-36 Measured Wall Temperatures from AAR-RPI Test #3 (from Reference (6)) 66
2-37 Estimated Liquid Level from AAR-RPI Test #3 (from Reference (6)) 67
2-38 Measured Fire Temperature in AAR-RPI Test #6 (from Reference (4)) 69
2-39 Measured Tank Pressure from AAR-RPI Test #6 (from Reference (4)) 70
2-40 Measured Lading Temperatures from AAR-RPI Test #6 (from Reference (4)) 71

LIST OF FIGURES (Cont'd)

FIGURE PAGE

2-41 Key to Thermocouple Locations for AAR-RPI Test #6 (from Reference (4)) 72
2-42 Measured Wall Temperatures for AAR-RPI Test #6 (from Reference (4)) 74
2-43 Estimated Liquid Level for AAR-RPI Test #6 (from Reference (4)) 75
2-44 Measured Fire Temperature in AAR-RPI Test #7 (from Reference (5)) 76
2-45 Measured Tank Pressure from AAR-RPI Test #7 (from Reference (5)) 78
2-46 Measured Lading Temperatures from AAR-RPI Test #7 (from Reference (5)) 79
2-47 Key to Thermocouple Location for AAR-RPI Test #7 (from Reference (5)) 80
2-48 Measured Wall Temperatures for AAR-RPI Test #7 (from Reference (5)) 81
2-49 Estimated Liquid Level for AAR-RPI Test #7 (from Reference (5)) 82
2-50 Results from Bare Plate Torch Fire Tests (from Reference (8)) 84
2-51 Results from Tank-Car Torch Fire Tests (from Reference (8)) 85
2-52 Results from Insulated Plate Torch Fire Tests (from Reference (8)) 87
2-53 Results from Insulated Tank-Car Torch Fire Tests (from Reference (8)) 88
2-54 Predicted Tank Pressure and Measured Tank Pressure for Enigma Test (from Reference (3)) 90
2-55 Predicted Wall Temperatures and Measured Wall Temperatures from Enigma Tests (from Reference (3)) 91
2-56 Predicted Liquid Level and Measured Liquid Level for Enigma Test (from Reference (3)) .. 92
2-57 Predicted Tank Wall Stresses and Material Strength for Enigma Test (from Reference (3)) 93
2-58 Predicted Tank Pressure and Measured Tank Pressure for Nova Test (from Reference (3)) . 95
2-59 Predicted Wall Temperatures and Measured Wall Temperatures from Nova Test (from Reference (3)) 96
2-60 Predicted Liquid Level and Measured Liquid Level for Nova Test (from Reference (3)) 97

LIST OF FIGURES (Cont'd)

FIGURE PAGE

2-61 Predicted Tank Wall Stresses and Material Strength for Nova Test (from Reference (3)) . 98

2-62 Predicted Tank Pressure and Measured Tank Pressure for RAX-201 Test (from Reference (2)) 101

2-63 Predicted Wall Temperatures and Measured Wall Temperatures from RAX-201 Test (from Reference (2)) 102

2-64 Predicted Liquid Level and Measured Liquid Level for RAX-201 Test (from Reference (2)) . 103

2-65 Predicted Tank Wall Stresses and Material Strength for RAX-201 Test 104

2-66 Predicted Tank Pressure and Measured Tank Pressure for RAX-202 Test (from Reference (2)) 108

2-67 Predicted Wall Temperatures and Measured Wall Temperatures from RAX-202 Test (from Reference (2)) 109

2-68 Predicted Liquid Level and Measured Liquid Level for RAX-202 Test (from Reference (2)) . 110

2-69 Predicted Tank Wall Stresses and Material Strength for RAX-202 Test 111

2-70 Predicted Tank Pressure and Measured Tank Pressure for Test #3 (from Reference (6)) ... 115

2-71 Predicted Wall Temperatures and Measured Wall Temperatures from Test #3 (from Reference (6)) 116

2-72 Predicted Liquid Level and Measured Liquid Level for Test #3 (from Reference (6)) 117

2-73 Predicted Tank Wall Stresses and Material Strength for Test #3 118

2-74 Predicted Tank Pressure and Measured Tank Pressure for Test #6 (from Reference (4)) ... 122

2-75 Predicted Wall Temperatures and Measured Wall Temperatures from Test #6 (from Reference (4)) 123

2-76 Predicted Liquid Level and Measured Liquid Level for Test #6 (from Reference (4)) 124

2-77 Predicted Tank Wall Stresses and Material Strength for Test #6 125

2-78 Predicted Tank Pressure and Measured Tank Pressure for Test #7 (from Reference (5)) ... 128

LIST OF FIGURES (Cont'd)

FIGURE PAGE

2-79 Predicted Wall Temperatures and Measured Wall Temperatures from Test #7 (from Reference (5)) 129
2-80 Predicted Liquid Level and Measured Liquid Level for Test #7 (from Reference (5)) 130
2-81 Predicted Tank Wall Stresses and Material Strength for Test #7 131
2-82 Predicted Tank Pressure for Torch Fire Test . 134
2-83 Predicted Wall Temperatures and Measured Wall Temperatures from Torch Fire Test (from Reference (8)) 135
2-84 Predicted Liquid Level for Torch Fire Test .. 136
2-85 Predicted Tank Wall Stresses and Material Strength for Torch Fire Test 137

3-1 Predicted Tank Pressure for Unprotected Tank from Program Runs Using Different Time Steps 140
3-2 Predicted Wall Temperatures for Unprotected Tank from Program Runs Using Different Time Steps 141
3-3 Predicted Liquid Level for Unprotected Tank from Program Runs Using Different Time Steps 142
3-4 Predicted Tank Wall Stresses and Material Strength for Unprotected Tank from Runs Using Different Time Steps 143
3-5 Predicted Tank Pressure for Insulated Tank (with steel jacket) from Program Runs Using Different Time Steps 146
3-6 Predicted Wall Temperatures for Insulated Tank (with steel jacket) from Program Runs Using Different Time Steps 147
3-7 Predicted Liquid Level for Insulated Tank (with steel jacket) from Program Runs Using Different Time Steps 148
3-8 Predicted Tank Wall Stresses and Material Strength for Insulated Tank (with steel jacket) from Program Runs Using Different Time Steps 149
3-9 Predicted Tank Pressure for Insulated Tank (no steel jacket) from Program Runs Using Different Time Steps 152

LIST OF FIGURES (Cont'd)

FIGURE PAGE

3-10 Predicted Wall Temperatures for Insulated Tank (no steel jacket) from Program Runs Using Different Time Steps 153
3-11 Predicted Liquid Level for Insulated Tank (no steel jacket) from Program Runs Using Different Time Steps 154
3-12 Predicted Tank Wall Stresses and Material Strength for Insulated Tank (no steel jacket) from Program Runs Using Different Time Steps 155
3-13 Predicted Tank Pressure for an Unprotected Tank from Program Runs Using Different Pool Fire Temperatures 158
3-14 Predicted Wall Temperatures for Unprotected Tank from Program Runs Using Different Pool Fire Temperatures 159
3-15 Predicted Liquid Level for Unprotected Tank from Program Runs Using Different Pool Fire Temperatures 160
3-16 Predicted Tank Wall Stresses and Material Strength for Unprotected Tank from Program Runs Using Different Pool Fire Temperatures 161
3-17 Sketch of Pool Fire Showing Idealized Shape Used in Pool Fire Heat Transfer Model (from Reference (1)) 164
3-18 Variation in Fire Transmissivity Around Tank for Different Flame Absorption Coefficients (from Reference (1)) 165
3-19 Variation in Radiant Heat Transfer Around a Tank for Different Flame Absorption Coefficients (from Reference (1)) 166
3-20 Predicted Tank Pressures for a Tank Exposed to Torch Fires of Different Temperatures ... 169
3-21 Predicted Tank Wall Temperatures for a Tank Exposed to a Torch Fire (Torch Temperature 1090 deg. C) 170
3-22 Predicted Tank Wall Temperatures for a Tank Exposed to a Torch Fire (Torch Temperature 980 deg. C) 171
3-23 Predicted Tank Wall Temperatures for a Tank Exposed to a Torch Fire (Torch Temperature 870 deg. C) 172

LIST OF FIGURES (Cont'd)

FIGURE PAGE

3-24 Predicted Tank Wall Temperatures for a Tank Exposed to a Torch Fire (Torch Temperature 760 deg. C) 173

3-25 Predicted Liquid Levels for a Tank Exposed to Torch Fires of Different Temperatures 175

3-26 Predicted Tank Wall Stresses and Tank Wall Material Strengths for a Tank Exposed to Torch Fires of Different Temperatures 176

3-27 Predicted Tank Pressures for a Tank Exposed to Torch Fires Applied at Different Angles from the Tank Top-Dead-Centre 179

3-28 Predicted Tank Wall Temperatures for a Tank Exposed to a Torch Fire (applied at 0 Degrees from TDC) 180

3-29 Predicted Tank Wall Temperatures for a Tank Exposed to a Torch Fire (applied at 30 Degrees from TDC) 181

3-30 Predicted Tank Wall Temperatures for a Tank Exposed to a Torch Fire (applied at 60 Degrees from TDC) 182

3-31 Predicted Tank Wall Temperatures for a Tank Exposed to a Torch Fire (applied at 90 Degrees from TDC) 183

3-32 Predicted Tank Wall Temperatures for a Tank Exposed to a Torch Fire (applied at 120 Degrees from TDC) 184

3-33 Predicted Liquid Levels for a Tank Exposed to Torch Fires of Different Temperatures 186

3-34 Predicted Tank Wall Stresses and Tank Wall Material Strengths for a Tank Exposed to a Torch Fire (applied at 0 degrees from TDC) .. 188

3-35 Predicted Tank Wall Stresses and Tank Wall Material Strengths for a Tank Exposed to a Torch Fire (applied at 30 degrees from TDC) . 189

3-36 Predicted Tank Wall Stresses and Tank Wall Material Strengths for a Tank Exposed to a Torch Fire (applied at 60 degrees from TDC) . 190

3-37 Predicted Tank Wall Stresses and Tank Wall Material Strengths for a Tank Exposed to a Torch Fire (applied at 90 degrees from TDC) . 191

LIST OF FIGURES (Cont'd)

FIGURE PAGE

3-38 Predicted Tank Wall Stresses and Tank Wall Material Strengths for a Tank Exposed to a Torch Fire (applied at 120 degrees from TDC) 192

3-39 Predicted Tank Pressures for Unprotected Tanks with Different Roll Angles Exposed to an Engulfing Fire 194

3-40 Predicted Tank Wall Temperatures for Unprotected Tanks with Different Roll Angles Exposed to an Engulfing Fire 195

3-41 Predicted Liquid Levels for Unprotected Tanks with Different Roll Angles Exposed to an Engulfing Fire 196

3-42 Predicted Tank Wall Stresses and Tank Wall Material Strengths for Unprotected Tanks with Different Roll Angles Exposed to Engulfing Fires 197

3-43 Predicted Tank Pressures for Unprotected Tanks with Different Pitch Angles Exposed to an Engulfing Fire 201

3-44 Predicted Tank Wall Temperatures for a Pitched, Unprotected Tank Exposed to an Engulfing Fire (pitch angle = 0 deg.) 203

3-45 Predicted Tank Wall Temperatures for a Pitched, Unprotected Tank Exposed to an Engulfing Fire (pitch angle = 10 deg.) 204

3-46 Predicted Tank Wall Temperatures for a Pitched, Unprotected Tank Exposed to an Engulfing Fire (pitch angle = 20 deg.) 205

3-47 Predicted Tank Wall Temperatures for a Pitched, Unprotected Tank Exposed to an Engulfing Fire (pitch angle = 40 deg.) 206

3-48 Predicted Tank Wall Temperatures for a Pitched, Unprotected Tank Exposed to an Engulfing Fire (pitch angle = 60 deg.) 207

3-49 Predicted Tank Wall Temperatures for a Pitched, Unprotected Tank Exposed to an Engulfing Fire (pitch angle = 90 deg.) 208

3-50 Sketch Showing how the Liquid Level Changes for Different Pitch Angles 209

3-51 Predicted Liquid Levels for Unprotected Tanks with Different Pitch Angles Exposed to an Engulfing Fire 211

LIST OF FIGURES (Cont'd)

FIGURE PAGE

3-52 Predicted Tank Wall Stresses and Tank Wall Material Strengths for Unprotected Tanks with Different Pitch Angles Exposed to Engulfing Fires 212
3-53 Predicted Tank Pressure for an Unprotected Tank Pitched 30 Degrees 214
3-54 Predicted Tank Wall Temperatures for a Pitched, Unprotected Tank Exposed to an Engulfing Fire (test section at mid plane, tank pitch = 30 degrees) 215
3-55 Predicted Tank Wall Temperatures for a Pitched, Unprotected Tank Exposed to an Engulfing Fire (test section at 1/3 L from tank top, tank pitch = 30 degrees) 216
3-56 Predicted Tank Wall Temperatures for a Pitched, Unprotected Tank Exposed to an Engulfing Fire (test section at 1/6 L from tank top, tank pitch = 30 degrees) 217
3-57 Predicted Liquid Levels at Different Axial Positions in a Pitched, Unprotected Tank Exposed to an Engulfing Fire (Pitch = 30 degrees) 218
3-58 Predicted Tank Wall Stresses and Tank Wall Material Strengths at Different Axial Positions in a Pitched, Unprotected Tank Exposed to an Engulfing Fire (Pitch = 30 degrees) 220
3-59 Predicted Tank Pressures for Unprotected Tanks Filled with Different Ladings, Exposed to an Engulfing Fire 222
3-60 Predicted Tank Wall Temperatures for an Unprotected Tank Containing Propane, Exposed to an Engulfing Fire 224
3-61 Predicted Tank Wall Temperatures for an Unprotected Tank Containing Butane, Exposed to an Engulfing Fire 225
3-62 Predicted Tank Wall Temperatures for an Unprotected Tank Containing Pentane, Exposed to an Engulfing Fire 226
3-63 Predicted Tank Wall Temperatures for an Unprotected Tank Containing Propylene, Exposed to an Engulfing Fire 227

LIST OF FIGURES (Cont'd)

FIGURE PAGE

3-64 Predicted Liquid Levels for Unprotected Tanks Containing Different Ladings, Exposed to Engulfing Fires 229

3-65 Predicted Tank Wall Stresses and Tank Wall Material Strengths for an Unprotected Tank Containing Propane, Exposed to an Engulfing Fire 230

3-66 Predicted Tank Wall Stresses and Tank Wall Material Strengths for an Unprotected Tank Containing Butane, Exposed to an Engulfing Fire 231

3-67 Predicted Tank Wall Stresses and Tank Wall Material Strengths for an Unprotected Tank Containing Pentane, Exposed to an Engulfing Fire 232

3-68 Predicted Tank Wall Stresses and Tank Wall Material Strengths for an Unprotected Tank Containing Propylene, Exposed to an Engulfing Fire 233

4-1 Predicted Tank Pressure for Insulated Tanks with Different Thicknesses of Insulation, Exposed to an Engulfing Fire 236

4-2 Predicted Tank Wall Temperatures for Insulated Tanks with Different Thicknesses Insulation, Exposed to an Engulfing Fire 237

4-3 Predicted Liquid Level for Insulated Tanks with Different Thicknesses of Insulation, Exposed to an Engulfing Fire 238

4-4 Predicted Tank Wall Stresses and Tank Wall Material Strengths for Insulated Tanks with Different Thicknesses of Insulation, Exposed to an Engulfing Fire 239

4-5 Predicted Tank Pressures for Tanks Equipped with Different Numbers of Fusible Plugs, Exposed to an Engulfing Fire 243

4-6 Predicted Tank Wall Temperatures for Tanks Equipped with Different Numbers of Fusible Plugs, Exposed to an Engulfing Fire 244

4-7 Predicted Liquid Level for Tanks Equipped with Different Numbers of Fusible Plugs, Exposed to an Engulfing Fire 245

LIST OF FIGURES (Cont'd)

FIGURE PAGE

4-8 Predicted Tank Wall Stresses and Tank Wall Material Strengths for Tanks Equipped with Different Numbers of Fusible Plugs, Exposed to and Engulfing Fire 246
4-9 Predicted Tank Pressures for Tanks Equipped with Fusible Plugs with Different Melting Temperatures, Exposed to an Engulfing Fire .. 247
4-10 Predicted Tank Wall Temperatures for Tanks Equipped with Fusible Plugs with Different Melting Temperatures, Exposed to an Engulfing Fire 248
4-11 Predicted Liquid Level for Tanks Equipped with Fusible Plugs with Different Melting Temperatures, Exposed to an Engulfing Fire .. 249
4-12 Predicted Tank Wall Stresses and Tank Wall Material Strengths for Tanks Equipped with Different Numbers of Fusible Plugs, Exposed to an Engulfing Fire 250
4-13 Predicted Tank Pressures for Tanks Equipped with Explosafe of Different Annular Thicknesses, Exposed to an Engulfing Fire ... 254
4-14 Predicted Tank Wall Temperatures for Tanks Equipped with Explosafe of Different Annular Thicknesses, Exposed to an Engulfing Fire ... 256
4-15 Predicted Liquid Level for Tanks Equipped with Explosafe of Different Annular Thicknesses, Exposed to an Engulfing Fire ... 257
4-16 Predicted Tank Wall Stresses and Tank Wall Material Strengths for Tanks Equipped with Explosafe of Different Annular Thicknesses, Exposed to an Engulfing Fire 258
4-17 Predicted Tank Pressures for Tanks Equipped with Explosafe of Different Orientation, Exposed to an Engulfing Fire 260
4-18 Predicted Tank Wall Temperatures for Tanks Equipped with Explosafe of Different Orientations, Exposed to Engulfing Fire 262
4-19 Predicted Liquid Level for Tanks Equipped with Explosafe of Different Orientations, Exposed to an Engulfing Fire 263
4-20 Predicted Tank Wall Stresses and Tank Wall Material Strengths for Tanks Equipped with Explosafe of Different Orientations, Exposed to an Engulfing Fire 264

1.0 INTRODUCTION

This report documents the work conducted in Phases III and IV of the Tank-Car Thermal Computer Model Project, DSS Contract Number 0SD-00086. The report presents the results of the Tank-Car Model validation and testing.

The Tank-Car Thermal Computer Model was developed to study the effectiveness of new concepts in thermal protection for rail tank-cars. The technical details of this computer model are presented in the TDC report entitled, "User Documentation for the Rail Tank-Car Thermal Analysis Program (TNKCAR)".

As part of the validation of the model, a fire test was conducted to study the effects of a burning relief valve flare on a tank-car that is already engulfed in fire. The results of this fire test are presented in a separate TDC report entitled, "Fire Test to Study the Significance of a Burning Relief Valve Flare from a Tank-Car Engulfed in Fire".

The following sections present the results of a program validation, and sensitivity analysis. Example simulations of tank-cars equipped with different thermal protection systems are also presented.

1.1 PROJECT BACKGROUND

As already mentioned, this report presents the results of Phases III and IV of the Tank-Car Thermal Computer Model Project (TCTCMP). The overall project was organized into four phases as follows:

Phase I : Model Formulation
Phase II : Model Development
Phase III: Model Validation
Phase IV : Model Simulations

This project was part of the Tank Car Explosion Protection Program (TCEPP). The overall objective of the TCEPP is, "to develop a technique of protecting rail, road and marine tankers carrying LPG, from the dangers of thermally induced ruptures and explosions".

The original intended use of the Tank-Car Thermal Computer Model was to analyze the results of partial scale experimental test programs conducted to understand the role of Explosafe[1] in protecting tank-cars from accidental fire impingement.

---

[1] Explosafe Division, Vulcan Industrial Packaging ...

Explosafe is an expanded aluminum mesh which is placed within the tank-car. The original belief was that the Explosafe, made of high thermal conductivity aluminum, would conduct heat from the hot regions within the tank (the vapour space and contacting wall areas) to the cooler regions (the liquid space and contacting wall areas), thereby reducing the risk of thermally induced ruptures caused by local weakening of the tank wall by thermal degradation. Further details of the Explosafe explosion suppression system can be found in the report entitled, "Explosafe Installation Design", Transport Canada report TP4398E.

The model was also to be used to identify preferred design alternatives of the Explosafe explosion suppression system for full-sized rail tank-cars, and to compare the performance of these systems with conventional protection systems.

1.2 TECHNICAL BACKGROUND

The TCTCM is a digital computer based model capable of simulating the response of a rail tank-car and its lading, to the conditions of external fire impingement (engulfing fire or 2-dimensional torch). The program is written in the FORTRAN IV programing language, and is presently running on a PDP 11/23 mini computer under the RT-11 operating system, and on the DEC VAX 11/780 under the VMS operating system.

The two-dimensional capabilities of the TCTCM have been validated (1) by comparing predictions with experimentally obtained data from previously conducted full and fifth-scale fire tests (2,3). Details of this validation process can be found in Reference (1).

Prior to the development of this model, it was necessary to conduct full or partial scale fire tests on tanks outfitted with candidate thermal protection systems. These tests proved to be very expensive and usually rendered little statistically significant data because of the highly uncontrolled nature of the test fires.

The model can consider several system configurations such as a rolled or pitched attitude of the tank, different fire conditions, different thermal protection schemes, and different ladings. Table 1.1 summarizes the various system configurations which can be considered by the program.

LADING	THERMAL PROTECTION	TANK ORIENTATIONS	FIRE CONDITIONS
propane n-butane n-pentane propylene	thermal insulation (three types) (with/without steel jacket) thermal radiation shielding special pressure relief devices (ie. fusible plugs) 'Explosafe'	variable roll angle variable pitch angle (pseudo 3-D)	engulfing fire 2-D torch fire

TABLE 1-1 SYSTEM CONFIGURATION CONSIDERED IN TNKCAR

The TCTCM is capable of predicting tank pressure, tank wall temperatures, relief valve flow rates, tank fill condition, tank wall stresses and tank wall failure, all as functions of time from fire ignition. The TCTCM is also capable of simulating the effects of a variety of thermal protection devices such as thermal insulation (with/without steel jacket, with/without thermally induced degradation), thermal radiation shielding, special pressure relief devices (fusible plugs or temperatures sensitive valves), and 'Explosafe'. The model can consider a large number of different tank/lading/fire configurations.

The overall tank-car model is made up from a series of sub-models which represent the various processes taking place in and around the tank. These sub-models represent the following processes,

i) flame to tank heat transfer,
ii) heat transfer through the tank wall and associated coverings,
iii) interior surface heat transfer,
iv) pressure relief device operating characteristics,
v) thermodynamic properties of the lading,
vi) thermodynamic process taking place within the tank, and,
vii) wall stresses and material properties.

The TCTCM consists of a main program and a series of subroutines. The main program controls some of the I/O, initializes the variables and matrices, and controls the subroutine calling sequence. The subroutines contain the various process sub-models.

1.3 OBJECTIVES

The objectives of Phases III and IV of the Tank-Car Thermal Computer Model Project were as follows:

i) **Validate the Tank-car Thermal Computer Model (TCTCM) using data available from fire tests and laboratory tests,**

ii) **Perform a sensitivity analysis on the TCTCM to establish the effects of input variables on the model predictive capabilities,**

iii) Perform Simulations on a variety of thermal protection systems, including Explosafe, to investigate the performance of these systems when critical parameters are varied, and

iv) If the assessment of the Explosafe thermal protection system is satisfactory, determine the most effective design configuration of Explosafe for use in full-sized rail tank-cars.

All of the above mentioned project objectives have been achieved.

1.4 SUMMARY

As stated above, all of the project objectives have been achieved. The tank-car model has been validated with available fire test data. A sensitivity analysis has been performed to determine the effects of varying important inputs, and a number of simulations have been performed to show the predicted performance of different thermal protection schemes, including EXPLOSAFE.

The TCTCM validation has included data from a number of tests including full and partial scale pool fire tests and some torch fire tests. The validation results presented in this report are more comprehensive than those shown in Reference (1) because of the use of additional fire test data. The validation presented in this report applies for the enhanced TCTCM which includes the rolled tank capabilities and the pseudo-3D analysis of pitched tanks. The validation presented in Reference (1) only applied to the original 2-D version of the TCTCM.

In addition to the validation resulting from the comparison of model simulations with fire test data, a major model assumption has been validated with the results of a indoor fire test conducted to simulate the effects of a burning relief valve flare on a tank which is already engulfed in fire. Details of this test are presented in Appendix A. The test results support the assumption that the burning relief valve flare has little or no effect on the tank-car when it is already engulfed in fire. This assumption played a major role in the development of the fire heat transfer sub-model.

The results of the validation show that the TCTCM is quite accurate at predicting tank pressure, liquid level and wall temperatures. However, the TCTCM did not accurately predict the time to failure in all cases. This, of course, stems from the fact that tank failure is determined by material properties and these are usually statistically based with some degree of variation from tank to tank. In addition, valve performance also plays a key role in tank failure because of its effect on the rate at which the tank is emptied, and tank-car relief valves are also known to have significant variations from nominal performance characteristics.

In general, for the purposes of comparing different thermal protection systems on an equal basis, the TCTCM is a valuable tool. However, there are parts of the overall model that require some further development such as in the thermodynamic process model, the interior surface heat transfer models, and the valve flow submodels.

The sensitivity analyses showed that the TCTCM is a very flexible tool and its numerical operations remain stable and accurate for a wide range of input. However, users should beware of those inputs that can result in program instabilities and inaccuracies in the simulation results. As expected, the model simulations are extremely sensitive to the external boundary conditions, namely, the fire temperatures and radiating properties. The simulation results are also extremely sensitive to the valve operatings characteristics because these effect the liquid level which dictates how the wall temperatures increase.

The example simulations that were performed show that a number of thermal protection schemes can prolong the life of a tank-car within an engulfing fire or torch fire environment. Some methods increase the tanks survivability by slowing the heating process to maintain lower tank pressures and wall temperatures, others reduce the tank pressure by venting the lading more rapidly, and some act to reduce the wall temperatures in the vapour space by increasing the heat transfer from the tank inner surface in these areas.

The methods which reduce the heat flow to the tank usually involve a thermal insulating layer or radiation shielding, or both. Under the ideal conditions of the simulations, these systems proved to be extremely effective at protecting the tank-car. The only apparent drawback of these methods is that they prolong the time where a nearly full tank remains exposed to fire. A full tank is potentially a bigger bomb.

An example of a system which vents the lading more rapidly involves fusible plugs. These devices work by opening orifices through which the lading can pass. When the fusible plug temperature exceeds some critical value it causes a metallic core to melt and open a flow orifice. Fusible plugs do not affect the heat transfer rate significantly but work by reducing the internal pressure (lower than is possible by a standard relief valve) and by venting the tank contents as rapidly as possible. The advantage of such systems is their ability to empty the tank and thereby remove the explosive charge. However, the disadvantage of these systems stems from the fact that once a fusible plug is opened it cannot be easily closed, and if the fire is quenched the tank will continue to vent the hazardous material into the atmosphere.

The internal protection scheme considered in this study involves the material known as Explosafe. The simulations performed for Explosafe equipped tank-cars show, as expected, that the Explosafe acts by increasing the heat transfer coefficient on the inner surface of the tank wall which is in contact with vapour. This increase in heat flux in these areas results in lower wall temperatures in the vapour space and thereby increases the survivability of a tank. However, this increase in heat flux also results in a slightly higher peak tank pressure which somewhat offsets the positive effects of the reduced wall temperatures.

Of all of the systems considered in the simulations, thermal insulation appears to be the most effective means of thermal protection. Thermal insulation covered with steel jacket is recommended because the steel jacket acts as a radiation shield. Fusible plugs also appear to be effective devices for protecting a tank-car. If the problem associated with the non-reversible nature of fusible plugs can be overcome with a temperature sensitive valve, such devices might be considered as back-up measures to thermal insulation. The Explosafe material did not, based on the simulations conducted, prove to be as effective as thermal insulation or fusible plugs.

The results of the validation, sensitivity analyses, and simulation activities have identified some weaknesses with the overall thermal model. These weaknesses are associated with the thermodynamic process model, the interior surface heat transfer model and the relief flow analyses. Future development of the TCTCM should concentrate on these areas.

2.0 VALIDATION

This chapter presents the results of the validation of the overall tank-car thermal model. In the following sections comparisons are made between available experimental data and model simulations.

2.1 VALIDATION METHOD

Before the tank-car model can be used as a design and development tool, its predictive capabilities must be verified. The purpose of this section is to describe the validation process used.

The sub-models which make up the overall tank-car model were developed using the fundamentals of heat transfer, fluid mechanics, thermodynamics and stress analysis. Each sub-model has been developed to satisfy the governing conservation laws, and these conservation laws in themselves act as one means of verification. For example, the heat balance analysis which models the thermodynamic process taking place within the tank must simultaneously satisfy continuity (conservation of mass), volume (fix tank volume) and energy (heat in minus vented energy equals internal energy rise) relations.

The separate verification and validation of each of the sub-models will not be discussed further here. For further details of the sub-model formulations and verification, the reader is directed to Reference (1). The remainder of this chapter will deal with the validation of the overall model. However, as will be seen in the following pages, the separate verification of the major sub-models is implicit in the overall model validation.

The validation process concentrates on the overall models ability to predict the basic tank conditions which dictate the rupture process. These conditions include, tank pressure, lading temperatures, liquid level, wall temperatures, wall stresses, and wall material strength. With this data it is theoretically possible to predict time to failure or time to empty for the tank. The above data, and much more, are predicted by the tank-car model.

It is not appropriate to present all of the model outputs in the validation process. The main reason for this is that there is no way of validating all of the model predictions because of a lack of experimental data. Therefore, the model outputs have been condensed into four summary plots which present the most significant information. The four summary plots are:

- pressure vs. time
- wall temperature vs. time
- liquid level vs. time
- wall stress and strength vs. time.

These four plots were chosen because they present data in a way that is similar to that used in the presentation of the fifth and full-scale fire test results.

The overall model validation involved the comparison of the four summary plots with experimentally obtained data. The sources of this data will be discussed in the following section.

For the purposes of the validation, the model inputs, such as tank initial fill, lading initial temperature, relief valve size, etc., were chosen to match, as closely as possible, the actual test conditions which existed for a given data set. In some cases where this data was not recorded, some judgement was used to approximate these boundary conditions. However, it should be stressed that model inputs were not varied until the desired outputs were obtained. All constants that are used in the sub-models were left alone during the overall model validation process.

2.2 AVAILABLE DATA

For the purposes of validating the tank-car model, data is required which accurately describes an entire fire event, from start to finish (tank rupture or empty). Therefore, this data must include, as a minimum, the following information:

- tank initial conditions (fill level, lading type, equilibrium temperature and internal pressure).
- tank wall temperatures at various circumferential locations, during the test.

- lading temperatures at various locations in the liquid and vapour (preferably at different vertical locations), during the test.

- tank internal pressure, during the test.

- tank dimensions (length, diameter, wall thickness) and,

- relief valve size and operating range.

In addition to these basic data needs, it is very desirable to have data on the relief valve stem lift, fire temperatures, and liquid level. With the above data, it is possible to simulate the test conditions with the tank-car model and then compare the model predictions with the actual experimental test results.

To obtain the desired data, a literature search was conducted. The scope of the literature search was confined to data relating to the response of rail tank-cars, or pressure vessels, exposed to external fire impingement.

The most useful data obtained so far has been that from fifth-scale tests conducted in Canada (3), full and fifth-scale engulfing fire tests and torch fire tests conducted in the U.S. (2, 4, 5, 6, 7, 8), and some smaller scale tests conducted in the UK (9) and the FRG (10).

Of this very useful data only the results from the Canadian and U.S. tests have been used directly in the validation of the model. Although the tests conducted in the UK and FRG were highly successful, the tank scales and the extent of the instrumentation resulted in data that was not easily reproducible by the tank-car model.

There is, of course, other data available on the thermal response of tanks exposed to external fire impingement. There have been a number of fire tests conducted with small scale tanks filled with propane or water. There have also been a number of small scale laboratory type tests, the most extensive being those conducted at the University of New Brunswick in Canada (11, 12, 13). The data from the above mentioned tests have not been used directly in the validation process. The reasons for not using the data varied from test to test, and included; a lack of recorded dated, scaling problems, test fluids other than those considered by the tank-car model, and undocumented heat input conditions. In many cases the data collection in these tests concentrated on one aspect of the event, such as boiling in the liquid, or relief valve flow, and as a result, there was not enough data to truely validate the overall model. For example, it is a simple matter to predict wall temperatures or tank pressures by themselves, it is much more difficult to predict pressure, lading temperatures, wall temperatures, liquid level and tank failure simultaneously.

The following sections introduce the tests and the results that were used directly in the validation process. Parts of these sections are excerpts from Reference (1).

2.2.1 TDC Tests

The Transportation Development Centre of Transport Canada has been a key supporter of R & D in the area of tank-car safety. As well as supporting the present research project, TDC has funded a number of other projects, both theoretical and experimental in nature.

The following section does not attempt to critique all of the tank-car related studies funded by TDC. The intention is to summarize the fifth-scale fire test program, from which data has been extracted for the purposes of validating the overall tank-car model.

The test program of most interest was conducted for the Transportation Development Centre, and involved the testing of six 1/5 linear scale tanks filled with LPG, and exposed to fires fueled by JP4. The tests were performed between June 1979 and April 1980 at the Defence Research Establishment (DRES) in Suffield, Alberta, Canada. Basically, the tests were undertaken to evaluate the performance of the internal protection device known as 'Explosafe'. Of the six tanks that were tested, two were unprotected and four contained the 'Explosafe' material in different configurations.

The test tanks were 1/5-scale models of DOT 114A340W tank-cars. The wall thicknesses of these tanks were such that the bursting pressure of the models was the same as for the equivalent full-scale tank. The relief valves used on the tanks were sized in accordance with the approved method for such devices. This method of sizing the valve is based on the total surface area of the tank, and as a result, the relief valves were approximately 1/5 (orifice area approximately 1/25) the size of those used on full-scale tanks. In each of the tests, the tanks were filled to 85 percent capacity with commercial grade propane. The tanks were partially protected from cross winds by barriers which were erected around the fire pan.

The tanks were instrumented to measure wall, lading and flame temperatures, and the tank internal pressure. No attempt was made to measure the position of the liquid surface using a separate instrument as a result of the problems experienced in other tests. Details of the instrumentation used in the tests can be found in Reference (3).

The different 'Explosafe' configurations that were tested are shown in Figure 2-1. The first configuration known as style #1 is shown in Figure 2-1a and consisted of a 76 mm deep annulus of circumferentially layered material with the 457 mm diameter core filled with cylindrically wound material. Style #2 shown in Figure 2-1b consisted of twelve vertically layered, pie shaped elements. Style #3 is shown in Figure 2-1c and it consisted of a 76 mm thick annulus of circumferentially layered material and was held against the wall by expandable retainer rings.

As mentioned, there were six tanks in total. The tests were given the code names, 'Baseline', 'Dres Special', 'Howler', 'Nova', 'Diablo', and 'Enigma'. The first test conducted was code-named 'Baseline', and was a datum case involving an unprotected tank. This tank ruptured after approximately ten minutes in the fire but as a result of instrumentation failure no data was obtained.

The second test was code named 'Dres Special', and this tank contained 'Explosafe' in the style #1 configuration. The vessel survived the test without rupturing, but fuel starvation at approximately five minutes into the test caused the flame intensity to drop dramatically. Although the instruments recorded the response of the tank/lading system, the results were of little use because of the widely changing flame conditions. As a result of the test failure, another test code named 'Diablo' was conducted using the same 'Explosafe' configuration as in 'Dres Special'.

The problem of varying flame conditions did not only occur in the 'Dres Special' test. Figure 2-2 presents the fire mean radiating temperatures based on the fire temperatures measured during the tests. Of the four tests that were considered successful, 'Diablo' shows a continuously dropping flame temperature during the test. Therefore, it

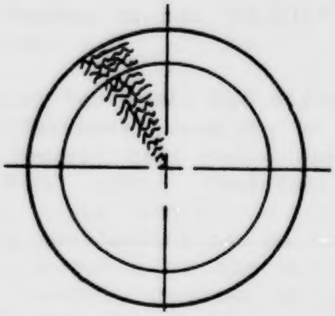

2-1a style #1 as tested in 'Dres Special' and 'Diablo'.

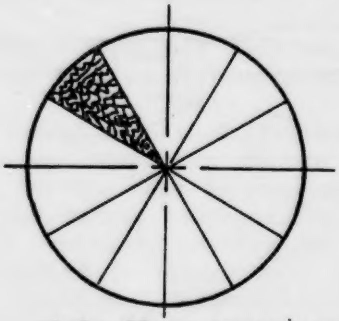

2-1b style #2 as tested in 'Howler'.

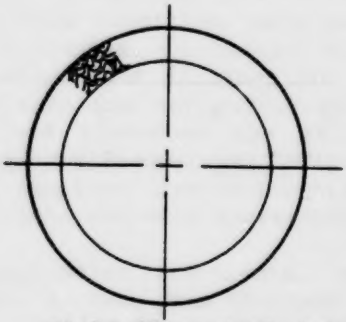

2-1c style #3 as tested in 'Nova'.

FIGURE 2-1 SKETCH SHOWING THE DIFFERENT STYLES OF 'EXPLOSAFE' IN THE TDC FIFTH-SCALE FIRE TESTS (from Reference (3))

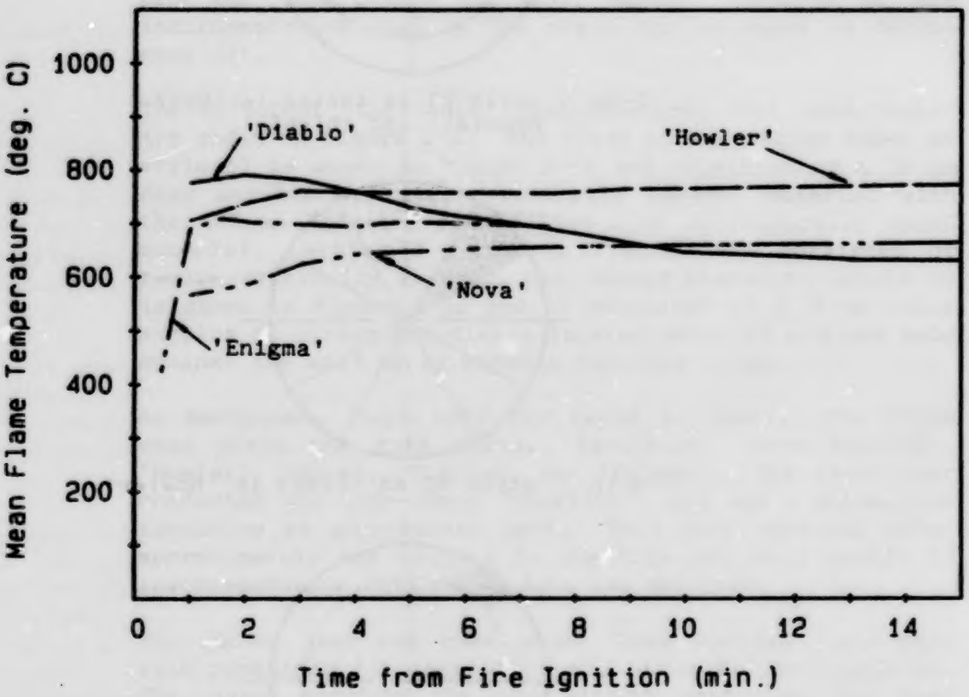

FIGURE 2-2 MEAN FLAME RADIATING TEMPERATURES FROM TDC FIFTH-SCALE FIRE TESTS (from Reference (1))

is questionable whether or not 'Diablo' should be considered as a valid test.

The three remaining tests all had differing flame conditions. These differences translate to potential radiant fluxes in the 'Howler' test being approximately double those in the 'Nova' test. Therefore, because of the widely differing flame conditions it is questionable whether or not any conclusions can be drawn from the tests regarding the performance of the different 'Explosafe' configurations. However, because no other data on the performance of 'Explosafe' in tank-cars exists, the data from these tests was used for the development of the 'Explosafe' equipped tank-car model.

The following sections present some of the results from the four tests that were considered successful.

'Howler': This vessel contained 'Explosafe' in the style #2 configuration as shown in Figure 2-1b. The tank pressure history for the test is presented in Figure 2-3, while the wall and lading temperatures are presented in Figures 2-4, 2-5 and 2-6. A key to the thermocouple locations is presented in Figure 2-7. The raw data from this test can be found in Reference (3).

From Figure 2-3 it can be seen that the tank pressure rose rapidly once the fire conditions were established. After approximately two minutes, the relief valve opened for the first time. At this point in time, the vapour generation rate within the tank was not sufficient to maintain the tank pressure, and therefore the relief valve cycled between the open and closed state. After the second valve cycle the valve remained open and continued to vent the lading from the tank, but with increasing tank pressure.

After the initial valve transients, the tank pressure continued to rise, as seen from the tank pressure history. The changes in the slope of the pressure/time curve clearly seen in Figure 2-3, may have been due to valve characteristics or the effects of varying flame intensities. Eventually, the rate of vapour generation was reduced as a result of the dropping liquid level, and therefore the tank pressure began to drop. At approximately 11 minutes into the test the valve began to cycle again until the tank emptied completely at approximately 15 minutes into the test.

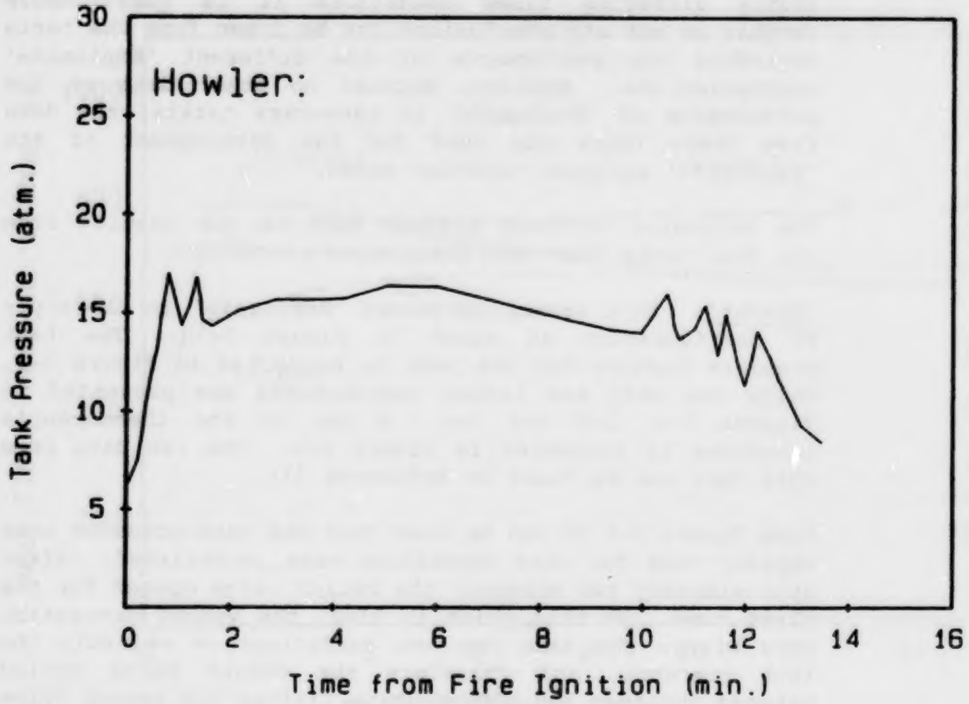

FIGURE 2-3 MEASURED TANK PRESSURE FOR 'HOWLER' TEST (from Reference (3))

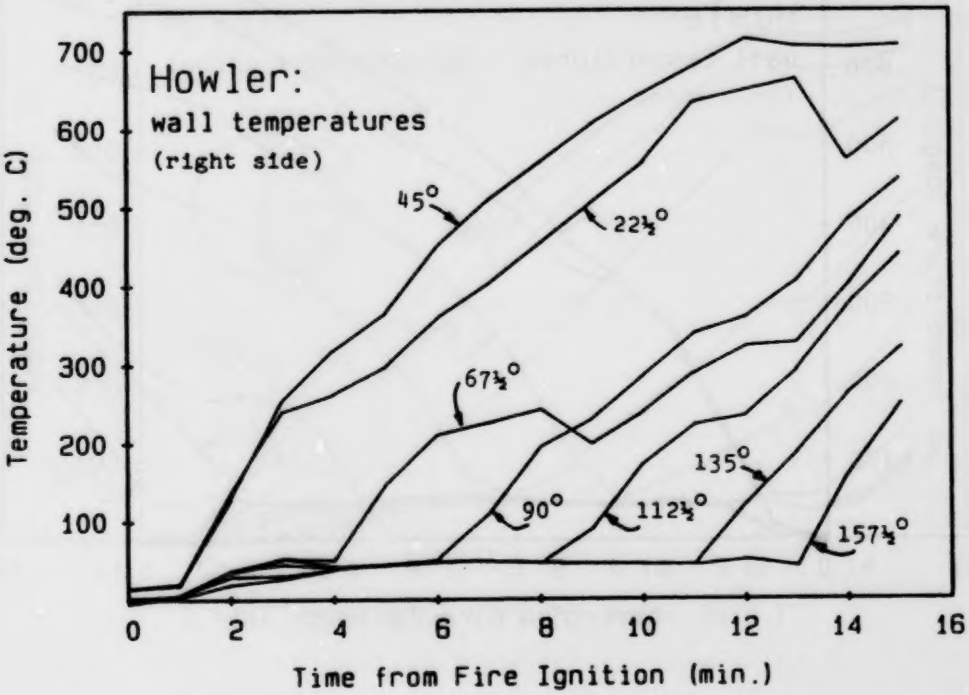

FIGURE 2-4 MEASURED INNER WALL TEMPERATURES (RIGHT SIDE) FROM 'HOWLER' TEST (from Reference (3))

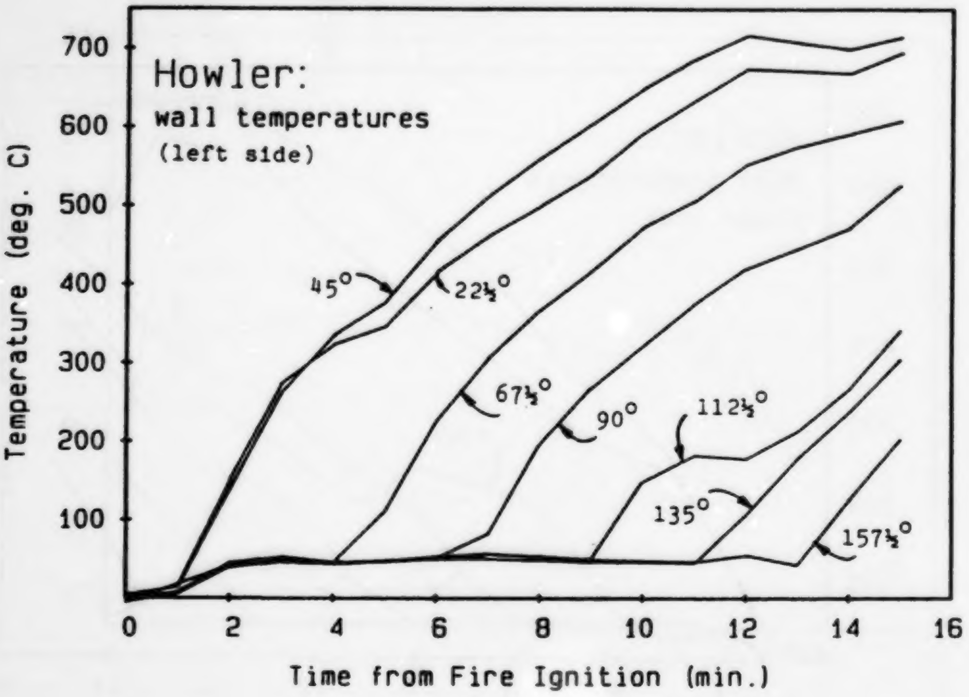

FIGURE 2-5 MEASURED INNER WALL TEMPERATURES (LEFT SIDE) FROM 'HOWLER' TEST (from Reference (3))

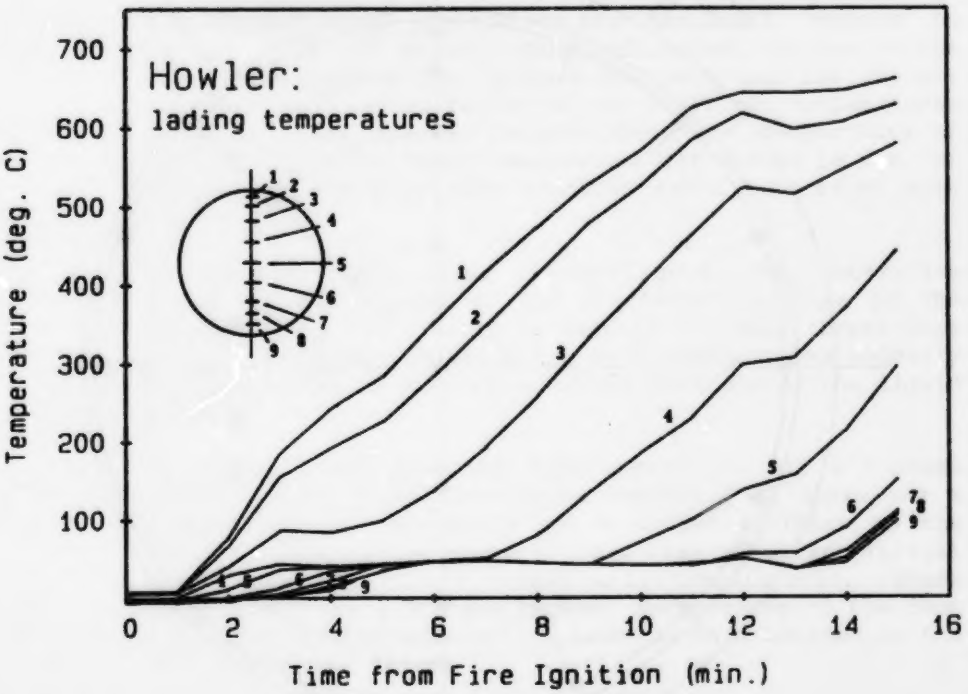

FIGURE 2-6 MEASURED LADING TEMPERATURES FROM 'HOWLER' TEST (from Reference (3))

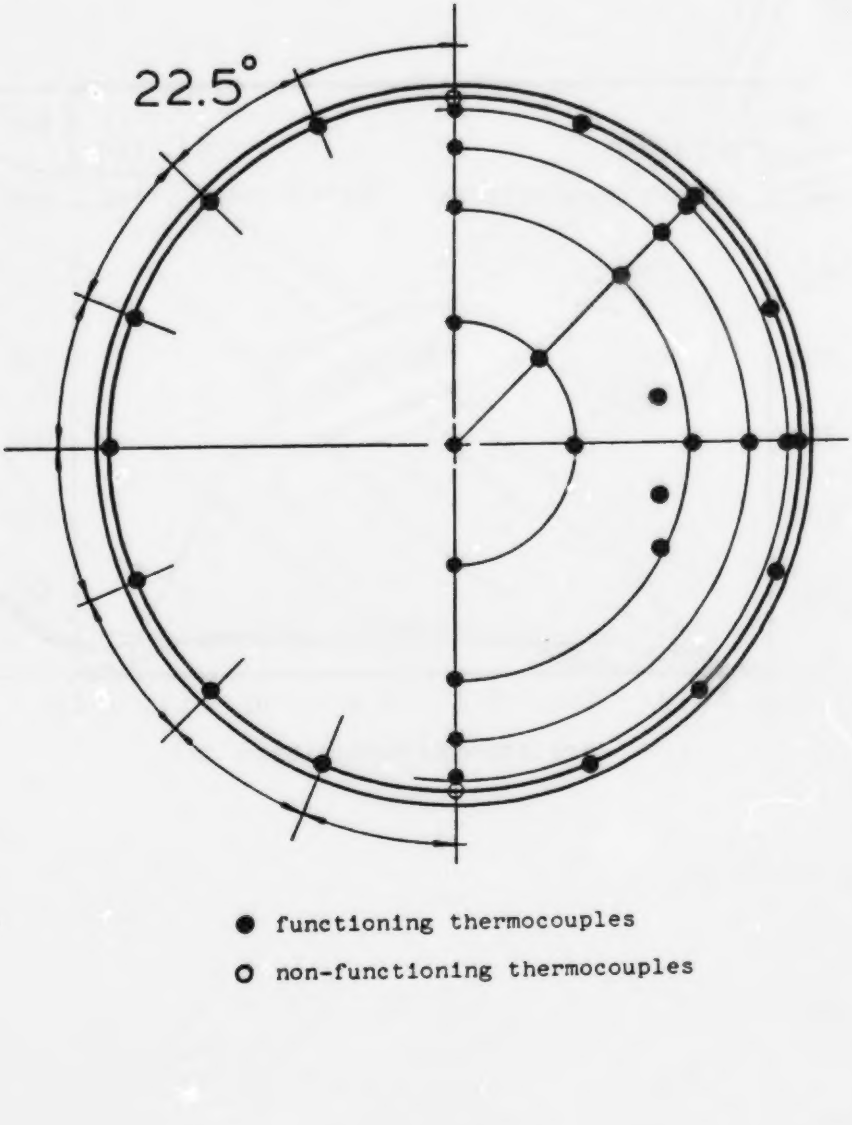

● functioning thermocouples

○ non-functioning thermocouples

FIGURE 2-7 KEY TO THERMOCOUPLE LOCATIONS IN 'HOWLER' TEST (from Reference (3))

The wall temperature data is presented in Figures 2-4 and 2-5. The two figures present data for each side of the tank, and therefore give some indication of the symmetry of the fire conditions. The locations of the various thermocouples are shown in Figure 2-7.

From these figures it can be seen that rapid increases in temperature were experienced by the wall regions in contact with the vapour. This, of course, is due to the low heat transfer rate between the wall and the vapour. In the liquid wetted region of the wall, the temperatures are only a few degrees celsius above the temperature of the liquid. This small temperature difference is due, of course, to the high heat transfer rates associated with boiling.

As the wall comes clear of the liquid, its temperature rises rapidly because of the inefficient cooling by the vapour. This can clearly be seen in the wall temperature plots. The times at which the wall temperatures suddenly increase gives an indication of the position of the liquid surface.

It is not clear from the data whether or not a 2-phase region exists above the liquid surface. If there was a 2-phase region, one would see a sudden increase in the slope of temperature curve a short time after its initial break from the liquid wetted wall temperatures. There most likely was a 2-phase region, but because of the tank scale its effects were not as large as will be seen in the full-scale tank tests.

In general, the wall temperatures experienced by 'Howler' were very high and are very similar to those of the unprotected tank 'Enigma' which ruptured. This will be discussed further later.

The lading temperatures for this test are presented in Figure 2-6. The shape of the curves are very similar to those of the wall temperatures. The break times, once again, give an indication of the position of the liquid level.

The lading temperature data shows one very interesting feature; temperature stratification. Temperature stratification in both the liquid and vapour regions are seen to have existed. The thermocouple data for the vapour temperatures must be treated with caution because thermocouples near the wall will probably be affected by radiant exchange between the wall and the thermocouple, and therefore data from these regions may not be true indications of vapour temperatures. The temperature data for the liquid region also shows that temperature variations existed there. The liquid near the walls and at the liquid surface was warmer than the liquid in the core. This temperature stratification died out at approximately five minutes into the test. At this point in time the liquid became nearly isothermal and was near saturated equilibrium.

The test concluded with the tank empty. At the end of the test the tank was examined and it was found that one end of the tank had bulged, and therefore the tank had been very near failure. This was considered to be a result of poor contact between the wall and the 'Explosafe' material. Poor wall contact has been shown (14) to cause reductions in the effectiveness of the 'Explosafe' material.

'Nova': This vessel contained 'Explosafe' in the style #3 configuration as shown in Figure 2-1c. The tank pressure history for the test is presented in Figure 2-8. Wall and lading temperatures are presented in Figures 2-9, 2-10 and 2-11. A key to the various thermocouple locations can be found in Figure 1-12. An estimate of the liquid level is shown in Figure 2-13.

From Figure 2-8, it can be seen that the tank pressure rapidly rose once the fire conditions were established. When the tank pressure reached approximately 13 atmospheres, there was a change in the pressurization rate which may have been caused by premature leaking of the relief valve. At approximately two minutes into the test, the relief valve opened for the first time. The vapour generation rate within the tank was not sufficient to maintain the tank pressure, and therefore the valve cycled. The remainder of the pressure plot appears similar to that of the 'Howler' test.

Wall temperatures recorded during this test are presented in Figures 2-9 and 2-10. As can be seen from these figures, the wall temperatures increased rapidly in the vapour wetted wall region and slowly in the liquid wetted wall region. The rate of temperature increase is seen to be considerably less than observed in the 'Howler' data. This may be due to improved contact between the wall and the 'Explosafe' material, or it may be the result of different fire intensities.

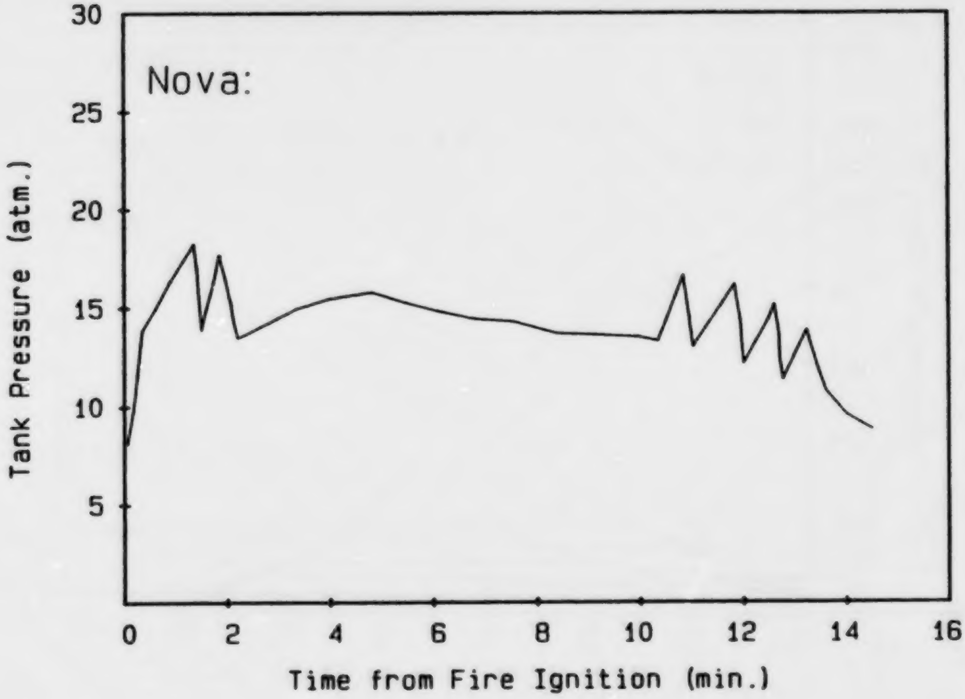

FIGURE 2-8 MEASURED TANK PRESSURE FOR 'NOVA' TEST (from Reference (3))

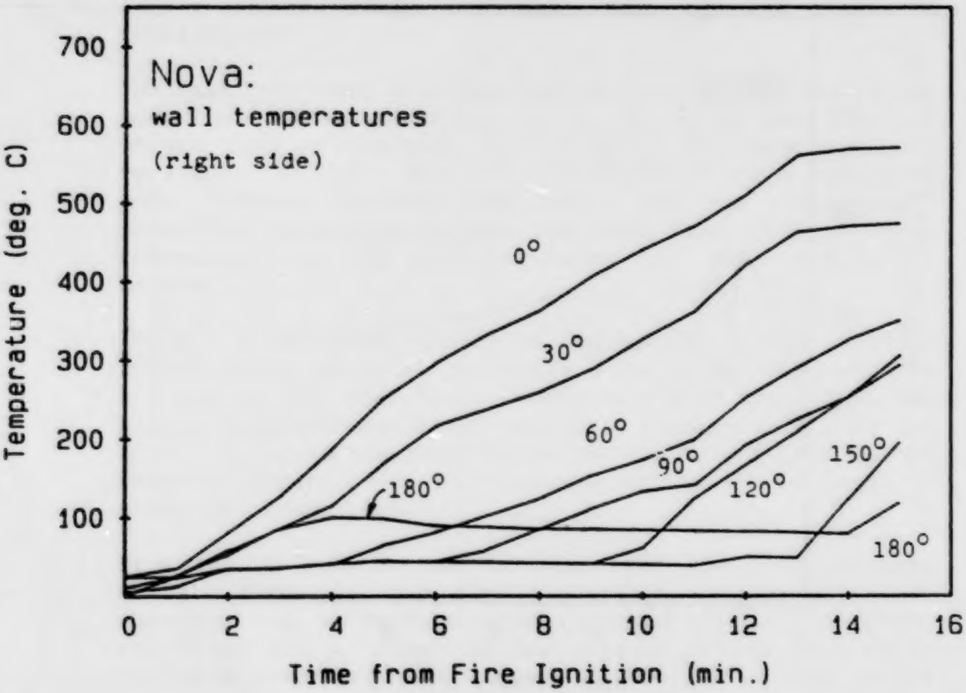

FIGURE 2-9 MEASURED INNER WALL TEMPERATURES (RIGHT SIDE) FROM 'NOVA' TEST (from Reference (3))

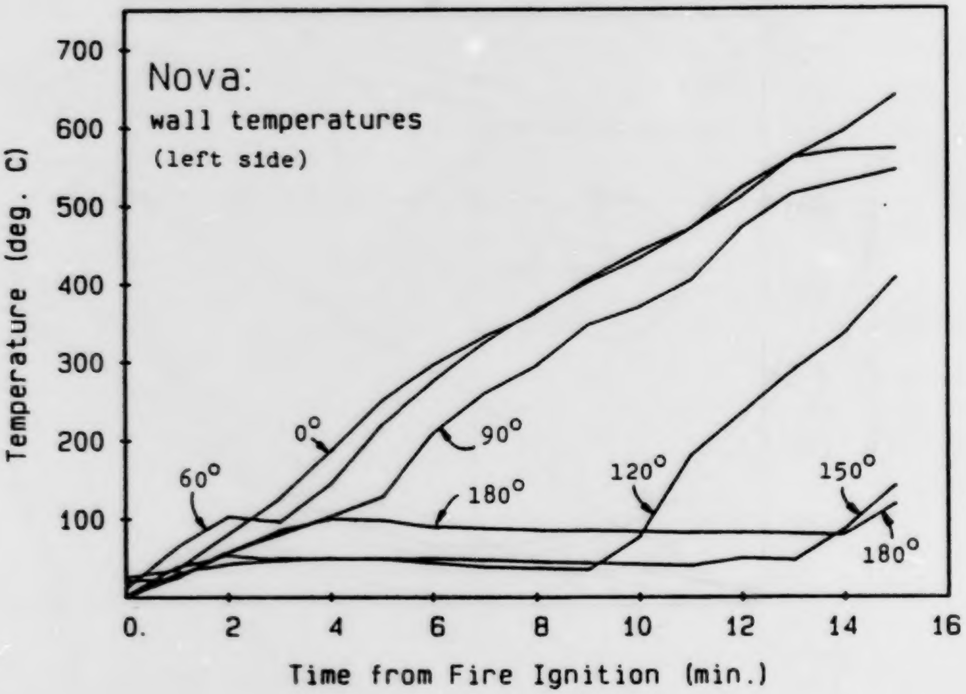

FIGURE 2-10 MEASURED INNER WALL TEMPERATURES (LEFT SIDE) FROM 'NOVA' TEST (from Reference (3))

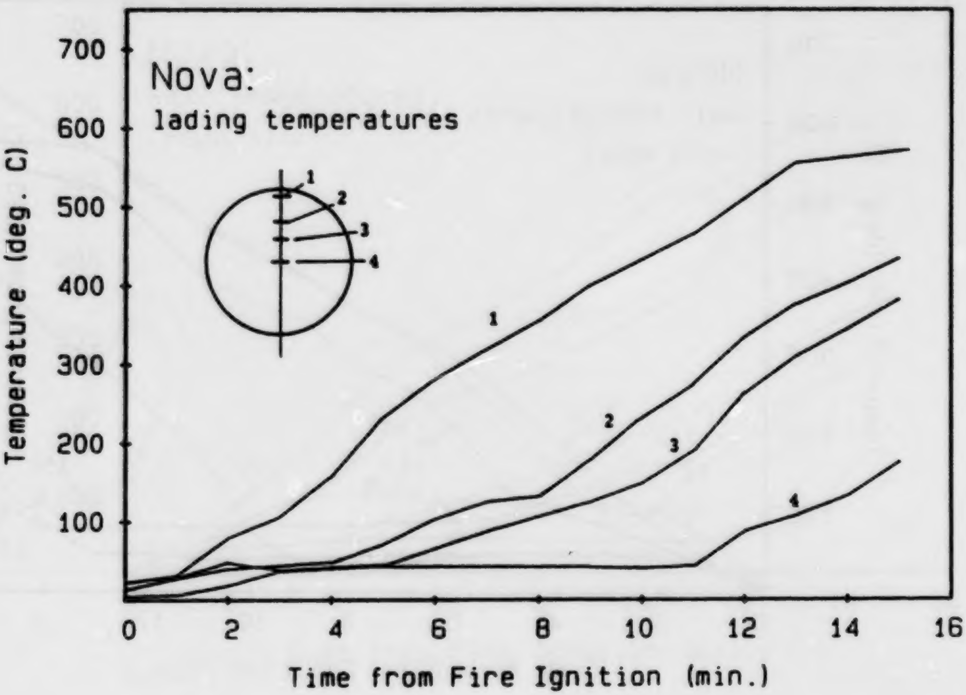

FIGURE 2-11 MEASURED LADING TEMPERATURES FROM 'NOVA' TEST (from Reference (3))

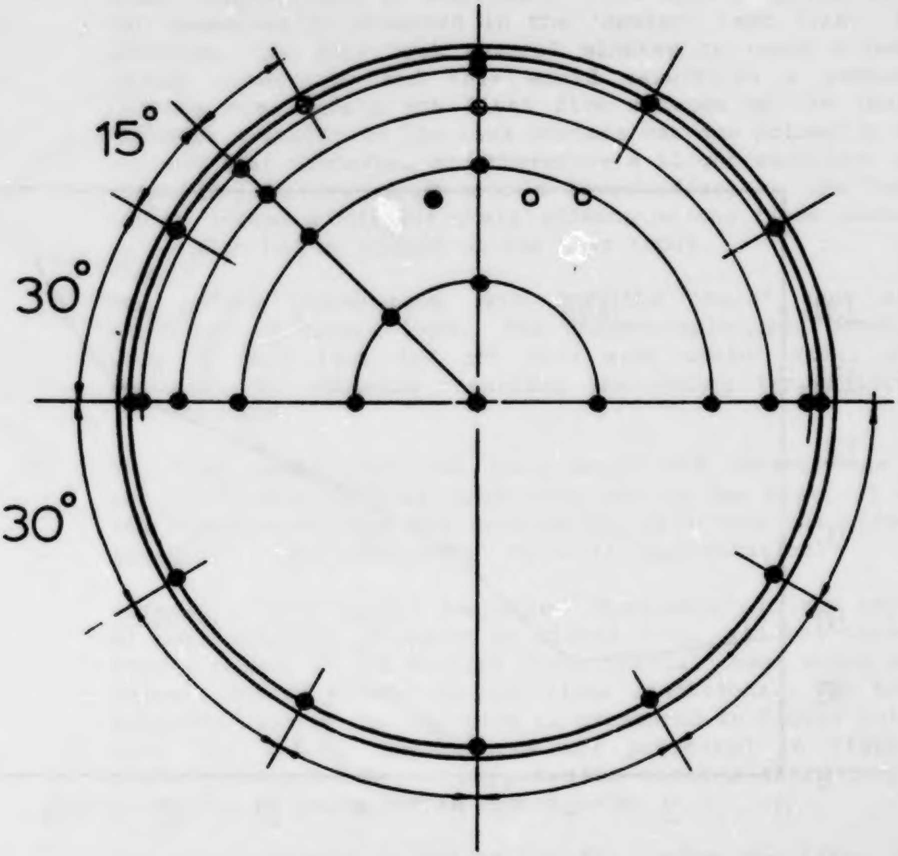

● functioning thermocouples

O non-functioning thermocouples

FIGURE 2-12 KEY TO THERMOCOUPLE LOCATIONS IN 'NOVA' TEST (from Reference (18))

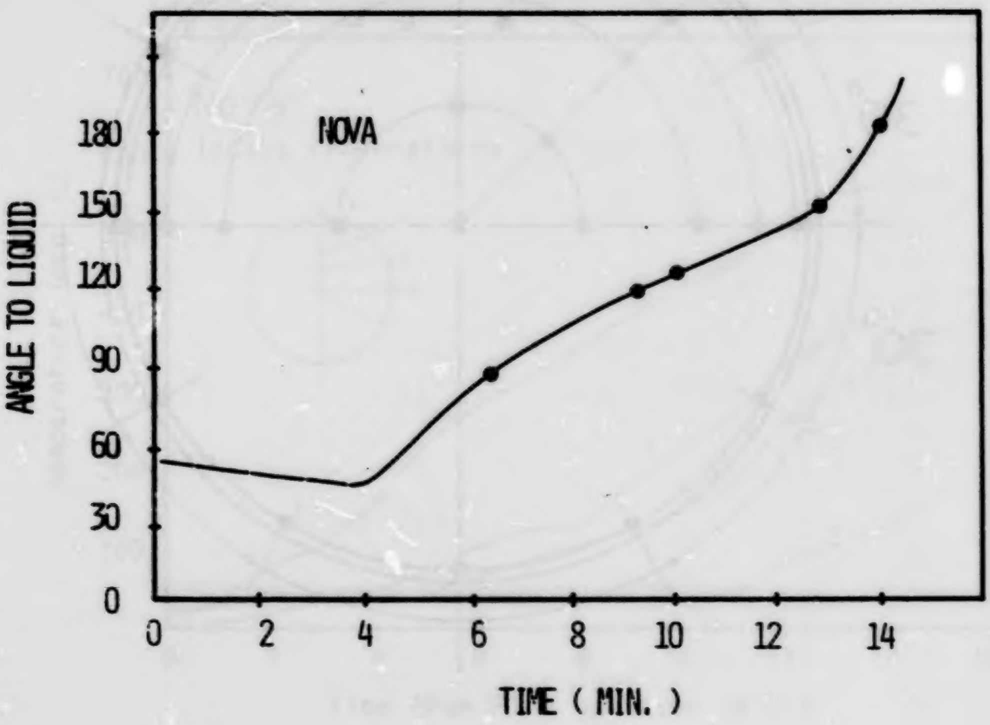

FIGURE 2-13 ESTIMATED LIQUID LEVEL FOR 'NOVA' TEST (from Reference (3))

Fire temperatures that were recorded showed generally lower temperatures in the 'Nova' test when compared with the temperatures observed in the 'Howler' test fire. In addition, the fire took several minutes to reach a near steady condition, and this would result in a reduced heating rate during the first five minutes of the test. The heat transfer to the tank surface was due primarily to radiant heat transfer, and therefore a slight reduction in flame temperature would have a large effect on the heat input. Cross winds and their effects on the flame geometries also had an effect on the heat input.

The lading temperature data for the 'Nova' test are presented in Figure 1-24. The thermocouple grid network used in this test did not give much useful data, and therefore no comments regarding the lading temperatures will be made.

The test ended with the tank empty and intact. As a result of varying fire conditions during the test, it is not possible to draw any conclusions regarding the effectiveness of the 'Explosafe' style #3 configuration.

'Diablo': This vessel contained 'Explosafe' in the style #1 configuration as shown in Figure 2-1a, and was therefore a repeat of the earlier 'Dres Special' test which was suspect due to widely varying flame conditions. The tank pressure history for the test is presented in Figure 2-14. Wall and lading temperatures are presented in Figures 2-15, 2-16 and 2-17. A key to the various thermocouple locations is presented in Figure 2-18.

The tank pressure increased rapidly during the first two minutes of the test. At approximately two minutes into the test, the relief valve opened for the first time. The vapour generation rate within the tank was not sufficient to maintain the tank pressure, and therefore the tank pressure dropped but the valve remained open. In this test there was no valve cycling period. The remainder of the pressure results appear similar to that of 'Nova' and 'Howler'.

The wall temperatures observed during the test are presented in Figures 2-15 and 2-16. In this test the wall temperatures increased rapidly during the initial four minutes. As with all the tests, the wall temperatures in the vapour wetted regions increased much more rapidly than those in the liquid wetted areas. At approximately four minutes into the test, the wall temperatures in the vapour

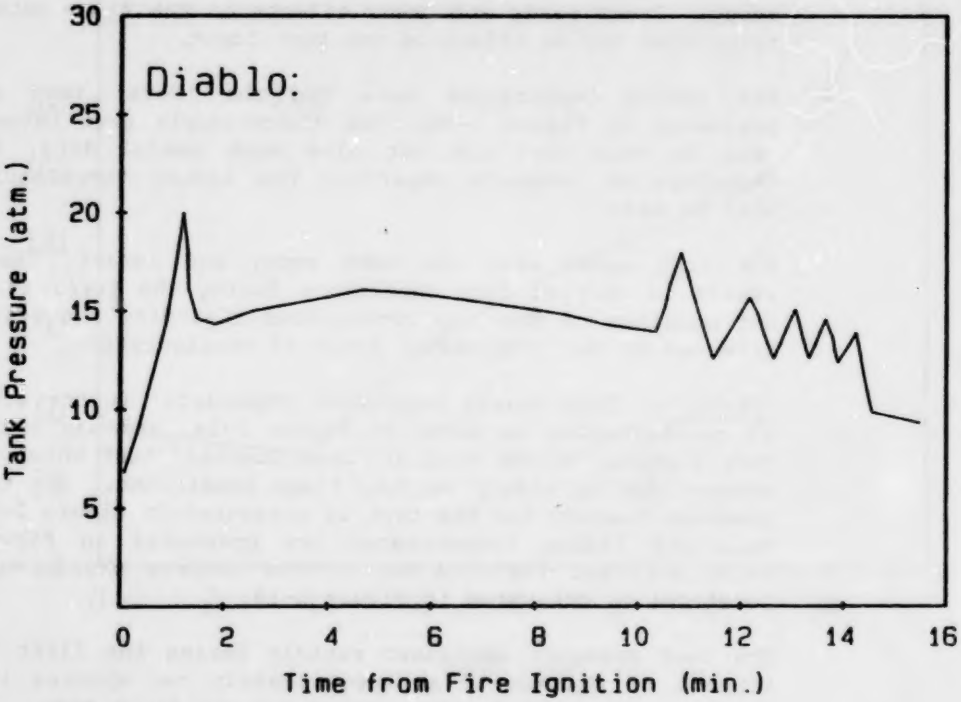

FIGURE 2-14 **MEASURED TANK PRESSURE FOR 'DIABLO' TEST (from Reference (3))**

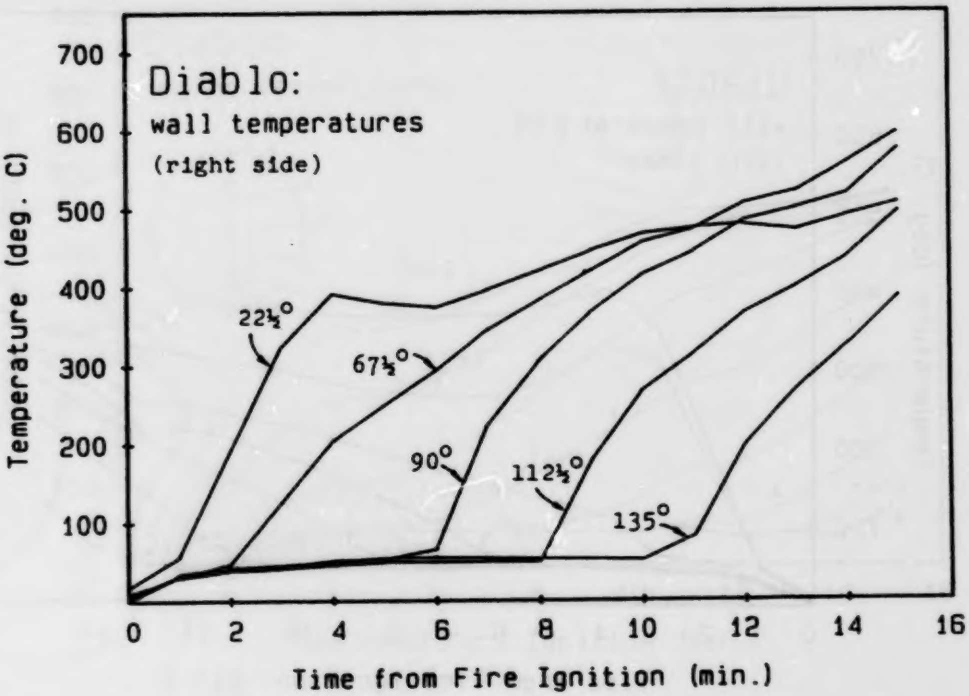

FIGURE 2-15 MEASURED INNER WALL TEMPERATURES (RIGHT SIDE) FROM 'DIABLO' TEST (from Reference (3))

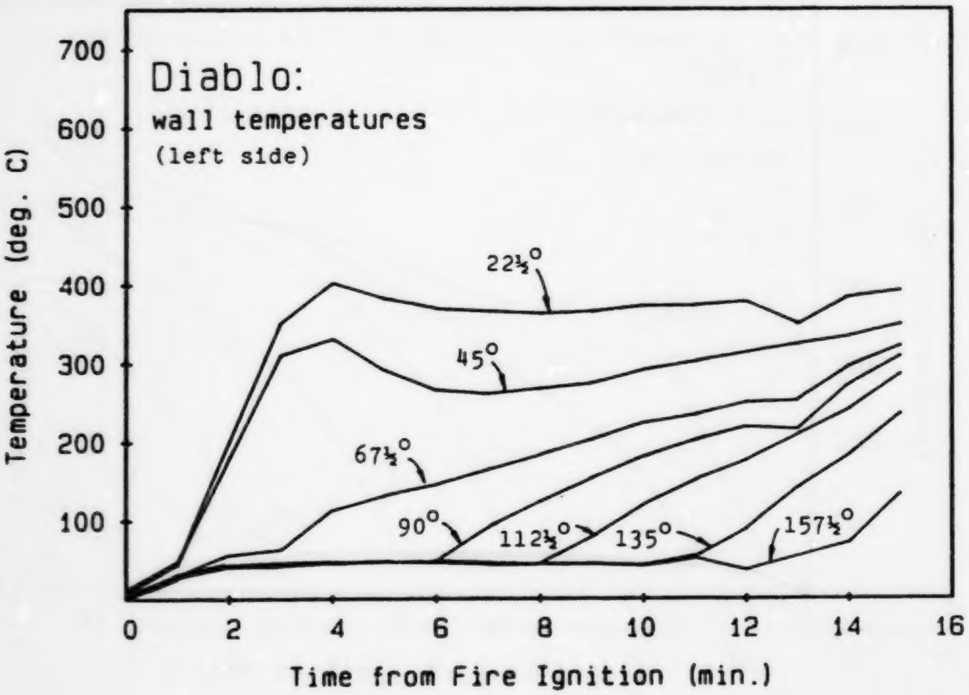

FIGURE 2-16 MEASURED INNER WALL TEMPERATURES (LEFT SIDE) FROM 'DIABLO' TEST (from Reference (3))

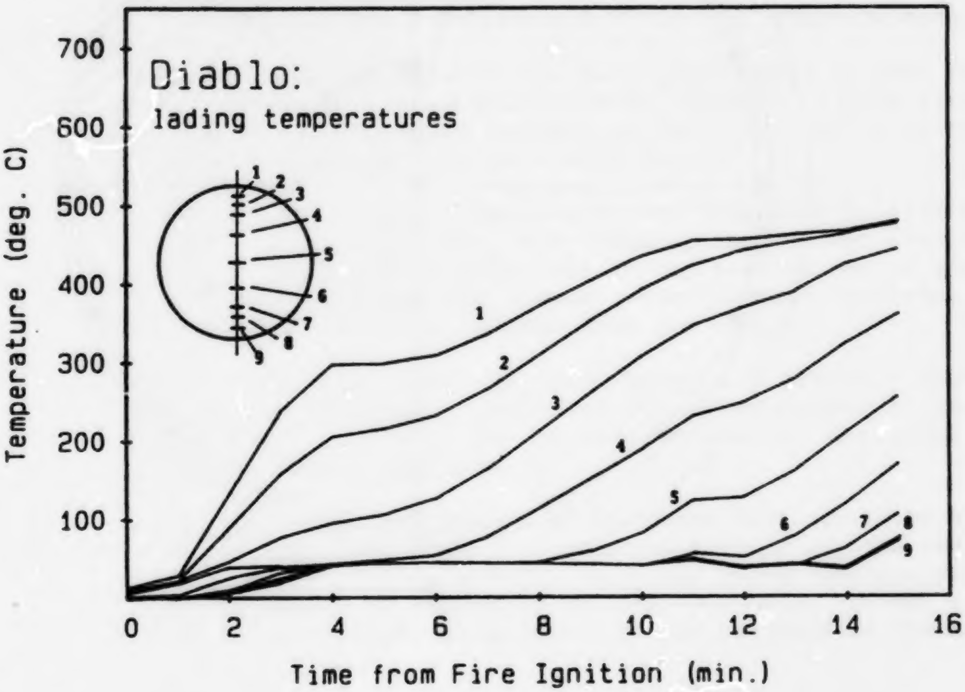

FIGURE 2-17 MEASURED LADING TEMPERATURES FROM 'DIABLO' TEST (from Reference (3))

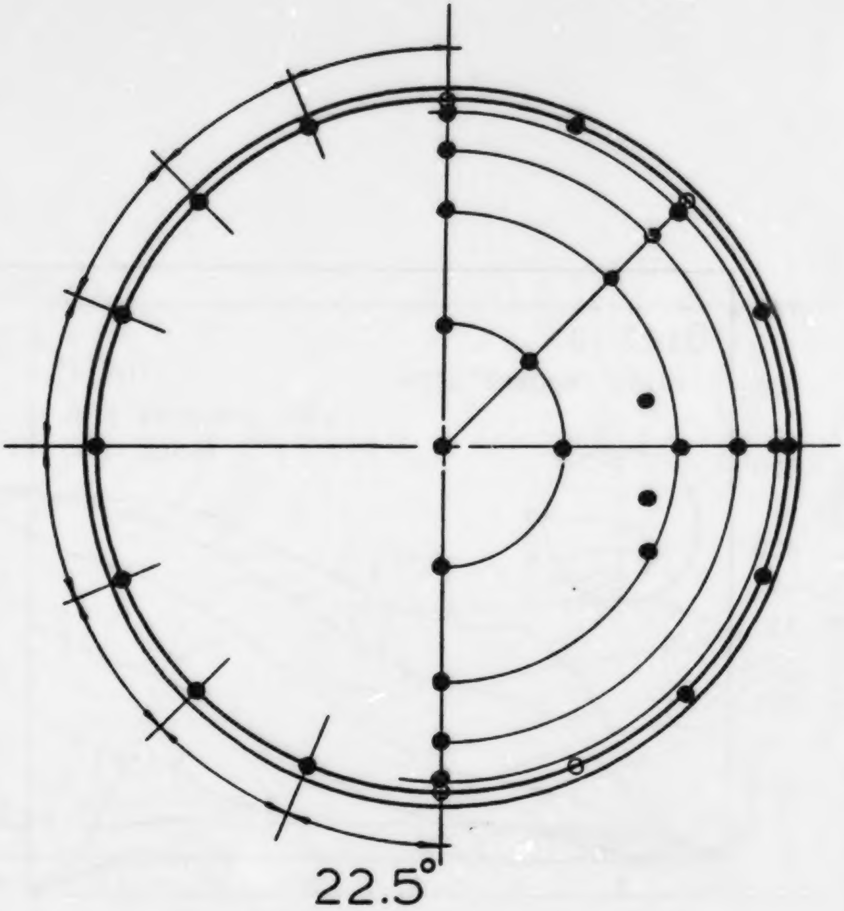

● functioning thermocouples

○ non-functioning thermocouples

FIGURE 2-18 KEY TO THERMOCOUPLE LOCATIONS IN 'DIABLO' TEST (from Reference (3))

wetted areas levelled off, this effect being particularly noticeable in the results obtained from the left side of the tank, as shown in Figure 2-16. This indicates an asymmetrical fire condition possibly resulting from cross winds encountered during the test. Flame temperature measurements taken during the test indicated a drop in the flame temperatures at approximately four minutes, and this would explain the levelling off of the wall temperatures.

The initial rise rate of the wall temperatures is seen to be greater than that experienced by 'Howler'. If the fire intensity had remained constant in this test, it is quite probable that the tank would have failed.

The measured lading temperatures are presented in Figure 2-17. As can be seen, the temperatures of the vapour region thermocouples level off in the same manner as the wall temperatures. The liquid region becomes isothermal at approximately four minutes into the test.

The test ended with the tank empty and intact. Once again, no conclusions regarding the effectiveness of the 'Explosafe' material can be made because of the widely varying flame conditions.

'Enigma': This was repeat of the datum test involving an unprotected tank. The tank pressure history for the test is presented in Figure 2-19. Wall and lading temperatures are presented in Figures 2-20, 2-21 and 2-22. A key to the various thermocouple locations can be found in Figure 2-23.

As with all the 1/5-scale tests, the tank pressure increased rapidly during the first two minutes of the test. At approximately two minutes the relief valve opened for the first time. The vapour generation rate within the tank was not sufficient to maintain the tank pressure, and therefore the valve cycled.

In this test, the valve cycled three times before the pressure in the tank began to rise with the valve operating.

The tank pressure continued to rise as with the previous tests. The tank pressure peaked at approximately 6 minutes into the test, and then the tank pressure began to drop. The tank ruptured at approximately 7.5 minutes into the test.

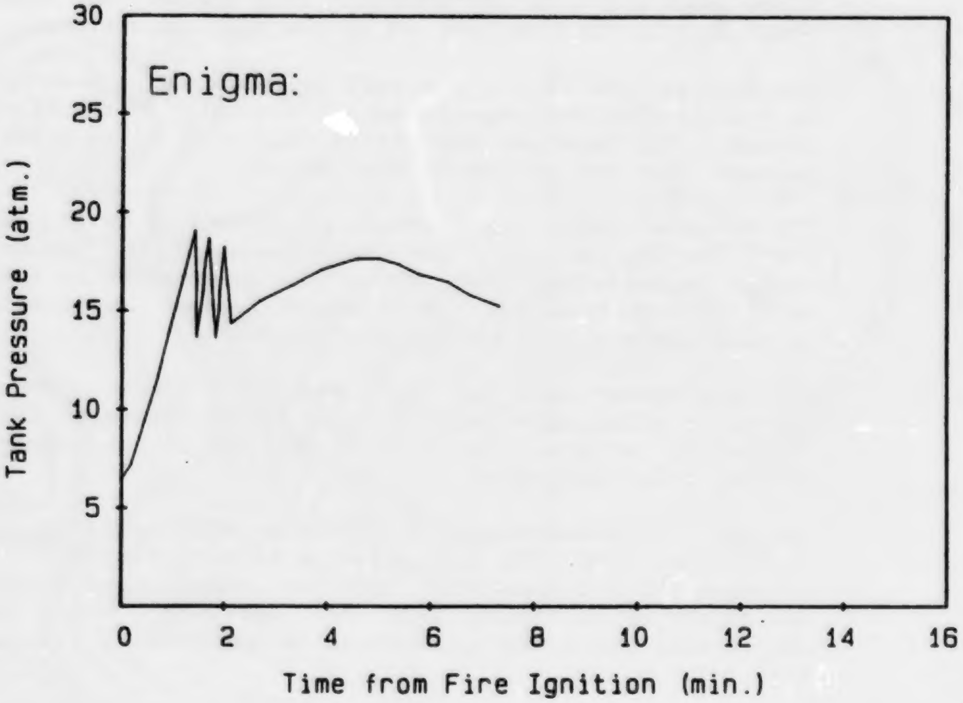

FIGURE 2-19 MEASURED TANK PRESSURE FOR 'ENIGMA' TEST (from Reference (3))

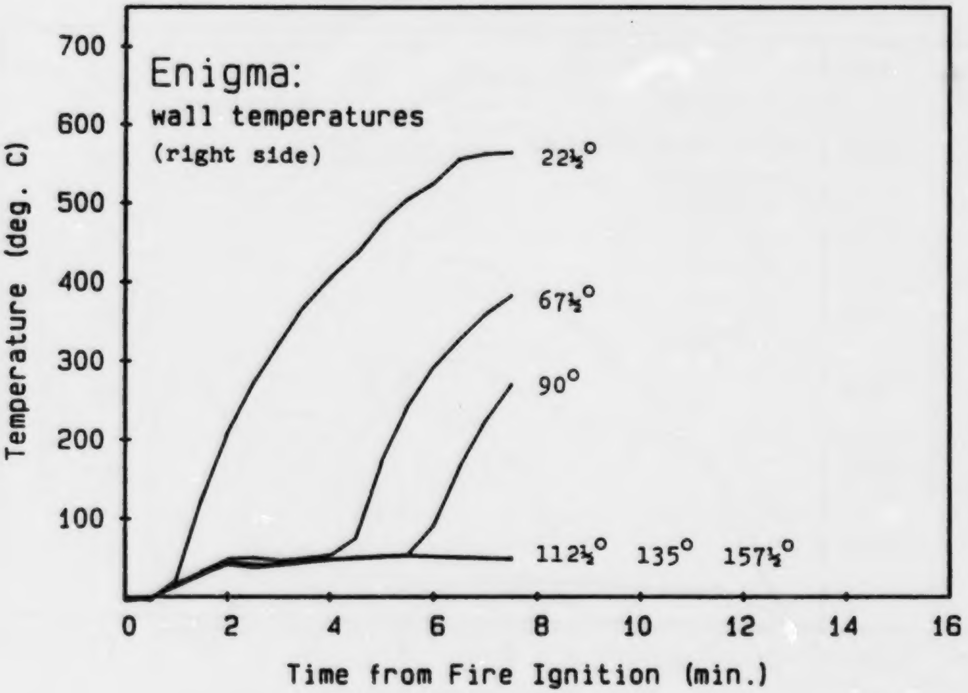

FIGURE 2-20 MEASURED INNER WALL TEMPERATURES (RIGHT SIDE) FROM 'ENIGMA' TEST (from Reference (3))

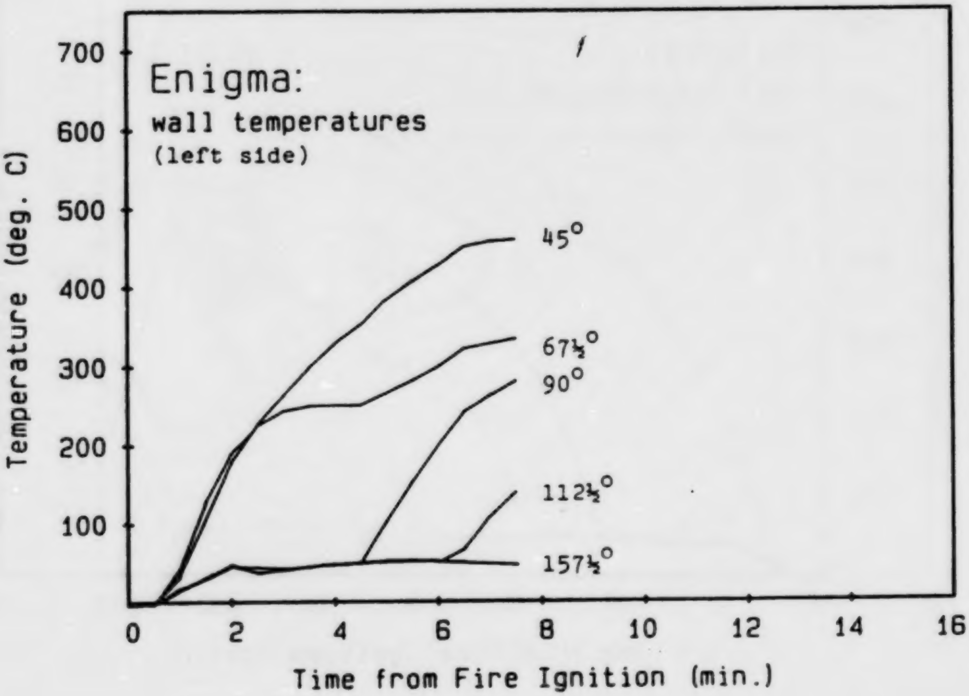

FIGURE 2-21 MEASURED INNER WALL TEMPERATURES (LEFT SIDE) FROM 'ENIGMA' TEST (from Reference (3))

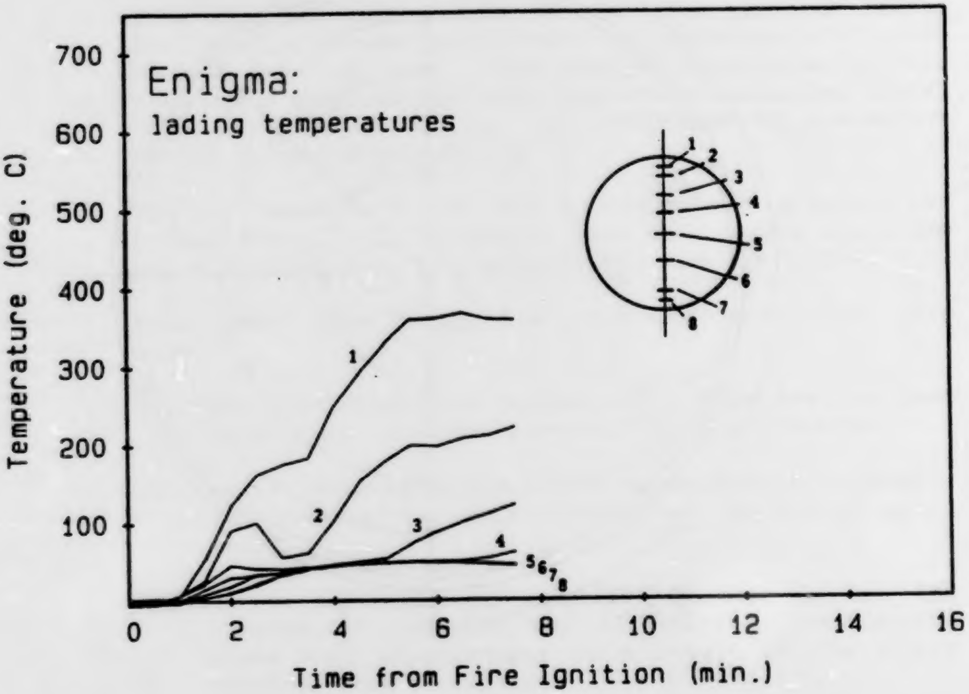

FIGURE 2-22 MEASURED LADING TEMPERATURES FROM 'ENIGMA' TEST (from Reference (3))

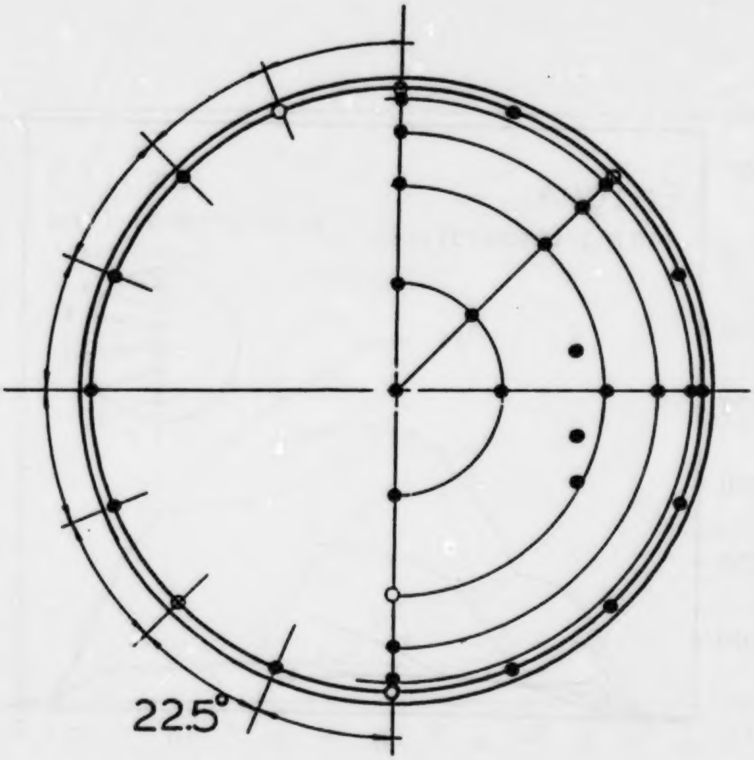

● functioning thermocouples

○ non-functioning thermocouples

FIGURE 2-23 KEY TO THERMOCOUPLE LOCATIONS IN 'ENIGMA TEST (from Reference (3))

The wall temperatures are presented in Figures 2-20 and 2-21. The wall temperatures in the vapour wetted area of the wall increased rapidly. This rate of increase is very similar to that observed in the 'Howler' test, and also during the initial periods of the 'Diablo' test. The wall temperatures continued to rise until the vessel failed.

The lading temperatures are presented in Figure 2-22. They show the same trends as seen from previous tests. The liquid became isothermal at approximately three minutes into the test. This time to saturation is less than that observed for the 'Explosafe' equipped tanks. This is probably due to the inhibition of convective mixing by the 'Explosafe' matrix.

The test ended with the tank rupturing and releasing its contents into the atmosphere. The tank failed along its upper surface where the temperatures were the highest.

From these four tests, the following conclusions were made.

i) The fire conditions varied widely from test to test as a result of cross winds and fueling problems.

ii) Valve characteristics played a key role in determining whether the safe venting of the lading would occur.

iii) It is difficult to establish whether or not the 'Explosafe' material was effective in maintaining lower wall temperatures as a result of the widely varying flame conditions.

iv) It is difficult to compare the performance of the three 'Explosafe' configurations as a result of the varying flame conditions.

v) The presence of the 'Explosafe' has some effect on venting rate, probably due to the flow restriction by the aluminum mesh.

vi) The presence of the 'Explosafe' seems to slow down the convective mixing processes in the tank as shown in the time-to-liquid-saturation data.

2.2.2 AAR - RPI Tests

In 1970 a major study was initiated by the Federal Railroad Administration/Department of Transportation (FRA/DOT), American Association of Railroads (AAR), the Railway Progress Institute (RPI), major railroads, tank-car builders, and various shipping organizations. The objectives of this study were as follows:

"To develop through study, tests, and research, improved knowledge of factors that cause punctures and ruptures of tank-car tanks in accidents."

"To develop, through the use of this knowledge, practical and proven means to improve the resistance of tank-cars to such punctures and ruptures."

The project scope was to cover all types of tank-cars and hazardous materials, but with emphasis being placed on pressure cars carrying materials which are commonly involved in severe accidents such as LPG, ammonia, and vinyl chloride. The study was broken down into thirteen phases, which covered a wide range of research activities. Of these, phase 6, 7 and 11 are of specific interest to the present study. Phases 6 and 7 dealt with the operation of safety relief devices, and phase 11 dealt with thermal effects, thermal effects being defined as effects of a fire on the conditions of the tank wall and contents.

Phases 6 and 7 included experimental and theoretical analysis of liquid and vapour flows through relief valves. The design and analysis of special devices such as improved relief valves and fusible plugs were also included as part of these phases of study.

Phase II involved studies related to the thermal effects of fire impingement on tank-cars. Work done in this phase included several experimental studies, the early fifth (4, 5, 6, 7) and full-scale (2) fire tests as well as the development of a computer model (15).

Results obtained in studies sponsored by this tank-car safety research program form the major portion of the data base used in the present study. The results obtained from the full-scale fire tests were the primary source of data for the development of the present computer model.

The following sections discuss some of the results from these U.S. experimental studies.

2.2.2.1 AAR-RPI: Full-Scale Tests

The full-scale fire tests were conducted in the early 1970's as part of Phase II of the AAR-RPI tank safety research project. In the tests, a full-scale unprotected tank and a full-scale thermally coated tank were exposed to engulfing fires fueled by JP4.

The engulfing flame was used because it represents what many consider to be the worst case possible in an accident situation. The use of JP4 as the fuel source made the test conditions somewhat more extreme than the conditions that would be expected in a real accident. This is because the radiating properties of a JP4 fueled fire would cause a higher heat input to the tank than would be expected from a fire fueled by LPG, a more probable fuel in an actual accident situation. It should be kept in mind that the tests were not necessarily designed to represent a real fire situation; they were experiments to compare the relative performance of an unprotected tank and a thermally coated tank.

The fires were contained in a pit to shield the tests from cross wind effects. However, the shielding effect of the pit was not entirely successful, and as a result the flame conditions varied throughout the tests. Some of the inconsistencies which appear in the test results may have been caused by the varying flame conditions.

The tanks were instrumented with thermocouples, liquid level indicators, pressure sensing devices, relief valve lift indicators, and heat input measuring devices. Details of the instrument types and locations can be found in Reference (2).

Due to the extreme conditions existing in the tests, many of the instruments failed. The measured results of most interest to the present study were the internal fluid temperature distributions, the tank wall temperatures and the tank internal pressure. The data regarding the valve lift, liquid level and heat input conditions would have been very useful, but unfortunately instrument problems make them highly suspect.

The fire characteristics played a key role in the overall response of the tank/lading system. The flames were observed to be highly turbulent, and very sooty as a result of oxygen starvation. A ramp in the fire pit caused a swirling action at one end of the tank, and as a result, the flame temperatures were considerably higher there. These effects can clearly be seen in the tank wall temperature data.

Results of radiometer measurements on both the JP4 fueled fire and the burning relief valve flare yielded questionable results, and were not used in any way in the present study. Radiometer measurements were not taken during the test of the thermally coated tank. The fire condition for the thermally coated tank test was considered to be less severe based on flame thermocouple data. This, of course, makes performance comparisons between the two tests very difficult.

The actual heating rates from the fires were calculated in a number of different ways, and a wide range of heating rates were estimated. These calculations did not attempt to account for heat input variations around the circumference of the tank, or along its length. They were also subject to large errors because they were based on the assumption that the tank lading was in saturated equilibrium. The test results clearly indicate that this assumption was in error for much of the heating period. Based on measured flame temperatures, the heating rates were likely in the range of 60 to 100 kw/m^2 (20000 to 40000 $btu/hr/ft^2$).

The lading in both of the full-scale tests was LPG with the following chemical constituents.

Normal-butane	0.01 %
Iso-butane	0.07
Ethane	1.96
Propane	97.96
	100.00%

In Reference (2), all data analysis was based on the use of thermodynamic data for pure propane. This approach was also used in the present study for the development of the computer model. Errors introduced by this assumption were considered to be small, based on the results presented in Reference (2).

The tests conducted on the full-scale tanks will now be discussed separately.

Unprotected Tank: Details of the full-scale unprotected-tank (RAX 201) tests can be found in Reference (2). The tank was filled to approximately 95% capacity (i.e. filled to within 28 cm. from the top) with LPG at a mean temperature of 25° C. This fill condition was, of course, determined from standard fill tables for LPG, based on the test ambient temperatures. The pressure relief valve was set to open at 20 atm. The pool fire was ignited and the tank and lading response was recorded.

The internal pressure response during the test is presented in Figure 2-24. As seen from this figure, the pressure rose rapidly for approximately 2 minutes before the first venting action took place. When the relief valve first opened, the rate of vapour generation was not sufficient to maintain the tank pressure and the tank pressure quickly dropped below the valve closing pressure. The pressure then rose again until the valve reopened. This response continued for three valve cycles (approximately 2 minutes) before continuous venting occurred. After the third valve cycle, when the valve was supposedly in the open condition, the pressure rise rate was almost as high as it was when the valve was closed. This may be an indication that the valve was not venting energy as rapidly as it was in the previous cycles. There are two possible reasons for this, either the valve was passing a 2-phase mixture, or the valve was not fully open. The effectiveness of a relief valve can be drastically reduced if a 2-phase mixture is flowing through the valve rather than a dry vapour.

When the tank pressure once again reached the normal valve opening pressure, there was a sudden change in the slope of the pressure curve. This probably indicates that on the last valve cycle, the valve closed only partially, and as a result, the reduced rate of venting was sufficient to allow a build up in the internal pressure. When the pressure inside the tank once again reached the normal valve opening pressure, the valve opened fully. This period over which the valve was probably in the partially open state, lasted for approximately 4 minutes, and may have considerably shortened the valve cycling period. This type of valve behavior is not what is expected, and it indicates the importance of the operating characteristics of the pressure relief devices on the overall tank/-lading response.

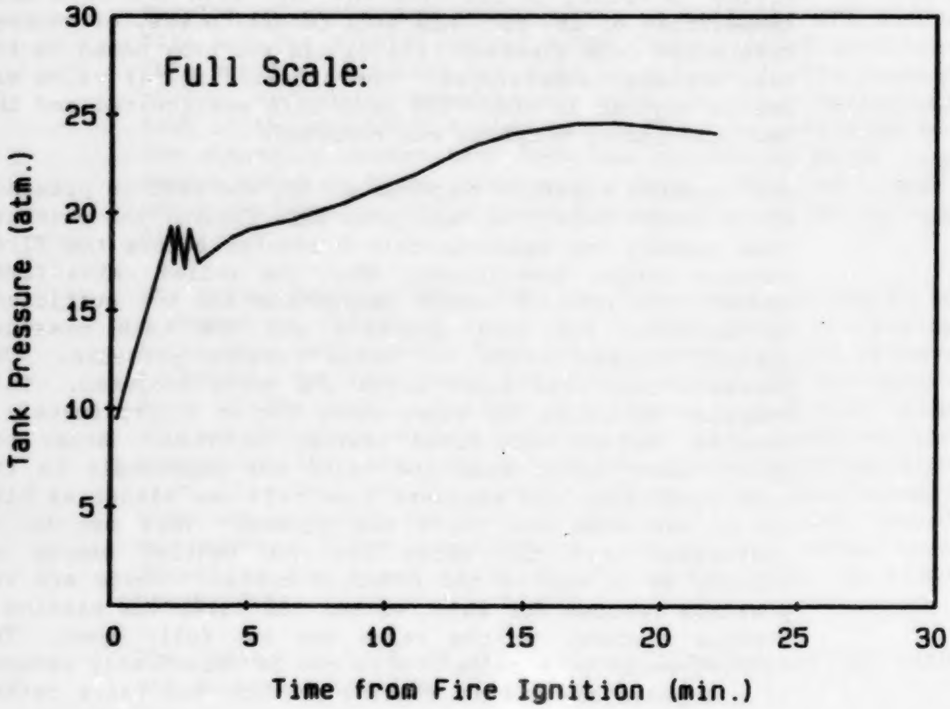

FIGURE 2-24 MEASURED TANK PRESSURE FROM AAR-RPI FIRE TEST # 8 (from Reference (2))

After the valve transient, the tank pressure continued to rise slowly until the tank ruptured at approximately 24 minutes into the fire. The relief valve maintained the tank pressure well below the normal tank bursting pressure of approximately 58 atm. From this it was concluded that the rupture was due to thermally induced degradation of the tank wall properties.

The measured lading temperature distribution is presented in Figure 2-25. The locations of the thermocouples are shown in Figure 2-26. The data points have been joined by straight lines for clarity. The raw data obtained from the test can be found in Reference (2). The data clearly shows that large temperature variations were present in the lading, and therefore any calculations based on the assumption that the lading was in saturated thermodynamic equilibrium would be in error.

The data clearly shows the rapid increase in temperature of the thermocouples located within the vapour space of the tank. This rapid temperature rise was expected because of the low thermal capacity of the vapour. The rate of change of the temperatures in the liquid space was much less than that observed for the vapour space. This was also expected because of the high thermal capacity of the liquid lading.

The data indicates that temperature variations existed in both the liquid and vapour spaces. The temperature variations within the lading existed because the external heating rate was so intense that heat transfer processes within the tank could not distribute the heat uniformly throughout the lading. Warm fluids tend to rise due to the effects of buoyancy, and therefore the temperature of the liquid near the liquid surface were higher than in the core of the liquid. Fluid temperatures near the walls of the tank were also higher, of course, due to the establishment of a thermal boundary layer. The temperature distribution within the tank is important to the modelling considerations because any thermodynamic model that is developed must partially account for these temperature variations.

As time passed in the test, the temperature distributions within the liquid became more uniform, until at around the 10 minute mark, the liquid became almost isothermal. This occurred some time after the relief valve had opened and it is clearly shown in Figure 2-25. Isothermal conditions were established because the venting process causes the

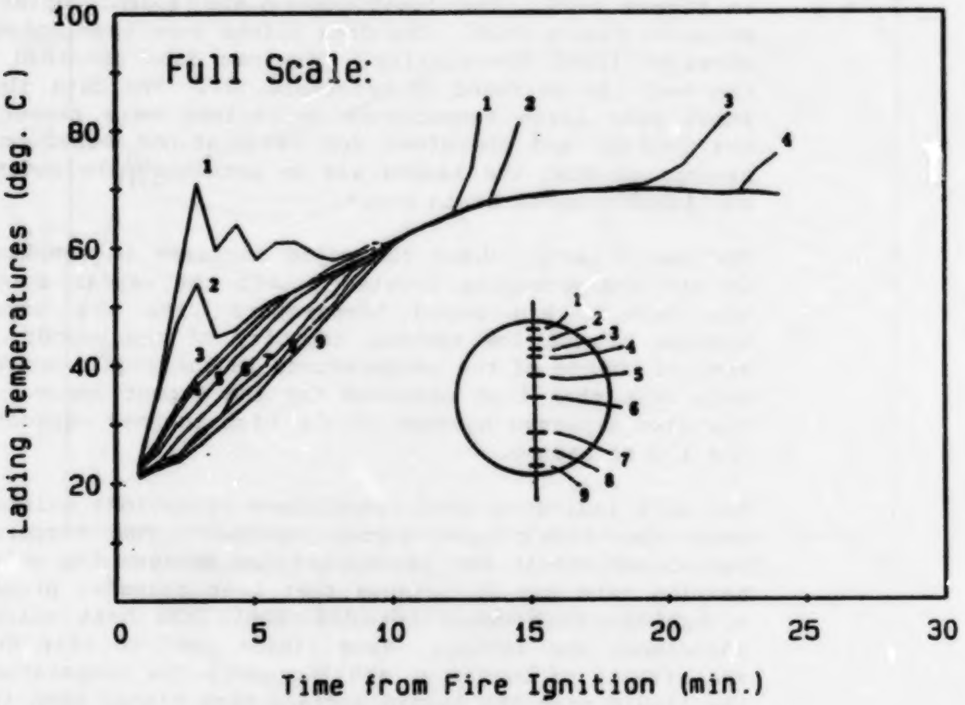

FIGURE 2-25 **MEASURED LADING TEMPERATURES FROM AAR-RPI FIRE TEST # 8 (from Reference (2))**

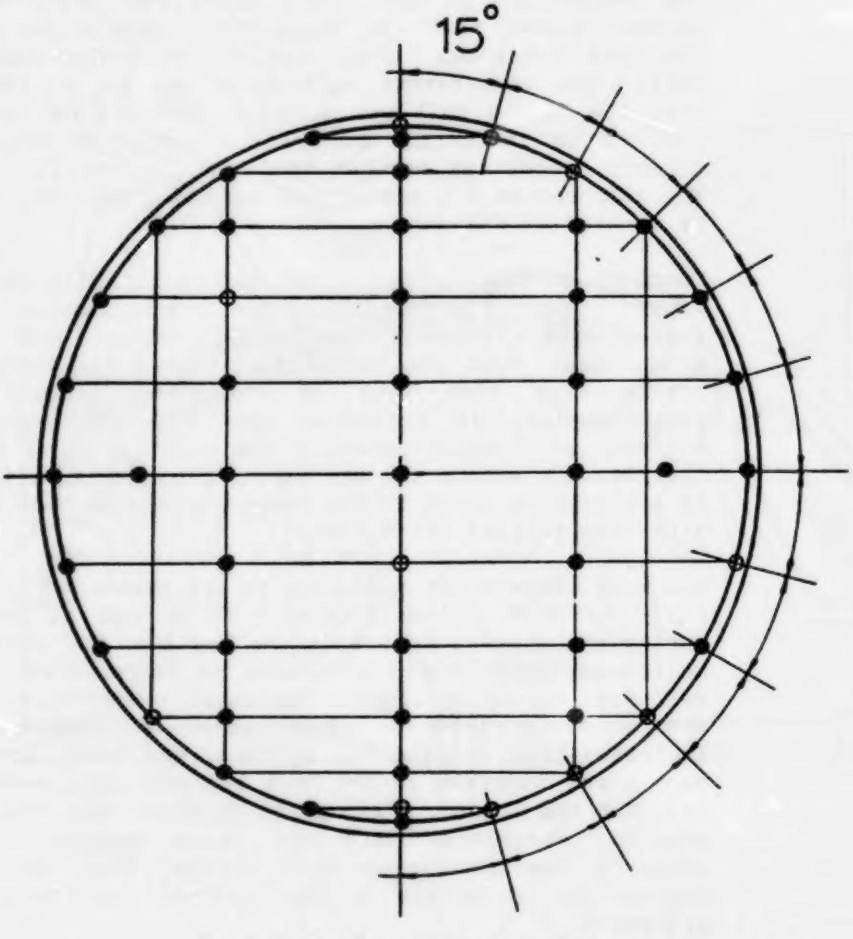

● functioning thermocouples

o non-functioning thermocouples

FIGURE 2-26 KEY TO THERMOCOUPLE LOCATIONS IN THE AAR-RPI TEST # 8 (from Reference (2))

convective mixing actions within the tank to increase because of the churning action of the vapour formation within the liquid.

The temperature of the liquid after this time was a few degrees higher than the saturation temperature based on the tank pressure. There are two possible reasons for this. The temperature difference may be an indication that the liquid bulk was slightly superheated, or it may just be an indication of the difference in the thermodynamic properties between the pure propane and the LPG. The temperature difference was approximately 3°C, and will be ignored in the present study.

There is no distinct interface between the liquid and the vapour region. In reality, a frothing, bubbling, 2-phase region exists between the liquid surface and the dry vapour cap. When the temperature of a given thermocouple breaks away from that of the other liquid wetted thermocouples, it indicates that the thermocouple has entered the 2-phase region. The point in time when the thermocouple enters the dry vapour region may be indicated by a change in slope of the temperature/time plot sometime after the initial break time.

The wall temperature measurements are presented in Figures 2-27 and 2-28. From Figure 2-27 it can be seen that during the initial period of the heating, the entire tank wall experienced rapid increases in temperature. In the wall area wetted by liquid, the rapid temperature increase was suddenly reduced after about 2 minutes. This indicates that boiling had started, and there had been a very large increase in the heat transfer rate between the wall and the liquid. This point in time, when the boiling started, correlates with the valve opening time and supports the conclusion made earlier that the venting process has an effect on the internal convective mixing processes.

Once the boiling process had started, the wall temperatures in the region wetted by liquid rarely exceeded the liquid temperatures by more than 10°C. This small temperature difference existed because of the high heat transfer coefficient that occurs with boiling. The critical heat flux for pure propane on a flat plate is in the order of 630 kW/m^2. (200000 $Btu/hr/ft^2$). The estimated heat fluxes from the fire to the wall of the tank are in the range of 60 to 100 kW/m^2, and therefore it is expected that nucleate boiling was taking place at the liquid wetted surfaces.

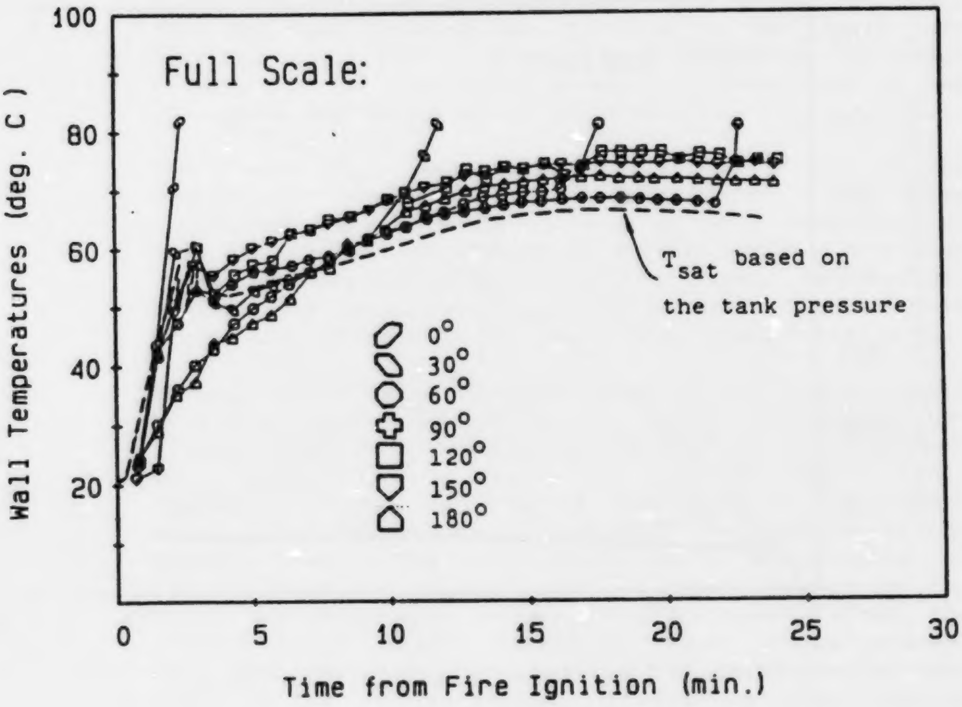

FIGURE 2-27 MEASURED WALL TEMPERATURES FROM THE AAR-RPI FIRE TEST #8 (from Reference (2))

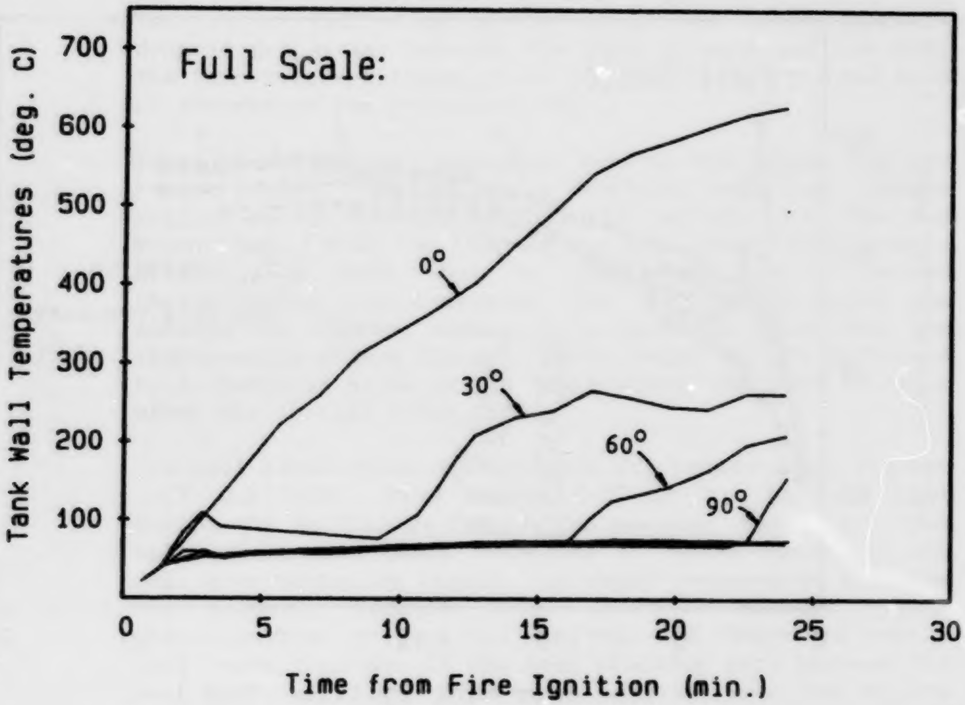

FIGURE 2-28 MEASURED WALL TEMPERATURES FROM THE AAR-RPI FIRE TEST #9 (from Reference (2))

For reference purposes, the saturation temperature for pure propane, based on the recorded tank history, has been plotted along with the recorded wall temperatures in Figure 2-27. The recorded wall temperatures in the liquid wetted wall regions follow this saturation temperature very closely, except for a 10°C offset. If it is assumed that the fluid in contact with this wall region was approximately 10°C cooler than the wall (the temperature difference required for boiling), then it would appear that the tank pressure was dictated by the liquid very near the wall. This of course, is a reasonable conclusion because most of the vapour generation takes place at the wall where nucleation sites are plentiful.

There were also temperatures variations in the liquid wetted wall regions as indicated in Figure 2-27. These variations are seen to be as large as 10°C. The temperature differences are seen to be erratic and may have been caused by non-uniformities in the fire. On average, however, the temperatures near the bottom of the tank were higher than those near the top of the liquid wetted area.

As the liquid level dropped, more of the liquid wetted wall area became exposed to the vapour and 2-phase regions. When the thermocouples located in these regions were exposed to the vapour and 2-phase fluids, their temperatures rose rapidly. As mentioned earlier, these break times can be used to estimate the location of the liquid level. The wall temperature measurements as presented in Figure 2-27 show distinct changes in the rates at which the temperatures increased after the initial break time. Possibly, these slope changes indicated the point in time when the thermocouples came clear of the 2-phase region. If this is true, then it appears as if the vapour cap was completely displaced by the frothing 2-phase region because the upper-most thermocouple readings also show these slope changes. Of course, there is considerable scatter in the test data and this conclusion cannot be fully substantiated.

In the vapour wetted wall region the temperatures rose rapidly, as shown in Figures 2-27 and 2-28, because of the ineffective cooling at this location. This was, of course, because of low convective and radiant heat transfer rates. As high wall temperatures were reached, the heat transfer due to thermal radiation became increasingly important.

The test ended with the tank rupturing at approximately 24.5 minutes into the fire. Since the tank pressure was well below the normal bursting pressure of the tank, it could be concluded that the tank failure was a result of local weakening in the tank wall due to high temperatures.

Coated Tank: This test involved a tank (RAX 202) which was spray insulated with a 3.2 mm. thick coat of 'Korotherm' intumescent thermal barrier, and was loaded with propane to approximately 85% capacity. Detailed records of the test conditions were not taken and it was therefore assumed that the test conditions were similar to those for the unprotected tank test (RAX 201). Results of the test can be found in Reference (2).

The test involving the thermally coated tank was plagued with instrumentation failures. All but one of the pressure transducers failed during the test, and the single remaining transducer had poor response characteristics. The tank pressures presented in the report were approximated from the wall temperatures and mean vapour temperatures. There is little evidence to indicate that this method of predicting the tank pressure was appropriate, and therefore the predicted tank pressures were not considered very accurate.

Figure 2-29 presents the estimated tank pressure history for RAX 202. As can be seen from the figure, the tank pressurized rapidly for the first five minutes, then the pressure remained constant for seven minutes, then increased rapidly until the valve opened at approximately sixteen minutes into the fire. It is difficult to explain this pressurization pattern. It is likely, however, that the initial pressurization rate shown is inaccurate and that the pressure history followed the dashed line shown on the figure.

As mentioned previously, the tank pressure history was estimated from wall temperatures and the mean vapour temperatures. There is little evidence to prove that this method of predicting the tank pressure is accurate. In fact, if one studies the results from the RAX-201 tests, the tank pressurization more closely follows the saturation pressure based on the liquid wetted wall temperatures. The dashed line in Figure 2-29 is based on the measured liquid wetted wall temperatures from RAX-202. This pressurization history (dashed line) is the typical ramp increase in pressure seen in all of the tank-car fire tests.

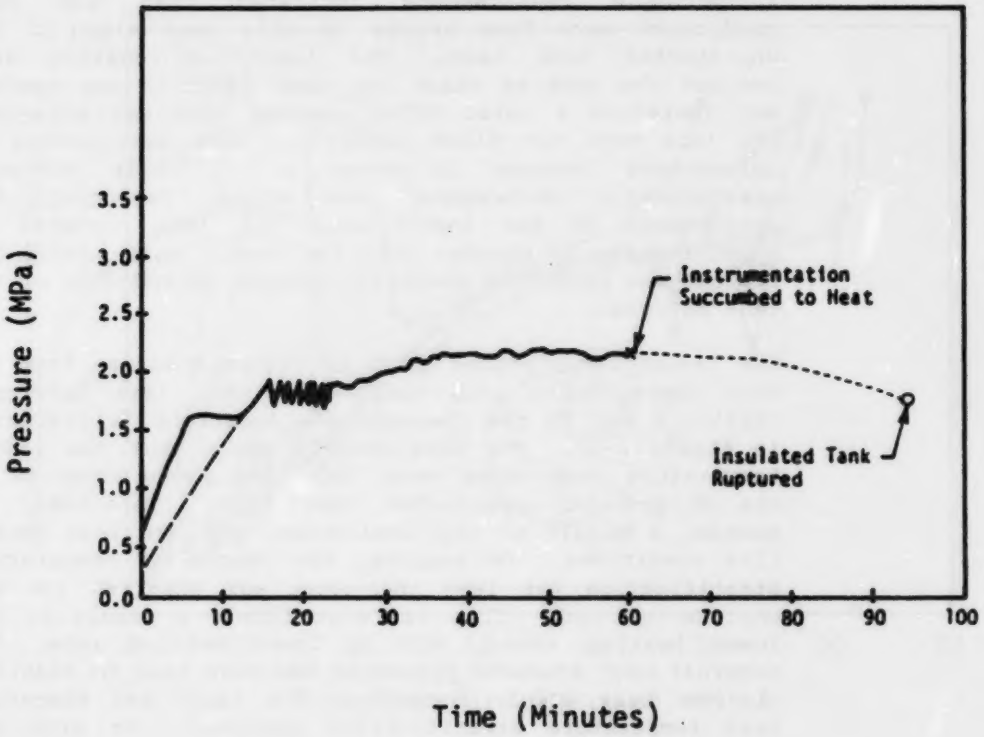

FIGURE 2-29 MEASURED TANK PRESSURE FROM AAR-RPI TEST #9 (from Reference (2))

The remainder of the pressure history appears to show the basic trend seen in all the fire tests. The only difference being the duration of the test. The insulation layer resulted in a lower heat input to the tank and therefore the time scale of the test was lengthened.

The later valve opening time, as compared to the unprotected tank test, was a result of two things. Flame thermocouple measurements indicated that the fire conditions were less severe in this test than in the unprotected tank test. The insulation coating also reduced the rate at which heat was added to the system, and therefore a later valve opening time was expected. The fact that the flame conditions were less severe is unfortunate because it makes it difficult to make statistically defendable conclusions regarding the performance of the insulation. The tank ruptured at approximately 93 minutes into the test. Once again, the rupture was caused by thermally induced degradation of the tank material.

The lading temperatures shown in Figure 2-30 are from the rear thermocouple grid within the tank (see Reference (16)). A key to the thermocouple locations is presented in Figure 2-31. The data clearly shows that the lading temperature rise rates were less than those observed in the full-scale unprotected tank test. This was, of course, a result of the insulation, and the less severe fire conditions. On average, the degree of temperature stratification was less than what was observed for the unprotected tank. This was most likely a result of the lower heating rate. With a lower heating rate, the internal heat transfer processes had more time to distribute the heat evenly throughout the tank, and therefore less temperature stratification occurred. As with the unprotected tank test, the liquid became near isothermal sometime after the relief valve had opened. The lading reached near saturation conditions at approximately 35 minutes into the test. As mentioned, temperature readings beyond 45 minutes into the test are suspected to include large errors.

The wall temperatures recorded from the rear thermocouple grid are presented in Figure 2-32. The wall temperatures in the vapour wetted region followed the same trends as observed from the unprotected tank test data. Because of the poor cooling effect of the vapour, the wall temperatures in the vapour wetted region increased rapidly. The development of the frothing 2-phase region eventually

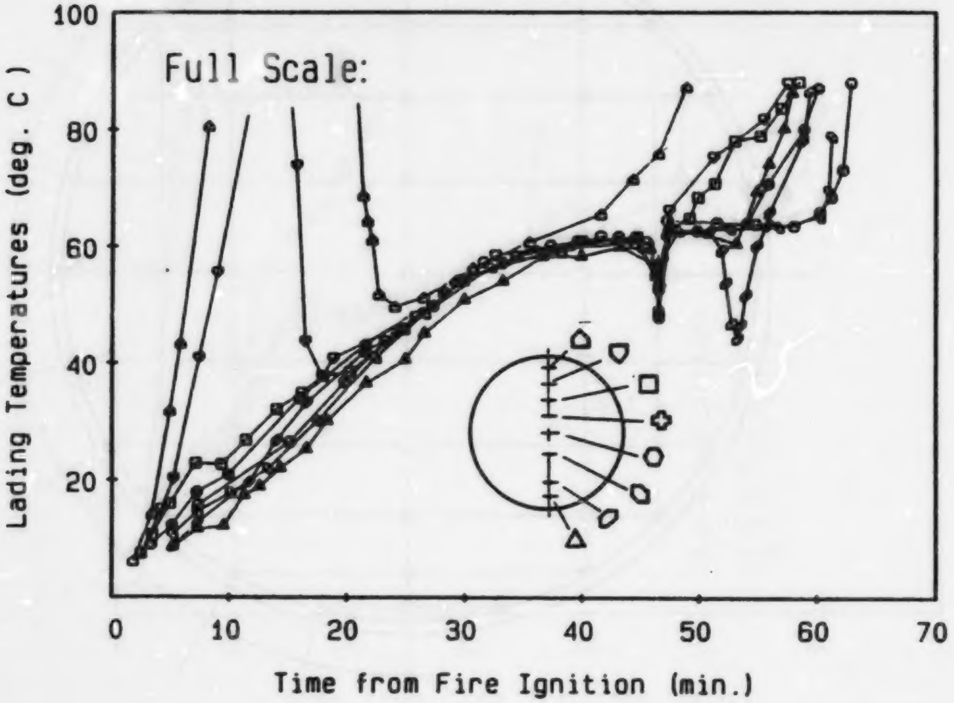

FIGURE 2-30 MEASURED LADING TEMPERATURES FOR AAR-RPI TEST #9 (from Reference (2))

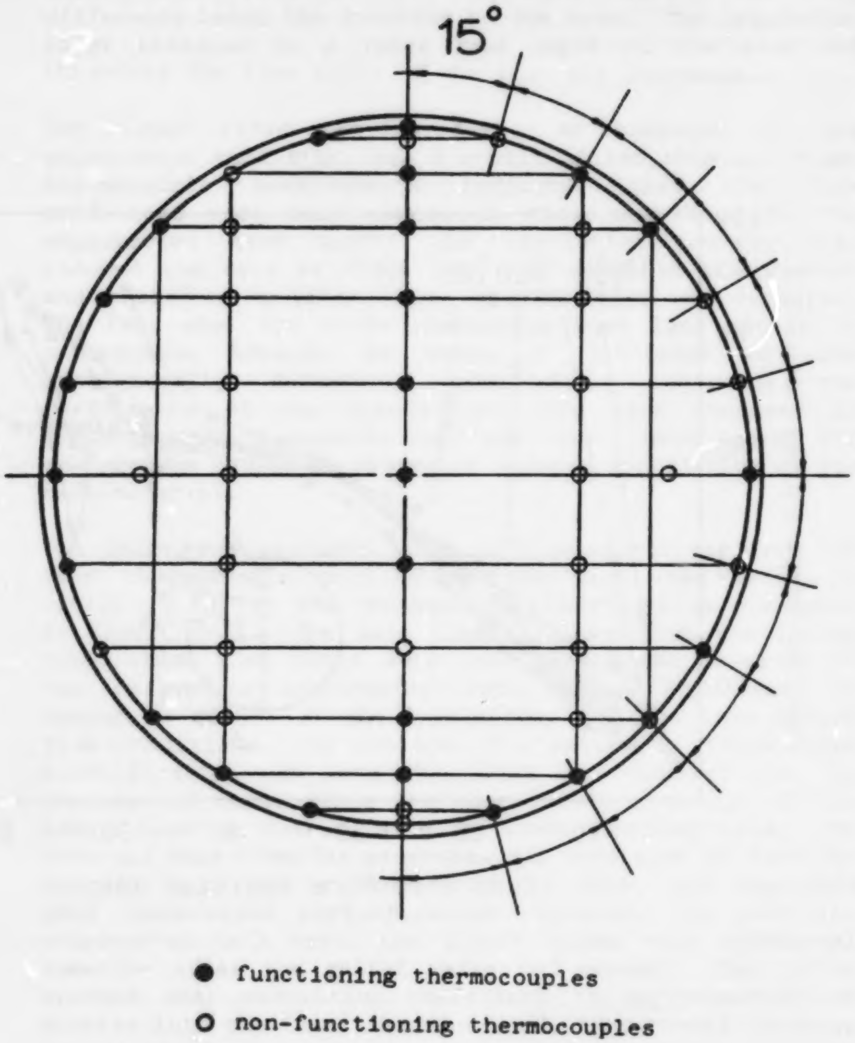
15°
● functioning thermocouples
○ non-functioning thermocouples

FIGURE 2-31 KEY TO THERMOCOUPLE LOCATIONS FOR AAR-RPI TEST #9 (from Reference (2))

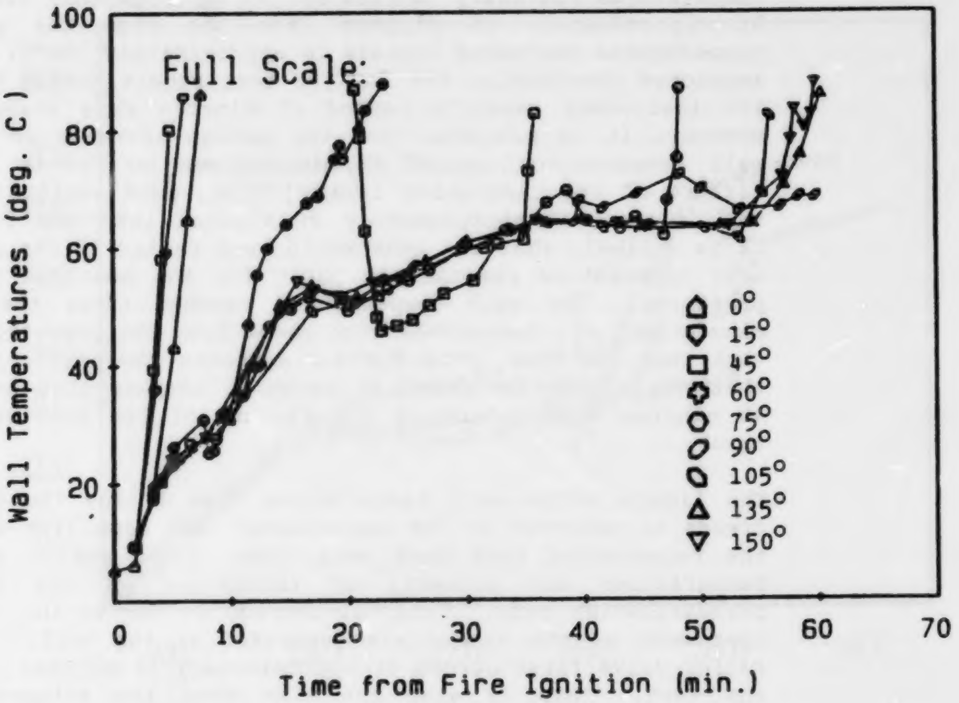

FIGURE 2-32 MEASURED WALL TEMPERATURES FROM AAR-RPI TEST #9 (from Reference (2))

caused wet fluid to cover some of the upper thermocouples. As these thermocouples were covered, their temperatures rapidly dropped. It appears that the uppermost thermocouple was not covered by the 2-phase region, and therefore the vapour cap was never completely displaced, as it was observed in the unprotected tank test.

The top-dead-centre wall temperatures are shown in Figure 2-33. As can be seen from this figure the tdc wall temperatures initially leveled off at approximately 320°C. At approximately 45 minutes into the test the wall temperatures increased rapidly to approximately 700°C. As mentioned previously, the RAX-202 test report stated that the instrument readings beyond 45 minutes were suspect. However, it is possible that the sudden increase in tdc wall temperatures beyond 45 minutes was caused by the failure of the insulating layer. This would explain the tank rupture at approximately 90 minutes into the fire. It is unlikely that the tank would have failed if the peak wall temperature remained at 320°C for the measured tank pressures. The wall temperatures reached after the 45 minute mark are comparable with those from the unprotected tank test RAX-201. This further supports the possibility that the sudden increases in measured temperatures after 45 minutes were caused by the failure of the insulation layer.

The liquid wetted wall temperatures also follow the same trends as observed in the unprotected tank case. As with the unprotected tank test data, the liquid wetted wall temperatures are probably an indication of the tank pressurization rate. This, of course, is due to the fact that most of the vapour was generated at the wall. The relief valve first opened at approximately 16 minutes into the test. This is also the time when the saturation pressure, based on the mean liquid wetted wall temperature, exceeded the valve opening set pressure. In other words, the actual tank pressure can be approximated by the saturation pressure based on the liquid wetted wall temperature. Assuming this is correct, the tank pressure never exceeded approximately 23 atmospheres.

The estimated liquid level history for RAX-202 is presented in Figure 2-34. The liquid level history is typical of the fire tests conducted. Initially the liquid level rises due to thermal expansion of the liquid and some lifting due to vapour generation in the liquid. During the valve cycling period, the liquid level remained relatively constant. During continuous venting, the liquid level dropped rapidly because of the high venting rate.

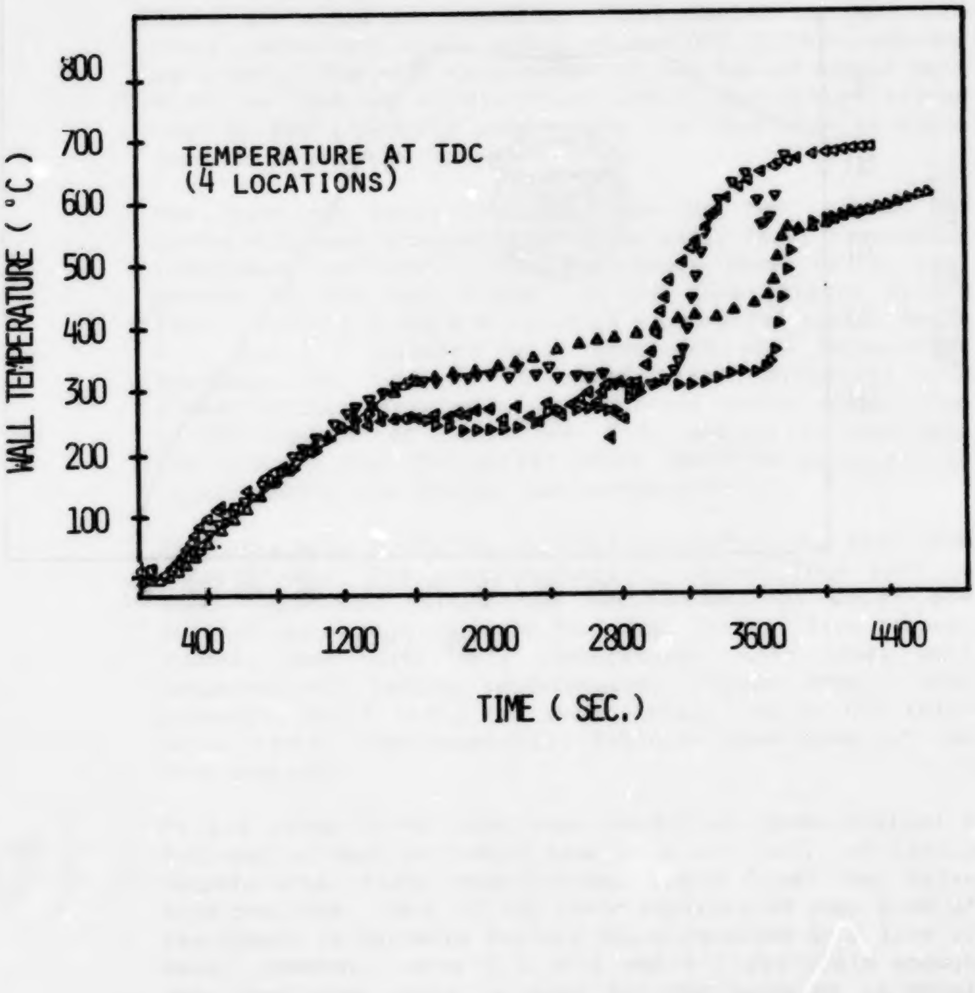

FIGURE 2-33 MEASURED WALL TEMPERATURES FROM AAR-RPI TEST #9 (from Reference (2))

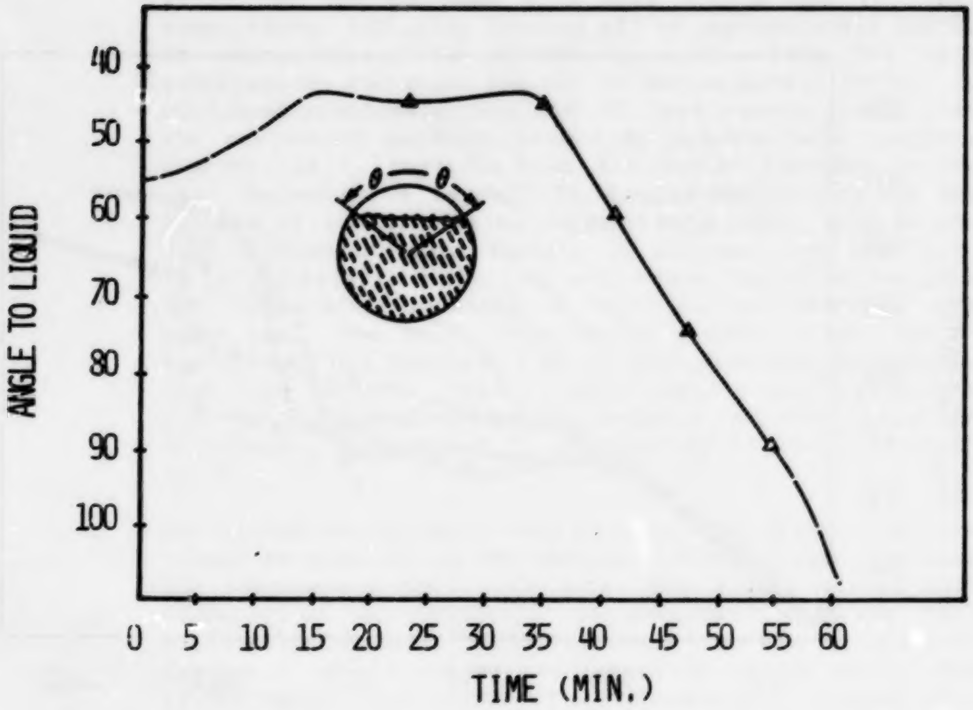

FIGURE 2-34 ESTIMATED LIQUID LEVEL FROM AAR-RPI TEST #9 (from Reference (2))

The results of this test show that external heat barriers can increase the life of a tank exposed to an engulfing fire. However, external heat barriers do not necessarily prevent a tank from rupturing.

2.2.2.2 AAR-RPI: 1/5 Scale Tests

The AAR-RPI 1/5 scale fire tests (4, 5 6, 7) were conducted as part of phase 11 of the AAR-RPI tank-car research program. These tests involved 1/5 linear scale tanks subjected to engulfing fires fueled by JP4. In total, seven such scale models of the DOT 112340W tank-car were used. The wall thicknesses of the Scaled models were equal to that of a full-scale tank. The relief valves used on the 1/5 scale models were the same size as those used on full-scale tank-cars.

The first two tests used water as the test fluid. No useful data was obtained from these early tests because of instrument failures. The remaining five tests used propane as the test fluid. Of the five propane filled tanks, tests # 3 and # 6 involved unprotected tanks, tests # 4, and # 5 involved tanks protected with intumescent coatings, and test # 7 involved a tank protected with foamed urethane insulation with a steel jacket cover. One of the unprotected tanks, test # 6, was rolled over onto its side so that the relief valve would be submerged in liquid during the initial heating period.

The tests were conducted in a pit to protect the fire from cross winds. The instrumentation varied from test to test. However, during the test series at least one attempt was made to measure fire heat fluxes, fire temperatures, tank outer wall temperatures, tank inner wall temperatures, lading temperatures, liquid level, tank pressure, valve lift, and sound level. As in the full-scale tests, instrumentation failures made some of the data suspect.

Of the seven tests that were conducted, none yielded a full-set of data including tank pressure, wall and lading temperatures, flame temperatures, liquid level, and valve stem position. Each of the tests experienced some kind of instrument or hardware failure which resulted in a loss of data. However, tests # 3, # 6 and # 7 did yield enough data that they could be used for the purposes of model validation. Some of this data is described in the following pages.

AAR-RPI Test # 3: This test involved the fire testing of a fifth-scale unprotected tank-car. The tank was in the upright position for the test and was equipped with a full-sized pressure relief valve. The tank wall thickness was equal to that of a full-scale tank-car.

The tank was equipped with lading, wall and fire thermocouples. Other details of the test can be found in References (6, 7). However, a publication relating only to test # 3 could not be found, and therefore some test details are not available.

It has been estimated that the initial temperature and fill were approximately 21°C (70°F) and 86% respectively. The fire temperature data for this test was also not found, and therefore it will be assumed that it was similar to the other AAR-RPI fifth-scale tests (ie ≅ 870°C).

Figure 2-35 presents the pre-venting pressurization data from test # 3. As can be seen from the figure, the relief valve first opened at approximately 60 seconds into the fire. The relief valve cycled through the entire test as expected, because of its oversizing for the 1/5 scale tank. During the test, the cycling pressure range, and frequency changed. This changing of the pressure relief valve set pressure is an indication of the complex operating characteristics of such devices.

Figure 2-36 presents the measured wall temperatures for test # 3. The wall temperatures show the typical response seen in all of the tank-car fire tests. Because of the short length of the test, the wall temperatures never reached any equilibrium level. The temperature break times are clearly seen as the liquid level dropped.

Figure 2-37 presents the estimated liquid level from the temperature data obtained from test # 3. As can be seen from the figure, the liquid level began to drop rapidly as soon as the relief valve started cycling open and closed. The tank did not, however, empty any more rapidly than the Transport Canada 1/5 scale tests even though the AAR-RPI test tanks were fitted with larger valves. This is because the venting rate is dictated by the heat input rate. Because the relief valve cycled during the entire test, the net venting rate was approximately the same as for a much smaller valve that remains open, as in the case of the Canadian fifth-scale tests.

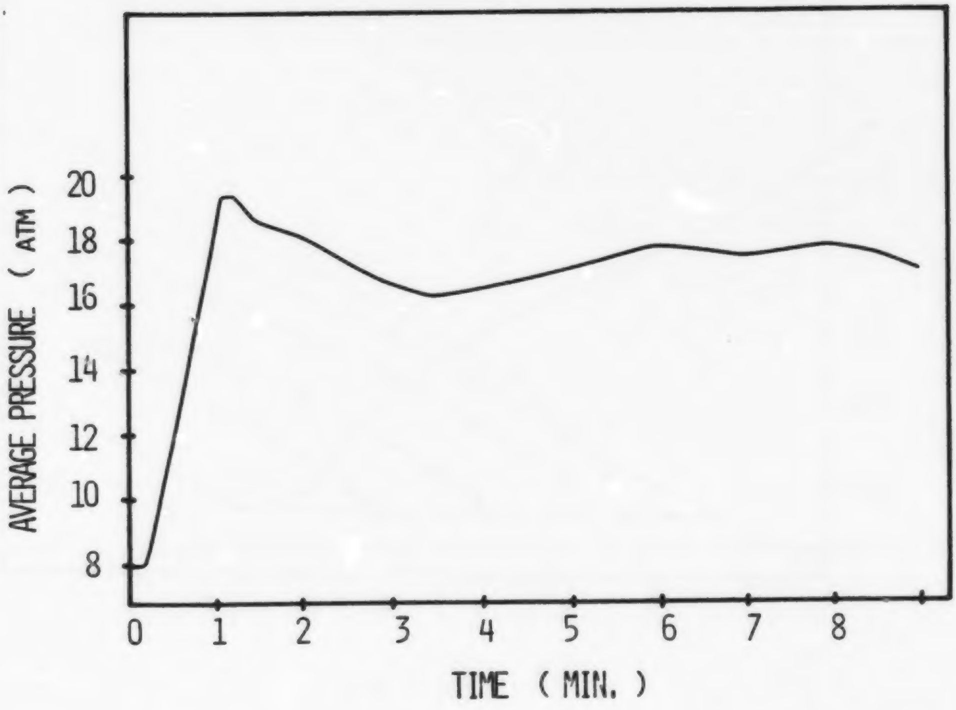

FIGURE 2-35 MEASURED TANK PRESSURE FROM AAR-RPI TEST #3 (from Reference (6))

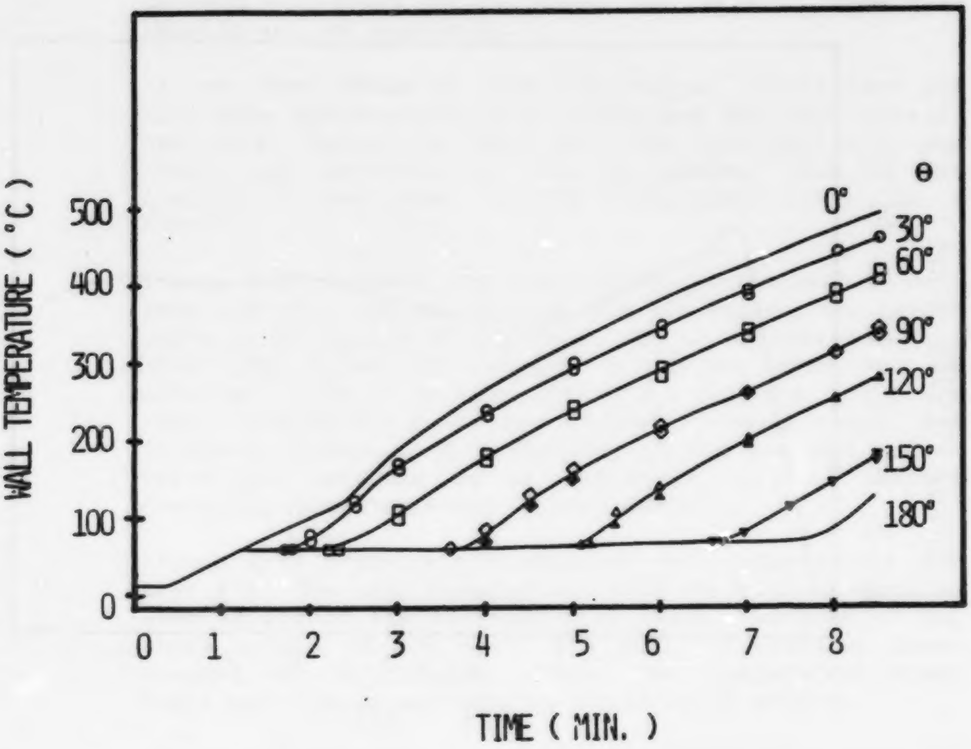

FIGURE 2-36 MEASURED WALL TEMPERATURES FROM AAR-RPI TEST #3 (from Reference (6))

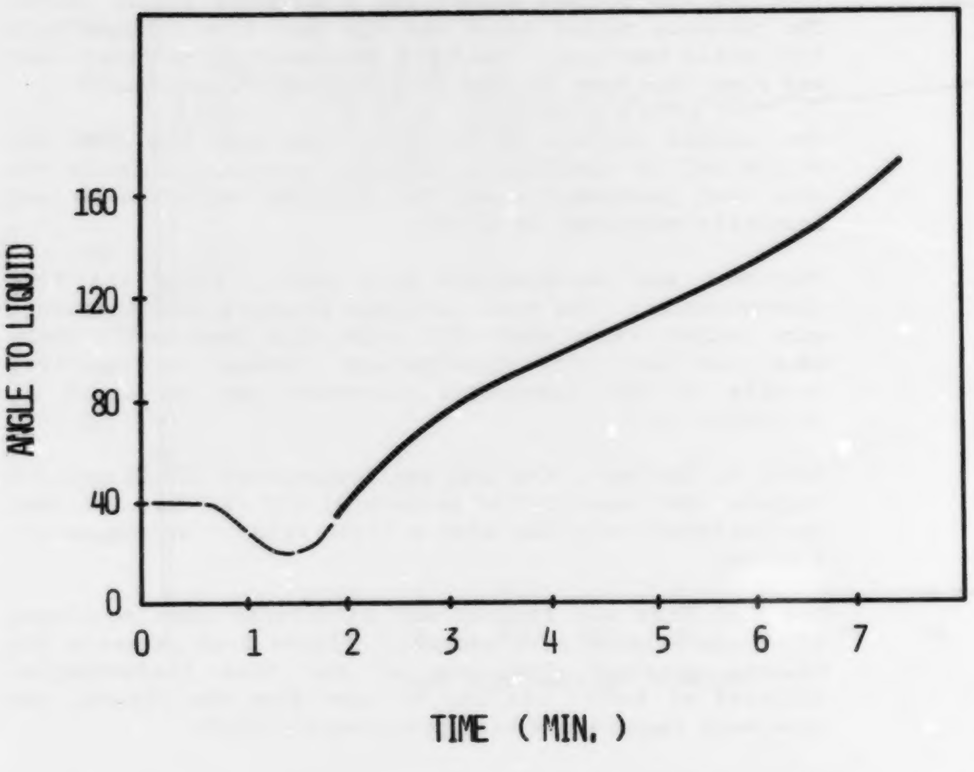

FIGURE 2-37 ESTIMATED LIQUID LEVEL FROM AAR-RPI TEST #3 (from Reference (6))

The test ended with the tank empty and intact. The tank did not fail because of a combination of effects including the low wall stresses because of the thicker wall (same thickness as full-scale tank), the lower peak wall temperatures, and the rapid emptying of the tank.

AAR-RPI Test # 6: This test involved a fifth-scale tank filled with propane, exposed to an engulfing fire. The tank was unprotected except for a pressure relief valve. The pressure relief valve was the same size as used on a full-scale tank-car. The wall thickness of the test tank was also the same as that of a full-scale tank-car.

The unusual feature of this test was that the tank was rolled 90° to simulate a derailed tank-car. This is the only test performed where the pressure relief valve was initially submerged in liquid.

The tank was instrumented with wall, lading and fire thermocouples. The tank internal pressure and the pressure relief valve stem lift were also measured. There were also heat flux calorimeters located in the fire. Details of the instrument placement can be found in Reference (4).

Prior to the test, the tank was loaded with 226 US gallons (approx. 85% capacity) of propane at 5°C (41°F). The test was performed on a day with a light wind of approximately 3 knots.

The pool fire was ignited and an intense fire developed after approximately 20 seconds. Figure 2-38 presents the results obtained from one of the fire thermocouples (located at 3:00). As can be seen from the figure, the fire mean temperature was approximately 850°C.

Figure 2-39 presents the pre-venting pressurization of the tank. For the first 30 seconds the pressurization rate is relatively slow due to the 20 second fire start-up time. After 30 seconds the tank pressurized rapidly until the relief valve opened for the first time at approximately 45 seconds into the fire. Valve cycling started at approximately 75 seconds. The valve continued to cycle until the pressure transducers failed at approximately 330 seconds.

Figure 2-40 presents some of the lading temperature data from the test. A key to the thermocouple locations is given in Figure 2-41. The scale of Figure 2-40 does not

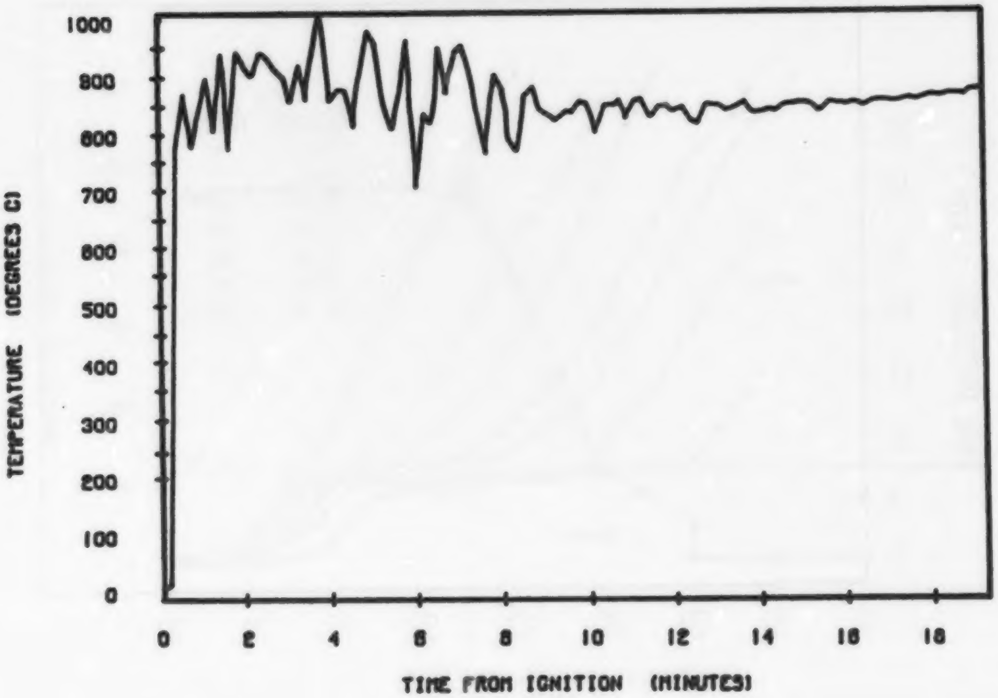

FIGURE 2-38 MEASURED FIRE TEMPERATURE IN AAR-RPI TEST #6 (from Reference (4))

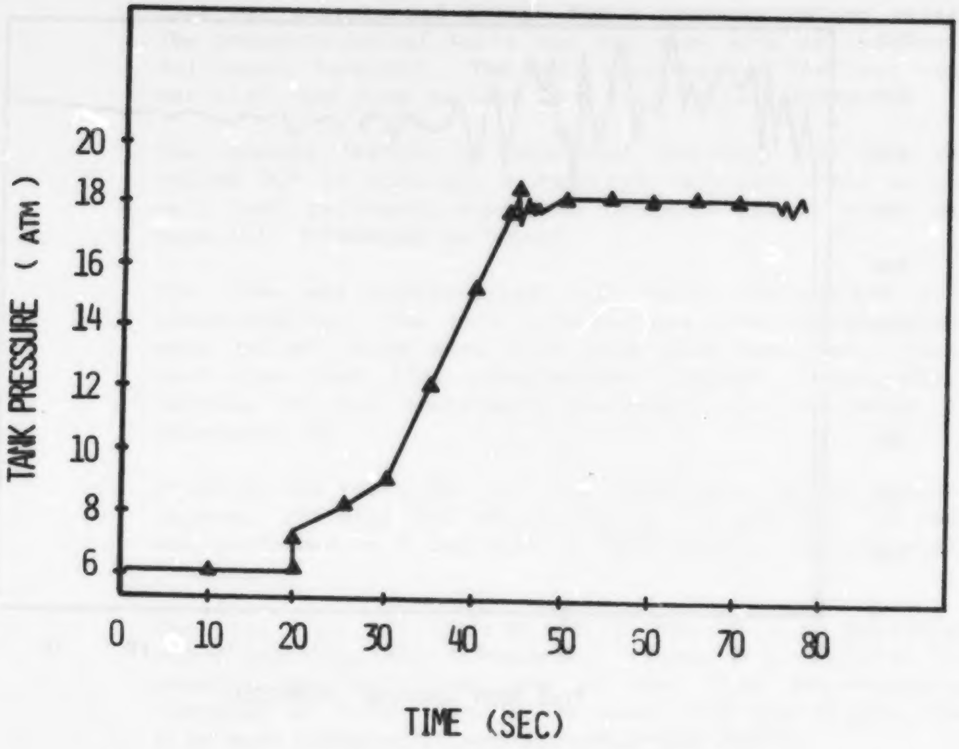

FIGURE 3-39 MEASURED TANK PRESSURE FROM AAR-RPI TEST #6 (from Reference (4))

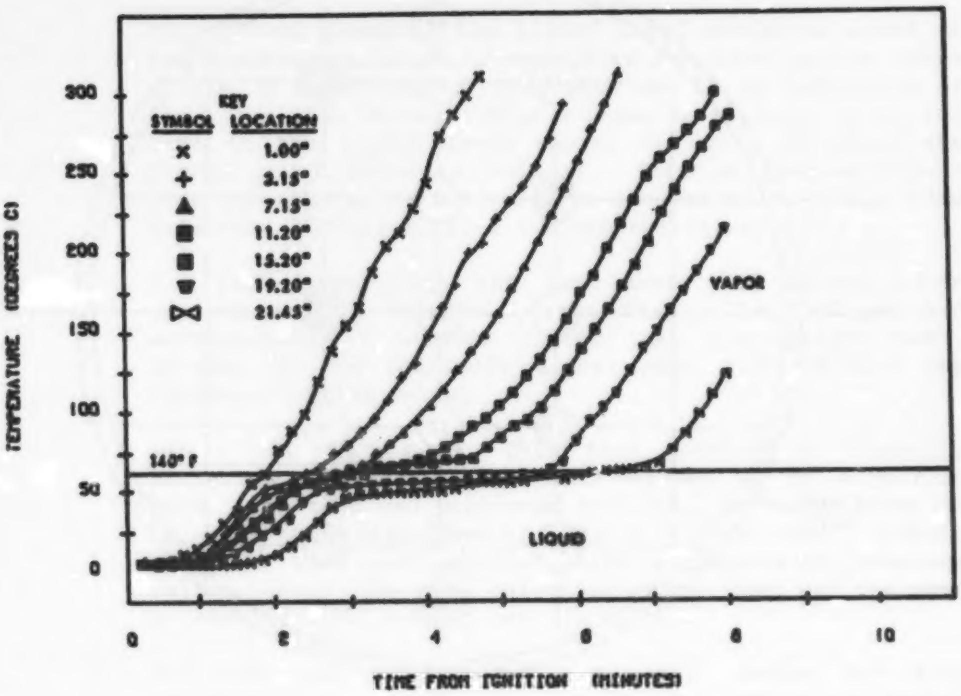

FIGURE 2-40 MEASURED LADING TEMPERATURES FROM AAR-RPI TEST #6 (from Reference (4))

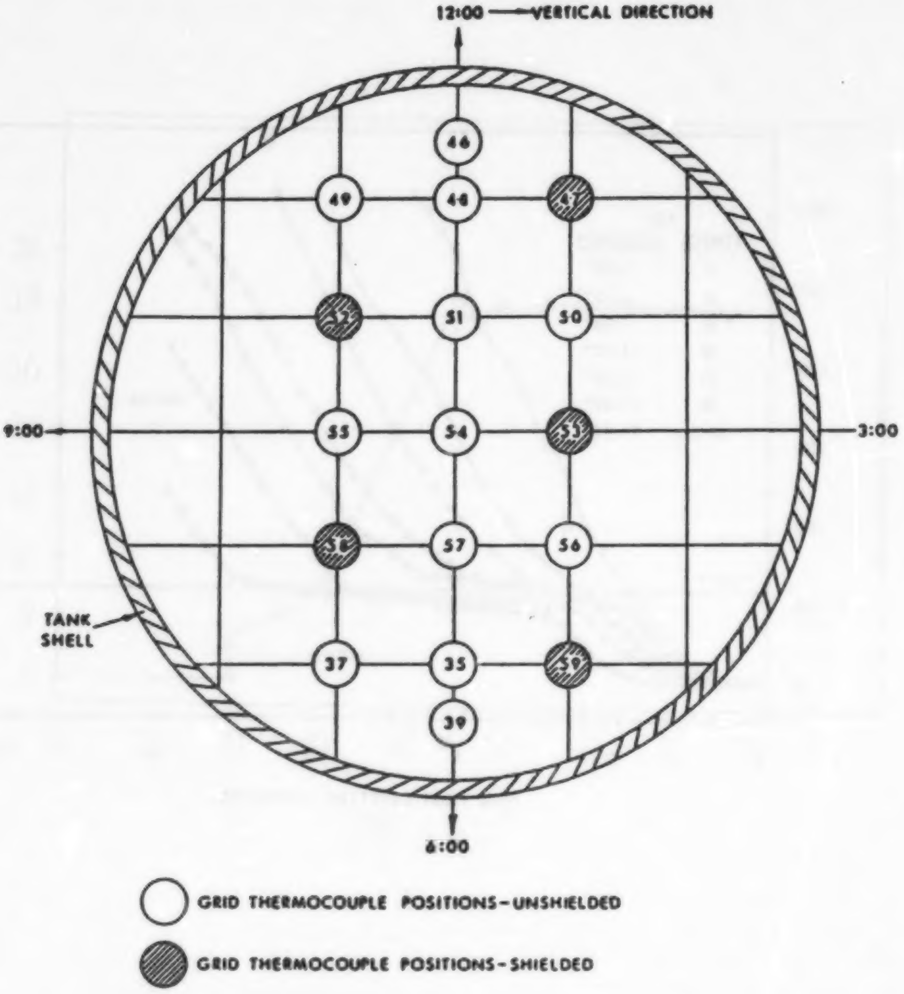
12:00 —VERTICAL DIRECTION
46
49
48
47
52
51
50
9:00
55
54
53
3:00
58
57
56
TANK SHELL
37
35
59
39
6:00
GRID THERMOCOUPLE POSITIONS-UNSHIELDED
GRID THERMOCOUPLE POSITIONS-SHIELDED

FIGURE 2-41 KEY TO THERMOCOUPLE LOCATION FOR AAR-RPI TEST #6 (from Reference (4))

allow for the identification of temperature stratification in the liquid. Figure 2-40 does, however, clearly show the temperature break times.

Figure 2-42 presents the measured wall temperatures from test #6. As can be seen from the figure, the wall temperature increases follow the typical pattern for all the fire tests.

Figure 2-43 presents the liquid level estimates based on the temperature break times. Note the bend in the curve at the 2½ minute mark. This bend may be an indication of the valve flow changing from 2-phase to vapour. After the bend in the liquid level curve, the rate at which the liquid level drops is reduced. This is because vapour flow through the relief valve results in a lower mass flow rate than for liquid flow through the valve.

The test ended with the tank empty and intact after approximately 6 minutes in the fire. The tank emptied approximately 2 minutes faster than the upright tank, because of the initially higher mass flow through the submerged relief valve.

AAR - RPI Test # 7: This test involved a thermally protected fifth-scale tank-car exposed to an engulfing fire. The tank was protected by a 10.2 cm thick layer of poly-urethane foam covered with a 0.3 cm steel jacket. The tank was also equipped with a full-sized pressure relief valve. The wall thickness of the tank was the same as that of a full-scale tank (1.59 cm).

The tank was instrumented with wall, lading and fire thermocouples and pressure transducers. There were also some fire heat flux calorimeters and valve lift indicators. Further details of the instrumentation and its placement can be found in Reference (5).

Prior to the test the tank was loaded with 226 US gal. of propane (approx 86% capacity). The initial propane temperature was 5.6°C (42°F). The fire was ignited and rapidly developed into an intense engulfing fire.

Figure 2-44 presents data taken from one of the fire thermocouples. It shows that the fire startup took approximately 30 seconds as with the other tests. The fire intensity was relatively constant up until approximately 45 minutes. The mean fire temperature was approximately 900°C (1650°F).

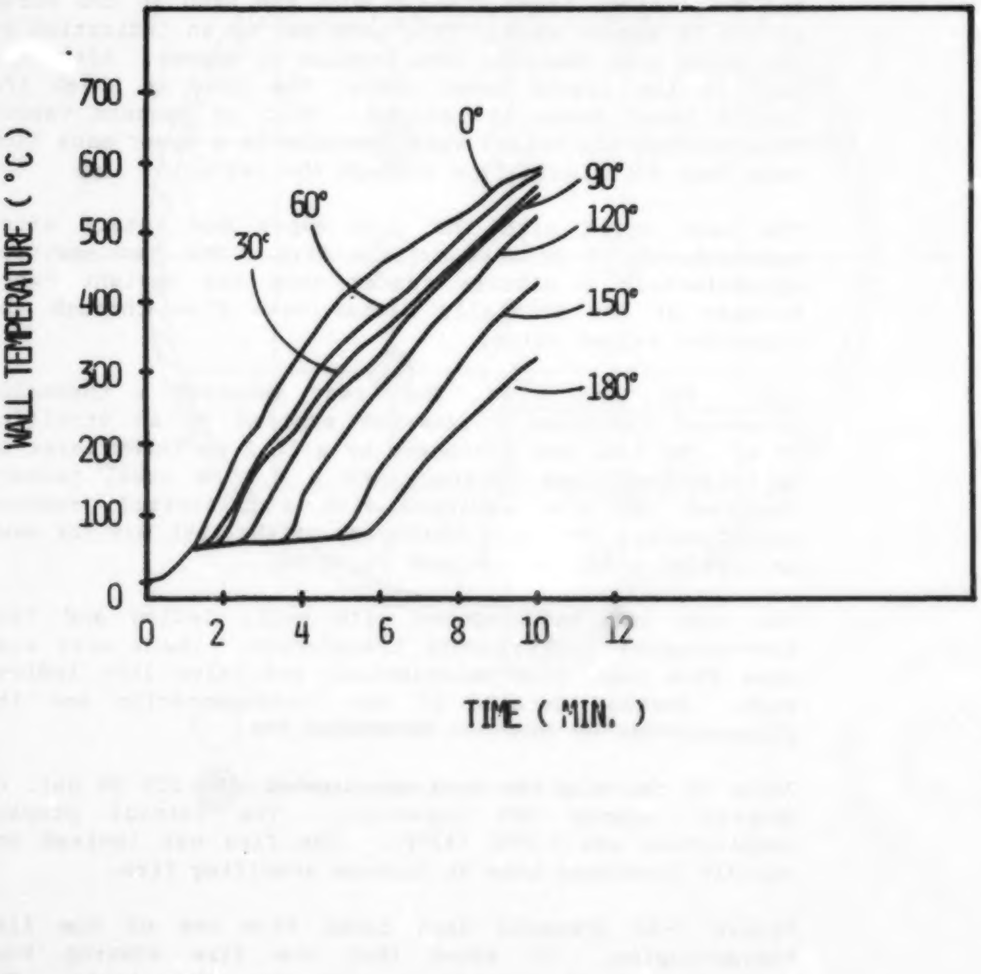

FIGURE 2-42 MEASURED WALL TEMPERATURES FOR AAR-RPI TEST #6 (from Reference (4))

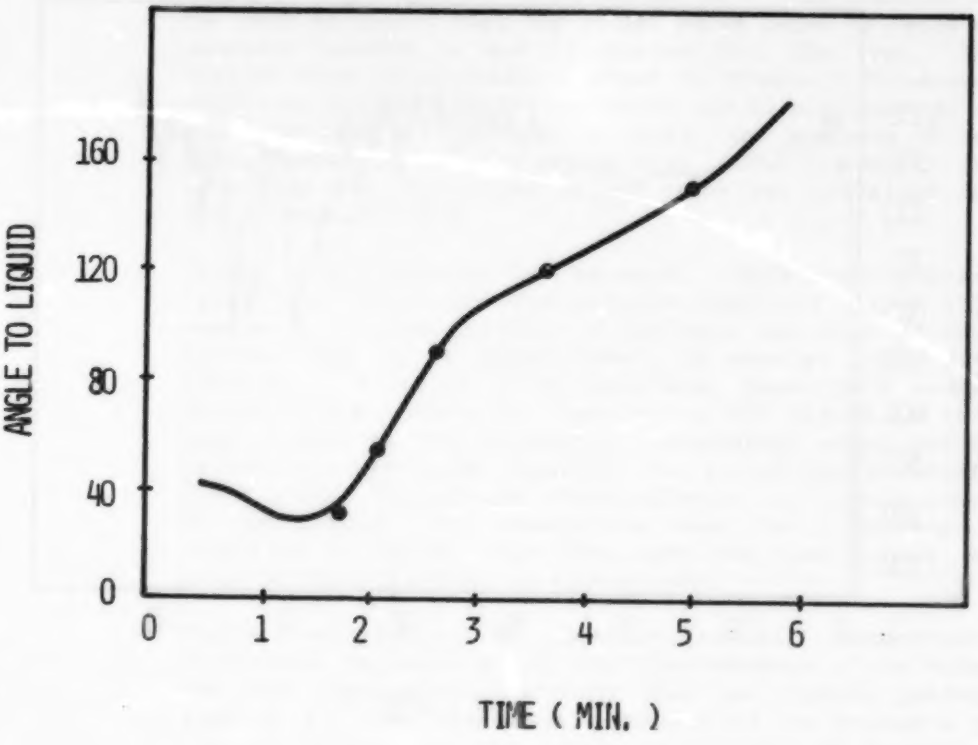

FIGURE 2-43 ESTIMATED LIQUID LEVEL FOR AAR-RPI TEST #6 (from Reference (4))

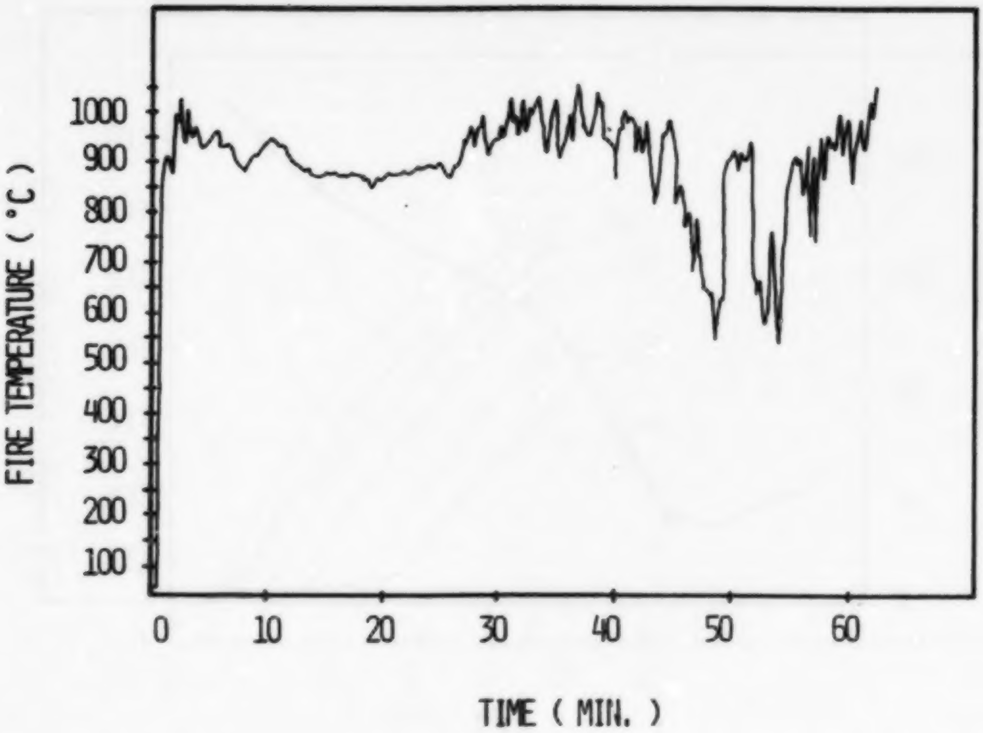

FIGURE 2-44 MEASURED FIRE TEMPERATURE IN AAR-RPI TEST #7 (from Reference (5))

Figure 2-45 presents the data obtained from one of the two pressure transducers. Data obtained prior to the 320 second mark were erratic due to a malfunction. The malfunction was corrected and the pressure data after approximately the 15 minute mark is accurate. Unfortunately the tank initial pressurization was lost due to the malfunction.

Based on the measured liquid wetted wall temperatures, it has been estimated that the relief valve began to cycle at sometime between 10 and 15 minutes into the test. The initial tank pressurization shown in Figure 2-45 assumes the valve opened first at approximately 15 minutes. As in the other AAR-RPI fifth-scale tests, the pressure relief valve cycled through the entire test. This was due to the fact that the full-sized relief valve was oversized for the fifth-scale tank.

Figure 2-46 presents the measured lading temperatures. Figure 2-47 shows the thermocouple locations. From this figure it is also possible to estimate the valve initial opening time to be approximately 15 minutes after fire ignition. It is at 15 minutes when there is a sudden change in the temperature rise rate of the liquid and this bend occurs at the saturation temperature which corresponds to a pressure equal to the relief valve setting (18.4 atm). Temperature stratification is clearly shown in the liquid. The temperature near the liquid/vapour interface is higher than that near the tank bottom, as expected from buoyancy considerations.

Figure 2-48 presents the inner surface wall temperatures at various locations around the circumference of the tank. The wall temperature increases show the typical pattern seen in all the fire tests. Because of the presence of the insulation, the time scale is expanded by roughly a factor of 10. In other words, the tank responds 10 times faster when it is not insulated. An interesting item to note on Figure 2-48 is the initial delay in the response of the tank to the fire. The inner wall temperatures do not increase significantly during the first 4 minutes of the test. This time lag could not have been caused by the fire start up which lasted about 1 minute. Possibly, during the first 4 minutes, the high temperatures degraded the urethane foam insulation, and this degradation process absorbed some of the heat added from the fire.

Figure 2-49 presents the liquid level in the tank estimated from the measured wall temperatures. As can be

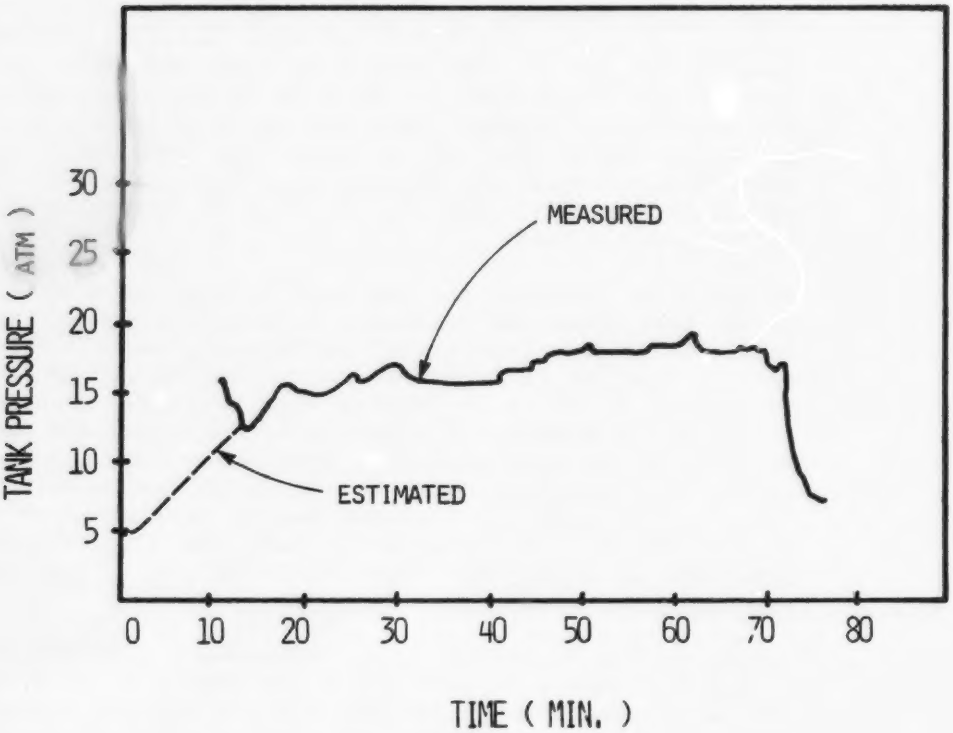

FIGURE 2-45 MEASURED TANK PRESSURE FROM AAR-RPI TEST #7 (from Reference (5))

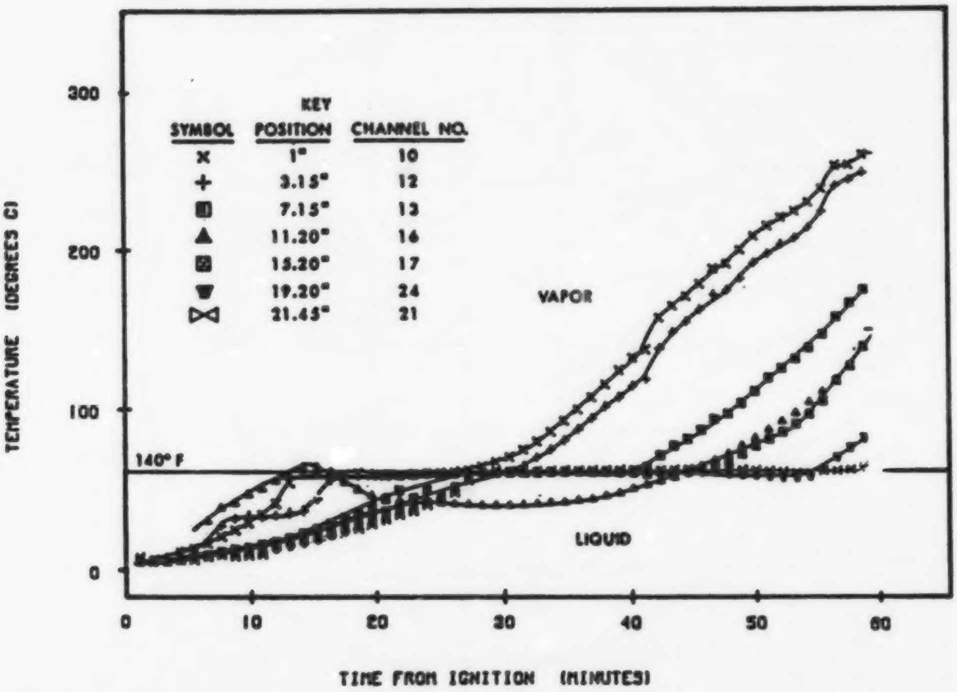

FIGURE 2-46 MEASURED LADING TEMPERATURES FROM AAR-RPI TEST #7 (from Reference (5))

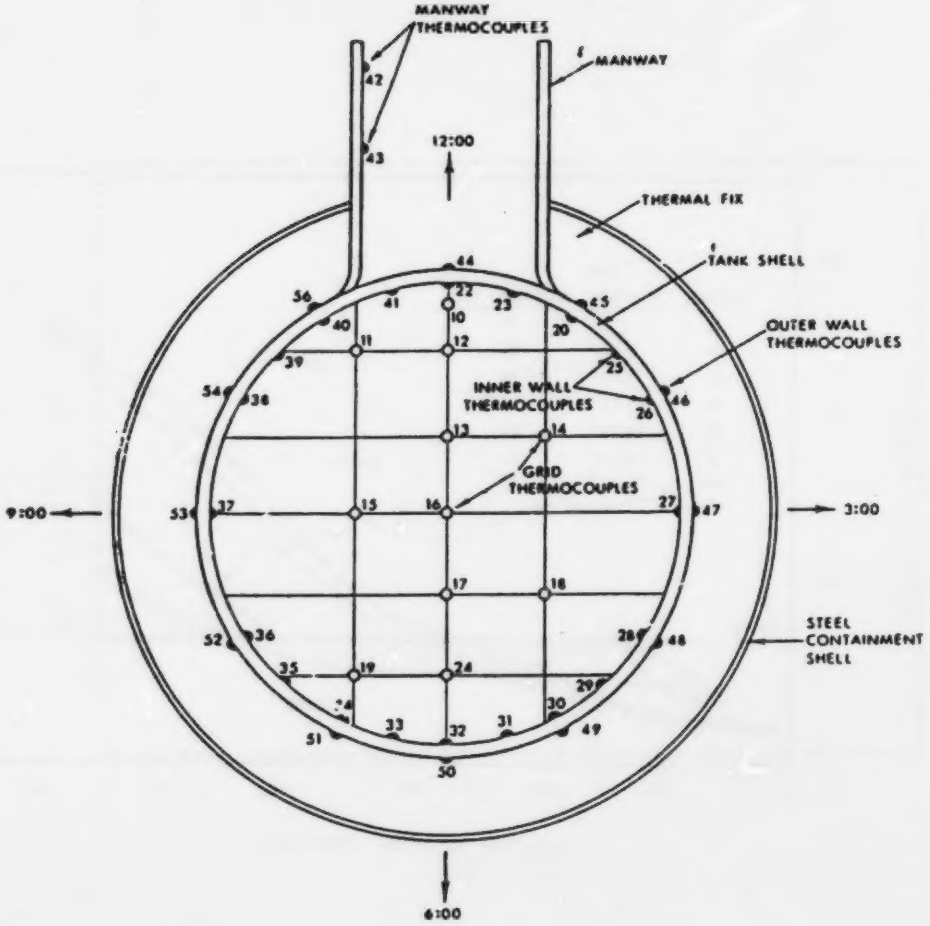
MANWAY THERMOCOUPLES
MANWAY
12:00
THERMAL FIX
TANK SHELL
OUTER WALL THERMOCOUPLES
INNER WALL THERMOCOUPLES
GRID THERMOCOUPLES
STEEL CONTAINMENT SHELL
9:00
3:00
6:00
42
43
44
22
10
41
23
45
56
40
20
11
12
39
25
54
38
46
26
13
14
15
16
27
47
53
37
17
18
52
36
28
48
35
19
24
29
34
30
33
31
32
51
49
50

FIGURE 2-47 KEY TO THERMOCOUPLE LOCATION FOR AAR-RPI TEST #7 (from Reference (5))

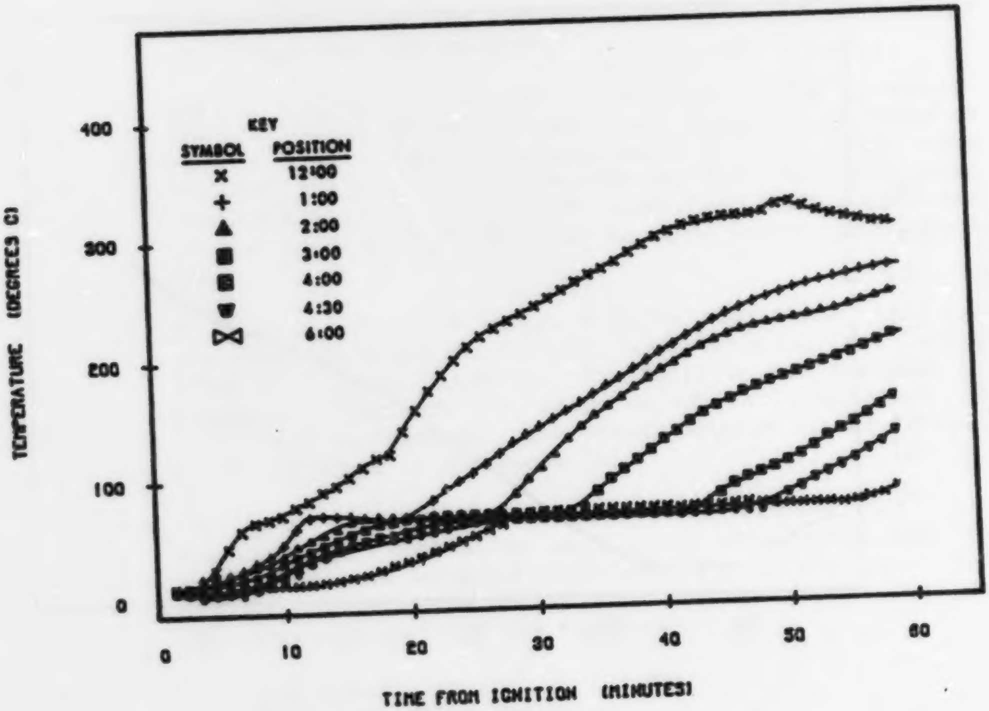

FIGURE 2-48 MEASURED WALL TEMPERATURES FOR AAR-RPI TEST #7 (from Reference (5))

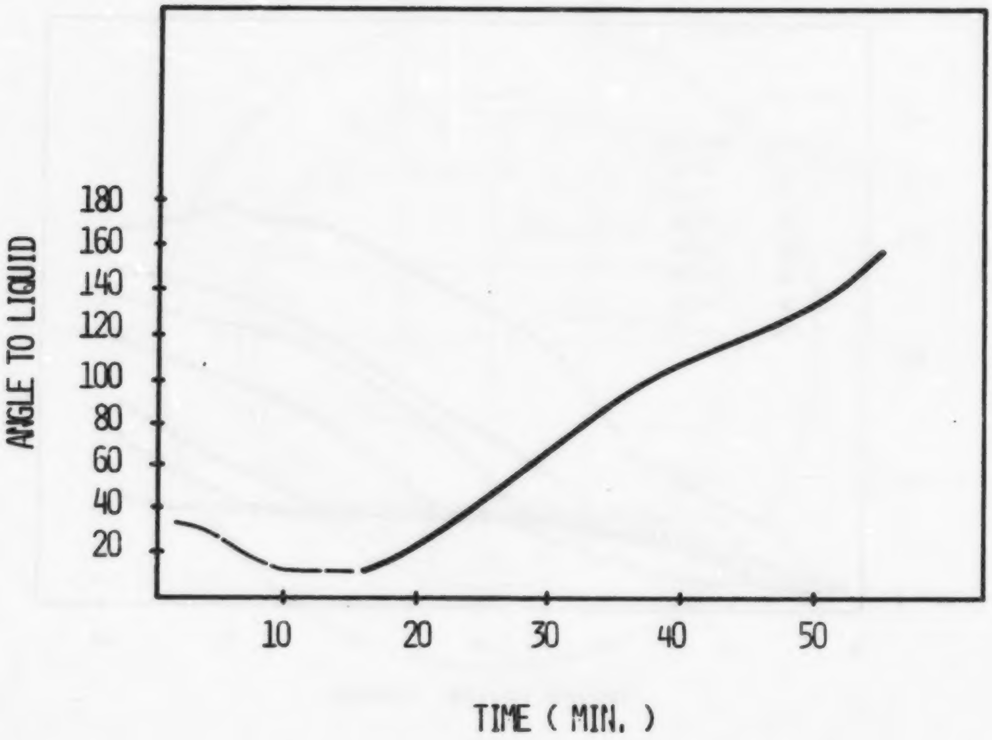

FIGURE 2-49 ESTIMATED LIQUID LEVEL FOR AAR-RPI TEST #7 (from Reference (5))

seen from the figure, the insulated tank took much longer to empty than the unprotected fifth-scale tank in test #3. It also appears that the tank approached the liquid full condition.

In summary, the test ended with the tank empty and intact after approximately 55 minutes in the fire. The thermal insulation and steel jacket significantly reduced the heat input to the tank and thereby lengthened the time scale over which the tank emptied.

AAR - RPI Torch Fire Tests: In addition to the US engulfing fire tests, torch fire tests (8) were also included as part of the tank-car safety work. These tests were included because it was recognized that tank-cars also require protection from torch fires, and that under some circumstances a torch fire can be more severe than a pool fire.

To conduct the torch tests, a torch simulation facility was constructed at the US DOT Transportation Test Centre (TTC) in Pueblo, Colorado. The facility was designed to accurately simulate the response of rail tank-cars to torch fire impingement. The design details of the facility can be found in Reference (8).

The torch simulator consisted of a propane jet (not premixed with combustion air) of a size sufficient to ensure that the level of turbulence was appropriate. The propane jet could be any quality 2-phase flow. The jet configuration used for the torch tests was:

fuel source pressure ≅ 1.5 MPa
orifice diameter = 0.95 cm
jet stand off = 3.66 m
impingement angle = 90 °

Because of economics, the torch simulator was not used on real tank-cars. Instead, the simulations were performed using 1.22 x 1.22 m steel plates. Figure 2-50 presents the results from a number of bare plate tests. The temperatures shown were averaged over the plate surface.

The objective of the torch simulator was to accurately represent a tank-car exposed to a torch environment. For this reason calibration tests were performed on a real tank-car. Figure 2-51 presents a comparison of results from a bare plate test and a tank-car test. The tank-car

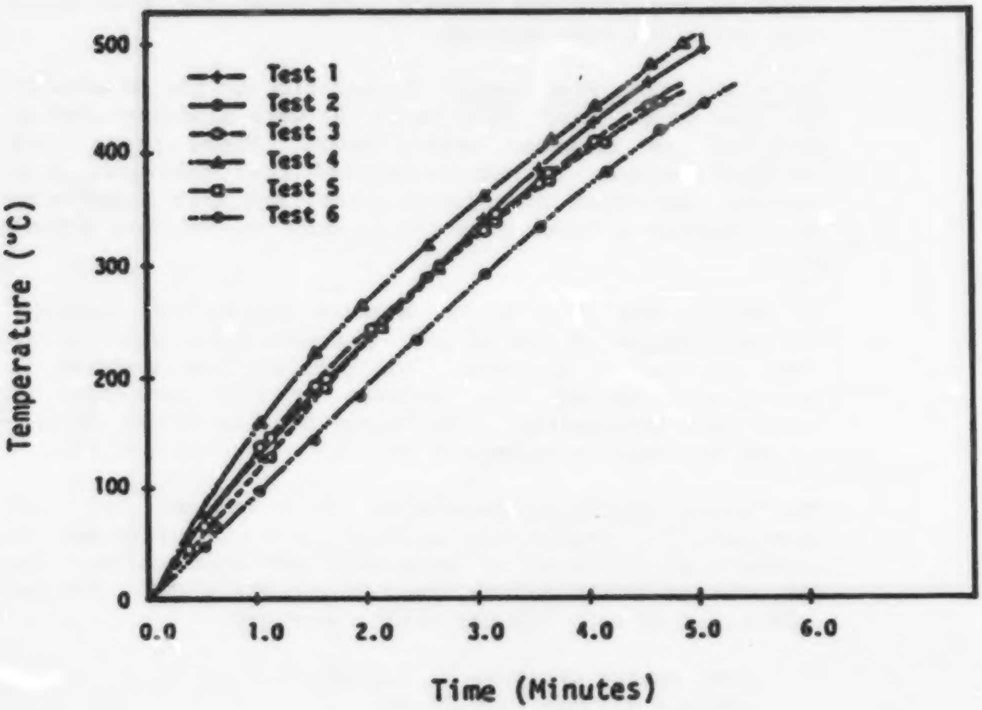

FIGURE 2-50 RESULTS FROM THE BARE PLATE TORCH FIRE TESTS (from Reference (8))

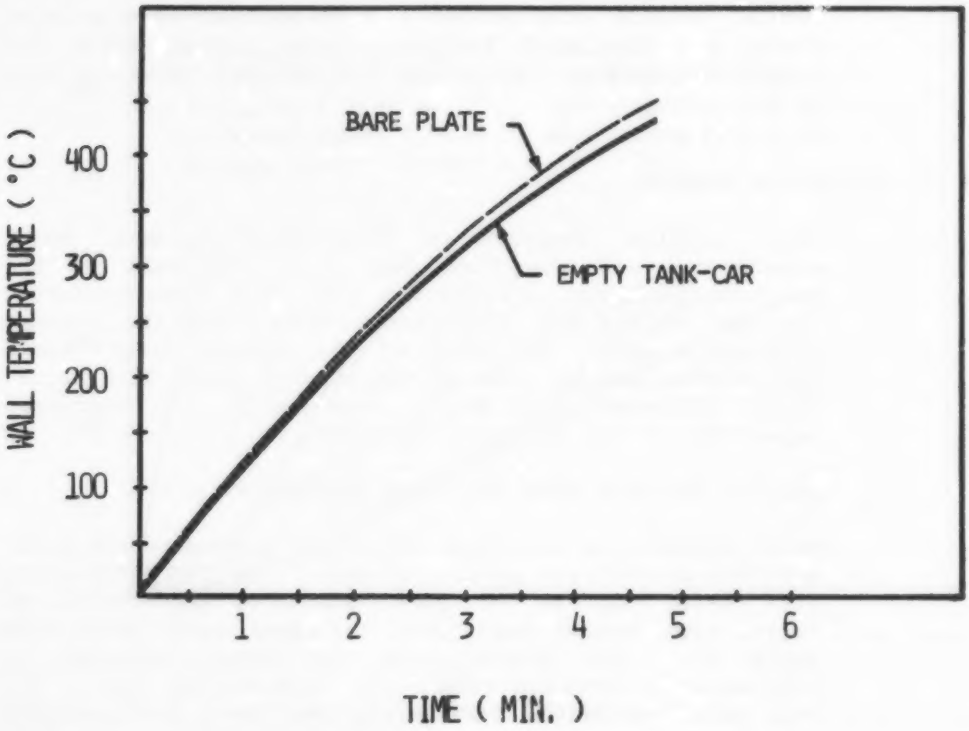

FIGURE 2-51 RESULTS FROM TANK-CAR TORCH FIRE TESTS (from Reference (8))

was empty in the test and therefore only wall temperature data was obtained. Clearly, the results indicated that the torch simulator acting on a bare steel plate is an accurate representation of the same jet applied to an empty tank-car.

The same kind of torch calibration tests were performed for insulated plates and an insulated tank-car. Figure 2-52 presents results from a number of insulated plate tests. Figure 2-53 presents a comparison of insulated plate and insulated tank-car tests. Once again the comparison between steel plate and tank-car tests are very good.

2.3 VALIDATION RESULTS

This section presents a comparison between model simulations and the fire test data discussed in the previous sections. Validation runs have been performed for two of the TDC fifth-scale tests, for the AAR-RPI full-scale tests, for three of the AAR-RPI fifth- scale fire tests, and for some of the AAR-RPI torch fire tests. These different validation runs will be discussed separately in the following sections.

2.3.1 TDC Test Data and Model Predictions

Model simulations have been performed to compare the model predictions with the results of two of the TDC fifth-scale fire tests. The two TDC tests considered were the Enigma tests (unprotected tank) and the Nova test (Explosafe Style 3). The Enigma data was chosen because it represents a baseline case of an unprotected tank. The Nova data was chosen because the Explosafe Configuration used in this case (annular configuration) is considered to be the most practical, from the standpoints of wall contact maintainability and cost effectiveness (this configuration does not fill the tank as did the other configurations considered in the TDC fifth-scale tests).

The following sections present the model predictions plotted along with fire test data. It should be noted that these two validation cases are the same as those reported in Reference (1). The only difference is that the simulations were performed using the enhanced version of the thermal model. The runs were performed using the two-dimensional analysis of the original thermal model.

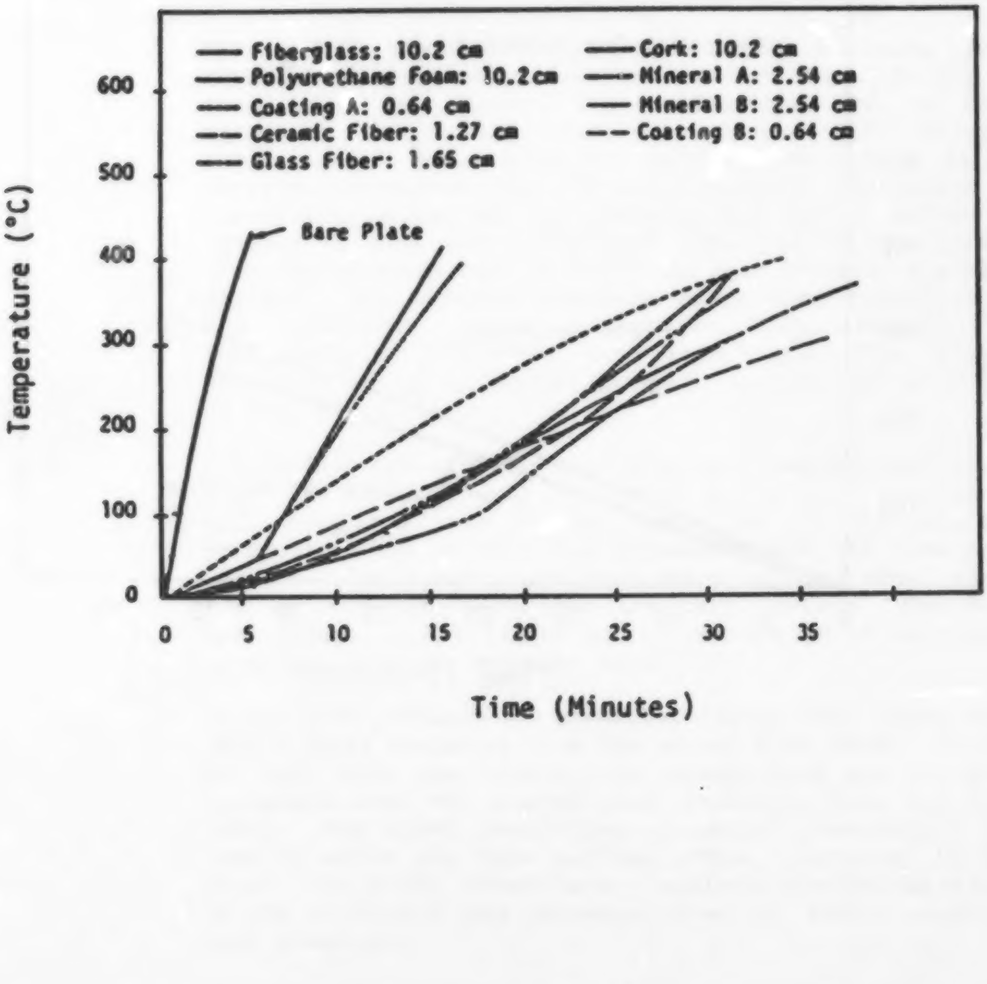

FIGURE 2-52 RESULTS FROM INSULATED PLATE TORCH FIRE TESTS (from Reference (8))

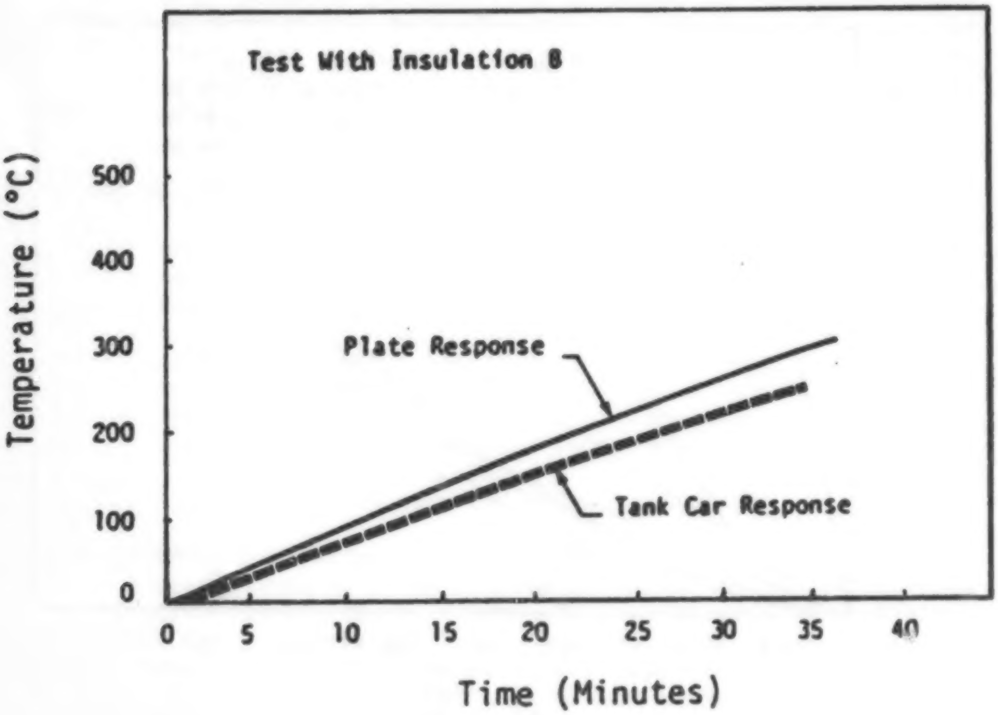

FIGURE 2-53 RESULTS FROM INSULATED TANK-CAR TORCH FIRE TESTS (from Reference (8))

2.3.1.1 Enigma Case

The tank-car model was used to predict the response of a fifth-scale unprotected tank exposed to an engulfing fire. The simulation was performed with boundary conditions which represented the actual fire conditions as closely as possible. The results of the simulation are presented in Figures 2-54 to 2-57 along with the actual measured data from the fire test.

Figure 2-54 presents the predicted tank pressure along with the measured pressures from the fire test. As can be seen from the Figure, the predictions are in good agreement with the test results. The initial pressurization rate prior to relief valve action is in excellent agreement with the tests results. The length of the cycling period and the pressure rise during continuous venting is also well predicted. The predictions depart from the measured results after the peak pressure has been reached. The measured pressure drops more rapidly than the predicted values prior to tank failure at approximately 7 minutes into the test. This slight departure in the predicted pressure is not considered to be overly significant.

Figure 2-55 presents the predicted wall temperatures along with the measured wall temperatures for three different wall locations. As can be seen from the figure, the predictions are in very good agreement with the fire test results. The temperature rise rates and the break times are in good agreement with the test results. The wall temperature in the liquid wetted regions is in excellent agreement with the measured data.

Figure 2-56 presents the predicted liquid level along with liquid level estimates from the actual fire tests. As can be seen from the Figure, the predictions are in good agreement with the limited data available from the fire tests. The model predictions slightly underpredict the rate at which the tank empties. This inaccuracy in the prediction of the liquid level could explain the departure of the predicted tank pressure from the actual measured tank pressure.

Figure 2-57 presents the predicted wall stresses and material properties for the Enigma test. The only data point from the fire tests shown on this figure is the actual time of failure of the tank at approximately 7½ minutes into the fire.

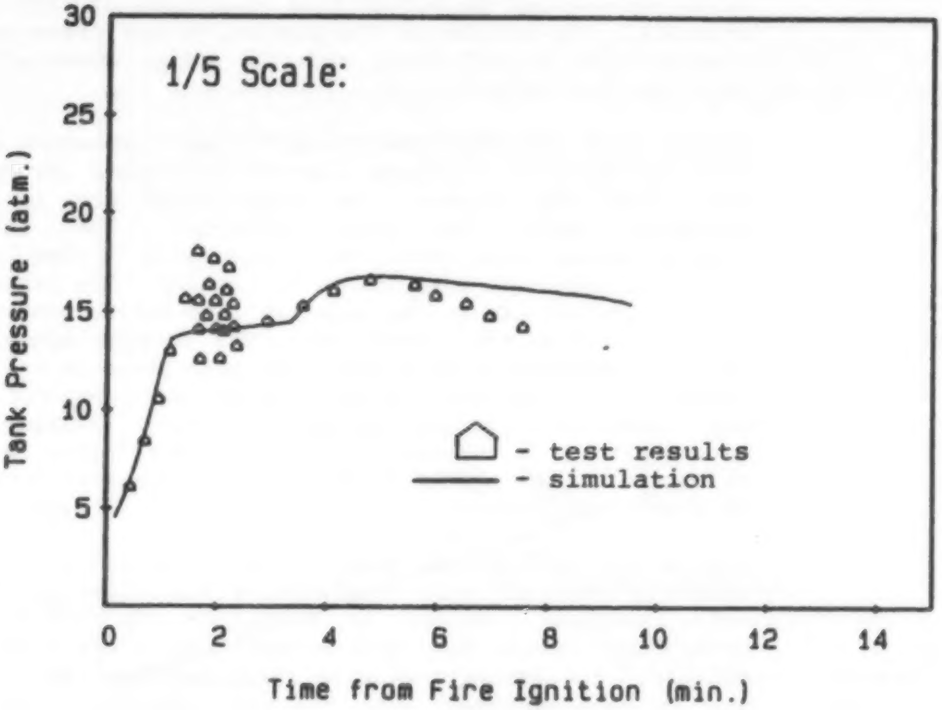

FIGURE 2-54 PREDICTED TANK PRESSURE AND MEASURED TANK PRESSURE FOR ENIGMA TEST (from Reference (3))

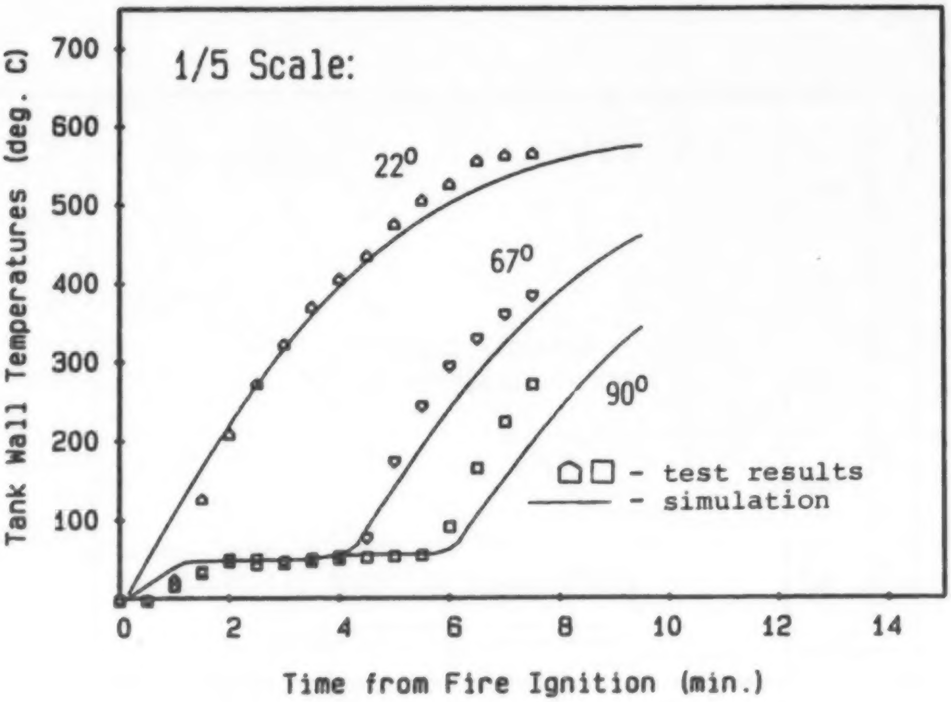

FIGURE 2-55 PREDICTED WALL TEMPERATURES AND MEASURED WALL TEMPERATURES FROM ENIGMA TEST (from Reference (3))

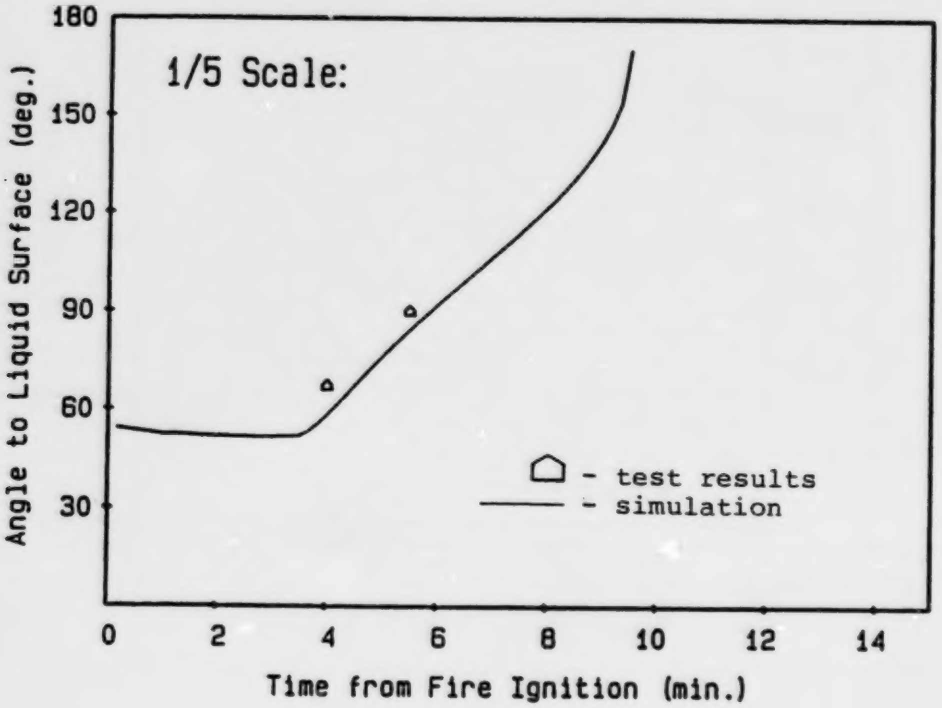

FIGURE 2-56 PREDICTED LIQUID LEVEL AND MEASURED LIQUID LEVEL FOR ENIGMA TEST (from Reference (3))

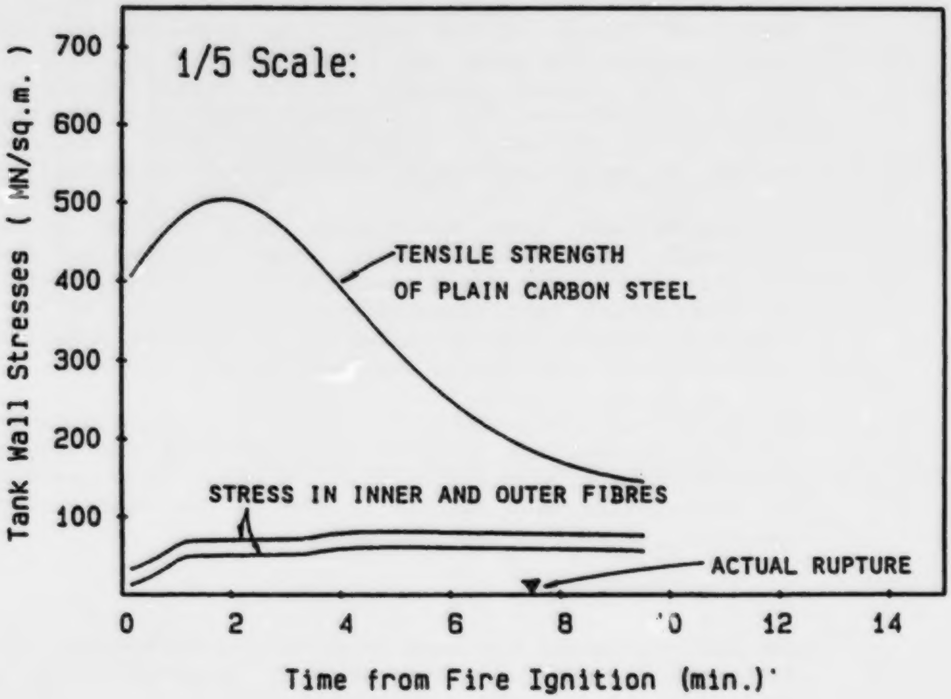

FIGURE 2-57 PREDICTED TANK WALL STRESSES AND MATERIAL STRENGTH FOR ENIGMA TEST (from Reference (3))

The figure shows the predicted tensile strength of the tank wall as a function of time from fire ignition. This tensile strength is of course a function of the wall temperature. The tensile strength shown is for the location on the tank wall where the maximum temperature is reached (at top-dead-centre).

The wall stresses at the inner and outer fibres of the tank wall are also shown. The maximum stresses occur at the inner fibres of the tank. The difference in the stress between the inner and outer fibres of the wall are due to the thermal gradient in the radial direction. Failure is indicated when the tensile strength of the wall drops below the stress levels in the wall. This, of course, is the maximum normal stress theory of failure.

As can be seen from the figure, tank failure is not predicted. This disagrees with actual observations from the fire test. The disagreement between the predictions and the actual test observations could be caused by a number of factors such as inclusions in the tank material, poor welds, or unpredicted hot spots in the tank wall.

To summarize, the model predictions for an unprotected fifth-scale tank are in good agreement with the results obtained from an actual fire test. A major departure from the actual fire test results is seen in the inability of the model to predict tank failure.

2.3.1.2 Nova Case

The tank-car model was used to predict the response of a fifth-scale tank-car protected with material known as Explosafe. As in the unprotected tank case considered earlier, Nova was exposed to an engulfing fire environment. The simulation was performed with boundary conditions which represented the actual fire conditions as closely as possible. The results of the simulation are presented in Figure 2-58 to 2-61 along with the actual measured data from the fire tests.

Figure 2-58 presents the predicted tank pressure along with the measured pressure from the fire test. As can be seen from the figure, the predictions are in good agreement with the test results. There is some disagreement in the initial pressurization rate prior to the relief valve cycling period, however, the length of the valve cycling period is well predicted. The tank

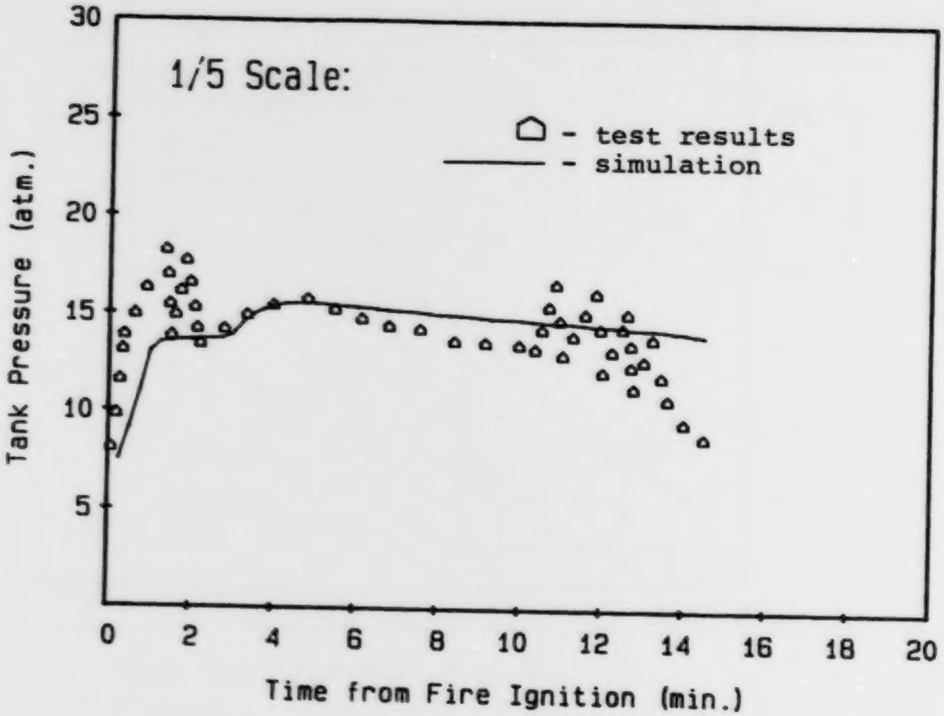

FIGURE 2-58 PREDICTED TANK PRESSURE AND MEASURED TANK PRESSURE FOR NOVA TEST (from Reference (3))

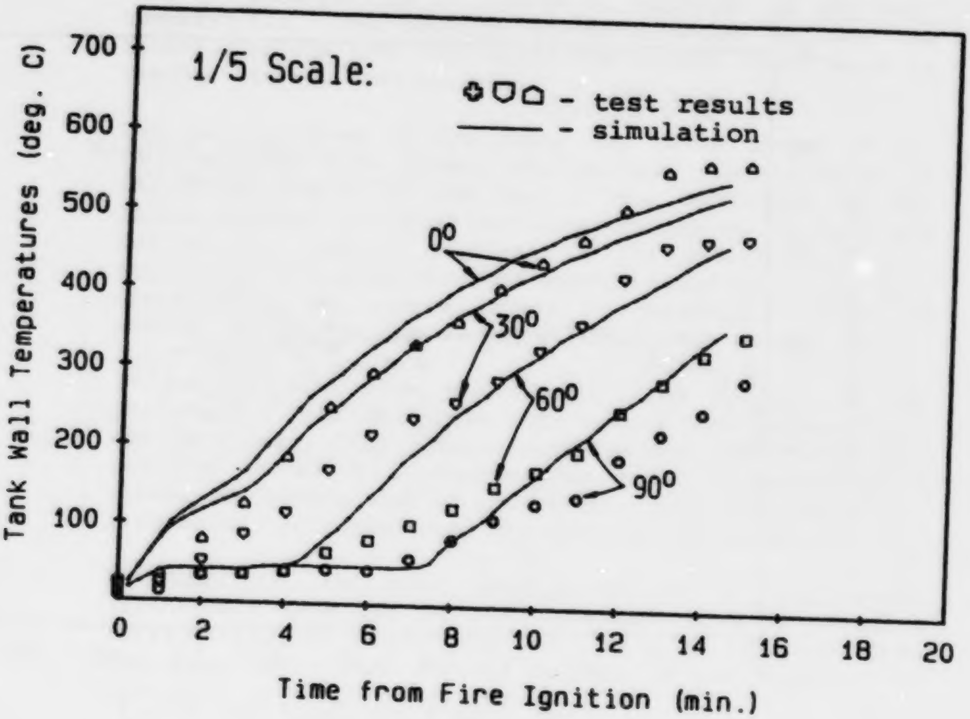

FIGURE 2-59 PREDICTED WALL TEMPERATURES AND MEASURED WALL TEMPERATURES FROM NOVA TEST (from Reference (3))

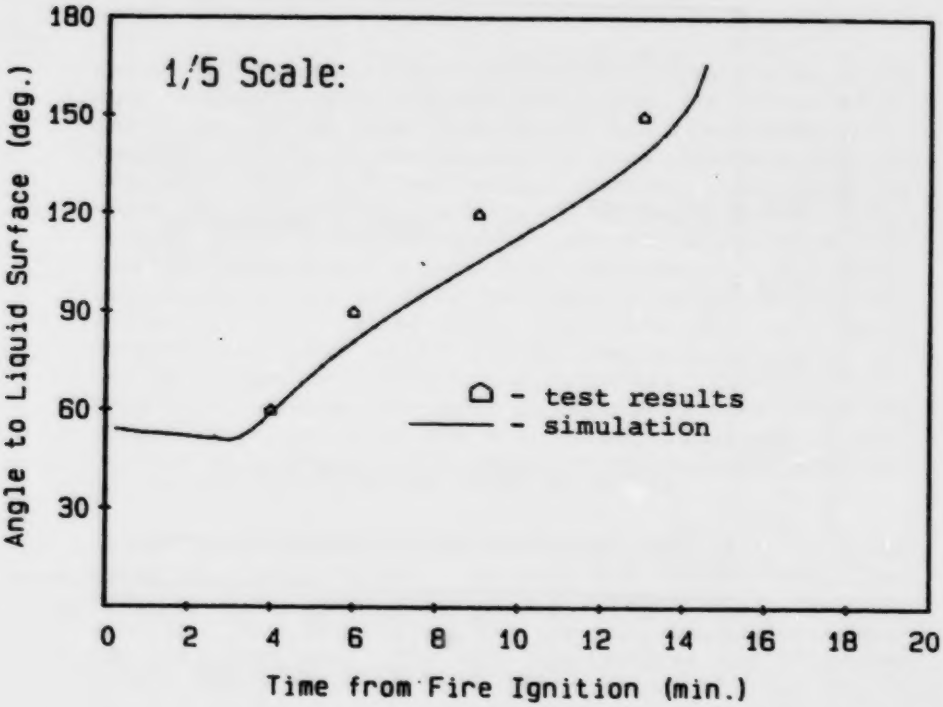

FIGURE 2-60 PREDICTED LIQUID LEVEL AND MEASURED LIQUID LEVEL FOR NOVA TEST (from Reference (3))

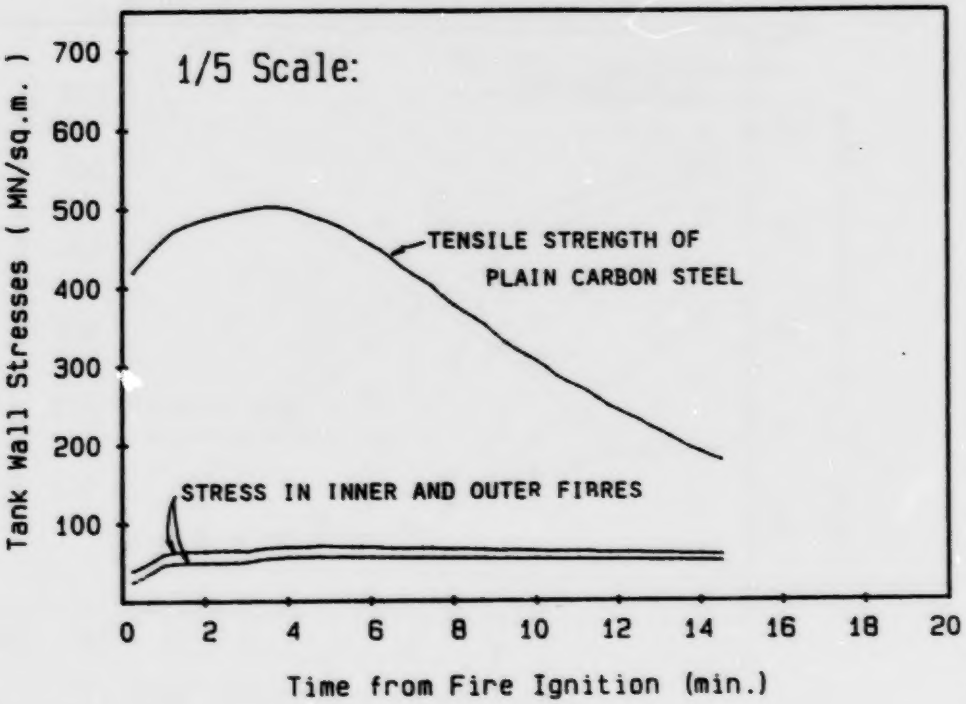

FIGURE 2-61 PREDICTED TANK WALL STRESSES AND MATERIAL STRENGTH FOR NOVA TEST (from Reference (3))

pressurization during continuous venting is also well predicted up to the time where the peak tank pressure for continuous venting is reached. As in the Enigma case, the tank pressure drops more rapidly than predicted by the model.

Figure 2-59 presents the predicted wall temperatures along with measured wall temperatures, from the actual fire test. As can be seen from the figure, the actual wall temperature predictions are not in good agreement for the different locations indicated. However, the rates at which the temperatures increase at the different locations (slopes of the different curves) are well predicted by the tank-car model. A possible explanation for this disagreement, may be that the heat transfer coefficient within a tank filled with Explosafe may vary more dramatically than predicted by the model. This, of course, requires further experimental investigation. Generally speaking, the model is capable of predicting the trends associated with the wall temperatures and is also capable of predicting the range of temperatures expected in the tank wall.

Figure 2-60 presents the predicted and experimentally obtained liquid levels. As with the Enigma case, the tank-car model underestimates the rate at which the tank empties. This may explain why the wall temperatures were not well predicted. The wall temperatures are of course significantly affected by the location of the liquid level. As the liquid level drops, more and more of the tank wall is exposed to vapour and in these regions the wall temperatures are much higher. The temperature break times for the different wall locations are of course caused by the liquid level dropping below the actual wall location, thereby exposing it to vapour. If the liquid level is not accurately predicted, one cannot expect the wall temperatures to be accurately predicted. Possible reasons for the departure in the prediction of the liquid level are, an underprediction in the rate of venting, an error in the internal surface heat transfer coefficients, or an error in the fire heat transfer.

Figure 2-61 presents the predicted wall stresses and the material properties for the Nova test case. In the actual fire test, the tank did not fail. As can be seen from the figure, the model predicts that the tank will not fail. However, it should be recalled that the tank-car model did not predict failure for the Enigma case either. As far as the model is concerned, neither Enigma nor Nova should have failed, and if one of them did fail, it was due to an effect other than simply wall temperatures and tank pressure.

In summary, the model predictions are in fair agreement with the results of the Nova fire test. There is some disagreement between the predictions and the actual test results in regards to wall temperatures. There is also some disagreement in the prediction of the liquid level, and this may have been the cause for the differences between the predicted and the measured wall temperatures.

2.3.2 AAR-RPI Tests

Model simulations have been performed to compare the model predictions with the results of a number of the AAR-RPI fire tests. Validation runs were performed to compare predictions with the AAR-RPI full-scale fire test of an unprotected tank, the full-scale fire test of a thermally protected tank, the fifth-scale fire test of an unprotected tank, the fire test of a fifth-scale unprotected tank rolled 90° so that the relief valve is initially submerged in the lading, the fifth-scale fire test of a thermally protected tank, and some torch fire tests conducted on empty, full-scale tank-cars.

2.3.2.1 RAX-201 Case

The tank-car model was used to predict the response of a full-scale unprotected tank exposed to an engulfing fire. Simulations performed had boundary conditions which represented the actual fire conditions as closely as possible. The results of the simulation are presented in Figures 2-62 to 2-65 along with the actual measured data from the fire test.

Figure 2-62 presents the predicted tank pressure along with the measured pressure from the fire test. As can be seen from the figure, the predictions are in fair agreement with the actual test results. The initial pressurization rate prior to the valve cycling is very well predicted. The model predicts a valve cycling period which is much longer than the valve cycling period observed in the fire test. A possible explanation of this disagreement may be that the relief valve on RAX 201 for some reason remained in a partially open state during the time when normal valve cycling would have occurred. This

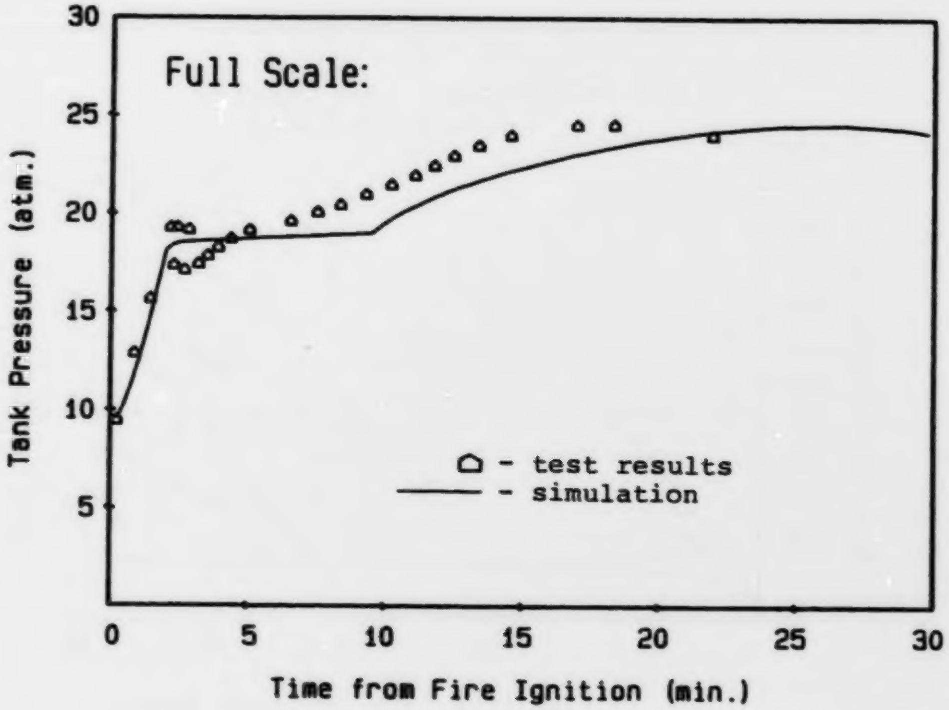

FIGURE 2-62 PREDICTED TANK PRESSURE AND MEASURED TANK PRESSURE FOR RAX-201 TEST (from Reference (2))

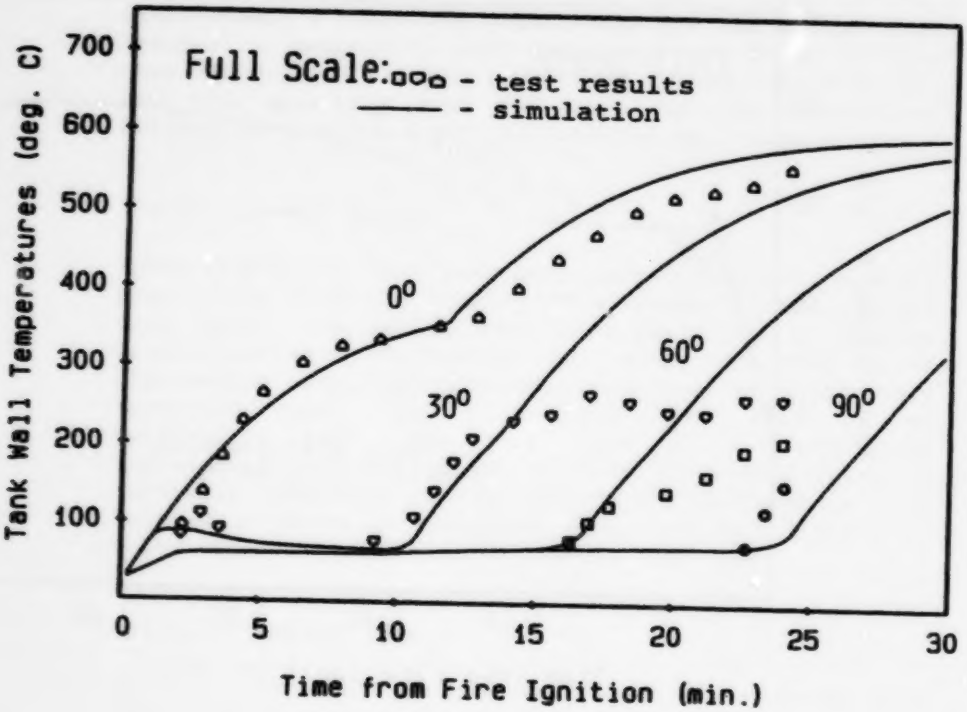

FIGURE 2-63 PREDICTED WALL TEMPERATURES AND MEASURED WALL TEMPERATURES FROM RAX-201 TEST (from Reference (2))

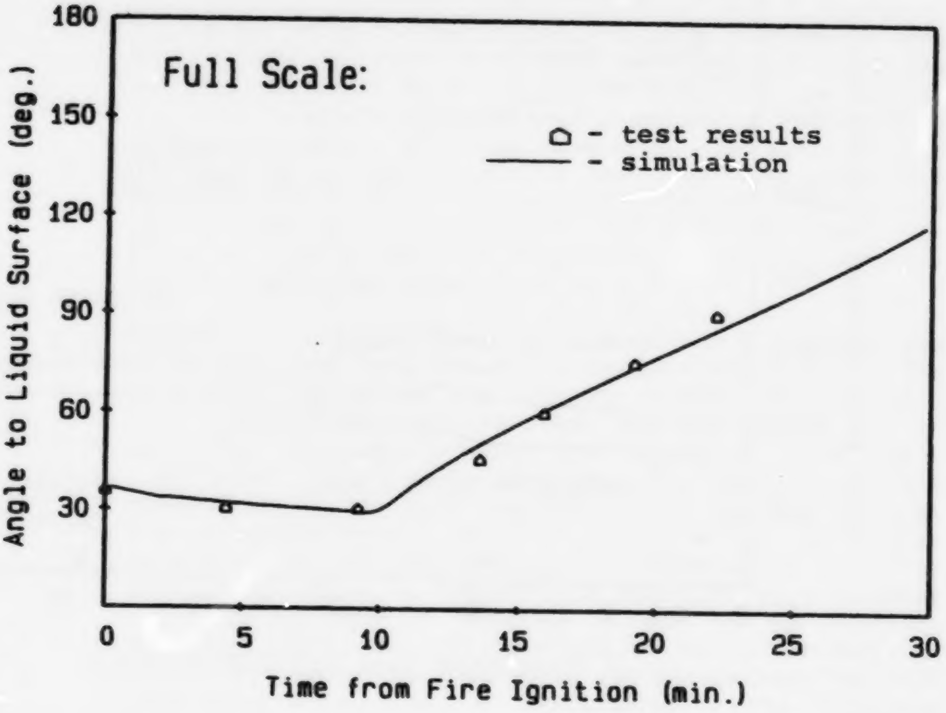

FIGURE 2-64 PREDICTED LIQUID LEVEL AND MEASURED LIQUID LEVEL FOR RAX-201 TEST (from Reference (2))

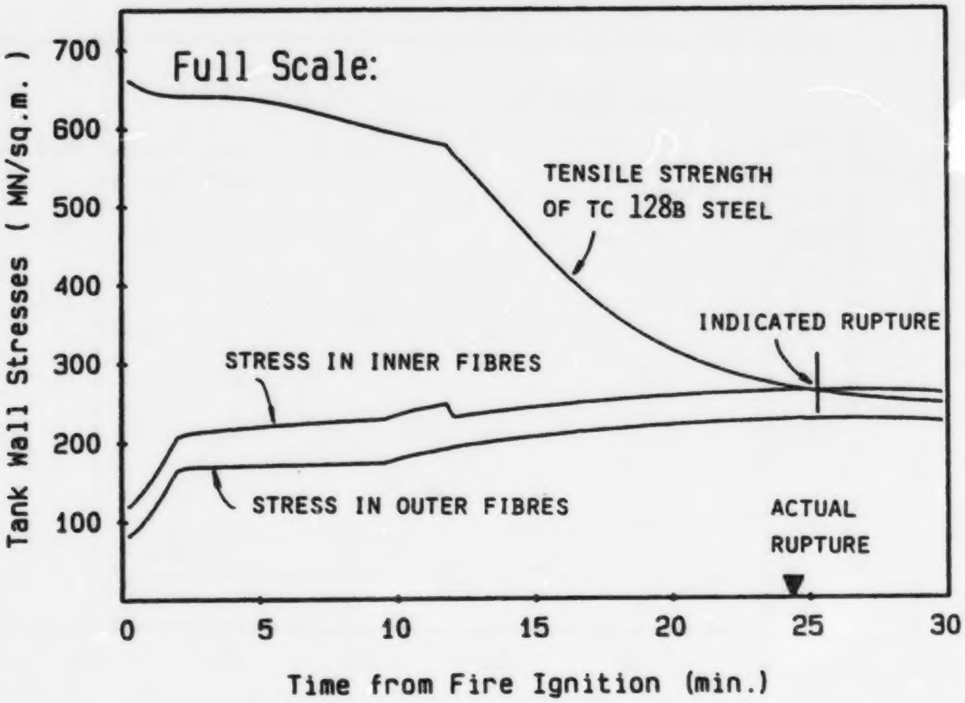

FIGURE 2-65 PREDICTED TANK WALL STRESSES AND MATERIAL STRENGTH FOR RAX-201 TEST

aspect of the fire test was discussed in a previous section. Because of this disagreement in the length of the valve cycling period, the model predictions for the tank pressure are in disagreement with the actually measured tank pressures. However, the disagreement in the tank pressure is not large.

Beyond the valve cycling period, the tank pressure is seen to continue to rise to a peak pressure and then the pressure begins to fall. As can be seen from the Figure, the model predicts that the peak pressure is reached at a later time. This error in predicting the time to peak pressure is of course due to the fact that the model predicted a much longer valve cycling period. However, as can be seen from the figure, the predicted tank peak pressure is in excellent agreement with the actually measured tank peak pressure.

Figure 2-63 presents the predicted tank wall temperatures along with the temperatures actually measured from the fire test. As can be seen from the figure, the predicted wall temperature for the tank top-dead-centre is in excellent agreement with the measured tank wall temperature. As can be seen from the figure, the wall temperature at the tank top-dead-centre appears to level off at approximately 350°C at approximately 10 minutes into the fire and then suddenly the temperature begins to rise again where it levels off again at approximately 600°C. This type of response is due to the frothing two-phase region that exists on top of the liquid surface. The first temperature plateau is reached because the tank wall temperature comes to equilibrium in the two-phase region. Eventually, however, due to venting of the tank lading, the liquid level drops and along with it the two-phase frothing region drops. Eventually, the wall is exposed to vapour, and again its temperature increases rapidly until it reaches an equilibrium again. This type of response is not as evident in the wall locations further around the side of the tank. This is because, the liquid level is dropping much more rapidly when the liquid level and the frothing level passes a location on the wall around the side of the tank. This means, that the wall does not have a chance to reach an equilibrium in the frothing region before it is exposed to the vapour.

As can be seen from the figure, the predicted wall temperatures for the 30, 60 and 90° locations around the tank do not agree well with the actual measured temperatures. There are two possible reasons for this, the first is that the low wall temperatures around the side of the tank are due to the uncontrollable nature of the fire, and the second reason may be that the frothing layer is much larger than predicted by the tank-car model. If the frothing layer is much larger than predicted, the wall regions around the side of the tank may be covered with frothing for a much longer period of time than predicted. If this were the case, the wall temperatures would reach an equilibrium at approximately 300° as they did for the top-dead-centre location. As can be seen from the figure, the 30° wall location reaches a temperature equilibrium of approximately 250°C. Therefore, from this it can be concluded that the frothing layer acts in a much more complex manner than is predicted by the tank-car model. This requires further study.

In general, the model predictions for wall temperatures are quite good. The wall temperatures at the top-dead-centre are predicted very well. It is the peak wall temperatures that dictate tank failure due to thermal degradation of the tank wall material. These peak wall temperatures generally occur at the top of the tank and it was seen from Figure 2-63 that the tank-car model is very accurate at predicting the top-dead-centre wall temperatures. Therefore, from this it can be concluded that the model should be adequate for predicting tank failure due to high temperatures at the tank-top-dead centre.

Figure 2-64 presents the predicted liquid level for the RAX-201 test. As can be seen from the figure, the predicted liquid level is in excellent agreement with the liquid level estimated from the wall temperature break times. It is very important that the model be able to predict the position of the liquid level accurately, because this liquid level determines the way in which the tank wall responds to the fire.

Figure 2-65 presents the predicted tank wall stresses along with the tank wall strength. Based on a maximum normal stress theory of failure, probable failure of the tank occurs when the tank wall strength drops below the maximum stress in the tank wall. As can be seen from Figure 2-65, the tank wall strength dips below the stress in the tank inner fibres at approximately 25 minutes. Also indicated in the figure, is the actually observed tank rupture time of approximately 24½ minutes. This excellent agreement is due to the accurate prediction of the peak wall temperature at the tank top-dead-centre, and the accurate prediction of the tank peak pressure.

In summary, the tank-car model predictions for the RAX-201 test condition are in very good agreement with the actual results obtained from the fire tests. Although the tank-car model predicts a longer valve cycling period, the predicted tank pressure is in good agreement with the measured tank pressure. The tank-car model predictions for the tank wall temperatures are in excellent agreement for the tank top-dead-centre, however, the wall temperature predictions for positions around the side of the tank are not in good agreement. This departure between predicted and measured wall temperatures is likely due to the model's failure in predicting the size and position of the frothing two-phase region which exists above the liquid surface. However, the tank-car model predicted the liquid level in the tank very accurately. As a result of the accurate predictions of the tank wall temperatures, and the tank pressure, the prediction of tank failure at 25 minutes is in excellent agreement with the actually observed tank failure.

2.3.2.2 RAX-202

The tank-car model was used to simulate the thermal response of a full-scale thermally insulated tank-car exposed to an engulfing fire. As with all the cases considered, the tank was filled with propane. The simulations were performed with boundary conditions that represented the actual fire test conditions encountered by RAX-202. The results of the simulation are presented in Figures 2-66 and 2-69 along with data recorded during the actual fire test.

Before the results of the simulation are discussed, it is important that some of the details of the thermal insulating material be described. As described in a previous section, RAX-202 was coated with a 3 mm thick layer of an ablative thermal barrier called Korotherm. Korotherm is made of an organic material that degrades at high temperature to form a char layer. During the degradation process, gases are released and these gases provide a transpiration cooling effect. In addition, the high thermal conductivity of the material provides a conventional type of thermal barrier. Unfortunately, the degradation process that provides the transpiration cooling effect is complex. Detailed data on the thermal properties of the Korotherm material (and how it changes with temperature) could not be found.

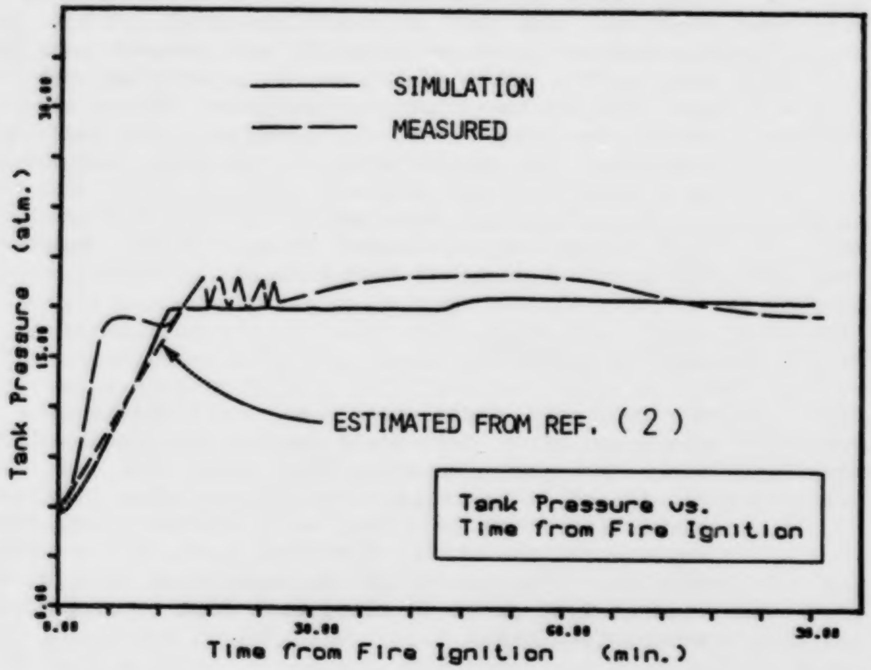

FIGURE 2-66 PREDICTED TANK PRESSURE AND MEASURED TANK PRESSURE FOR RAX-202 TEST (from Reference (2))

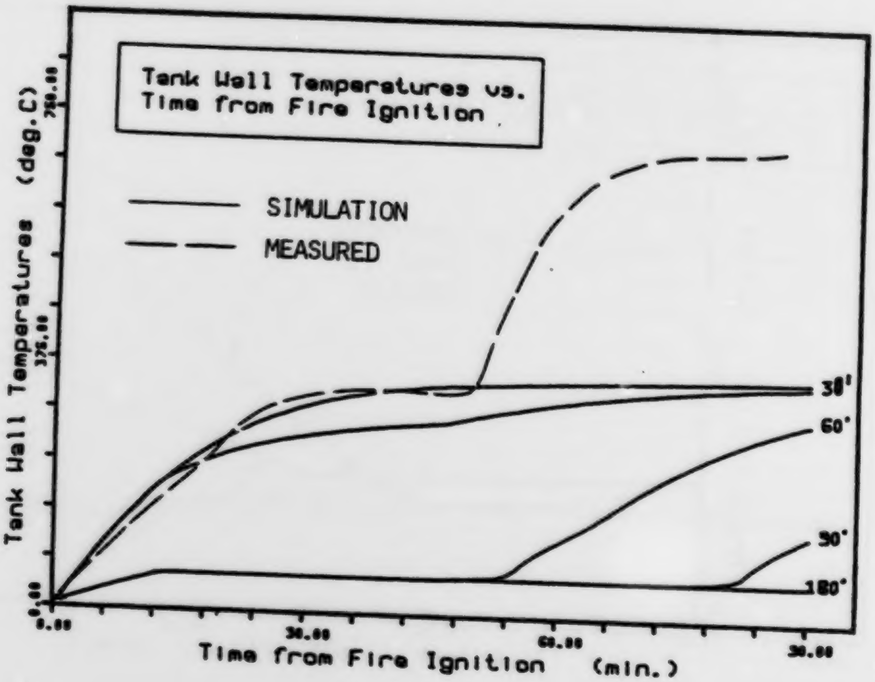

FIGURE 2-67 PREDICTED WALL TEMPERATURES AND MEASURED WALL TEMPERATURES FROM RAX-202 TEST (from Reference (2))

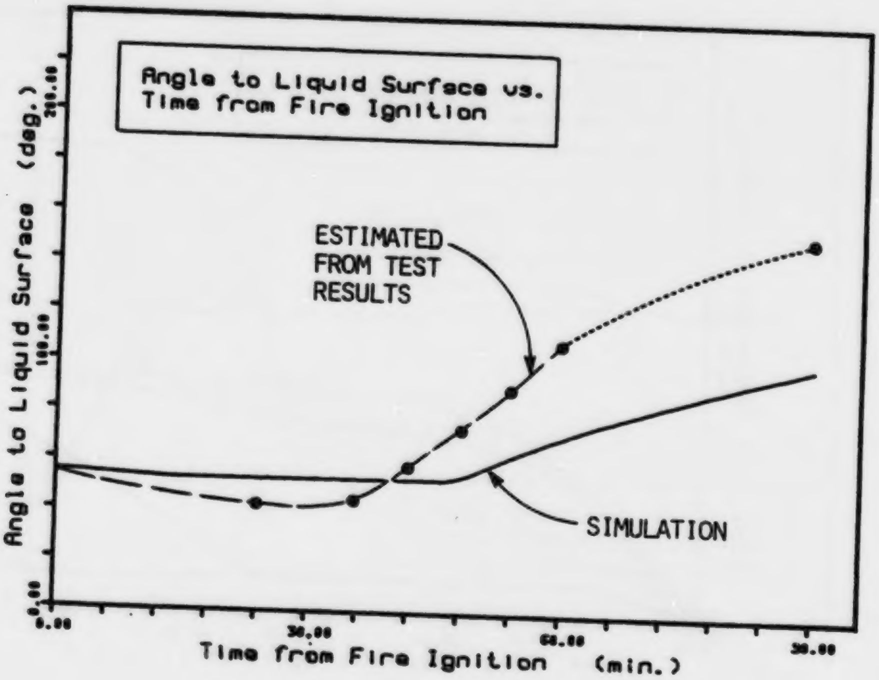

FIGURE 2-68 PREDICTED LIQUID LEVEL AND MEASURED LIQUID LEVEL FOR RAX-202 TEST (from Reference (2))

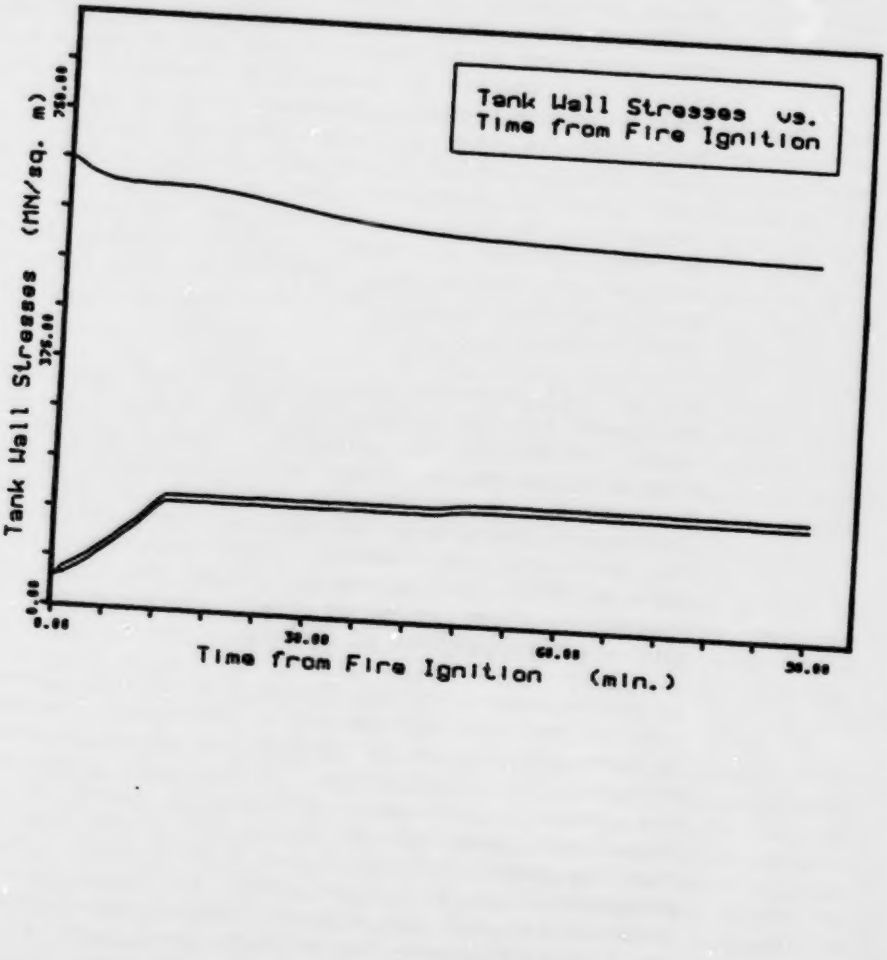

FIGURE 2-69 PREDICTED TANK WALL STRESSES AND MATERIAL STRENGTH FOR RAX-202 TEST

Because of the lack of data, it was not possible to model the action of the Korotherm in detail (this would have been possible if the data were available because the tank-car model can represent an ablative material if its temperature dependent performance characteristics are known). For the purposes of the simulation, it was assumed that the tank-car was insulated with a 3 mm thick layer of material with physical and thermal properties which are similar to those of asbestos. This material is different from the Korotherm material in many ways, the most important being, that it does not ablate and give off significant amounts of gases, and therefore transpiration cooling is not present. However, even though the assumed insulation is very different from the actual insulation used, the results of the present simulation case show the basic results expected when a tank-car is thermally insulated. As will be seen from the following plots, the agreement between the predicted tank response and the test results are quite good considering the fact that the operating details of the insulating material have been greatly simplified.

Figure 2-66 presents the predicted tank pressure and the estimated tank pressure from the actual fire test. The word "estimated" was carefully chosen because there is some question as to whether or not the tank pressure shown is correct. As mentioned in Reference (2) there were many instrument failures in RAX-202 and these failures included the pressure transducers. From Reference (2) but it appears that the pressure (from the fire test) was estimated from measured wall temperatures and the saturation properties of propane.

As can be seen from the figure, the initial pressurization rate is not well represented by the model. However, there is some question as to whether the pressure obtained from Reference (2) is accurate. If the tank pressure followed the saturation pressure (of propane) based on the liquid wetted wall temperatures, as it did in the case of RAX 201 then the model predictions would be correct. However, the pressure from the fire test is based on the wall temperatures and the average vapour temperatures. There is little evidence to confirm that such a method of predicting the actual tank pressure is correct. Therefore, it is difficult to conclude whether the model is right or wrong in the prediction of the initial pressurization rate. A piece of evidence in favour of the model predictions is the fact that in the fire test the relief valve first opened at about 15 minutes into the fire. In all fire tests conducted, the pre-venting pressurization has been a simple ramp increase up to the valve opening pressure. In the case of the "estimated" pressure for RAX-202, the initial pressurization is not a simple ramp increase but a rather unusual ramp, then drop, then increase to valve opening. It is difficult to explain this kind of pressurization sequence. The tank-car model predicts a valve opening time of approximately 13 minutes which is in good agreement with the actually observed valve opening time from the RAX-202 test.

Once the relief valve opened, the valve cycled for approximately six minutes in the actual fire test. The model, however predicts a much longer valve cycling time of approximately 30 minutes. This inaccuracy in predicting the valve cycling time is probably due to the specific characteristics of the relief valve used on RAX-202. This same inaccuracy in the model results was seen in the case of RAX-201. It is very difficult to conclude whether or not the model is wrong or whether it was the characteristics of the valve that resulted in the short valve cycling period. It should be noted that the peak tank pressure (based on the liquid wetted wall temperatures) remained within the valve open/close pressure range and therefore the valve could have reached some meta-stable position. This type of condition cannot be modelled presently by the tank-car model.

The remaining portion of pressure history, as shown in Figure 2-66 is reasonably well predicted by the tank-car model. The model basically predicts that the valve would cycle for much of the fire event, assuming of course, simple valve characteristics.

Figure 2-67 presents the predicted tank inner wall temperatures along with some measured wall temperatures from the actual fire test. The test data shown is the average measured temperature at the tank top-dead-centre. As can be seen, the model predictions for this single location are in excellent agreement for the first 50 minutes of the test and then the measured wall temperature increases rapidly. This increase is likely due to a break down in the effectiveness of the insulation layer. The temperatures eventually reached by the tdc location are in the order expected for an unprotected tank. This breakdown in the layer is of course not predicted by the tank-car model because of the simple assumptions used to represent the insulating material. Unfortunately instrumentation failures resulted in a lack of data for other wall locations.

Figure 2-68 presents the predicted liquid level along with the liquid level from the RAX-202 test. As can be seen from the figure, the model predictions are not in good agreement with the results from the fire test. Part of the inaccuracy is due to the error in the prediction of the length of the valve cycling period. A more significant error is likely due to the fact that the insulation on RAX-202 was eventually burned away in some areas and therefore the heating rate and subsequently the venting rate increased far above that expected for a completely insulated tank.

Figure 2-69 presents the predicted wall stresses and wall material strength at tdc. RAX-202 ruptured at approximately 90 minutes into the test. As can be seen from Figure 2-69 the tank-car does not predict failure. The reason for this discrepancy is the fact that in the RAX-202 test, very high wall temperatures were reached in areas where the insulation layer was burned away. These high wall temperatures in local areas (hot spots) resulted in the tank failure. Later examination of the tank fragments substantiate this claim.

In summary, the model predictions for the full-scale insulated tank are in fair agreement with the actual measured results. This is surprising considering the fact that a very simplistic approach to representing the Korotherm thermal barrier was used. The basic downfall of the simulation was the inability of the model to predict the failure of the insulating material in certain areas such as at the tank top-dead-centre (the model could have predicted this failure if data was available on the characteristics of the Korotherm material). The simulation shows how successful an ideal insulation can be, and how significant local breakdown of an insulating layer can be.

2.3.2.3 Test #3

This case involved the simulation of an unprotected fifth-scale tank filled with propane, exposed to an engulfing fire environment. The simulation was performed with boundary conditions matching those from the AAR-RPI test #3. As a special note, the tank was equipped with a full-sized (standard size for full-scale tank-car) pressure relief valve and the wall thickness was the same as for a full-sized tank-car. The results of the simulation are presented in Figures 2-70 to 2-73 along with the actual fire test results.

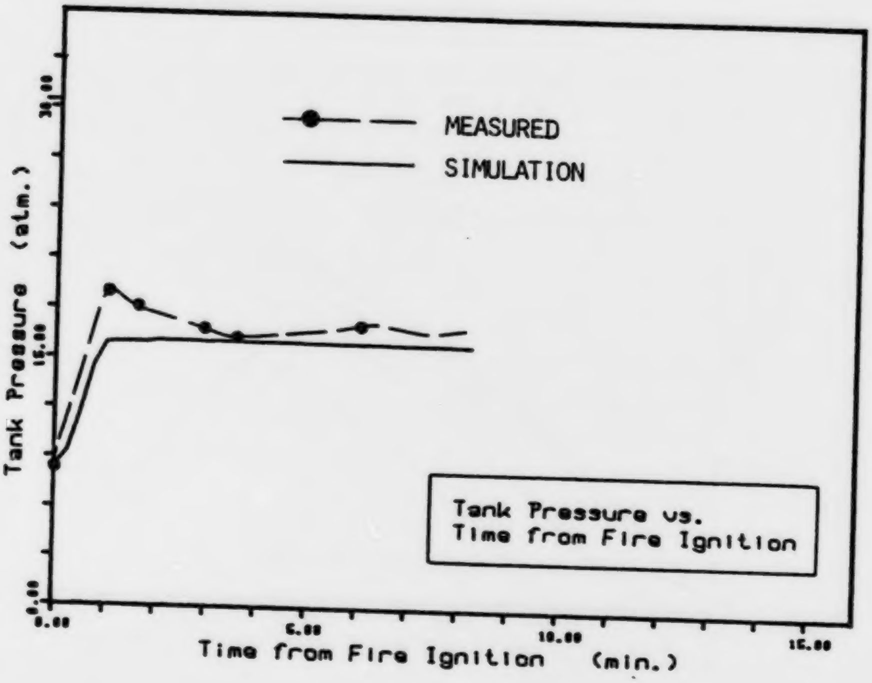

FIGURE 2-70 PREDICTED TANK PRESSURE AND MEASURED TANK PRESSURE FOR TEST #3 (from Reference (6))

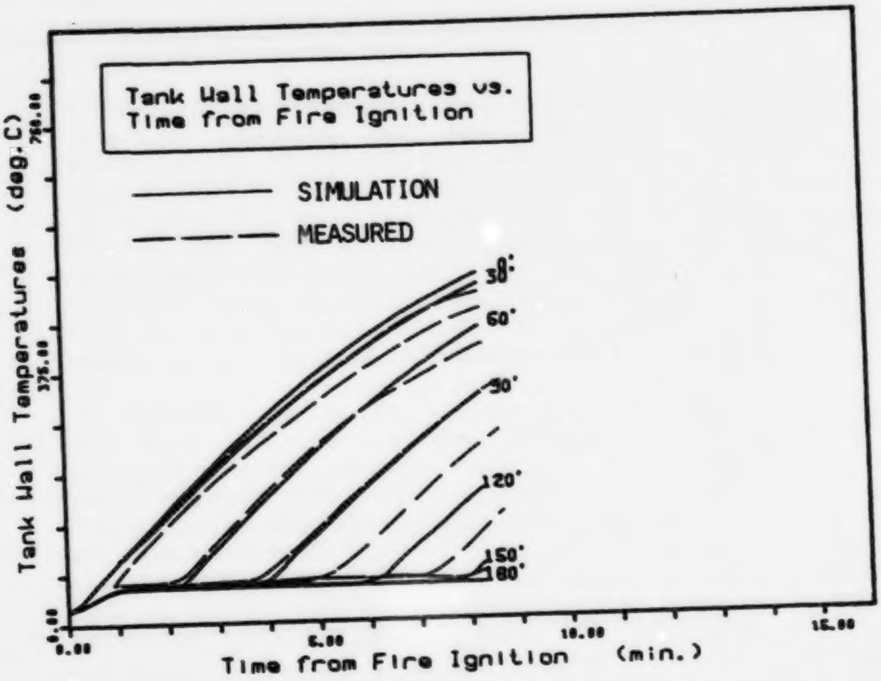

FIGURE 2-71 PREDICTED WALL TEMPERATURES AND MEASURED WALL TEMPERATURES FROM TEST #3 (from Reference (6))

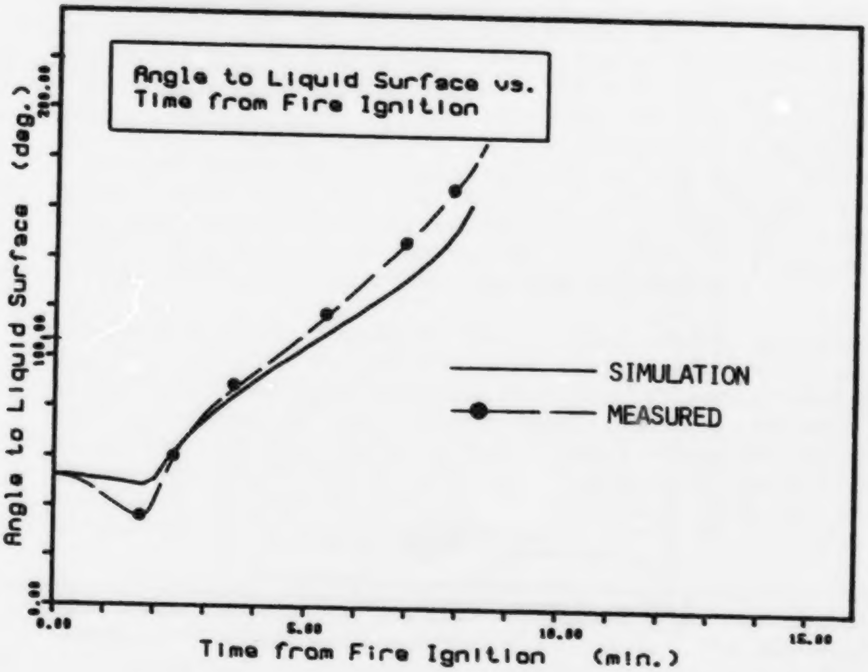

FIGURE 2-72 PREDICTED LIQUID LEVEL AND MEASURED LIQUID LEVEL FOR TEST #3 (from Reference (6))

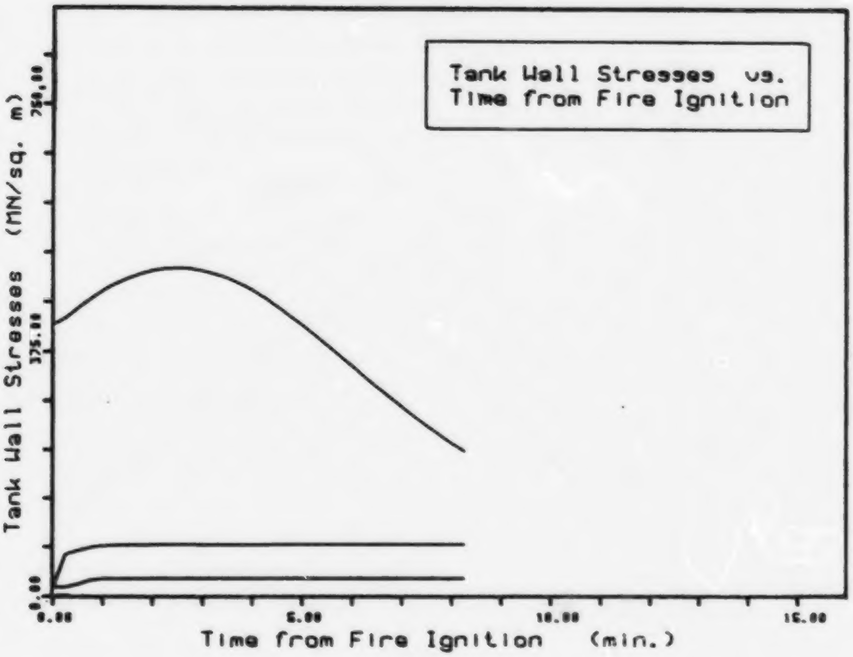

FIGURE 2-73 PREDICTED TANK WALL STRESSES AND MATERIAL STRENGTH FOR TEST #3

Figure 2-70 presents the predicted tank pressure along with the measured tank pressure from test #3. The test data shown represents the average pressure in the tank and does not show the actual pressure variations due to the valve cycling. The relief valve cycled throughout fire test #3 because of the fact that the relief valve was oversized for the fifth-scale tank.

As can be seen from Figure 2-70 the tank-car model predictions for the initial tank pressurization, prior to valve action, is very good. There is some disagreement in the actual valve opening pressure and this is clearly seen where there is a sudden leveling of the predicted pressure. This disagreement in the valve opening pressure is caused partially by the simplicity of the relief valve model, and also by the unknown variability in the operating characteristics of real pressure relief valves. This variability in relief valves is evident in every one of the simulations performed for the validation.

The predicted tank pressure remains level during the valve cycling period. As can be seen from Figure 2-70, the actual tank pressure obtained from test #3 varied during the remainder of the test. This pressure variation suggests that the actual relief valve open and close pressures varied during the test. This, of course, is difficult to explain and is a phenomenon that is not accounted for in the tank-car model.

As can be seen from Figure 2-70, the model prediction of the tank pressure is in good agreement with the actual measured pressure. The differences between the measured and predicted pressures are easily explained by the operating characteristics of real relief valves.

Figure 2-71 presents the predicted and measured wall temperatures for test #3. As can be seen from figure, the model predictions are in excellent agreement with the measured temperatures. There is some disagreement in the wall temperatures for the lower wall locations (120, 150 and 180° from tdc). These disagreements can be explained by slight errors in the prediction of the liquid level. This will be discussed further with reference to Figure 2-72 which shows the predicted and experimentally obtained liquid level.

As can be seen from Figure 2-72 the predicted liquid level is in fair agreement with the liquid levels derived from the actual fire test results. The fire test data shows that the tank approached the liquid full condition whereas the model does not predict this condition. The liquid levels from the fire test are based on wall temperature break times and therefore it is possible that the estimated liquid level from the fire test data is really the top of the frothing two-phase region. If this is the case, then the model predictions may be more accurate than they appear.

At approximately the two minute mark, the predicted liquid level agrees with the test results. From that point on the predicted and measured liquid levels diverge. The maximum error is approximately 20° in the angle to the liquid level. This error in predicting the liquid level results from errors in predicting the venting rate and have a significant effect on the wall temperature predictions. The disagreement between predicted and measured wall temperatures is caused by this error in the prediction of the liquid level because the temperature break times are directly related to the liquid level position.

Figure 2-73 presents the predicted wall stresses and material strengths for test #3. As can be seen, the model does not predict tank failure which is in agreement with the actual test results.

In summary, the model predictions are in good agreement with the fire test results. Basic errors in the prediction of the tank thermal response can be related directly to the difficulties in representing the characteristics of pressure relief valves. Even with these weaknesses in the overall thermal model, the model was capable of accurately predicting the peak wall temperatures and was also capable of predicting the time to tank empty condition within 20 seconds of the actual test #3 time to empty.

2.3.2.4 Test # 6

This case involved the simulation of an unprotected fifth-scale tank, filled with propane, exposed to an engulfing fire environment. This case was different than that of Test # 3 because the tank was rolled 90 degrees to one side so that the pressure relief valve was initially submerged in liquid. The simulation was performed with boundary conditions matching those from the AAR-RPI Test # 6. As with Test # 3, the tank was equipped with a full-size (standard size for full-scale tank-car) pressure relief valve and the wall thickness was the same as for a full-size tank-car. The results of the simulation are presented in Figures 2-74 to 2-77 along with the actual fire test results.

Figure 2-74 presents the predicted tank pressure along with the measured tank pressure from test # 6. The test data shown represents the average pressure in the tank and does not show the actual pressure variations due to the valve cycling. As a result of the valve oversizing, the valve cycled throughout the test.

As can be seen from Figure 2-74 the tank-car model predictions for the initial tank pressurization rate are in excellent agreement with the actual measured pressurization rate. As can be seen from the Figure, there is a sudden drop in the predicted tank pressure at the point where the pressure relief valve first opens. This drop in the predicted pressure is a result of an instability in the solution of the tank pressure caused by the very non-linear action of the relief valve opening. As can be seen from the Figure, the model eventually recovers and the tank pressure rises to be in very good agreement with the actual observed tank pressure from Test # 6.

Figure 2-75 presents the predicted tank wall temperatures and the measured tank wall temperatures from Test # 6. As can be seen from the figure, the predicted tank wall temperature at the tank top-dead-center are in excellent agreement with the actual measured wall temperature in that area. The predicted wall temperatures for the remaining areas are not in good agreement with the measured wall temperatures. However, the slopes of the various temperature curves agree very well with the slopes with the measured wall temperatures. This is an indication that the heat transfer rates are being well predicted. However, as will be seen in a following Figure, the prediction of the liquid level is not very accurate and this results in an error in the prediction of the temperature breakdown times for the wall locations around the side of the tank.

Figure 2-76 presents the predicted liquid level along with the liquid level estimated from the results of Test # 6. As can be seen from the figure the model under predicts the rate at which the tank emptied. As can be seen from the figure, the liquid level in Test # 6 began to drop

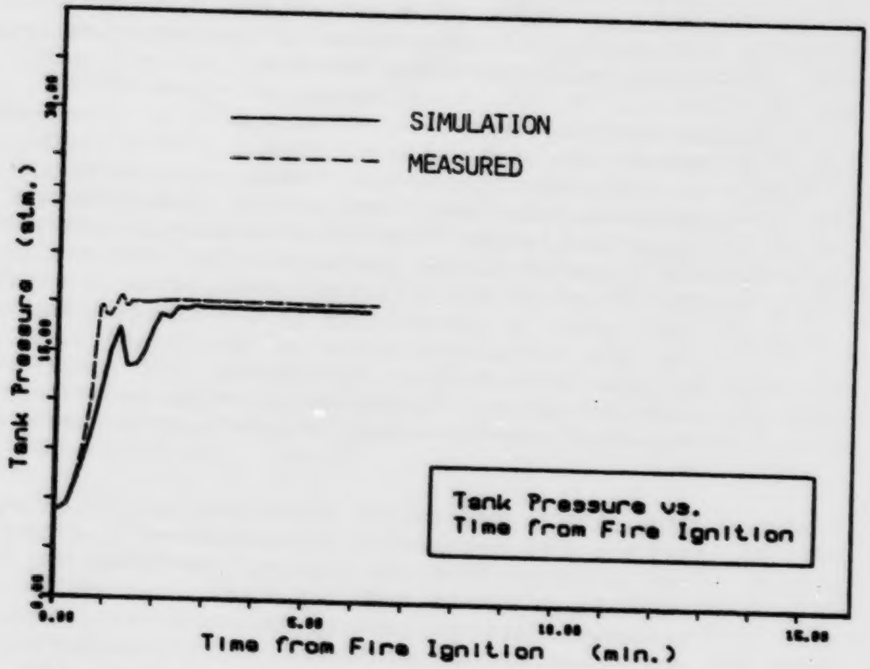

FIGURE 2-74 PREDICTED TANK PRESSURE AND MEASURED TANK PRESSURE FOR TEST #6 (from Reference (4))

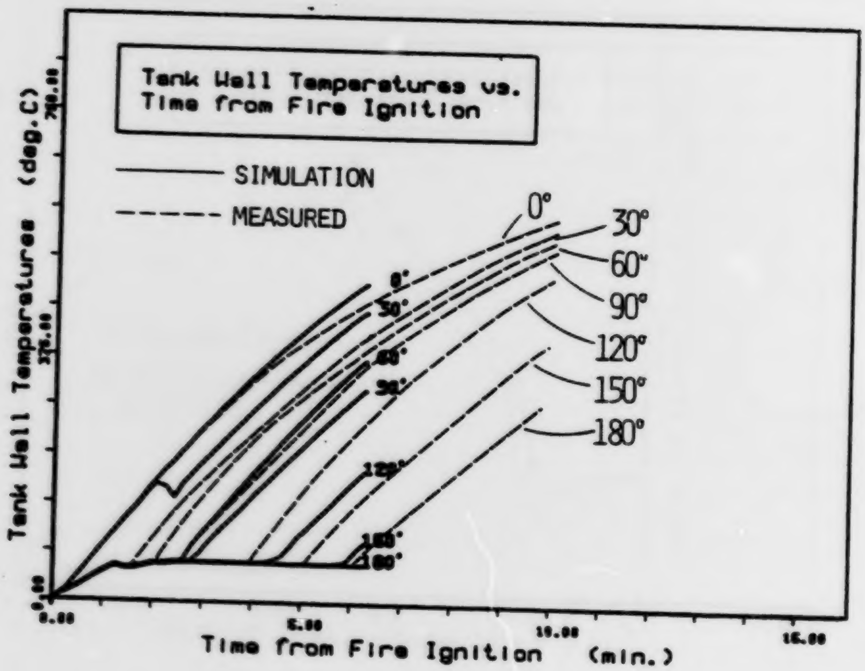

FIGURE 2-75 PREDICTED WALL TEMPERATURES AND MEASURED WALL TEMPERATURES FROM TEST #6 (from Reference (4))

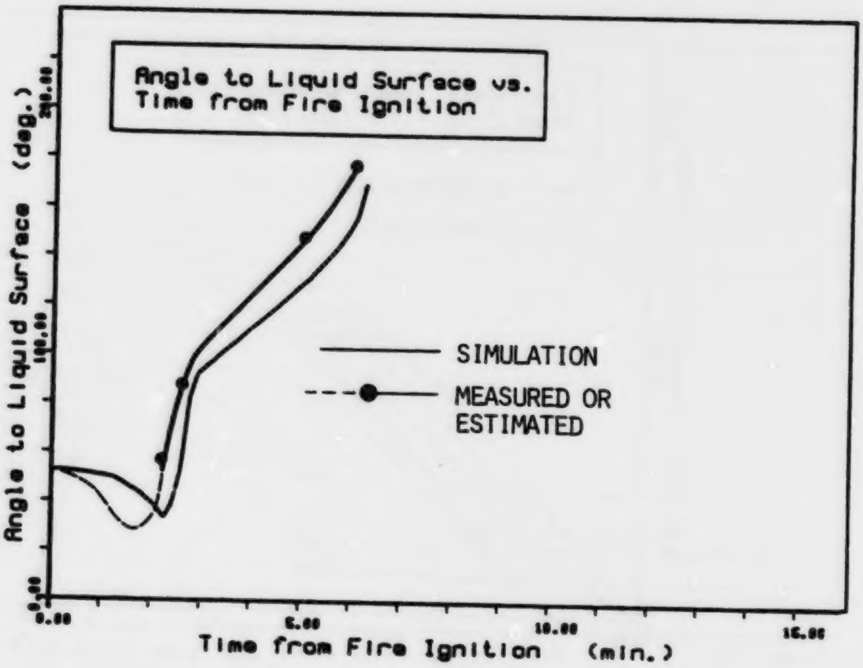

FIGURE 2-76 PREDICTED LIQUID LEVEL AND MEASURED LIQUID LEVEL FOR TEST #6 (from Reference (4))

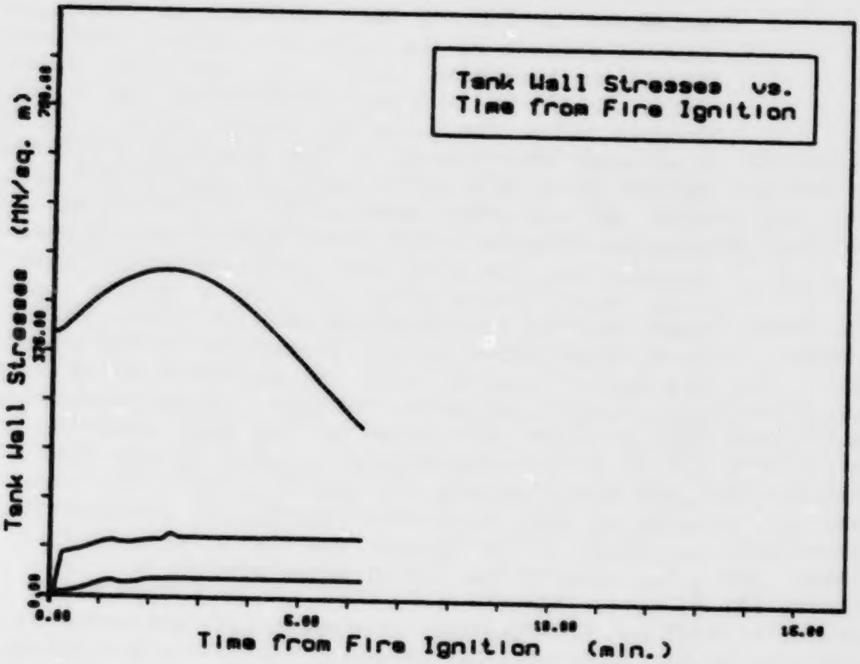

FIGURE 2-77 PREDICTED TANK WALL STRESSES AND MATERIAL STRENGTH FOR TEST #6

rapidly after 2 minutes into the test. The model predictions show a similar rapid drop in the liquid level but at a slightly later time, and this results in quite a substantial error in the prediction of location of the liquid level.

As mentioned previously, Test # 6 involved a tank rolled 90° to one side so that the relief valve would be submerged in liquid, and therefore at least during the initial periods of the tests the relief valve was passing liquid or two-phase fluid. At some point however, the valve would be passing vapour when the liquid level dropped below the pressure relief valve. The point in time when this change in the phase flowing through the relief valve occurs, is seen in the Figure as a sudden bend in the plot showing the liquid level. For the predicted level, this bend occurs at approximately 3 minutes into the fire test. For the actual test results, this bend occurs about 1/3 of a minute before that predicted by the tank-car model. Although there is a significant error in the prediction of the liquid level, the actual rate at which the liquid level is dropping is quite well predicted. The error in the prediction in the liquid level is caused by the fact that the predicted liquid level response is slightly shifted along the time axis with respect to the liquid level. This slight shifting results in the significant errors. This slight shifting is of course due to a slight error in the prediction of the relief valve action.

Figure 2-77 presents the predicted tank wall stresses and tank wall material strength for Test # 6. As can be seen from the figure, the tank-car model does not predict tank failure.

In summary, the model predictions are generally in quite good agreement with the actual results from Test # 6. The tank-car model prediction of the tank pressurization rate is quite good although there were some instability problems with the model of the relief valve flow rate. This problem is associated with the non-linear action with the relief valve and the fact that liquid is passing through the relief valve. The tank wall temperature rise rates were well predicted however the actual break times for the different wall locations were not well predicted because of the difference between the predicted liquid level and the actually observed liquid level. The prediction of the liquid level is very good in terms of the rate at which the liquid level dropped, however, the predicted liquid level is slightly shifted along the time axis with respect to the actually observed liquid level, and this results in rather significant errors. The rather significant errors are due to the fact that the liquid level is dropping very rapidly and because of the severe slope of the curves even a small offset results in a rather large difference in the liquid levels. The tank-car model did not predict tank rupture which is of course in agreement with the actual rest results.

2.3.2.5 Test # 7

This case involved the simulation of a thermally protected fifth-scale tank filled with propane exposed to an engulfing fire environment. The simulation was performed with boundary conditions matching those from the AAR/RPI Test # 7.

The tank was insulated with a 102 mm thick cover of poly-urethane foam insulation covered by a steel jacket. Poly-urethane foam is known to degrade at high temperatures. However, detailed data on this degration process could not be found and therefore this simulation did not include the accurate modelling of the insulation degradation. Instead, an effective thermal conductivity was used for the poly-urethane foam to account for the degradation process. The effective thermal conductivity was established by the calibration of the model predictions of the tank wall temperatures with the actual measured wall temperatures from Test # 7. This effective thermal conductivity was the only co-efficient or constant varied in the tank-car model to obtain the overall simulation results. As will be seen from the figures, the setting of this single effective thermal conductivity resulted in very good agreement for the predicted tank pressure, predicted tank wall temperatures, and the predicted tank liquid level. The results of the simulations are presented in Figures 2-78 to 2-81.

Figure 2-78 presents the predicted tank pressure along with the actual measured pressure from Test # 7. As can be seen from the figure, the tank initial pressurization rate is quite well predicted as is the average pressure during the valve cycling period. As with the other AAR/RPI fifth-scale tests, the tank was equipped with a full-size pressure relief valve and the tank wall was equal to the wall thickness of a full-size tank-car. As a result of the relief valve oversizing, the relief valve cycle during the entire test.

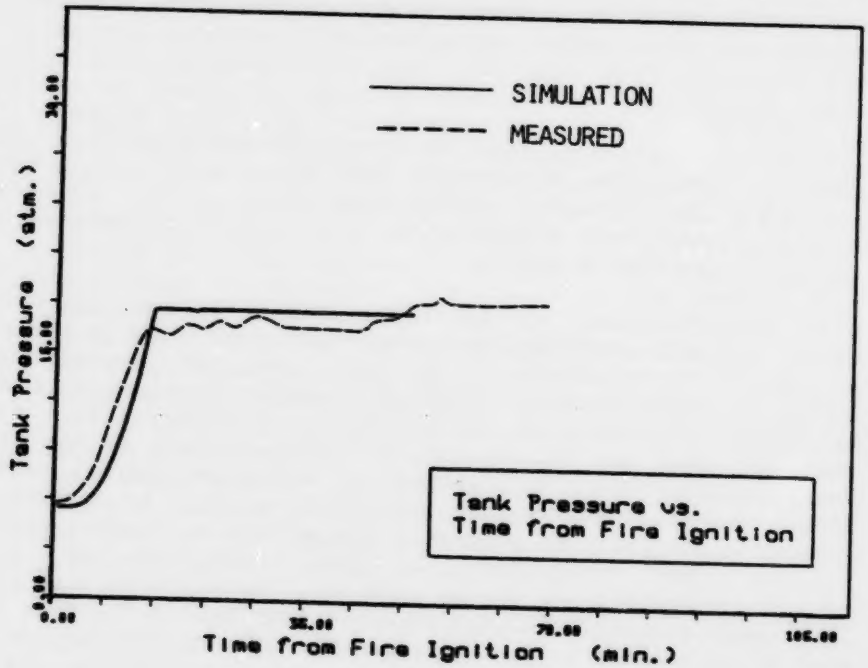

FIGURE 2-78 PREDICTED TANK PRESSURE AND MEASURED TANK PRESSURE FOR TEST #7 (from Reference (5))

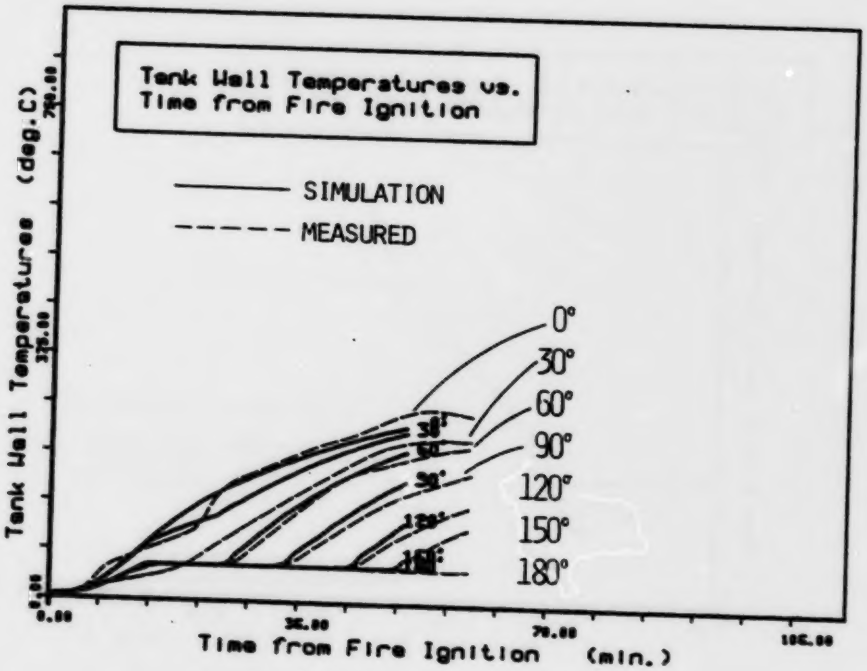

FIGURE 2-79 PREDICTED WALL TEMPERATURES AND MEASURED WALL TEMPERATURES FROM TEST #7 (from Reference (5))

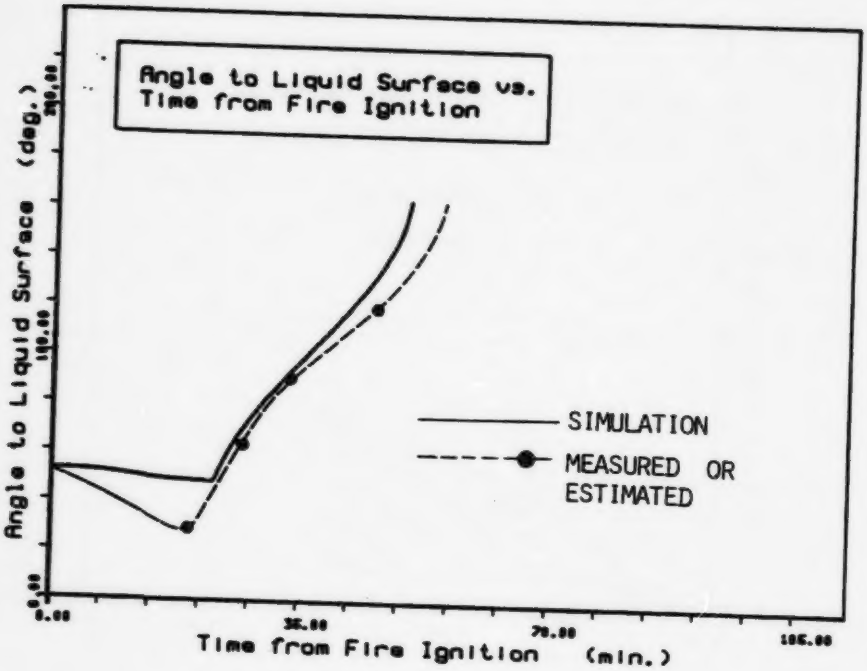

FIGURE 2-80 PREDICTED LIQUID LEVEL AND MEASURED LIQUID LEVEL FOR TEST #7 (from Reference (5))

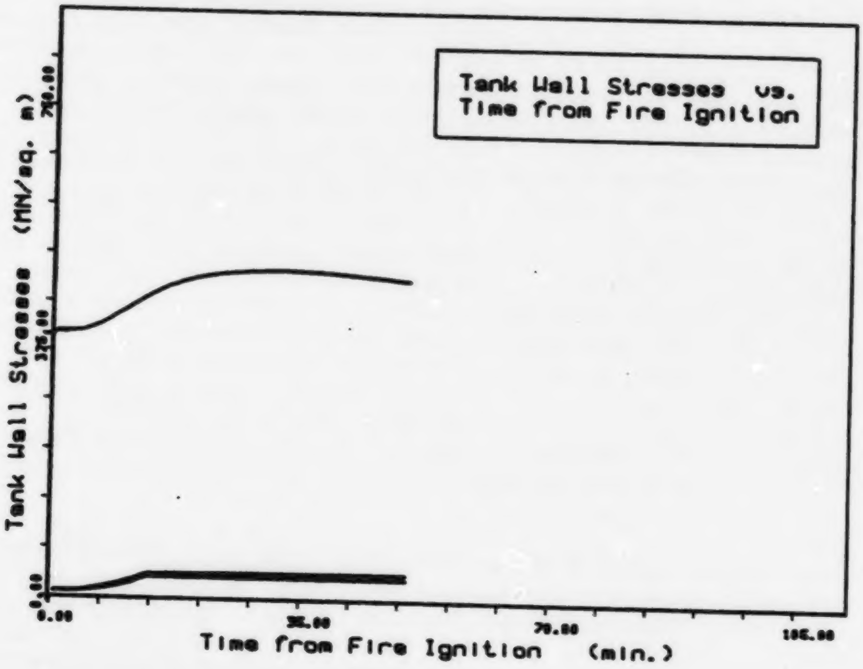

FIGURE 2-81 PREDICTED TANK WALL STRESSES AND MATERIAL STRENGTH FOR TEST #7

Figure 2-79 presents the predicted tank wall temperatures along with the actual measured wall temperatures from Test # 7. As mentioned earlier, the effective thermal conductivity used to represent the poly-urethane foam was established by calibrating the predicted wall temperatures with the actual measured wall temperatures. Therefore, the predicted wall temperatures are in good agreement for that reason. As can be seen from the figure, the wall temperatures are well predicted including the prediction of the wall temperatures around the side of the tank. This is an indication, that not only the temperatures were well predicted but the tank liquid level was well predicted as will be seen the next figure.

Figure 2-80 presents the predicted liquid level along with the estimated liquid level from the results of Test # 7. As can be seen from the figure, the test results seem to indicate that the tank reached the near liquid full condition. However, it may not be that the tank approached the liquid full condition it could also be that the frothing 2-phase region resulted in a perceived high liquid level. The model, does not predict that the tank reached the near liquid full condition. Beyond approximately 3 minutes, the model predictions are in good agreement with the estimated liquid level from Test # 7. The predicted and measured liquid levels diverged slightly in the later minutes of the fire.

Figure 2-81 presents the predicted tank wall stresses and the predicted tank wall material strength for Test # 7. As can be seen from the figure the model did not predict the tank failure. This, of course, is due to the fact that the tank wall temperatures were maintained well below levels that would result in significant degradation in the tank wall material strength. In addition, the presence of the insulation resulted in small radial temperature gradients in the tank wall which resulted in small thermal stresses.

In summary, the results of the simulation are in excellent agreement with the actual observed results of Test # 7. It should be noted, however, that these results were generated using an effective thermal conductivity which was calibrated to the tank wall temperatures measured from Test # 7. However, with the use of the single thermal conductivity, the tank-car model was able to predict all of the vital conditions of the tank-car including the tank pressure, tank wall temperatures, and the tank liquid level.

2.3.2.6 Torch Fire Tests

This simulation was performed to compare the results of the tank-car model with the torch fire tests conducted on bare metal plates and on an empty tank-car. The simulations involved a full-scale tank exposed to a torch type fire applied 30° from the tank top-dead-center. In this simulation, the tank was almost empty (10 % full of propane). The results of the simulation are presented in Figures 2-82 to 2-85.

Figure 2-82 presents the predicted tank pressure for the case of a nearly empty tank-car exposed to a torch fire. Because of the fact that the torch is applied near the top of the tank, and that the tank is almost empty the tank pressurization rate would be very slow.

Figure 2-83 presents the predicted wall temperatures along with the results from the bare plate and the empty tank torch fire tests. As can be seen from the figure, the predictions for the peak wall temperatures (at the center of torch application) are in excellent agreement with the measured temperatures at the center of the torch application for the bare plates and for the test conducted on the empty tank-car. No data was recorded for the other wall locations from the empty tank-car torch fire tests.

Figure 2-84 presents the predicted liquid level in the tank. As expected, the liquid level does not change over the duration of the test because of the fact that the torch is being applied far away from the liquid contents.

Figure 2-85 presents the predicted wall stresses and predicted wall material strength for the case of the nearly empty tank exposed to a torch fire. As can be seen from the figure, the tank-car model predicts that the tank would rupture sometime shortly after 10 minutes after the torch was applied. This is due to the fact at the center of the torch application, the tank wall temperatures are very high and these high temperatures result in a significant drop in the tank wall material strength. This drop in the material strength results in the failure of the tank.

In summary, the results of the simulation show that the tank-car model's representation of a torch compares well with the torch fire test facility constructed in the U.S. Therefore, it can be concluded that the two dimensional torch analysis used in the tank-car model is a fair representation of an accidental torch fire impingement.

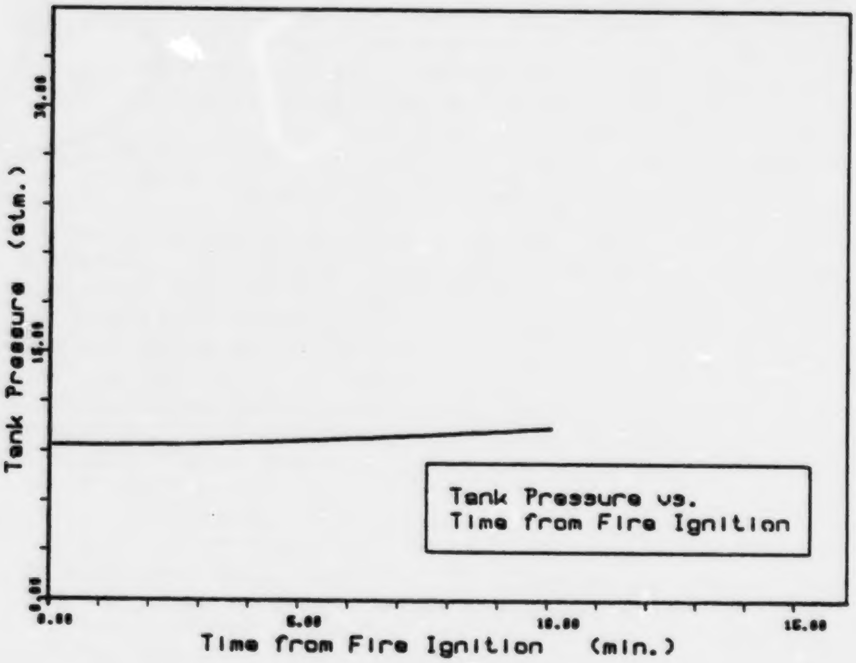

FIGURE 2-82 PREDICTED TANK PRESSURE FOR TORCH FIRE TEST

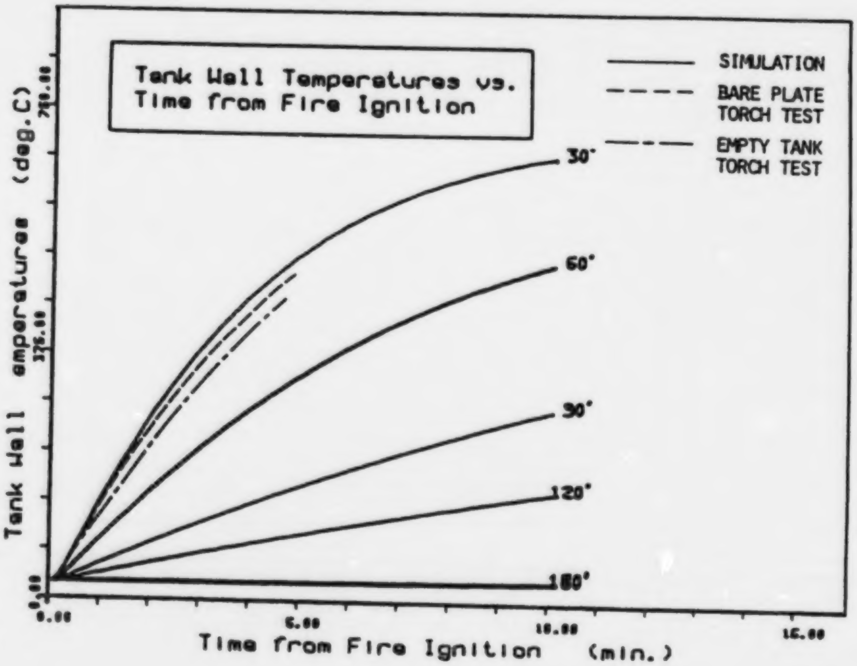

FIGURE 2-83 PREDICTED WALL TEMPERATURES AND MEASURED WALL TEMPERATURES FROM TORCH FIRE TEST (from Reference (8))

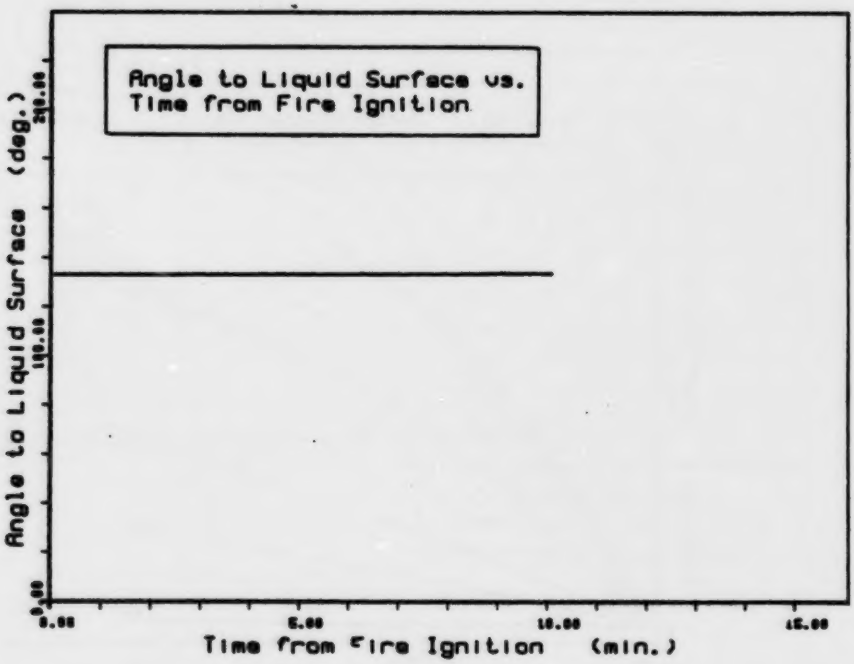

FIGURE 2-84 PREDICTED LIQUID LEVEL FOR TORCH FIRE TEST

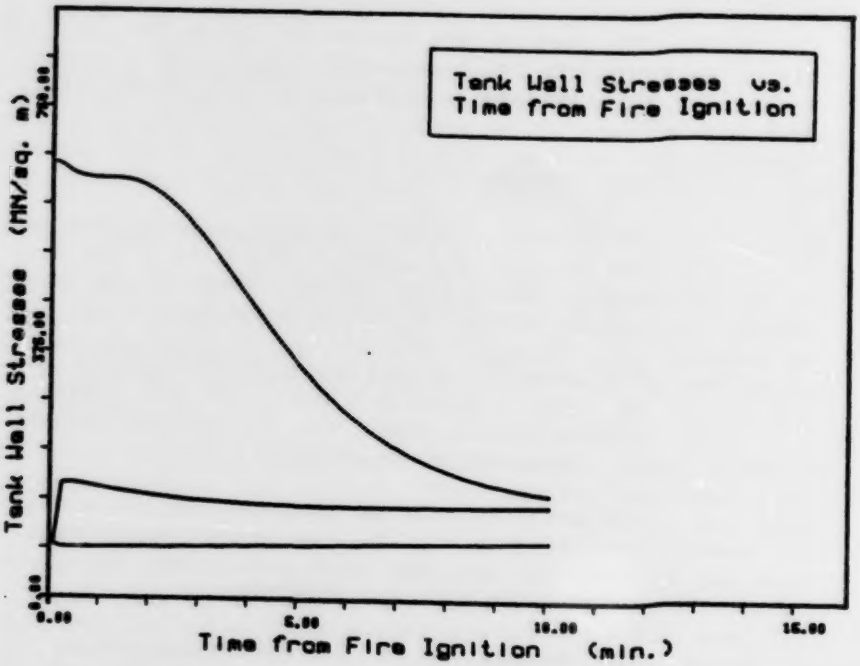

FIGURE 2-85 PREDICTED TANK WALL STRESSES AND MATERIAL STRENGTH FOR TORCH FIRE TEST

3.0 PROGRAM SENSITIVITY ANALYSIS

This section presents the results of a series of program runs conducted to test the sensitivity of the model to variations in key inputs. The inputs that were considered in the sensitivity analysis are, the time step, fire type and configuration, tank roll, tank pitch, and lading type. A following chapter considers the effects of different combinations and configurations of thermal protection.

The results are presented using the four summary plots; pressure vs. time, wall temperature vs. time, liquid level vs. time and wall stress conditions vs. time.

3.1 TIME STEP SENSITIVITY

The choice of the time step used in the program plays a key role in the model predictions. The size of the time step affects both the accuracy of the model predictions and the stability of the model solutions.

The accuracy of the model prediction is related directly to the implicit and explicit finite difference approximations used, the integration methods, and the use of linearization techniques.

The accuracy and the stability of the model solutions are most closely tied to the thermodynamic heat balance model (HTBAL7) and the tank wall (and associated coverings) temperature submodel (TNKTMP).

The calculation of the wall temperatures is based on an implicit finite difference solution of the governing equations. The effects of the thermal radiation are linearized by using explicitly determined heat transfer coefficients. The boundary conditions, such as fluid temperatures, heat transfer coefficients and heat inputs are also explicitly obtained. Explicit components of the solution give rise to solution instabilities. Other inaccuracies result due to integration errors.

The heat balance model is based on a simple numerical integration technique. Accuracy is therefore tied directly to the selection of the integration interval or time step. In addition, there are inaccuracies and potential stability problems associated with the very non-linear affects of the pressure relief valve action and the affects of temperature sensitive valves or fusible plugs.

The effects which have just been described will now be illustrated with two examples. The first is a simulation of an unprotected tank-car and it will be seen that the variation in time step has a small affect on the prediction of tank failure. However, in this particular case there are no stability problems. The second example, is a simulation of a tank with externally applied thermal insulation. It will be seen that increasing the time step in this particular case results in program instabilities and eventual model failure.

In both examples the time steps were increased while all other run parameters were kept constant. The results of the runs are presented in plots which present the tank pressure, wall temperature, liquid level and wall stresses as functions of time from fire ignition.

3.1.1 Unprotected Tank

This series of runs involved the simulation of a full-scale unprotected (except for standard size relief valve) tank-car filled to 95% capacity with propane at 25°C. In all the simulations the tank was exposed to an engulfing pool fire.

In total five time steps were considered, .5 sec, 1 sec., 5 sec., 10 sec., and 30 sec. The results from these runs are presented in Figures 3-1 to 3-4. As will be seen from these figures, there is very little difference between the .5 second and the 1 second runs and therefore it can been assumed that these time steps give accurate predictions. This was the basis for choosing a one second time step for all the validation runs which were presented in Chapter 2.

Figure 3-1 presents the predicted tank pressure for the different time step runs. As can be seen from the figure the different time steps have very little effect on the pressure predictions other than a shifting along the time axis. This is due to the fact that the large time steps caused the initial heat up period to be poorly represented. The rapid thermal response in the first moments of the fire requires small integration intervals, i.e., small time steps. As can be seen from the figure the length of the valve cycling period is not affected by the time step size. The peak tank pressure is also unaffected by the time step choice. The only affect, is the slight shifting along the time axis which was mentioned earlier.

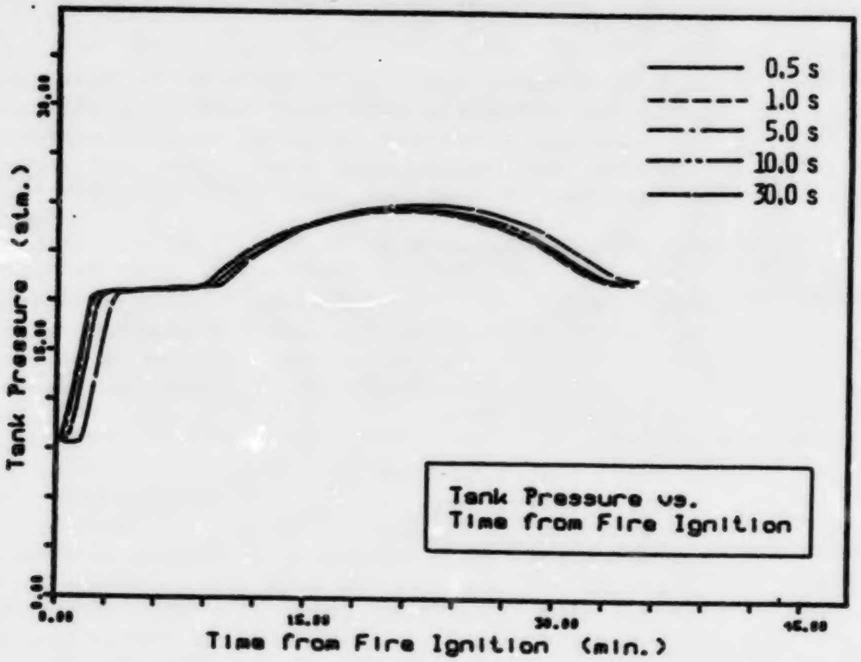

FIGURE 3-1 PREDICTED TANK PRESSURE FOR UNPROTECTED TANK FROM PROGRAM RUNS USING DIFFERENT TIME STEPS

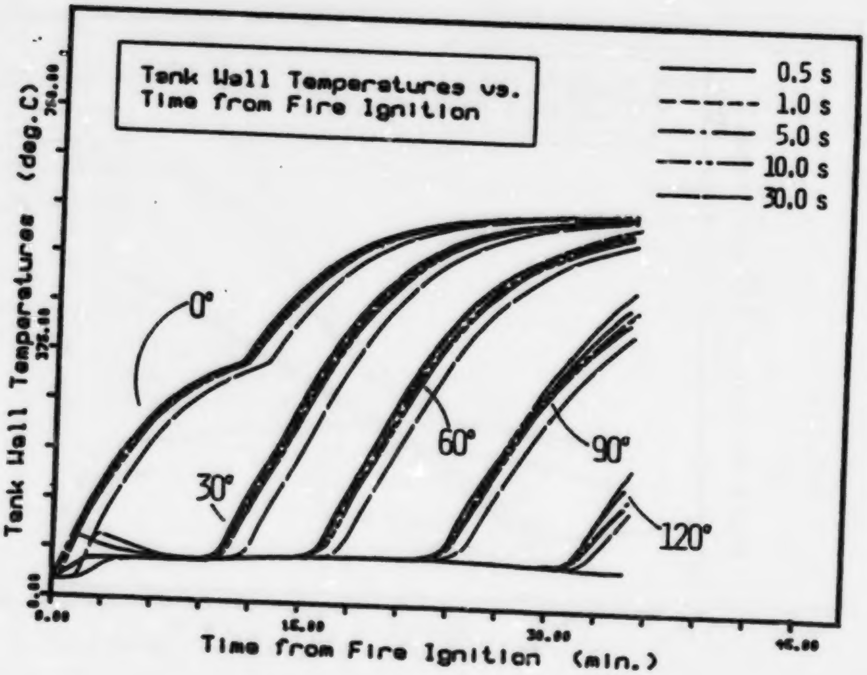

FIGURE 3-2 PREDICTED WALL TEMPERATURES FOR UNPROTECTED TANK FROM PROGRAM RUNS USING DIFFERENT TIME STEPS

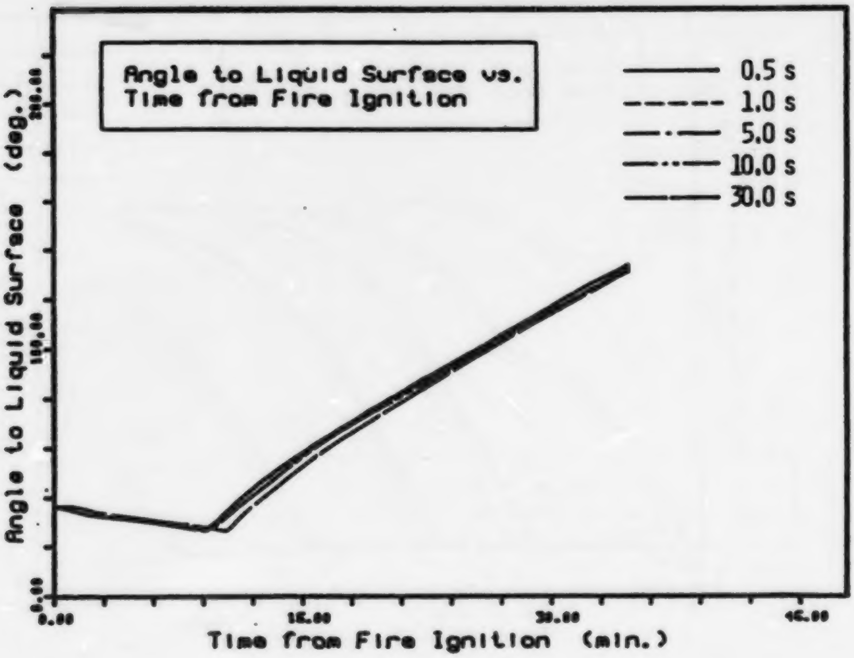

FIGURE 3-3 PREDICTED LIQUID LEVEL FOR UNPROTECTED TANK FROM PROGRAM RUNS USING DIFFERENT TIME STEPS

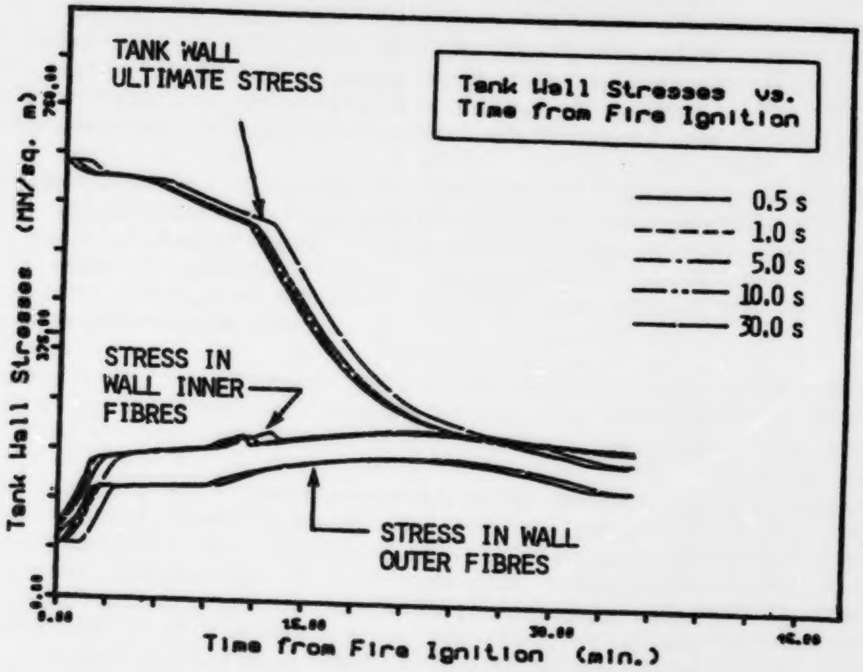

FIGURE 3-4 PREDICTED TANK WALL STRESSES AND MATERIAL STRENGTH FOR UNPROTECTED TANK FROM PROGRAM RUNS USING DIFFERENT TIME STEPS

Figure 3-2 presents the predicted tank wall temperatures for the different time step cases considered. As with the pressure predictions, the only effect that is seen is a slight shifting along the time axis. The peak wall temperatures are unaffected by the choice of the time step as is the length of time between temperature breaks. The slight shift along the time axis is again due to the poor representation of the initial heating period.

Figure 3-3 presents the predicted liquid level for the different time step cases considered. Again the only apparent affect is a slight shifting along the time axis. The actual slopes of the different curves are identical.

Figure 3-4 presents the predicted tank wall stresses and tank wall material strengths. As with all the plots, the only apparent effect is a slight shifting along the time axis. This shifting however, affects the time to failure predictions. The error in the prediction of the time to tank failure is directly related to the degree of shifting along the time axis of all the prediction results. However, the total time shift is only approximately 3 minutes for the 30 second time step case. This is not considered to be a large error.

In summary, the results indicate that the Tank Car model is relatively insensitive to changes in time step, up to approximately 30 seconds, for the specific case of an unprotected tank-car. It is recommended therefore that time steps of less than 30 seconds be used for all simulations of unprotected tanks. It is believed that a time step of 1 second gives accurate results.

3.1.2 Insulated Tank

This series of runs involved the simulation of a full-scale thermally insulated tank (with standard size relief valve) filled to 95% capacity with propane at 25°C. The tank was exposed to an engulfing pool fire. In the simulation, it was assumed that the thermal insulation consisted of 6.4 mm thick layer of material with thermal and mechanical properties similar to those of asbestos. Both steel jacketed and unjacketed cases were considered because the calculation procedure changes when steel jacket is added. As will be seen from the following results, the model sensitivity to variations of time step size are significantly affected by the steel jacket. This is because the steel jacket analysis has a stabilizing effect on the overall calculations.

The results are presented for both jacketed and unjacketed cases using time steps of 1, 5, 10 and 30 seconds. The results for the jacketed insulation case are presented in Figures 3-5 to 3-8. The results for the unjacketed case are presented in Figures 3-9 to 3-12.

Case 1; Jacketed Insulation (Figures 3-5 to 3-8)

Figure 3-5 presents the predicted tank pressures as a function of time from fire ignition. As can be seen from this figure the pressure prediction is not significantly affected by the variations of the time step. The only apparent effect is a slight shifting of the predicted response along the time axis. As with the case of an unprotected tank this shifting effect is caused by integration errors during the initial rapid heating of the tank/lading system. These inaccuracies however, have no affect on the overall peak pressure. This shifting along the time axis also has no effect on the length of the valve cycling period.

Figure 3-6 presents the predicted wall temperatures for the insulated and jacketed tank for the different time steps considered. Once again, the model predictions are shifted along the time axis as the time step size is increased. In addition, the predicted wall temperatures, especially at locations around the side of the tank, are significantly effected as the time step is increased. As the time step is increased the wall temperatures are reduced from those predicted using small (1 second) time steps. This deviation is due to a build up of integration error over the rather long real time duration of the simulation. This kind of build up of integration errors is not seen clearly with an unprotected tank case because the real time duration is much shorter for an unpredicted tank period. For the case of an unprotected tank, the real time duration may be approximately 30 or 40 minutes. Whereas, in the case of a thermally insulated tank, the real time duration may be as high as 300 to 400 minutes. This increase in the length of real time allows integration errors to build up until the point where they are very significant. This inaccuracy, however, does not affect the wall temperatures near the top of the tank significantly and since these are the peak temperatures which dictate the time to tank failure the actual prediction of failure is not significantly affected by this buildup of integration errors. This will be discussed further later.

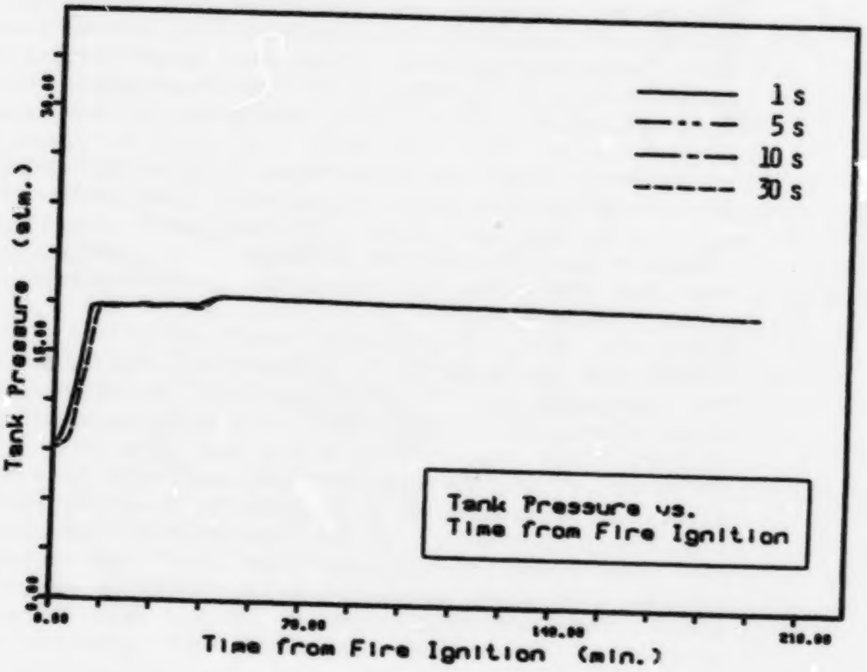

FIGURE 3-5 PREDICTED TANK PRESSURE FOR INSULATED TANK (WITH STEEL JACKET) FROM PROGRAM RUNS USING DIFFERENT TIME STEPS

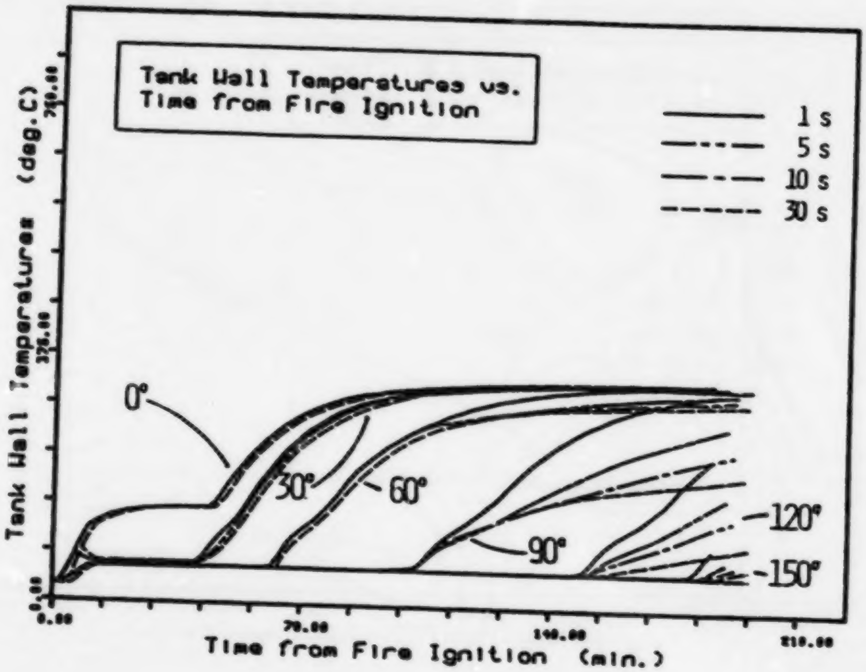

FIGURE 3-6 PREDICTED WALL TEMPERATURES FOR INSULATED TANK (WITH STEEL JACKET) FROM PROGRAM RUNS USING DIFFERENT TIME STEPS

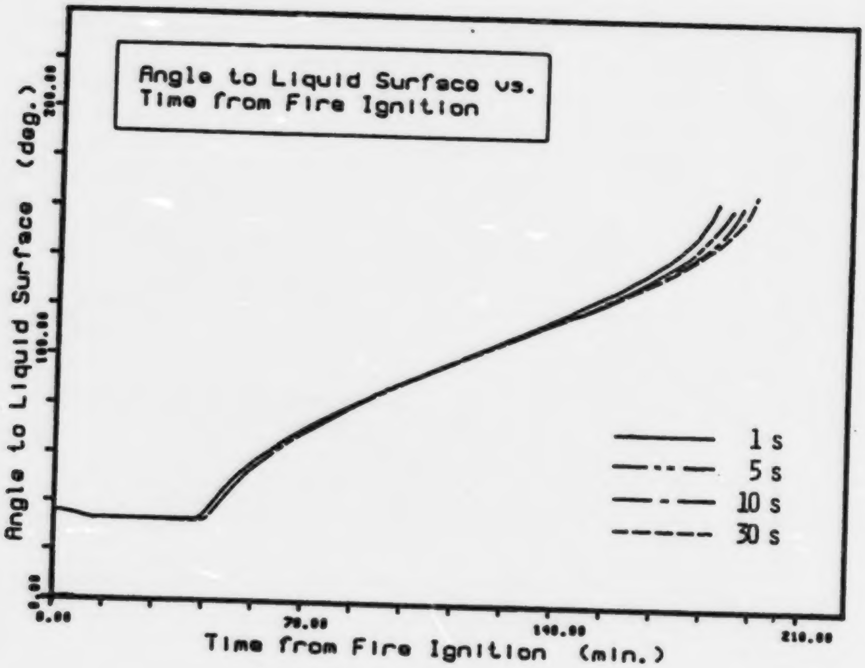

FIGURE 3-7 PREDICTED LIQUID LEVEL FOR INSULATED TANK (WITH STEEL JACKET) FROM PROGRAM RUNS USING DIFFERENT TIME STEPS

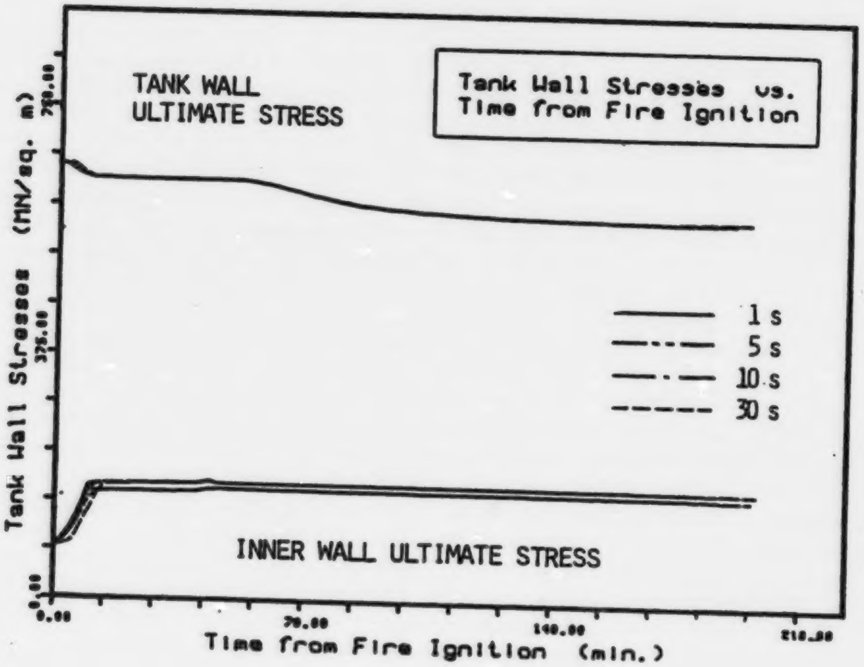

FIGURE 3-8 PREDICTED TANK WALL STRESSES AND MATERIAL STRENGTH FOR INSULATED TANK (WITH STEEL JACKET) FROM PROGRAM RUNS USING DIFFERENT TIME STEPS

The wall temperature predictions clearly show how important the proper choice of time step size is. As a general rule, integration errors will grow in proportion to the real time duration of a simulation. The real time being, the actual tank-car time, not the computer run time. Therefore, it is not advisable that long real time durations be associated with large time steps. This of course, will reduce computer run time, however it will also increase integration error.

Figure 3-7 presents the model predictions for the liquid level. The plots again show a slight shifting of the predicted liquid level along the time axis. Additional to the shifting effect of the increased time step, the location of the liquid level deviates more and more as time goes on because of integration errors which build up. The integration errors, of course, are associated with the large time steps. This error tends to keep the liquid level higher in the tank and this translates into the wall temperature prediction errors discussed earlier. The integration error is caused by the fact that over a time interval the relief valve mass flow is assumed to be constant. Because an insulated tank remains in a fire for a long period, the integration errors accumulate and eventually become significant. For this reason these integration errors are not as significant for the case of an unprotected tank because of the short simulation real time. To improve the integration of mass flow leaving the tank-car, one would have to know the mass flow rate at a point in time in the future. This can be done, however, it would require iteration which would significantly increase the run time of the tank-car program.

Figure 3-8 presents the predicted tank stress conditions for the case of thermally protected tank with steel jacket. As can be seen from the Figure the only apparent affect of the different time steps is a very slight shifting along the time axis for the highest time steps chosen. However, the actual wall stresses and material strengths are not significantly affected by the different time steps chosen.

The wall material strength is directly related to the peak wall temperature. In the case of a tank-car exposed to engulfing pool fire the peak wall temperature will occur at the top-dead-centre of the tank. It was shown earlier that the peak wall temperature at top-dead-centre was not significantly effected by integration errors. Therefore, different time steps appear to have little or no effect on the material strength. The tank wall stresses are of course dictated by the tank internal pressure and a temperature gradient through the tank wall. Neither of these are significantly effected by changes in the time step, and therefore, there is no significant change in the predicted wall stresses. These effects combine to give no significant change in the prediction of time to failure.

In summary, the results indicate that variations in the size of the program time step for the specific case of an insulated tank with steel jacket exposed to an engulfing pool fire have little or no effect on the prediction of time to failure. However, variations in the time step can have a significant effect on the prediction of wall temperatures. Therefore, it is recommended that for such cases the time step be kept below five seconds. If however, it is not important to accurately predict the wall temperatures, time steps can be increased to a limit of approximately 30 seconds.

Case 2: Insulation without Steel Jacket (Figures 3-9 to 3-12)

This series of simulations involved an insulated tank with the same thermal barrier as described in the previous case, however, there was no steel jacket present. This case was considered in the sensitivity analysis because it is known that the analysis used to represent the steel jacket has a stabilizing effect on the calculation of wall temperatures. It should be made clear that the time step sensitivities about to be discussed are typical of an explicit numerical solution technique.

Figures 3-9 to 3-12 present the results of the simulations. Time steps of 1, 5, 10 and 30 seconds were considered. The results shown in the figures include only the results from the 1 and 5 second time step runs. The results from the other runs (ie. 10 and 30 second time step) are not plotted because those runs terminated very early in the simulations because of instabilities in the numerical solutions. The instabilities causing the termination of the runs were associated with the subroutine TNKTMP which is used to calculate the temperature distribution in the tank and associated coverings. The details of the instability will be discussed in more detail at a later point in this section.

The results that are presented in Figures 3-9 to 3-12 for the 1 and 5 second time step cases are very nearly

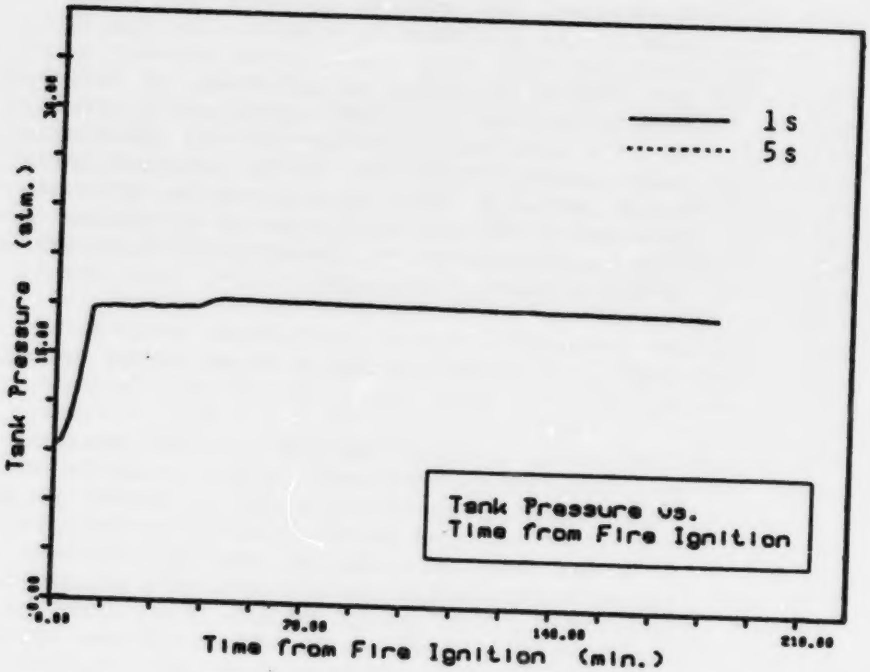

FIGURE 3-9 PREDICTED TANK PRESSURE FOR INSULATED TANK (NO STEEL JACKET) FROM PROGRAM RUNS USING DIFFERENT TIME STEPS

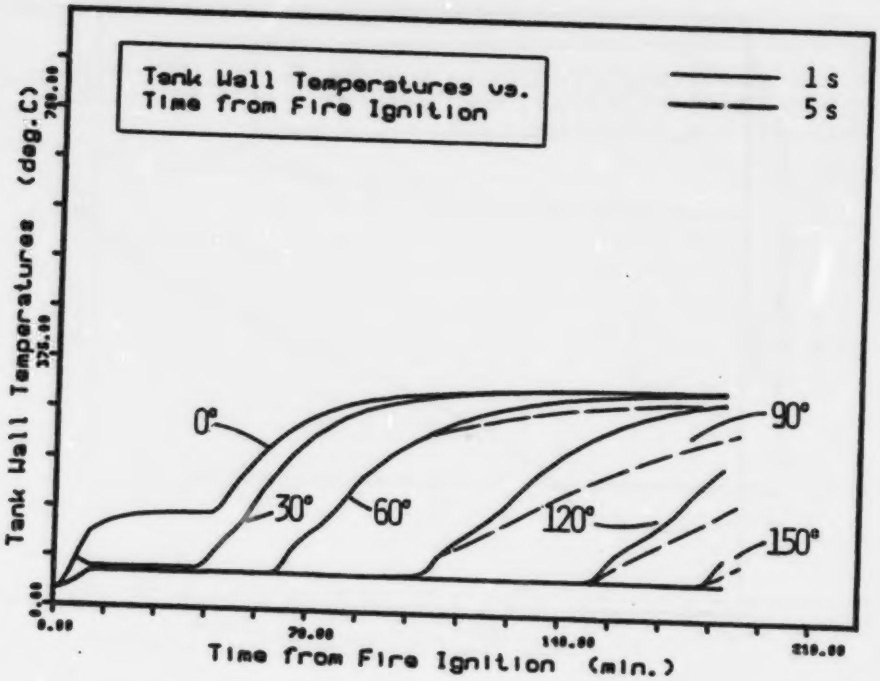

FIGURE 3-10 PREDICTED WALL TEMPERATURES FOR INSULATED TANK (NO STEEL JACKET) FROM PROGRAM RUNS USING DIFFERENT TIME STEPS

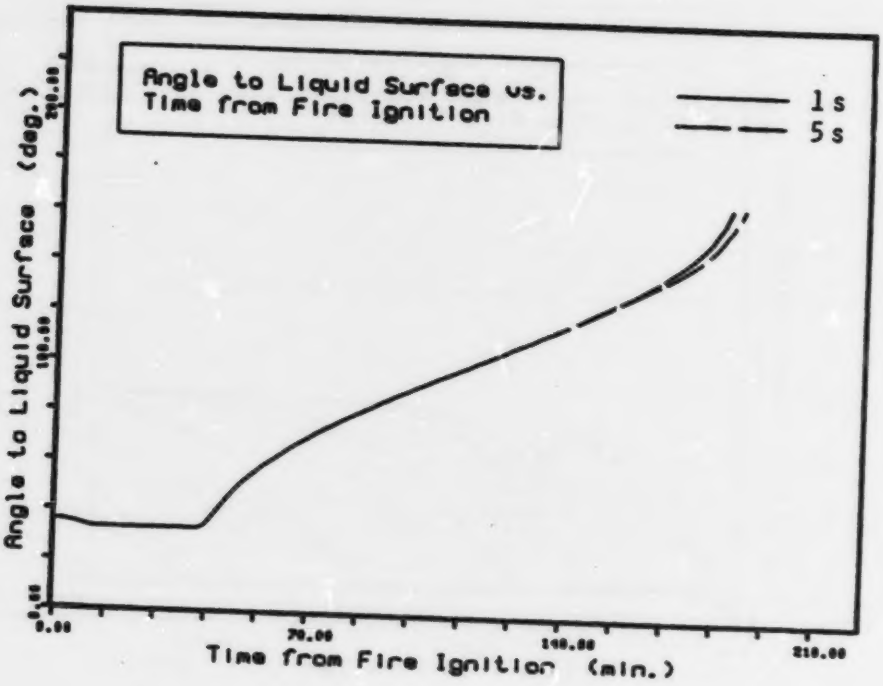

FIGURE 3-11 PREDICTED LIQUID LEVEL FOR INSULATED TANK (NO STEEL JACKET) FROM PROGRAM RUNS USING DIFFERENT TIME STEPS

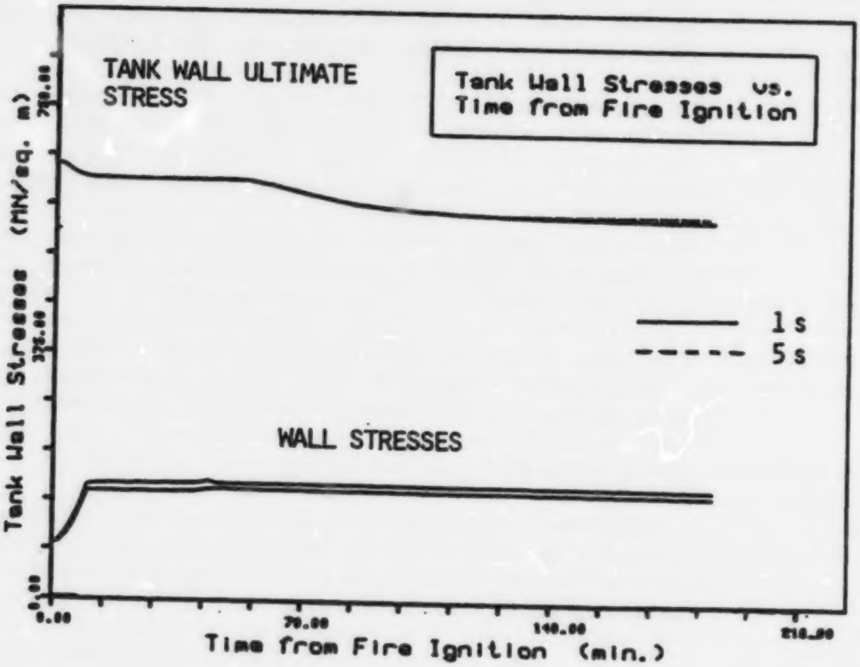

FIGURE 3-12 PREDICTED TANK WALL STRESSES AND MATERIAL STRENGTH FOR INSULATED TANK (NO STEEL JACKET) FROM PROGRAM RUNS USING DIFFERENT TIME STEPS

identical to those shown in the case of the insulated tank with steel jacket. This is an indication that the predictions for 1 and 5 second time steps for this case are accurate. It is expected that from a thermal standpoint the presence of the steel jacket does not affect the temperatures in the insulation and tank wall as long as the insulation stays in contact with the steel jacket. If the insulation shrinks away from the steel jacket then the jacket will act as a radiation shield, an additional resistance to the flow of heat to the tank.

The cases with the 10 and 30 second time steps terminated early in the simulations because of instabilities in the calculation of the wall and insulation temperatures. The instabilities were caused by the large time steps.

The calculation of the wall temperatures is based on a partially implicit, partially explicit finite difference solution technique. The explicit part of the procedure results from the fact that the fire heat transfer rates to the tank outer surface are calculated using wall temperatures from a previous time step. For small time steps this method is adequate. However, for large time steps the explicit procedure becomes unstable. The reasons for the instability are as follows.

During the initial moments of a fire, the outer surface of a tank wall experiences rapid increases in temperature. For an uninsulated tank, the outer surface temperatures are limited by the relatively high thermal conductivity of the steel, and the heat transfer from the tank inner surface. For an insulated tank, the outer surface temperatures will reach much higher levels because of the low thermal conductivity of the insulation (the insulation requires a much larger temperature difference applied through its depth to get the same heat transfer). For this reason the outer fibres of the insulation layer may experience temperatures which approach the fire temperature.

In sub-routine TNKTMP the heat transfer to the tank outer surface is based on the tank outer surface temperature from a previous time step. The calculated heat transfer is a non-linear function of the temperature differences between the tank outer surface and the fire because the heat transfer from the engulfing fire is primarily due to thermal radiation (heat transfer proportional to the temperature to the fourth power). If the time steps are large the calculated heat transfer rates will have very significant errors associated with them because of the fact that the surface temperatures are actually varying very rapidly. The calculated heat transfer rates are assumed constant over a time step and the errors can result in calculated outer surface wall temperature which exceed the fire temperature. This of course is not possible. During the next time step, the wall heat transfer rates will be negative (caused by the fact that the wall is hotter than the fire). This sets up an oscillation in the numerical solution with a growing amplitude. Eventually, the overall tank-car model fails to converge. This sequence of events caused the early termination of the 10 and 30 second time step runs.

This instability does not appear in the numerical solution if there is a steel jacket because the addition of the jacket mass to the outer most nodes in the wall/insulation model has a stabilizing effect. This added mass at the outer fibre nodes does not eliminate the instability problem, it simply shifts the problem to larger time steps. In other words, it is likely that the insulation with steel jacket case would go unstable if the time step was increased above 30 seconds.

In summary, when a simulation is to take place involving a tank-car with thermal protection, without a steel jacket the time step should be kept below 5 seconds. If the time step is increased above this the program solutions will become unstable and the program run will terminate.

3.2 FIRE CONDITION SENSITIVITY

This section deals with the effects of the fire condition on the overall tank-car model predictions. The runs that were performed were designed to show the effects of fire geometry (pool or torch at various angles of application) and fire temperature on the model predictions.

3.2.1 Pool Fire Temperature Sensitivity

In this case, simulations were performed involving a full-scale unprotected tank (except for standard sized relief valve) and filled with propane exposed to an engulfing fire. The fire mean radiating temperature was varied between 700 and 930°C in 55°C increments. The results of the runs are summarized in Figures 3.13 to 3.16. The runs clearly indicated that the predicted tank

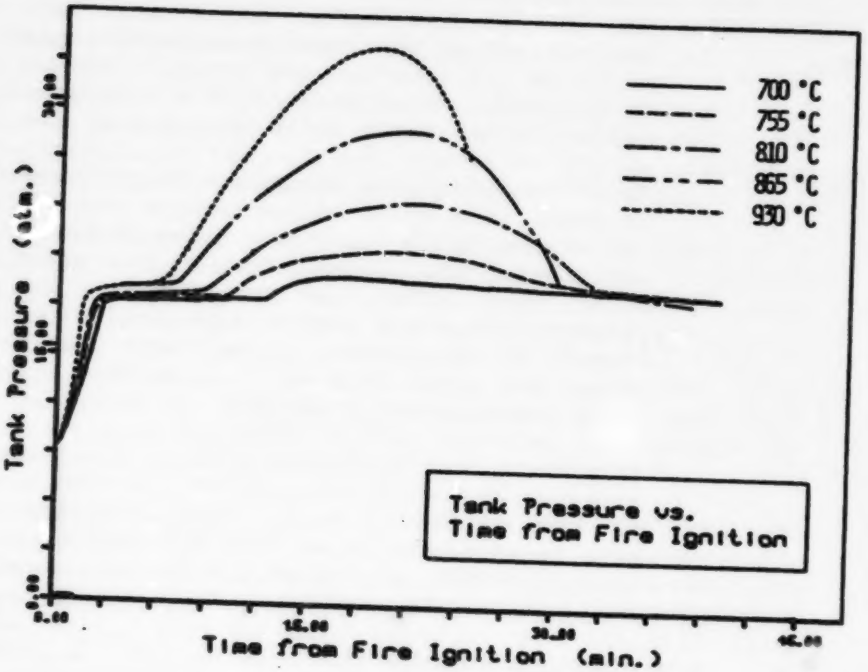

FIGURE 3-13 PREDICTED TANK PRESSURE FOR AN UNPROTECTED TANK FROM PROGRAM RUNS USING DIFFERENT POOL FIRE TEMPERATURES

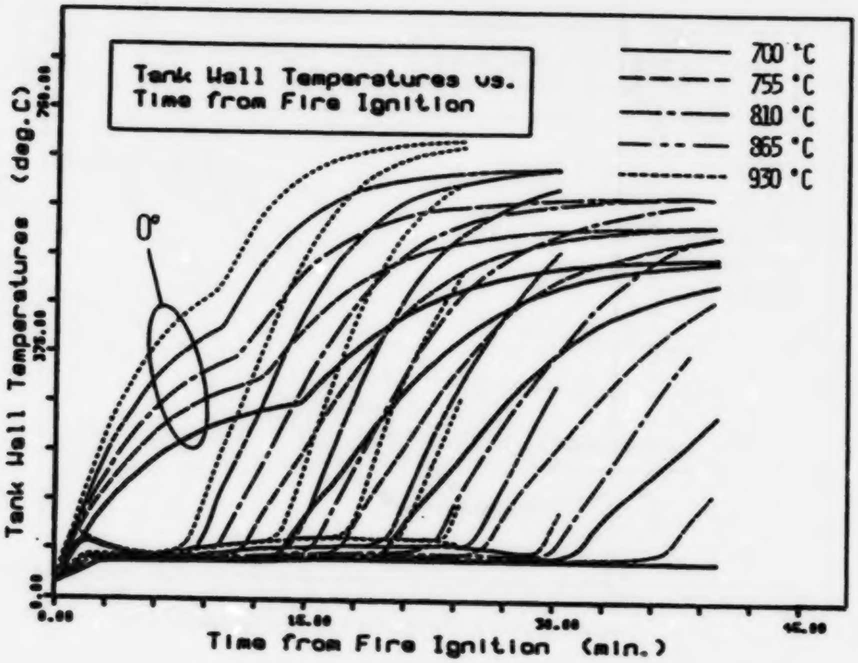

FIGURE 3-14 PREDICTED WALL TEMPERATURES FOR UNPROTECTED TANK FROM PROGRAM RUNS USING DIFFERENT POOL FIRE TEMPERATURES

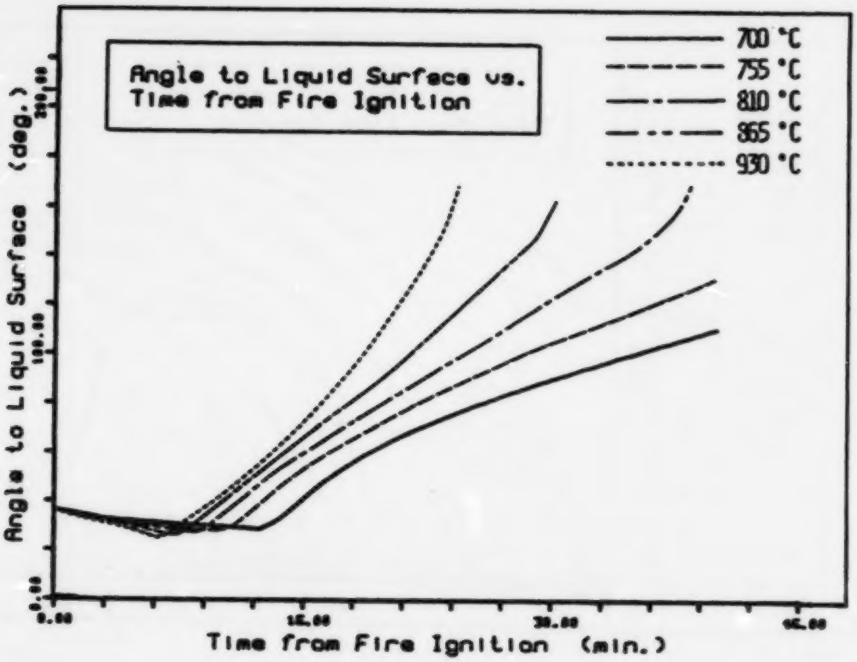

FIGURE 3-15 PREDICTED LIQUID LEVEL FOR UNPROTECTED TANK FROM PROGRAM RUNS USING DIFFERENT POOL FIRE TEMPERATURES

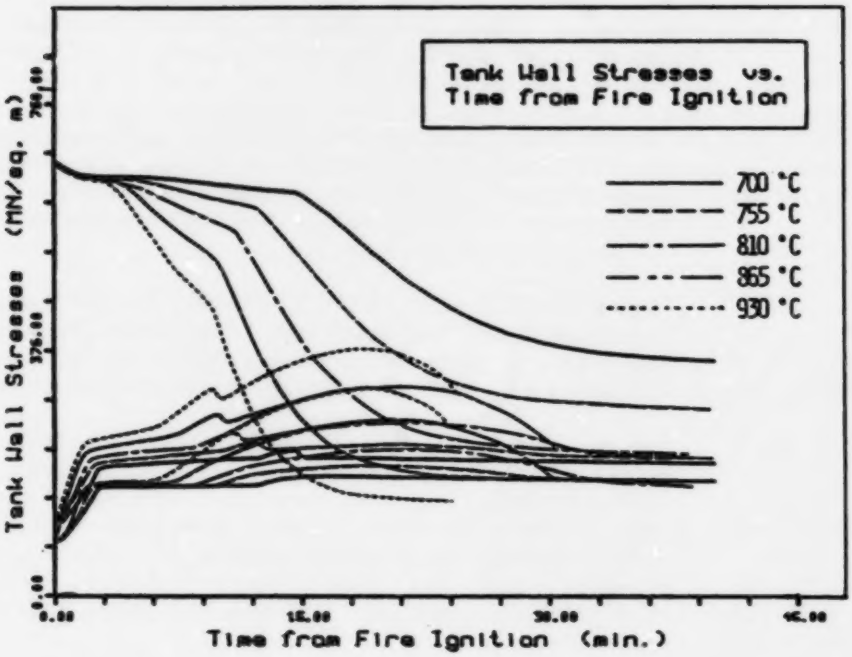

FIGURE 3-16 PREDICTED TANK WALL STRESSES AND MATERIAL STRENGTH FOR UNPROTECTED TANK FROM PROGRAM RUNS USING DIFFERENT POOL FIRE TEMPERATURES

response is very sensitive to the assumed flame temperature.

Figure 3-13 presents the predicted tank pressures for the different flame temperatures. As can be seen from the Figure, the tank pressurization rate and the peak pressure are very sensitive to assumed flame temperature. This is as expected because the heat input to the tank is primarily due to thermal radiation and this is proportional to the flame temperature to the fourth power (T^4).

Figure 3-14 presents the predicted wall temperatures for the different flame temperature cases. The predicted wall temperatures increase significantly as the flame temperature is increased. This is as expected because of the increased heat input.

Figure 3-15 presents the predicted liquid level for the different flame temperatures. The liquid level drops much more rapidly as the flame temperature is increased. This, again, is as expected because of the increased heat input.

Figure 3-16 presents the tank stress condition for the different flame temperatures. As can be seen, both the wall stresses and the tank wall ultimate strength are significantly effected by the flame temperature. The tank wall stresses are higher because of the increased tank pressure and the tank wall material strength is significantly reduced because of the increased wall temperatures.

The results shown here indicate that the flame temperature has a significant effect on the thermal response of a tank-car engulfed in fire.

3.2.2 Pool Fire Absorption Coefficient Sensitivity

This section considers the effects of mean flame absorptivity on the heat input conditions. For this sensitivity case no simulations were performed, however, the effects of flame absorptivity on the fire heat transfer, and the overall tank/lading response are described.

The pool fire heat transfer sub-model is described in detail in the TNKCAR user documentation. A brief description of the radiant heat transfer analysis is repeated here for convenience.

The radiant heat transfer model considers the two-dimensional case of an infinitely long horizontal cylinder engulfed in an upright free ambient fire. The shape of the fire is approximated by a rectangle with height to width ratio (≅ 2.0) as shown in Figure 3-17 based on data from actual fires. With this assumed geometry, the surface-to-surface and surface to volume radiant exchange factors are calculated for flame and tank dimensions appropriate for the full and fifth-scale fire tests. Exchange factors have been calculated for tank surface nodes at 10° circumferential increments. These exchange factors have been calculated for a range of flame absorption coefficients and are presented in Figure 3-18 for the case of a full-scale tank. The exchange factors are presented in terms of the surface transmissivity which is defined as:

$$A_{ij} = \tau_{ij} A_i \qquad (3\text{-}1)$$

where

A_{ij} = surface to surface exchange factor from surface i to surface j

A_i = area of surface zone i

τ_{ij} = surface to surface transmissivity from surface i to surface j

A surface to surface transmissivity of 1.0 indicates that fire does not act as an absorbing/emitting medium, but rather as a purely transmitting medium. If the surface transmissivity is 0.0 then the fire acts as a black body radiator. The transmissivity is shown for flame absorption coefficients ranging from 0.0164 m^{-1} to 1.97 m^{-1}. A very sooty fire (as in the case of a JP 4 fueled fire) would have a large absorption coefficient.

Figure 3-19 presents an example of radiant heat transfer rates at a condition where the fire is radiating at 870°C and the entire tank surface is 15°C. It is assumed that the infinite surroundings are also at 15°C.

As can be clearly seen from the figure, the distribution of flame to tank radiant heat transfer varies considerably with the flame absorption coefficient. With a very sooty fire (high flame absorption) the fire acts almost as a black surface surrounding the tank and therefore the heat transfer rate is almost uniform around the circumference

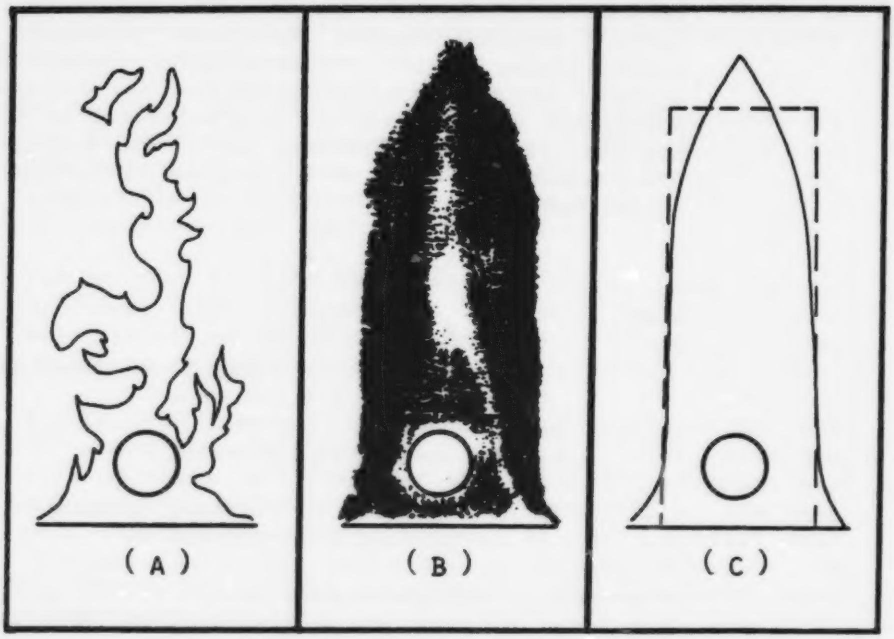

FIGURE 3-17 SKETCH OF POOL FIRE SHOWING IDEALIZED SHAPE USED IN POOL FIRE HEAT TRANSFER MODEL (from Reference (1))

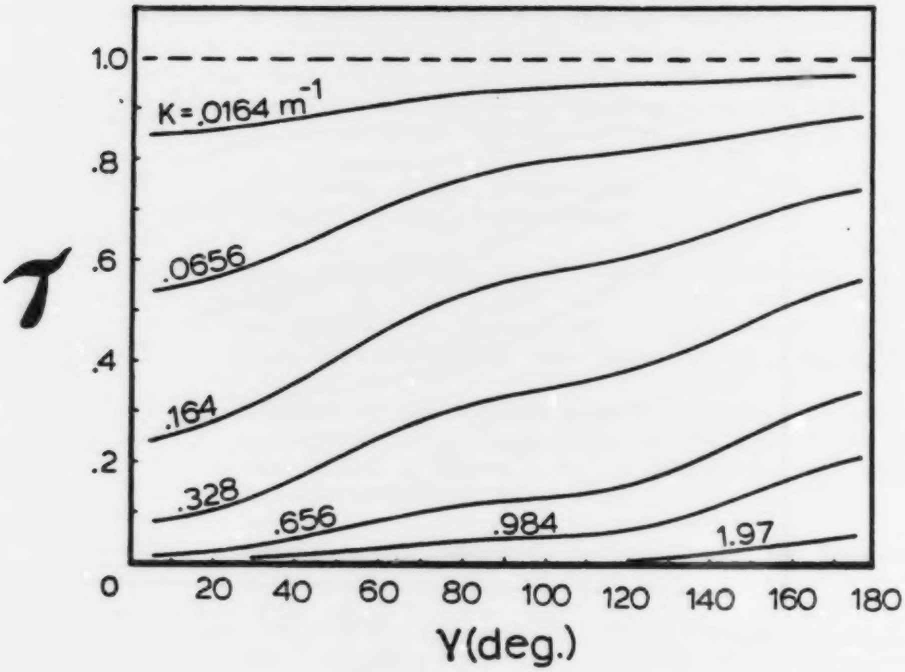

FIGURE 3-18 VARIATION IN FIRE TRANSMISSIVITY AROUND TANK FOR DIFFERENT FLAME ABSORPTION COEFFICIENTS (from Reference (1))

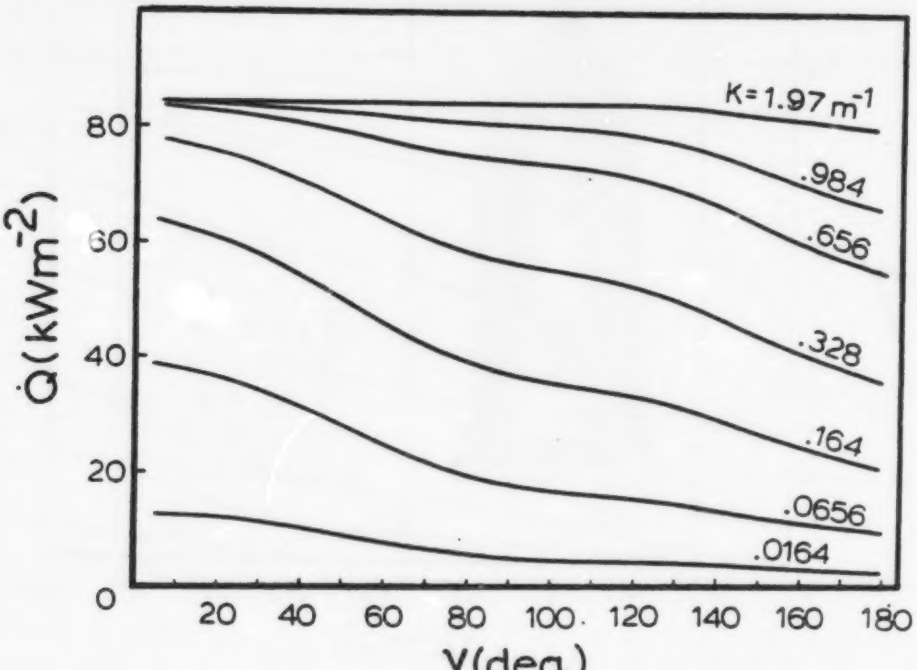

FIGURE 3-19 VARIATION IN FIRE TRANSMISSIVITY AROUND TANK FOR DIFFERENT FLAME ABSORPTION COEFFICIENTS (from Reference (1))

of the tank. For a flame with a low absorption coefficient the heat transfer rate varies considerably around the circumference of the tank because of the shape of the fire (the top element of the tank sees a thicker fire than an element at the side or bottom). Of course the magnitude of the heat transfer is higher for the fire with the high flame absorption coefficient.

A tank-car and its lading would respond very differently to the different heat transfer distributions shown in Figure 3-19. Low flame absorption coefficients would result in a reduction of the total heat input to the tank, and the top heavy distribution would result in very different wall temperature distributions in the tank. The net result of low flame absorption would be as follows:

- the tank would pressurize at a reduced rate because of the reduced heat input.
- wall temperatures would generally be higher at the top of the tank (not just because of the vapour wetted vs the liquid wetted wall condition, but also because of the heat transfer distribution).
- because of the reduced pressurization rate and the concentration of heat input at the top of the tank the relief valve will cycle longer and the lading release rate will be reduced.
- the time to failure would likely be increased because of the reduced heat input rate.

The existing tank-car model uses a flame absorption coefficient of 1.97 m^{-1}. This is based on the assumption that tank-car fires are likely to be very sooty. Experimental work is necessary to determine whether or not this assumption is adequate.

3.2.3 Torch Fire Temperature Sensitivity

This series of runs considered a full-scale unprotected tank (except for standard relief valve) filled with propane to 95% capacity, exposed to a torch type flame. The simulated torch was modelled after AAR/RPI torch fire test facility. Details of the torch configuration can be found in the tank-car model user documentation (Reference (16).

It should be noted that the torch analysis used in the overall model is two-dimensional. A two dimensional torch is a "slot jet" that runs along the length of an infinite cylinder. A true torch would require a full three dimensional analysis which is beyond the scope of the present study. The "slot jet" two dimensional torch analysis will result in predictions that are conservative, ie. more severe in nature than a three dimensional torch. The two dimensional torch analysis will predict higher tank pressurization rates, higher peak pressures, higher wall temperatures, more rapid venting rates and a shorter time to tank failure than a true three dimensional analysis would. However, for the purposes of comparing different thermal protection systems, the two dimensional torch analysis should be adequate.

In this series of runs the torch mean temperature was varied from 760°C (1400°F) to 1090°C (2000°F). All other parameters were held constant. In each of the simulations the torch application angle was 90 degrees from the tank top-dead-centre (ie. a horizontal torch applied at the tank mid-height). With this assumed application angle the torch was applied below the liquid surface. A following section considered the case of a torch applied above the liquid surface. In all cases the tank initial temperature was 25°C.

Figure 3-20 presents the predicted tank pressurization rates for the different torch temperatures. As can be seen from the figure, as the torch temperature is reduced, the initial tank pressurization rate is also reduced. The low torch temperatures also result in longer valve cycling times. The decreased torch temperature does not, however, seem to have a significant impact on the peak tank pressure. In all the cases the peak tank pressure does not rise significantly above the valve set pressure (ie. the average pressure between the valve leak pressure and the valve closing pressure).

The wall temperature predictions for the different torch temperatures are presented in Figures 3-21 to 3-24. As can be seen from these figures the vapour wetted wall temperatures are significantly affected by the torch temperatures. This is of course due to the reduction in the heat transfer rate as the torch temperature is reduced. This effect on the wall temperatures is very significant because it is the wall temperatures that determines whether or not the tank will fail. This will be discussed in more detail when the wall stress and failure plots are presented.

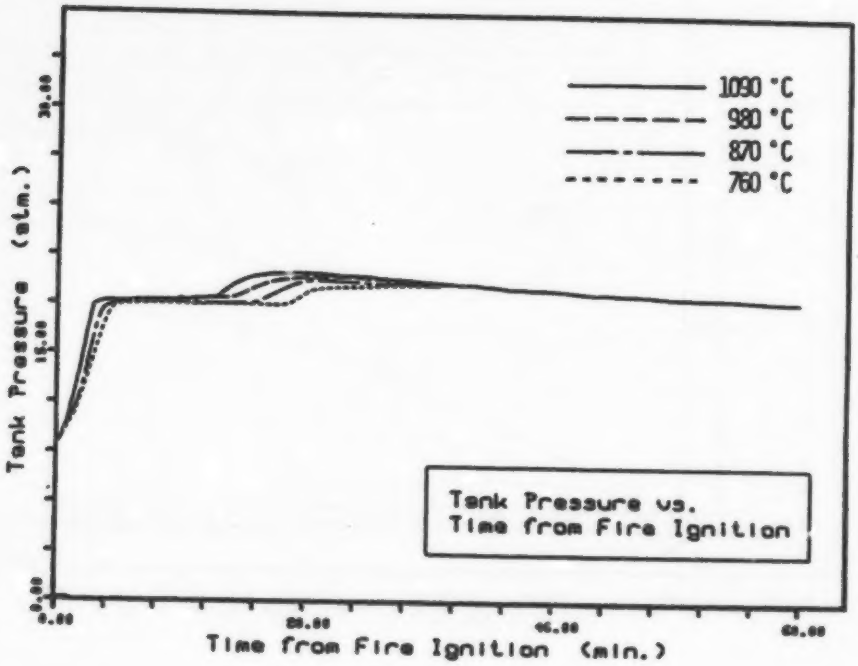

FIGURE 3-20 PREDICTED TANK PRESSURES FOR A TANK EXPOSED TO TORCH FIRES OF DIFFERENT TEMPERATURES

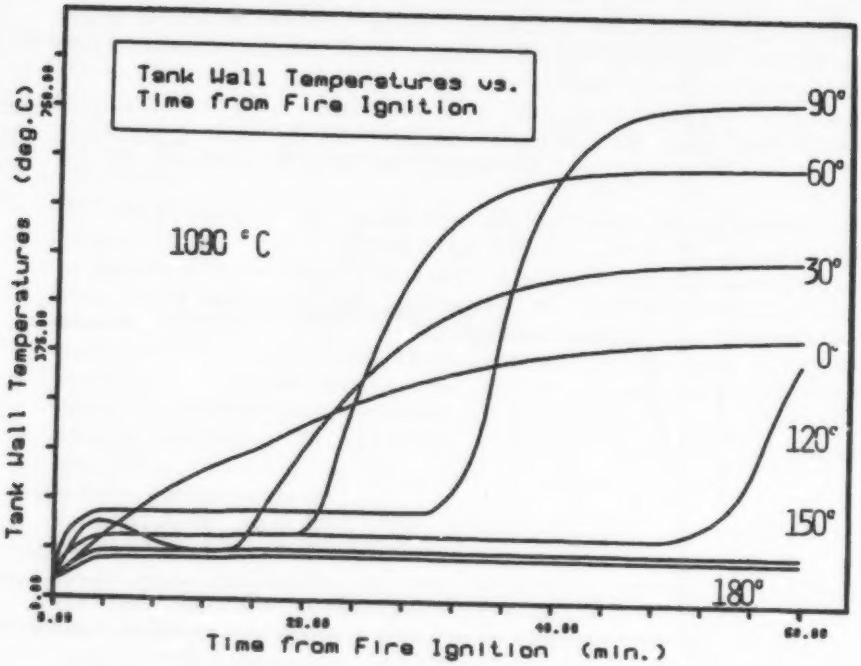

FIGURE 3-21 PREDICTED TANK WALL TEMPERATURES FOR A TANK EXPOSED TO A TORCH FIRE (TORCH TEMPERATURE 1090 deg. C)

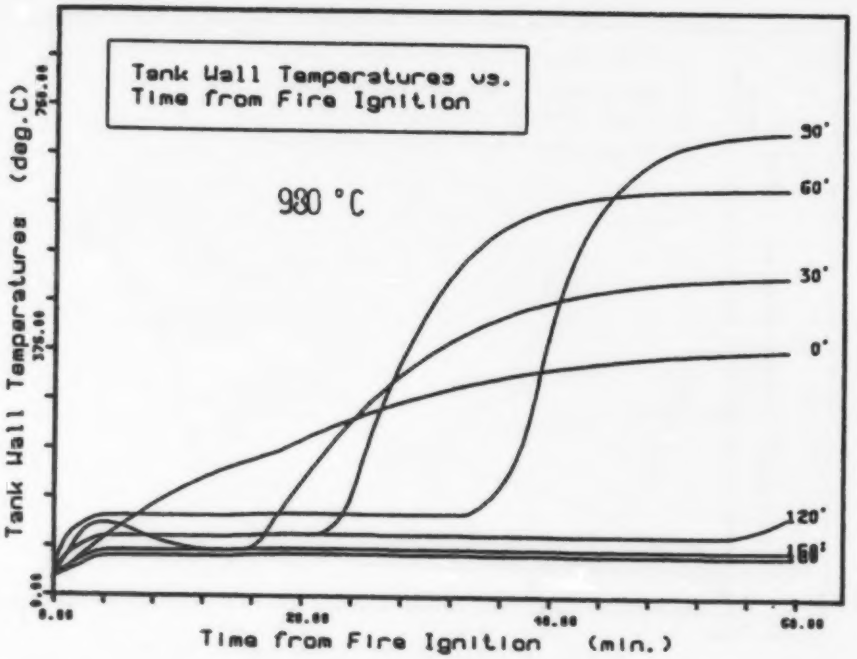

FIGURE 3-22 PREDICTED TANK WALL TEMPERATURES FOR A TANK EXPOSED TO A TORCH FIRE (TORCH TEMPERATURE 980 deg. C)

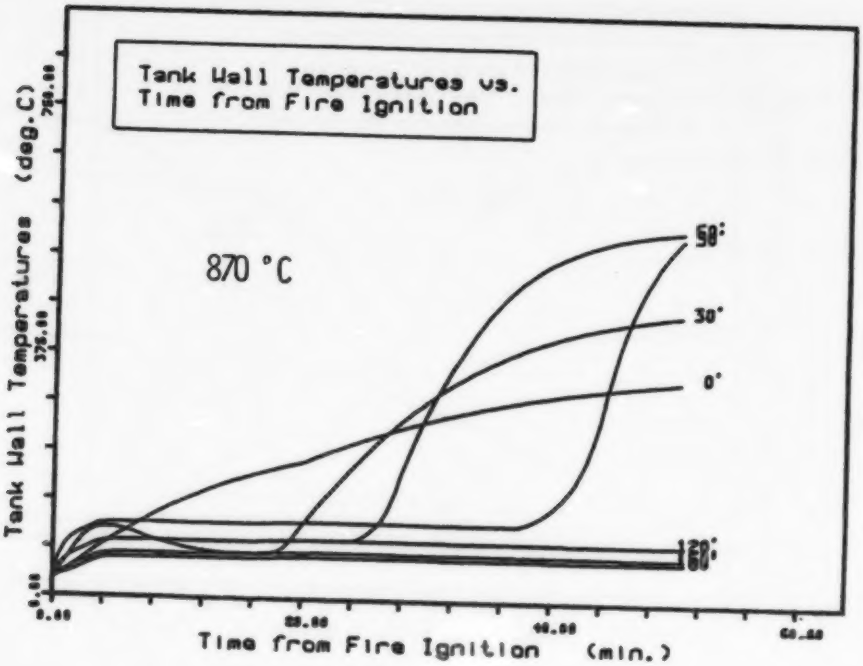

FIGURE 3-23 PREDICTED TANK WALL TEMPERATURES FOR A TANK EXPOSED TO A TORCH FIRE (TORCH TEMPERATURE 870 deg. C)

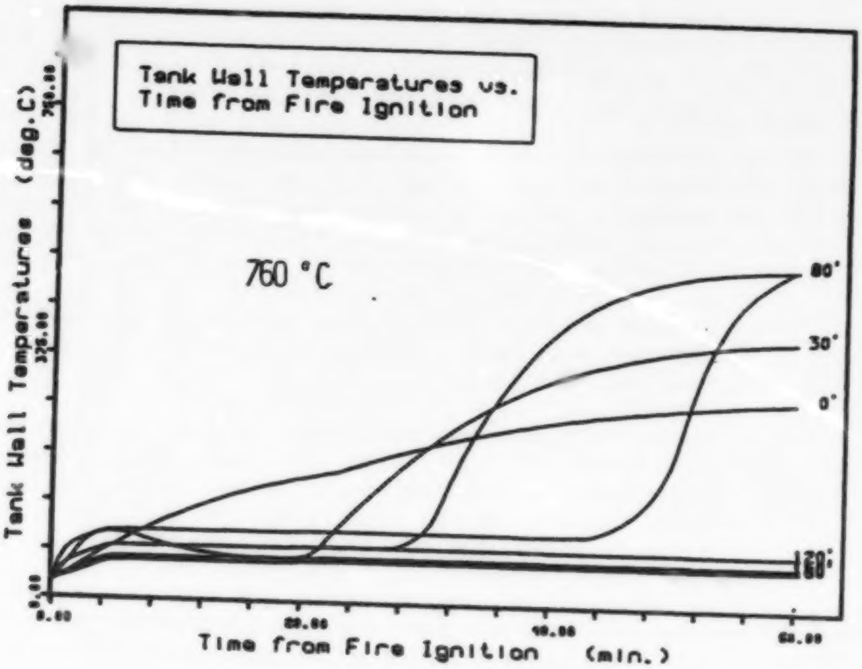

FIGURE 3-24 PREDICTED TANK WALL TEMPERATURES FOR A TANK EXPOSED TO A TORCH FIRE (TORCH TEMPERATURE 760 deg. C)

Figure 3-25 presents the predicted liquid levels for the cases considered. The results show that as the torch temperature is increased, the tank empties faster. The higher torch temperature results in a higher heat flux to the lading which in turn results in an increase in vapour generation within the tank. The model predicts that this increased vapour generation results in a shorter time to continuous venting through the relief valve. In other words, the increased torch heat flux results in a shorter period of valve cycling. This time to continuous venting is seen in Figure 3-25 where there is a sudden upturn in the plots. Beyond this bend in the liquid level vs time plots the slopes are very similar.

The liquid level has a significant affect on the time to failure because of the fact the torch is, in this case, initially below the liquid level. With the assumed torch configuration a tank would fail very early if the torch is applied to a vapour wetted area. Therefore, the time to tank failure is closely related to the liquid level, because once it drops below the torch application point the tank will fail. This will be seen in the plot showing tank wall stresses.

Figure 3-26 presents the predicted tank wall stresses and wall strength for the different torch temperatures considered. As can be seen from the figure the higher the torch temperature the sooner the tank will fail. In fact, the plot shows that the tank failure is very sensitive to the torch temperature. The time to failure is most affected by the liquid level and the vapour wetted wall temperatures. As mentioned earlier these two conditions are significantly affected by the torch temperature. As can be seen in the figures the wall strength drops significantly as soon as the torch central location is above the liquid surface. This drop in the wall material strength is the most important determinant of tank failure. The rate at which the wall ultimate strength drops is dictated by the wall temperature and this is, of course, determined by the torch heat flux (temperature). As can be seen from the figure, the wall strength drops most rapidly for the highest torch temperatures.

The tank failure is also affected by the wall stresses which are caused by the tank internal pressure and the thermal gradients in the tank shell. However, these stresses do not appear to vary significantly between the cases considered here. This is because the tank pressures

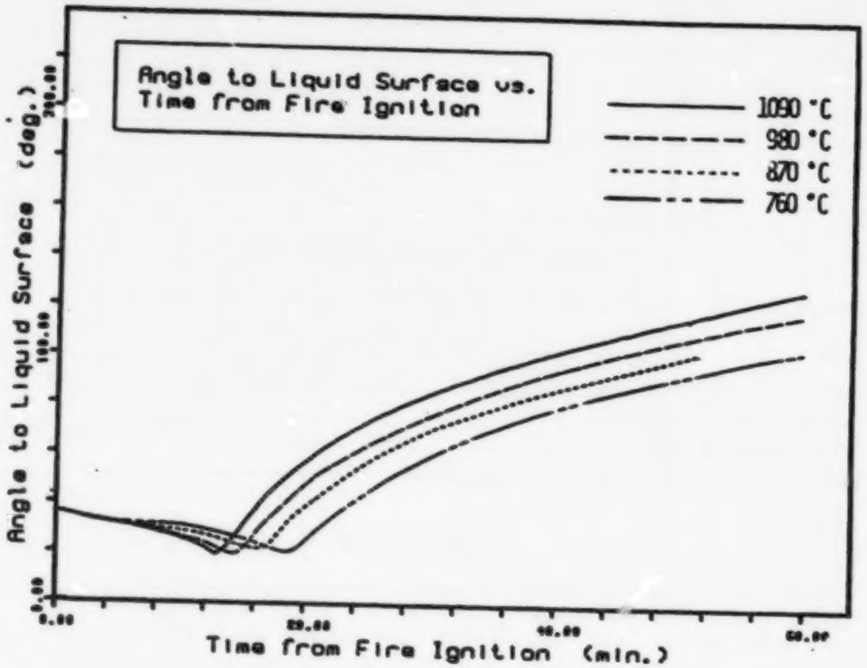

FIGURE 3-25 PREDICTED LIQUID LEVELS FOR A TANK EXPOSED TO TORCH FIRES OF DIFFERENT TEMPERATURES

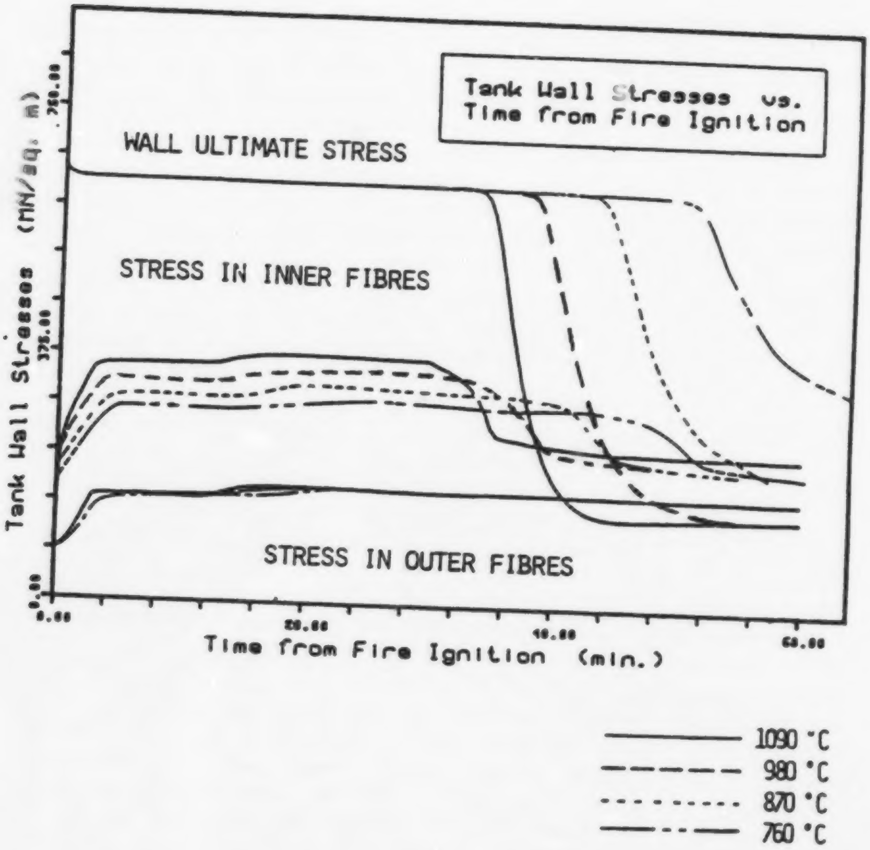

FIGURE 3-26 PREDICTED TANK WALL STRESSES AND TANK WALL MATERIAL STRENGTHS FOR A TANK EXPOSED TO TORCH FIRES OF DIFFERENT TEMPERATURES

were not significantly different between the cases considered. The thermal stresses are however quite significantly different between the cases. The thermal stresses are shown in the figure as the difference between the stresses in the wall inner and outer fibres. The stresses shown only consider radial temperature gradients and these are of course affected by the liquid level and the heat flux.

In summary, the torch temperature has a significant impact on the response of a tank-car to an impinging torch fire. The most important impact is that relatively small changes in the torch temperature can result in large changes in the time to tank failure. This is a clear indication that thermal protection from such uncontrollable conditions is a necessity.

3.2.4 Torch Fire Application Sensitivity

This series of runs considered a full-scale unprotected tank (except for standard relief valve) filled with propane to 95% capacity, exposed to a torch fire. The angle of application of the torch was varied from 0° (top-dead-centre) to 120°. As before, the torch is represented as a two-dimensional slot jet. In all the cases considered in this section, the torch temperature was fixed at 1090°C (2000°F).

As mentioned above, simulations considered tanks filled to 95% capacity at 25°C ambient condition. This will result in an initial fill angle of approximately 36½° from top-dead-centre. This means that for the cases where the torch is applied at 0° and 30° from top-dead-centre the torch is initially above the liquid level, whereas in the cases where the torch is applied at 60, 90 and 120° below top-dead-centre the initial torch application is below the liquid level. The location of the application of the torch whether it is above or below the liquid surface has a significant effect on the wall temperatures and therefore on the time to tank failure. This is because the heat transfer from the inner surface of the tank is significantly different when the tank wall is exposed to vapour or when it is exposed to liquid. In the case where the torch is applied to the outer surface of a vapour wetted wall, the heat transfer from the inner surface of the wall to the vapour is much less than the heat transfer to the wall from the torch. In this case the wall temperature rises very rapidly. When the torch is applied to the outer surface of liquid wetted wall, the heat transfer rate to the wall is similar to the heat transfer rate from the inner surface of the wall to the liquid, and therefore the wall temperature follows very closely to that of the liquid.

The effects on the tank caused by the location of the application of the torch is not limited to the wall temperatures. When the torch is applied to liquid wetted walls the net total heat transfer to the tank lading is much higher than it would be if the torch is applied to vapour wetted wall. All these effects will be discussed in more detail with the aid of the following plots.

Figure 3-27 presents the predicted tank pressures for the different cases considered. As can been seen from the plot, the most rapid pressurization rate takes place in the case where the torch is applied well below the liquid surface. This is, of course, because most of the heat transfer is being applied to the liquid wetted wall, and therefore the heat transfer is being carried into the lading. Because of the increased heat transfer to the lading, one also sees shorter valve cycling periods for the cases where the torch is applied below the liquid surface. For the case where the torch is applied 120° below the top-dead-centre, the valve cycling period only lasts approximately 10 minutes. In the case where the torch is applied at top-dead-centre, the valve cycling period lasts for approximately 30 minutes, or half the simulation time. As will be seen later, this time to continuous venting is a very important factor in determining how quickly the tank empties.

In general, the tank pressures do not rise significantly above the valve set pressures for all of the cases considered. In terms of the tank pressure, the most significant difference between simulations is the length of the valve cycling time. This will be discussed further, later.

The predicted wall temperatures are presented in Figures 3-28 to 3-32. As can be seen from the figures the wall temperatures are significantly affected by the application angle of the torch fire.

Figure 3-28 presents the predicted wall temperatures for the case where the torch is applied at the top-dead-centre of the tank. As can be seen from this figure the wall

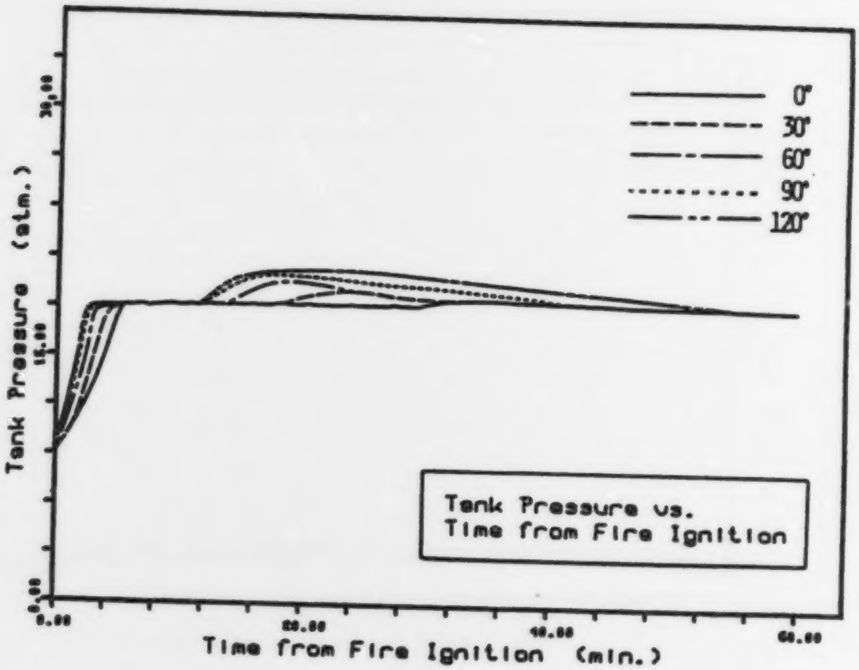

FIGURE 3-27 PREDICTED TANK PRESSURES FOR A TANK EXPOSED TO TORCH FIRES APPLIED AT DIFFERENT ANGLES FROM THE TANK TOP-DEAD-CENTRE

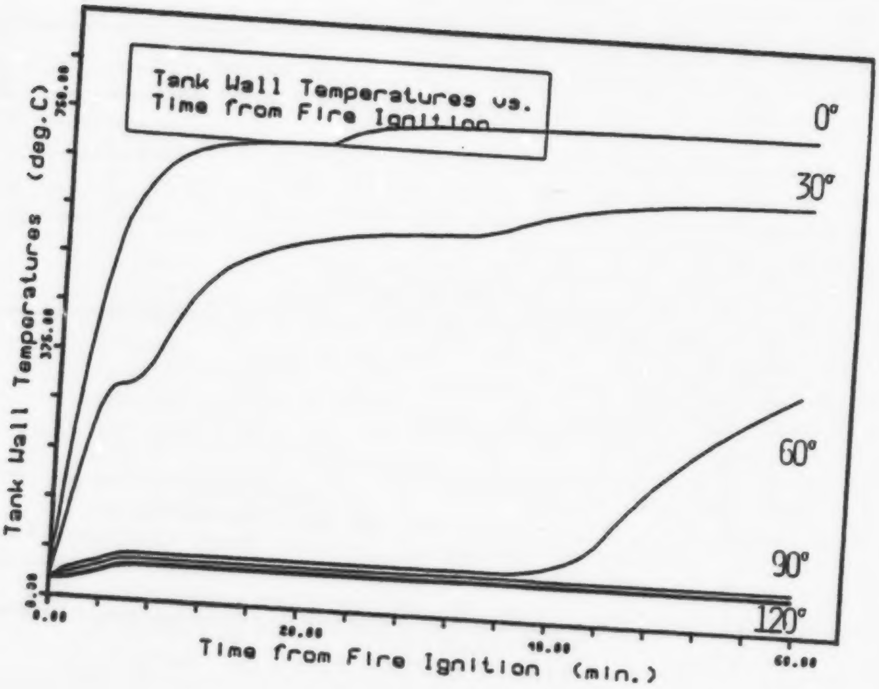

FIGURE 3-28 PREDICTED TANK WALL TEMPERATURES FOR A TANK EXPOSED TO A TORCH FIRE (APPLIED AT 0 DEGREES FROM TDC)

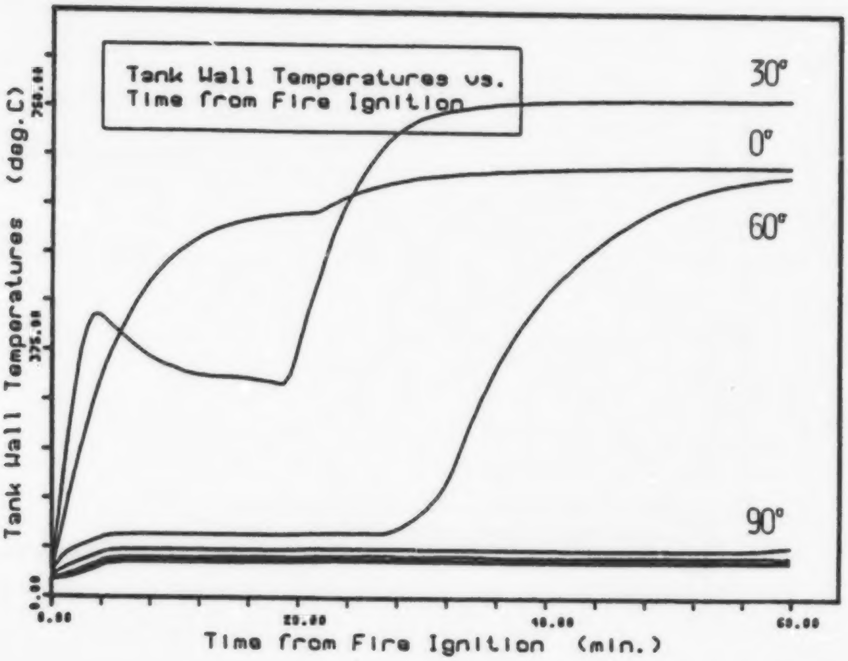

FIGURE 3-29 PREDICTED TANK WALL TEMPERATURES FOR A TANK EXPOSED TO A TORCH FIRE (APPLIED AT 30 DEGREES FROM TDC)

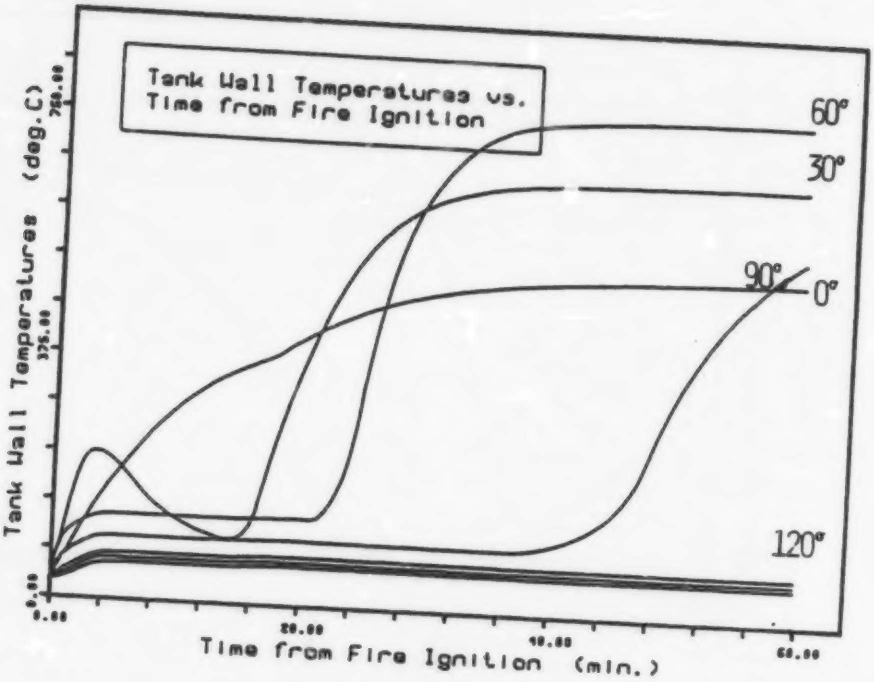

FIGURE 3-30 PREDICTED TANK WALL TEMPERATURES FOR A TANK EXPOSED TO A TORCH FIRE (APPLIED AT 60 DEGREES FROM TDC)

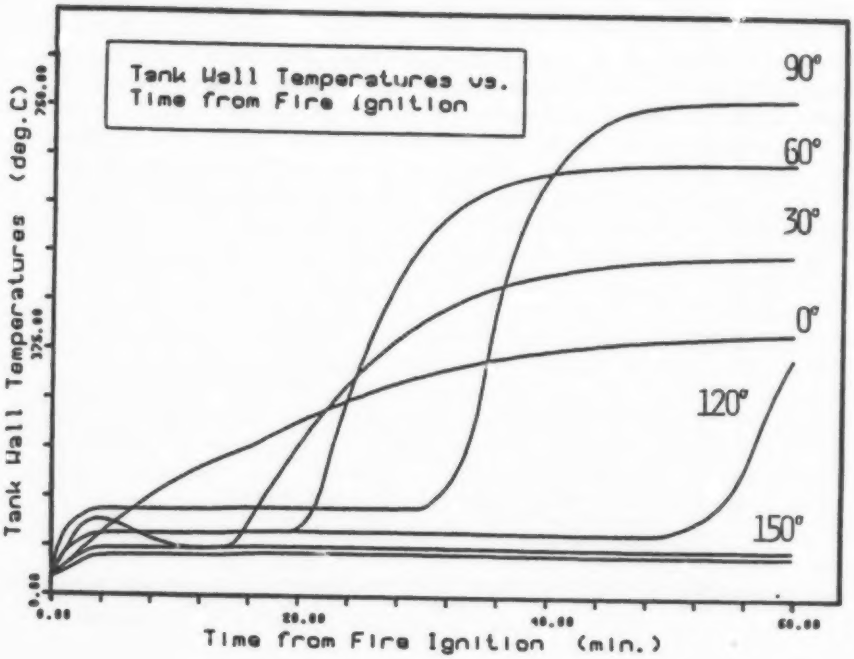

FIGURE 3-31 PREDICTED TANK WALL TEMPERATURES FOR A TANK EXPOSED TO A TORCH FIRE (APPLIED AT 90 DEGREES FROM TDC)

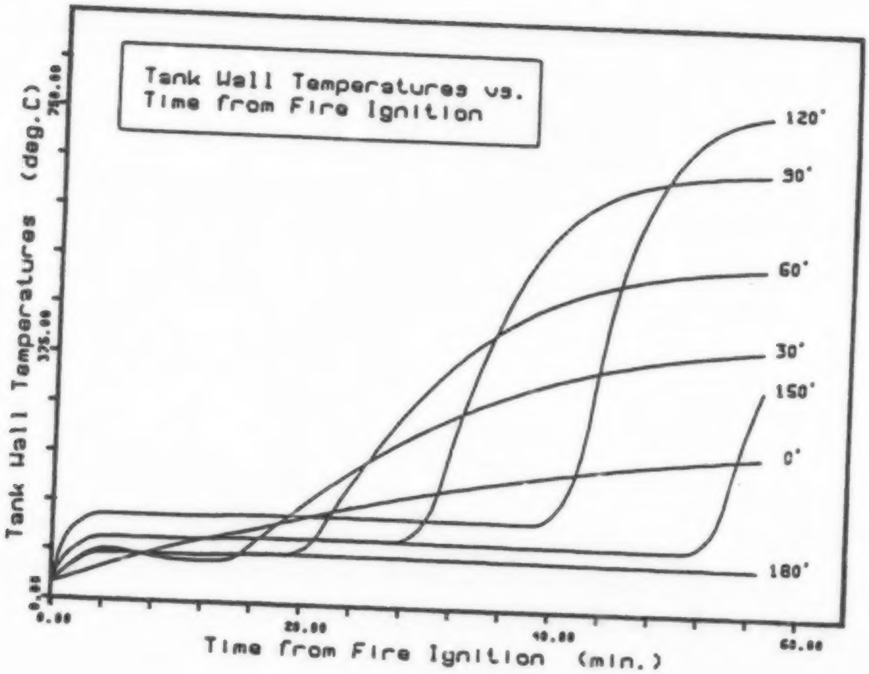

FIGURE 3-32 PREDICTED TANK WALL TEMPERATURES FOR A TANK EXPOSED TO A TORCH FIRE (APPLIED AT 120 DEGREES FROM TDC)

temperature at the top-dead-centre location rises extremely rapidly. This, of course, is due to the fact that the torch is impinging on the vapour wetted wall area on the tank surface.

Figure 3-29 shows the predicted wall temperature for the case where the torch is applied 30° from top-dead-centre. In this case, initially, the centre point of the torch, that is the 30° from top-dead-centre location, increases rapidly for the first few minutes of the simulation. After that point however, the wall temperature at the 30° location drops and levels. This is due to a rising of the liquid level due to thermal expansion and frothing. Eventually however, due to venting, the liquid level begins to drop again and it eventually drops below the application point of the torch. After this time, the temperature rises rapidly and levels off as shown in the figure. The period of rapid increase of wall temperature indicates the time when the wall is once again exposed to vapour.

Figure 3-30 presents the predicted wall temperatures for the case where the torch is applied at 60° below top-dead-centre. In this case the torch is applied to the wall area which is initially wetted by liquid. Therefore, initially the wall temperature at the centre of the impingement zone remains relatively low because of the efficient cooling effects of the liquid. At approximately 20 minutes however, the liquid level drops below the 60° location, and therefore the centre point of the torch impingement is exposed to vapour and the temperature rapidly rises and levels off.

In the remaining figures, Figure 3-31 and Figure 3-32 the same trends are shown. Initially the point of torch impingement is located below the liquid surface. Eventually however, the liquid surface drops below the point of impingement because of venting through the relief valve and at this time the wall temperatures rise rapidly due to the inefficient cooling effects of the vapour. In all cases the point of impingement eventually reaches the highest temperature.

Figure 3-33 presents the predicted liquid level for the different cases considered. As can be clearly seen from the figure the liquid level is significantly affected by the application angle of the torch. As can be seen the case where the torch was applied well below the liquid surface resulted in the most rapid emptying of the tank.

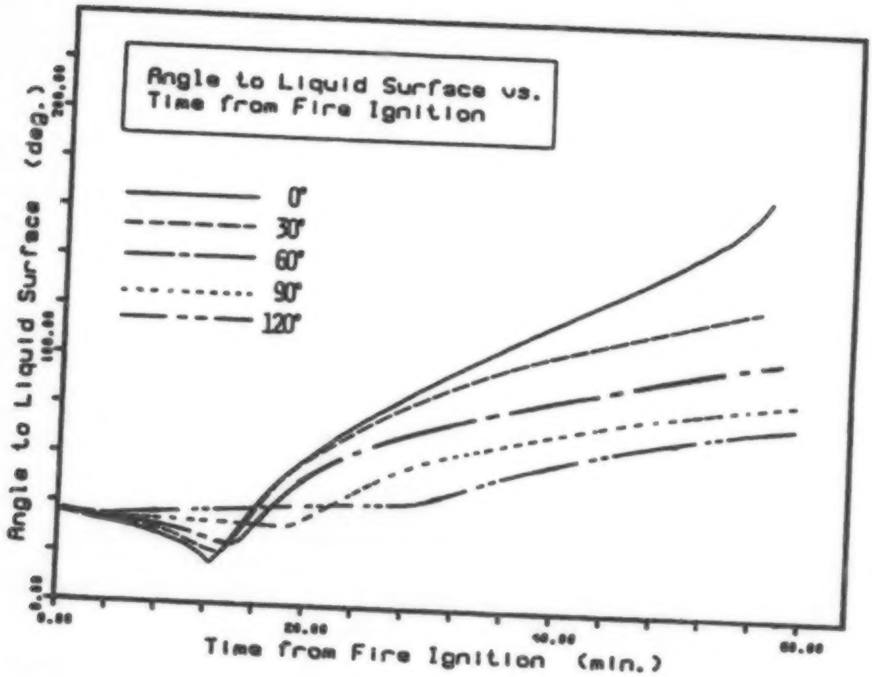

FIGURE 3-33 PREDICTED LIQUID LEVELS FOR A TANK EXPOSED TO TORCH FIRES OF DIFFERENT TEMPERATURES

Where the torch was applied at top-dead-centre, that is on the vapour wetted wall area, the tank emptied at the slowest rate. This is as expected because when the torch is applied below the liquid surface, the highest heat transfer to the lading occurs.

Figures 3-34 to 3-38 present the predicted tank wall stresses and tank material strengths for the different torch application angle cases. As can be seen from the figures the location of the torch application has a significant affect on the time to failure for the tank. For the case where the torch is applied at top-dead-centre the tank fails very shortly after time from fire ignition. This is of course due to the fact that the wall temperatures rise very rapidly at this location. The high temperatures result in rapid degradation of the wall material strength and the tank fails at relatively low wall stresses.

Figure 3-35 shows the predicted stresses and tank failure for the case where the torch is applied 30° from top-dead-centre. In this figure one sees that initially the material strength drops very rapidly and then has an upturn resulting from a sudden drop in the wall temperature. This drop, as discussed earlier, is due to rising of the liquid level due to thermal expansion and two-phase frothing. Eventually, however at approximately 20 minutes the wall temperatures begin to rise rapidly and at this time the material strength drops rapidly. At about 24 minutes the tank fails because the material strength drops below the wall stresses.

Figure 3-36 shows the predictions for the case where the torch is applied 60° from top-dead-centre. In this case the torch is applied initially below the liquid surface, and therefore the wall temperatures do not rise very rapidly. Eventually however, the liquid level drops below the point of torch application and the temperatures rise rapidly with resulting drop in material strength. Shortly after that time the tank fails. These same trends are shown in Figures 3-37 and 3-38 for the 90 and 120° application angles. Generally speaking, if a torch is applied well below the liquid surface, the tank will survive a longer period. For the tank to fail, the liquid level must drop below the point of torch application.

In summary, the point of application of the torch has a significant effect on the ultimate failure of a tank exposed to torch fire. If the torch is applied above the

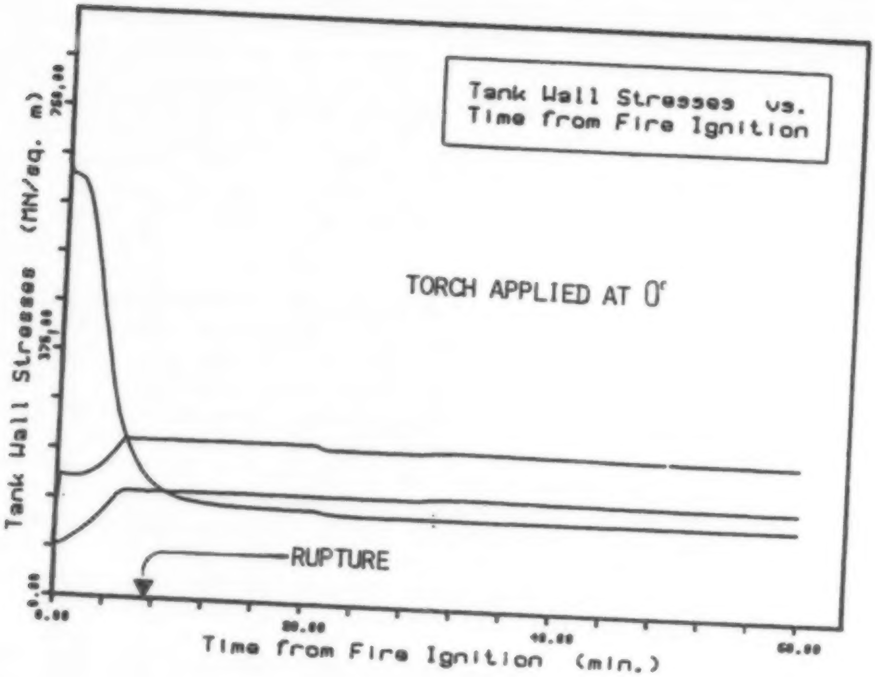

FIGURE 3-34 PREDICTED TANK WALL STRESSES AND TANK WALL MATERIAL STRENGTHS FOR A TANK EXPOSED TO A TORCH FIRE (APPLIED AT 0 DEGREES FROM TDC)

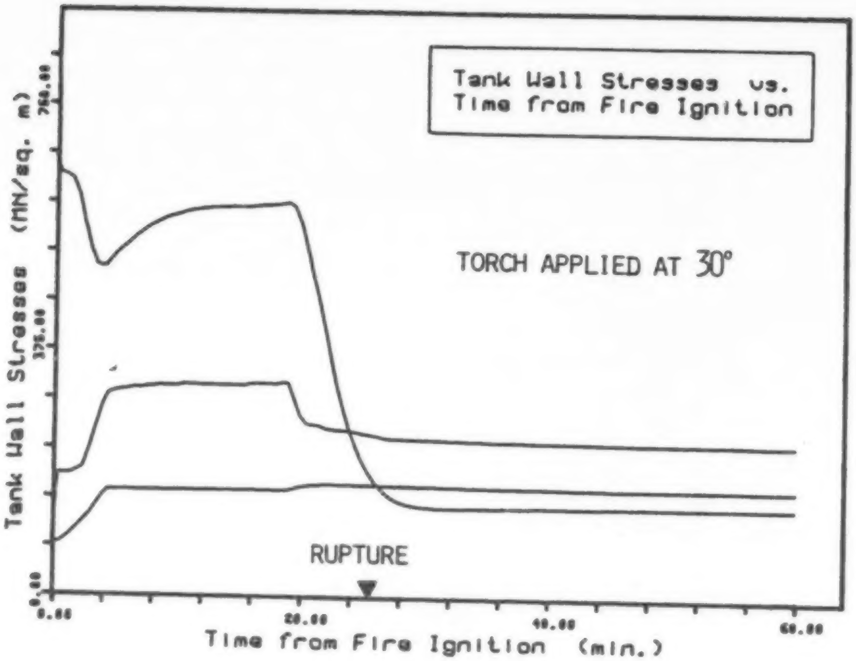

FIGURE 3-35 PREDICTED TANK WALL STRESSES AND TANK WALL MATERIAL STRENGTHS FOR A TANK EXPOSED TO A TORCH FIRE (APPLIED AT 30 DEGREES FROM TDC)

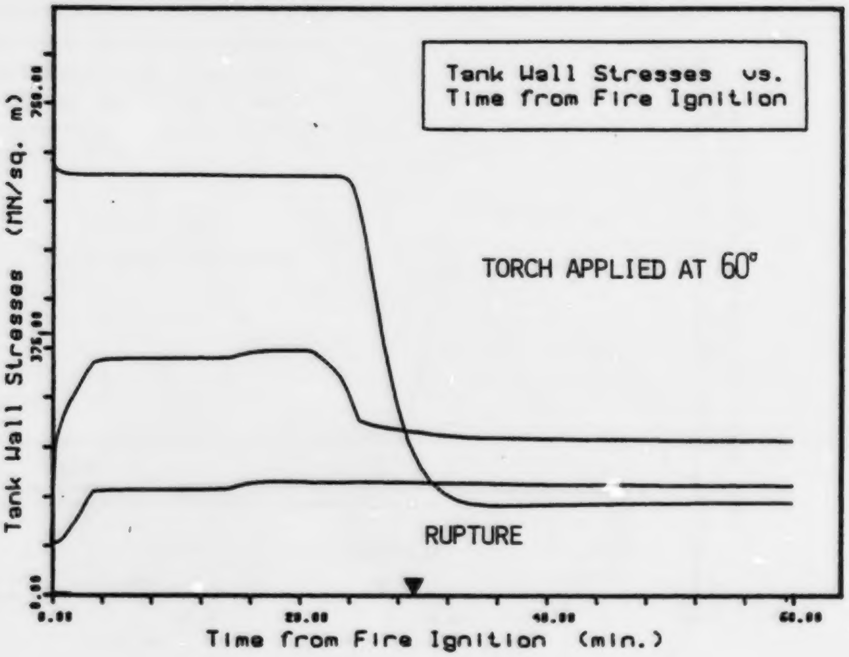

FIGURE 3-36 PREDICTED TANK WALL STRESSES AND TANK WALL MATERIAL STRENGTHS FOR A TANK EXPOSED TO A TORCH FIRE (APPLIED AT 60 DEGREES FROM TDC)

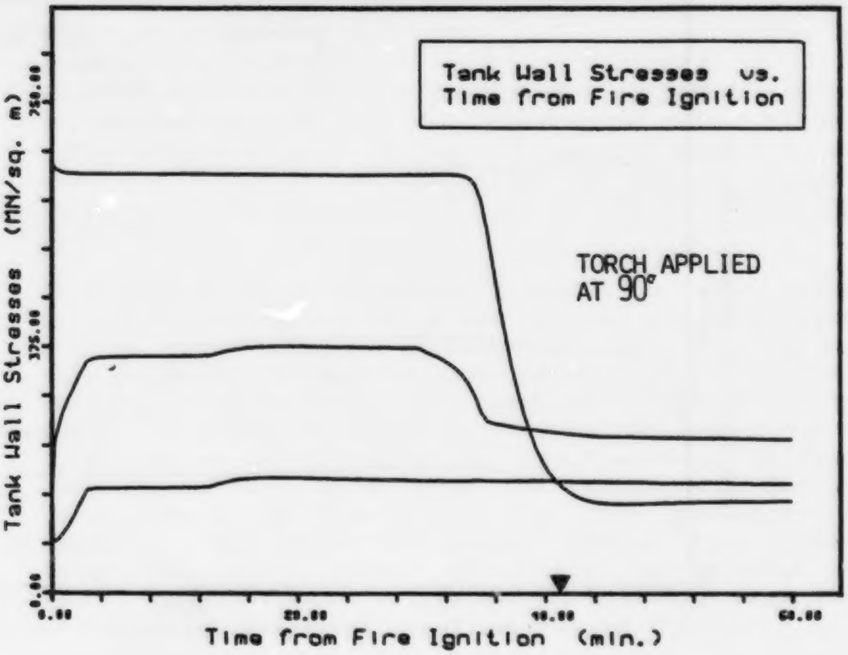

FIGURE 3-37 PREDICTED TANK WALL STRESSES AND TANK WALL MATERIAL STRENGTHS FOR A TANK EXPOSED TO A TORCH FIRE (APPLIED AT 90 DEGREES FROM TDC)

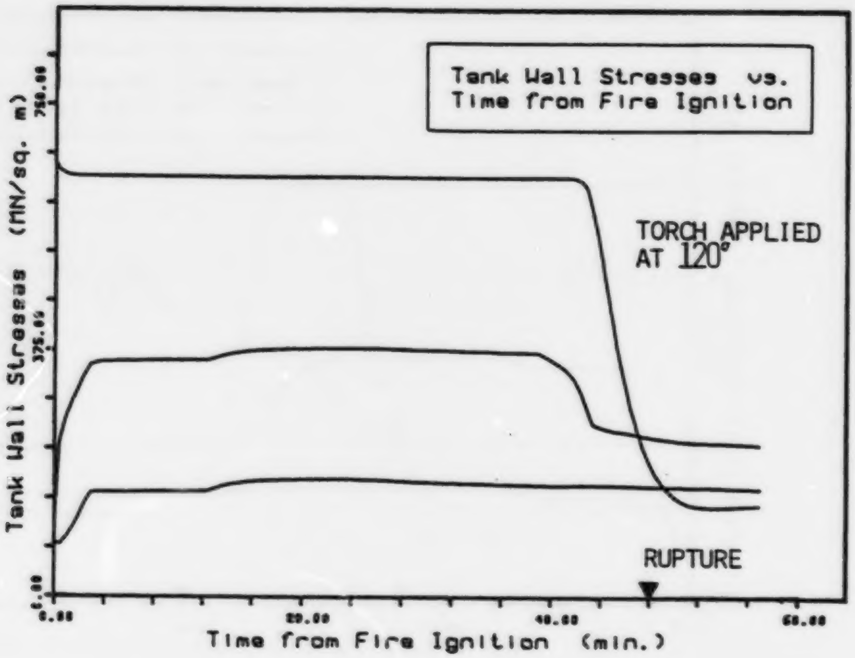

FIGURE 3-38 PREDICTED TANK WALL STRESSES AND TANK WALL MATERIAL STRENGTHS FOR A TANK EXPOSED TO A TORCH FIRE (APPLIED AT 120 DEGREES FROM TDC)

liquid surface then very high wall temperatures can be expected and the tank will fail due to thermal degradation of material properties. If the torch is applied below the liquid surface, the tank will remain relatively safe until the liquid surface drops below the point of torch application, and at this time the wall temperatures will rise rapidly and cause thermal degradation of the material properties.

3.3 TANK ROLL SENSITIVITY

This series of simulations considered a full-scale unprotected tank (except for a standard sized relief valve) filled with propane at 25°C to 95% capacity exposed to an engulfing fire. In the simulations the tank was assumed to have roll angles of 0, 30, 60, 90 and 120° from the vertical.

If a tank-car is in the upright position the relief valve will be located at the top of the tank and the valve inlet will be above the liquid surface. This means that vapour will be passing through the valve except for those periods when excessive frothing has raised the effective liquid level. If a tank is rolled to one side, the relief valve inlet will be located under the liquid surface. In this case, liquid will be entering the relief valve for at least part of the fire event. The larger the angle of tank roll, the longer the period during which liquid enters the relief valve. Eventually, as material is vented from the tank, the liquid level will drop below the relief valve, and vapour will flow through the valve.

Figures 3-39 to 3-42 present the four summary plots showing pressure vs time, wall temperature vs time, liquid level vs time and wall stress vs time.

The simulations indicate that as the tank is rolled the pressure relieving capability of the relief valve is improved and the tank empties more rapidly. The wall temperatures are also affected because it has been assumed that when the relief valve is submerged and liquid is being vented, the two-phase frothing region is not present.

The simulation results are in conflict with what is generally known about rolled tank responses to fires. This conflict is due to the simple flow model used when the relief valve is submerged in liquid. The "frozen

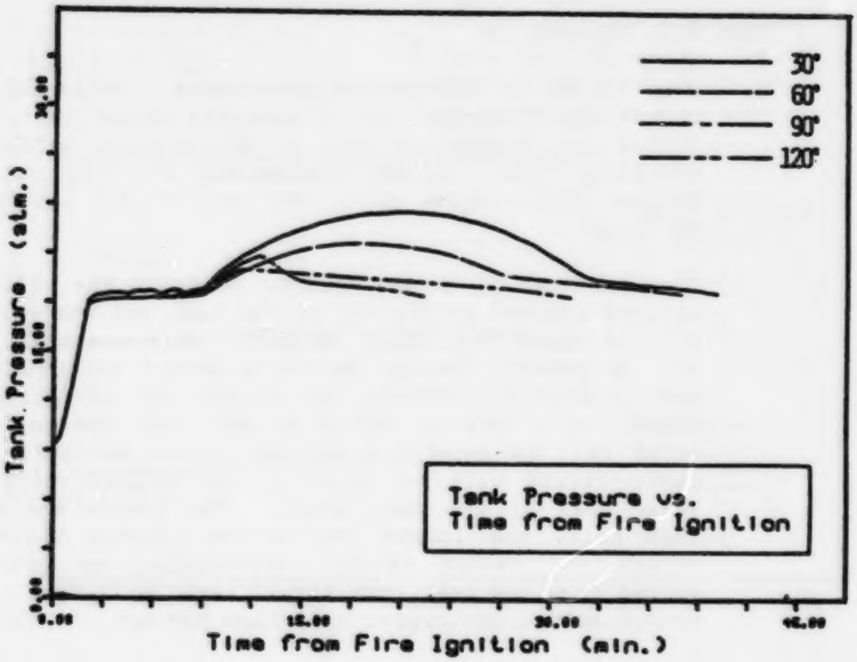

FIGURE 3-39 PREDICTED TANK PRESSURES FOR UNPROTECTED TANKS WITH DIFFERENT ROLL ANGLES EXPOSED TO AN ENGULFING FIRE

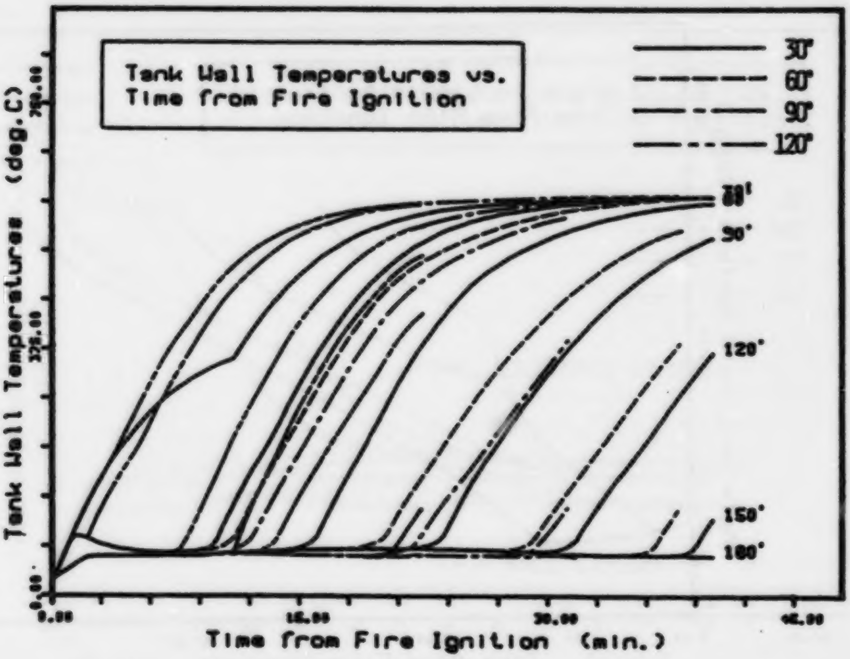

FIGURE 3-40 PREDICTED TANK WALL TEMPERATURES FOR UNPROTECTED TANKS WITH DIFFERENT ROLL ANGLES EXPOSED TO AN ENGULFING FIRE

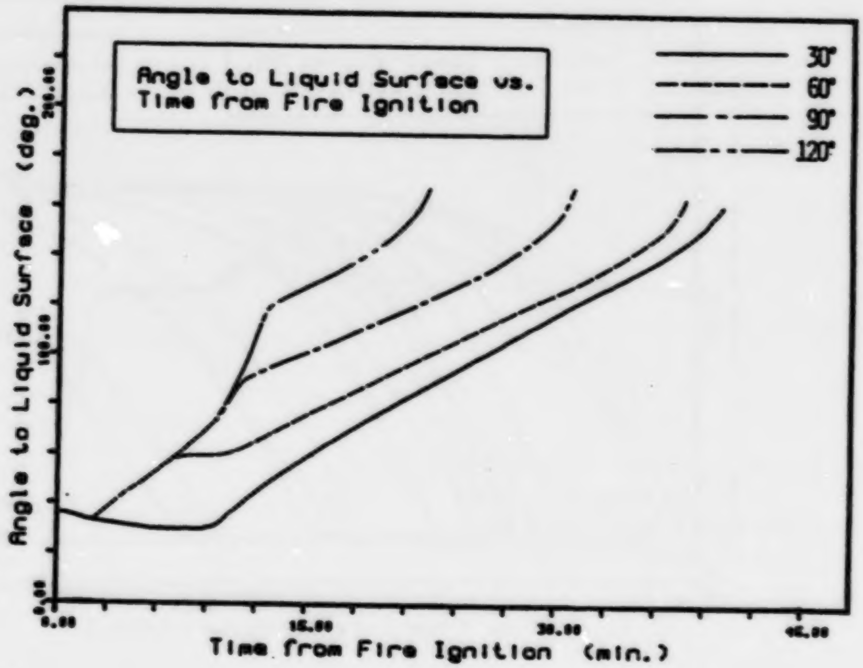

FIGURE 3-41 PREDICTED LIQUID LEVELS FOR UNPROTECTED TANKS WITH DIFFERENT ROLL ANGLES EXPOSED TO AN ENGULFING FIRE

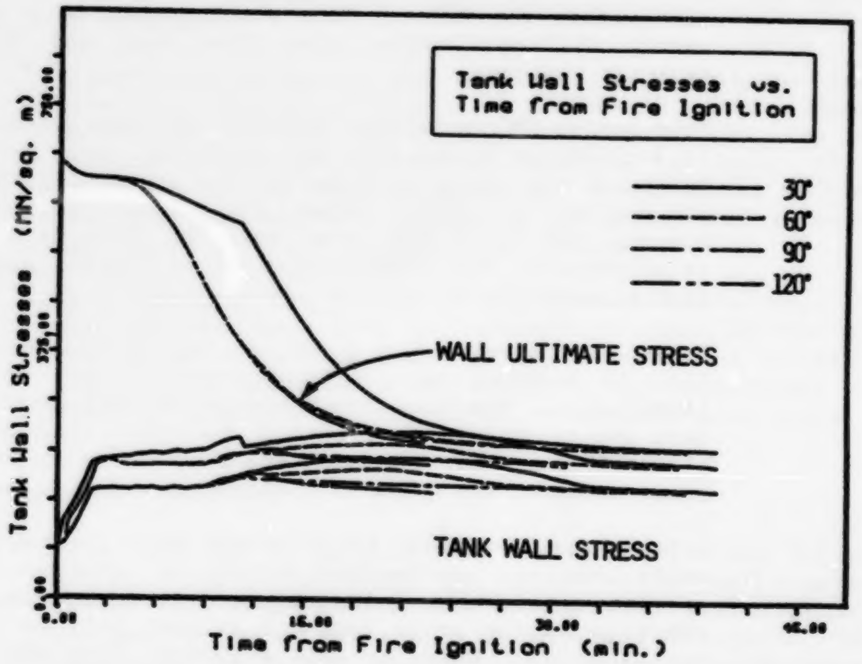

FIGURE 3-42 PREDICTED TANK WALL STRESSES AND TANK WALL MATERIAL STRENGTHS FOR UNPROTECTED TANKS WITH DIFFERENT ROLL ANGLES EXPOSED TO ENGULFING FIRES

flow" model for liquid flow through the relief valve assumes that the liquid entering the relief valve remains liquid until it exits the valve. This would be the case in reality if the liquid was sub-cooled as it entered the valve and if the pressure drop through the valve was not large. In the present case, the liquid may be slightly subcooled initially, but later in the fire event the liquid will be saturated. The pressure drop is quite large, however, and even with the subcooled liquid this large pressure drop would likely result in vapour formation within the valve. This would result in a significantly different valve mass flow rate and different tank-car response.

This series of simulations indicate that the overall model is working as it should, ie. when the tank is rolled, initially the valve is submerged but eventually the valve is exposed to vapour when the liquid level drops. However, the valve flow model when the valve is submerged is inadequate, and this results in an overall simulation that is unrealistic.

Presently the valve flow model has two options, either the flow is modelled as isentropic vapour flow, or frozen liquid flow. The flow model must be further developed to have the capability to represent two-phase flow under two circumstances - ie. two-phase entering the valve or single phase entering the valve with flashing in the valve.

A two-phase flow model for a relief valve is complex, and would require considerable effort to develop for the present application. In addition to this complexity, there is little or no tank-car related data to validate such a model. There is data available from the nuclear power industry on 2-phase relief valve flow that could be used for the present application.

Figure 3-39 presents the predicted tank pressures for the cases considered. As can be seen from the figure, the model predicts lower peak pressures for the rolled tanks. The lower peak pressures are caused by the fact that the relief valve flow model, for liquid entering the valve, (frozen liquid flow) results in an overestimate of the pressure relieving capabilities of the valve. A 2-phase flow model is needed to bring the model simulations more in line with reality.

Figure 3-40 presents the predicted wall temperatures for the different cases considered. As can be seen from the figure, the peak wall temperatures are not affected by the tank being rolled. Only the temperature break times are affected because of the fact that the submerged relief valve passes more mass and therefore the liquid level drops more rapidly when liquid is flowing through the valve.

Figure 3-41 presents the predicted liquid levels for the different cases considered. As can be seen from the figure, the liquid level drops more rapidly when the valve is submerged.

Figure 3-42 presents the predicted wall stresses and material strengths for the different roll cases considered. As can be seen from the figure, the time to failure is affected by the roll angle of the tank. This is caused by the fact that the wall temperatures at the tank top increase more rapidly in the rolled tank because the liquid level is dropping more rapidly.

When reviewing the results of the present simulations, it must be noted that they are somewhat in error because of the relief valve flow model used. As mentioned earlier, this liquid flow model will results in an overestimate of the relieving capabilities of the submerged relief valve.

3.4 TANK PITCH SENSITIVITY

If a tank-car is pitched from the horizontal two things happen, the distribution of liquid wetted and vapour wetted wall areas change, and if the tank is pitched far enough, the relief valve will be submerged in liquid. The change in the wetted areas affects the wall temperatures and the rate of heat addition to the tank and its lading. The submerged relief valve affects the pressure relieving capacity of the valve.

The tank-car model represents a horizontal tank as a two-dimensional system. This is possible because in a horizontal tank the liquid wetted and vapour wetted wall area distribution does not vary along the axis of the tank. The only three dimensional effects in a horizontal tank are those caused by the ends and these are small because of the length to diameter ratio of a rail tank-car (6:1).

When a tank-car is pitched, it can no longer be represented as a two dimensional system because the liquid level varies along the axis of the tank. This variation in the liquid level results in strong axial gradients in temperature and flow. The tank end effects are also complicated by the fact that the low end of the tank is filled with liquid and the high end is filled with vapour.

The tank-car model does not represent all of the three dimensional effects in a pitched tank. Such a full three-dimensional model would be complex and demanding of computer power. Instead, the tank-car model represents a pitched tank by using a pseudo-3D analysis consisting of two 2-D models, one representing a specific plane along the axis of the tank (the test plane) and the other representing the average condition in the tank. Further details of the pseudo-3D model can be found in Reference (16).

The following sections present a number of simulations involving a pitched unprotected tank. The sensitivity runs were performed to study the overall response of the tank/lading system at different angles of pitch, and also the axial variations in tank/lading response for a fixed angle of pitch.

In all of the following simulations the tank is full-scale, and unprotected except for a standard sized relief valve. The lading is propane at an initial temperature of 25°C. The tank initial fill was assumed to be 95% of capacity.

3.4.1 Variations in Pitch Angle

This series of runs were performed to study the effect of angle of pitch on the tank-car. Five different angles of pitch were considered, 0, 10, 20, 40, 60 and 80°. In all cases the test section was located at the mid-plane of the tank-car.

Figure 3-43 presents the pressure vs time plot for the five different pitch angles. As can be seen from the figure, the tank pressurization rate prior to relief valve opening is only slightly affected, however, once the relief valve opens the pressure response is significantly changed. It must be noted that for the present case of a 95% filled tank, the relief valve becomes submerged at very low pitch angles.

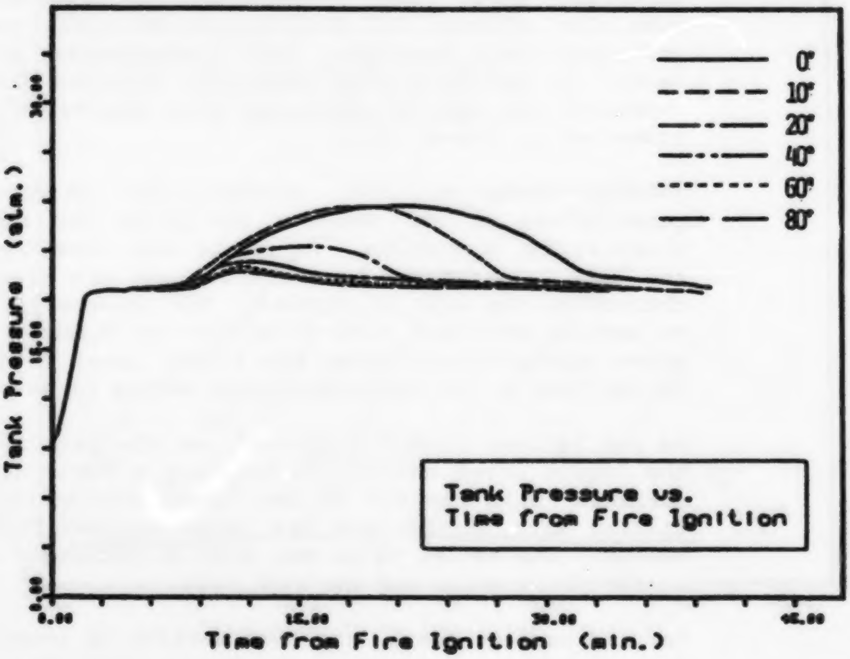

FIGURE 3-43 PREDICTED TANK PRESSURES FOR UNPROTECTED TANKS WITH DIFFERENT PITCH ANGLES EXPOSED TO AN ENGULFING FIRE

In the simulations the relief valve is initially submerged and therefore liquid is entering the relief valve. As in the case of a rolled tank (discussed in section 3.3) the tank-car model represents the flow through the submerged relief valve by using a "frozen flow" model. The frozen flow model is based on the assumption that no vapour generation occurs as the liquid passes through the relief valve, and therefore the frozen flow model is overestimating the pressure relieving capabilities of the submerged valve. This overestimate of the relief valve mass flow affects all of the tank-car model predictions including tank pressure, wall temperatures and liquid level. A two-phase flow model is required to properly represent the venting operation when the relief valve is submerged in liquid level.

Figures 3-44 to 3-49 present the predicted wall temperatures at the tank-car mid plane for the various pitch angles considered. As can be seen from the figures, the wall temperatures at the mid plane are significantly changed as the tank is pitched. The reasons for this can be easily explained with reference to Figure 3-50 which shows approximately where the liquid level is for a 95% filled tank at the different pitch angles of interest.

As can be seen from Figure 3-50, as the tank is pitched, the liquid level changes to maintain a horizontal liquid surface. This results in the lower section of the tank filling with liquid, and the upper section filling with vapour. The relief value may also be submerged depending on the pitch angle and the tank fill.

For the present cases, the test section is located at the tank mid plane. As shown in Figure 3-50 this plane is submerged initially for all of the pitch angles considered here. When the relief valve opens and material is vented from the tank, the liquid surface will move parallel with the horizontal. Eventually the point where the liquid level intersects the top-dead-centre of the tank will meet the tank mid plane and at that time the mid plane temperature at top-dead-centre will begin to rise rapidly. This, of course, is due to the charge from liquid wetted to vapour wetted wall conditions. This event will occur later for tanks with large angles of pitch, for obvious reasons.

The time between when the top-dead-centre of the tank and the bottom-dead-centre of the tank are exposed to vapour also depends on the pitch angle. In a vertical tank (90°

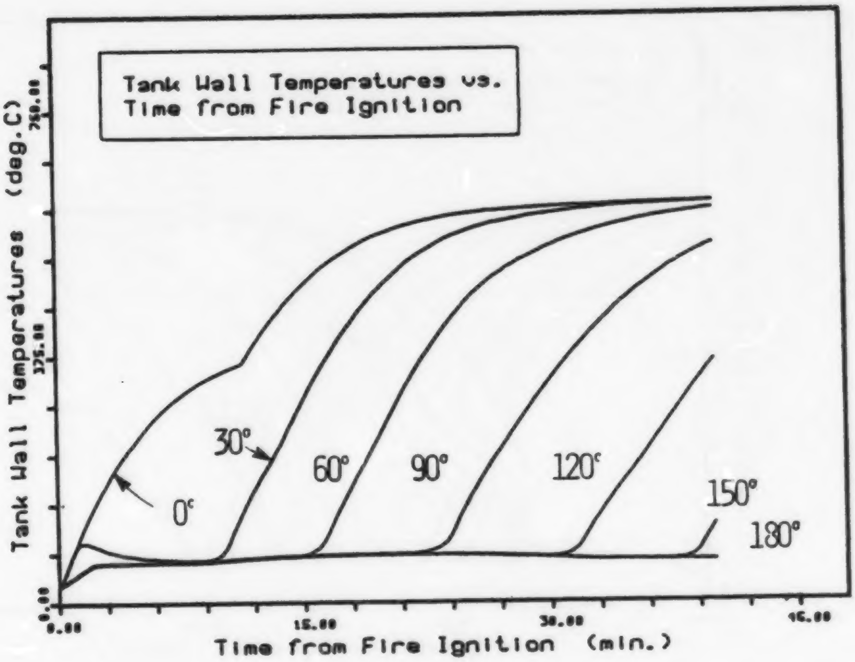

FIGURE 3-44 PREDICTED TANK WALL TEMPERATURES FOR A PITCHED, UNPROTECTED TANK EXPOSED TO AN ENGULFING FIRE (PITCH ANGLE = 0 deg.)

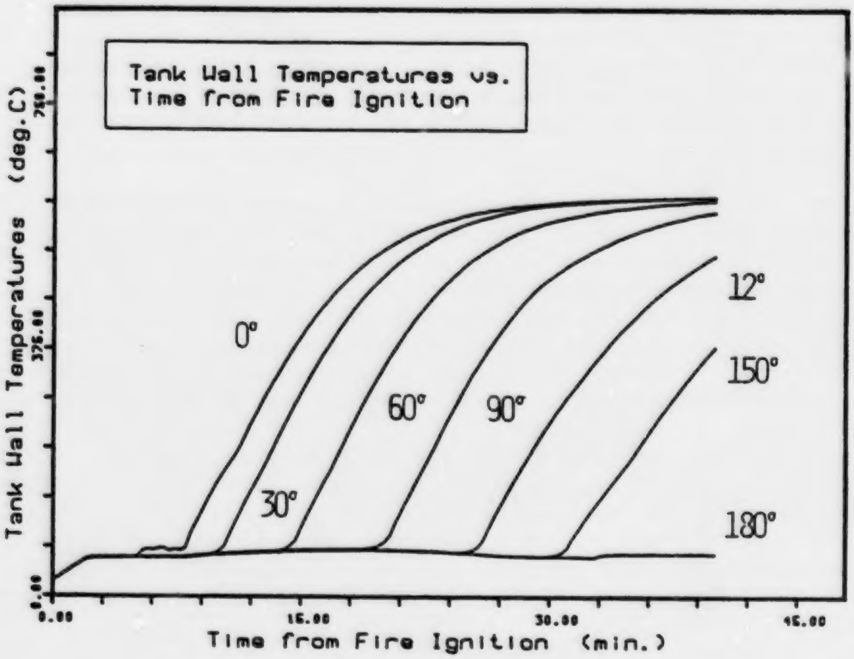

FIGURE 3-45 PREDICTED TANK WALL TEMPERATURES FOR A PITCHED, UNPROTECTED TANK EXPOSED TO AN ENGULFING FIRE (PITCH ANGLE = 10 deg.)

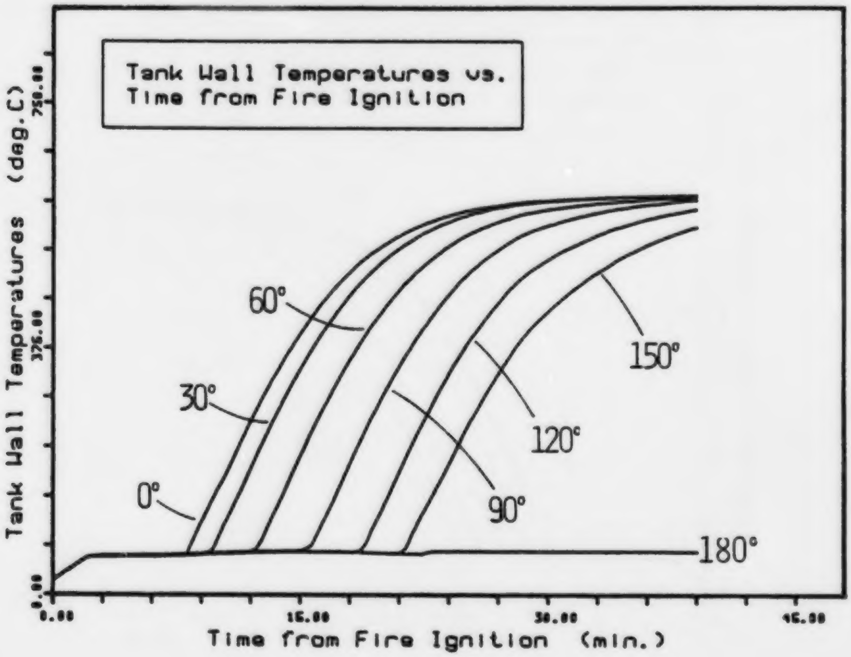

FIGURE 3-46 PREDICTED TANK WALL TEMPERATURES FOR A PITCHED, UNPROTECTED TANK EXPOSED TO AN ENGULFING FIRE (PITCH ANGLE = 20 deg.)

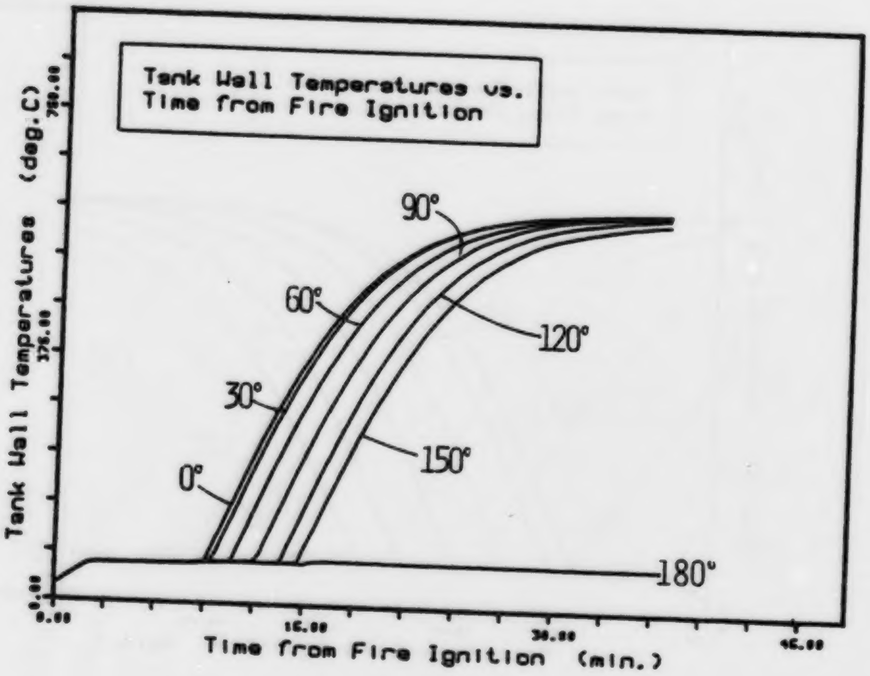

FIGURE 3-47 PREDICTED TANK WALL TEMPERATURES FOR A PITCHED, UNPROTECTED TANK EXPOSED TO AN ENGULFING FIRE (PITCH ANGLE = 40 deg.)

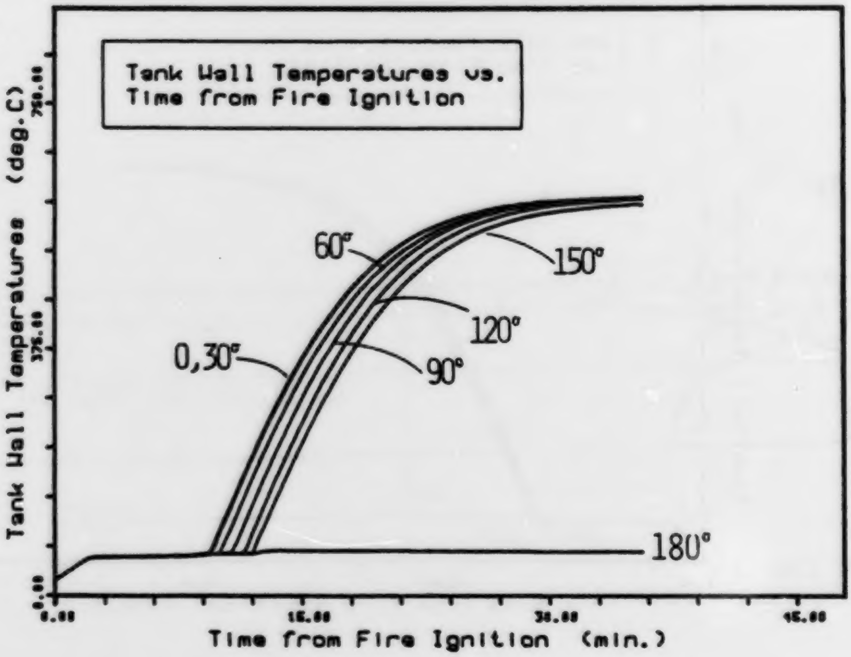

FIGURE 3-48 PREDICTED TANK WALL TEMPERATURES FOR A PITCHED, UNPROTECTED TANK EXPOSED TO AN ENGULFING FIRE (PITCH ANGLE = 60 deg.)

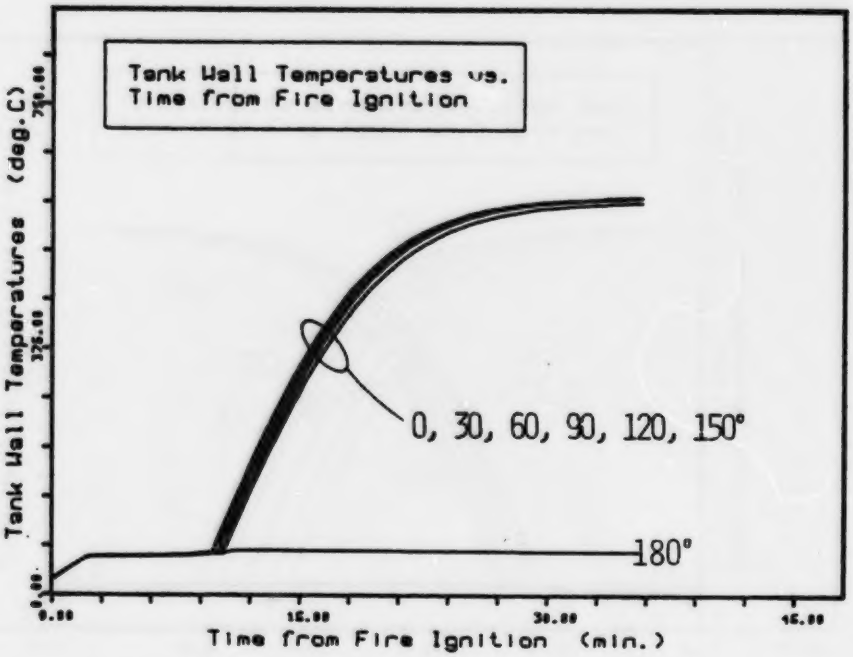

FIGURE 3-49 PREDICTED TANK WALL TEMPERATURES FOR A PITCHED, UNPROTECTED TANK EXPOSED TO AN ENGULFING FIRE (PITCH ANGLE = 90 deg.)

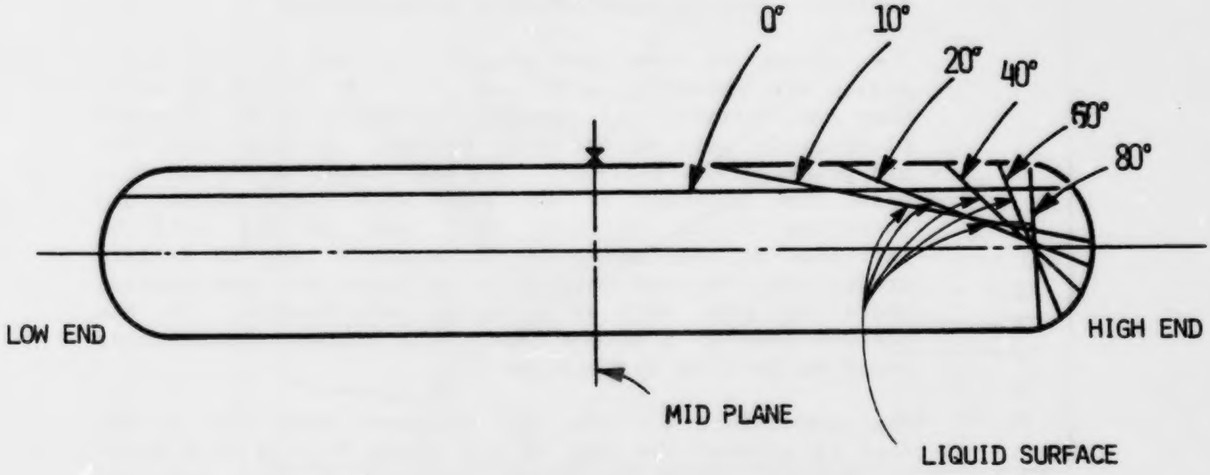
0°
10°
20°
40°
60°
80°
LOW END
HIGH END
MID PLANE
LIQUID SURFACE

FIGURE 3-50 SKETCH SHOWING HOW THE LIQUID LEVEL CHANGES FOR DIFFERENT PITCH ANGLES

pitch) the tdc and bdc locations are exposed to vapour at the same instant. This results in the temperature vs time plots where one cannot differentiate between the wall temperatures at bdc or at 60° around the side from tdc. This effect can be seen in Figures 3-44 to 3-49 in that the temperature plots for the different circumferential locations move closer together as the tank is pitched further from the horizontal.

This same effect can be seen in the liquid level predictions shown in Figure 3-51. As the tank is pitched from the horizontal the mid plane of the tank fills with liquid. The angle that the liquid surface makes with the mid plane dictates how quickly the level drops in that section. This is shown clearly in the Figure.

The stress vs time predictions for the various pitch angles are presented in Figure 3-52. It should be noted that the stresses and material strengths shown in these plots apply only at the test section, in this case, the mid plane of the tank-car. The mid plane is not, in this case, the location of the peak wall temperatures and therefore it is unlikely that tank failure will be initiated at this section. To obtain a time to failure prediction, the user would have to locate the test section where the peak wall temperatures are located. In the present case of a pitched tank, the highest temperatures would be found at the high end.

The predictions for the wall stresses show that as the tank is pitched the risk of mid plane failure initiation is reduced. This prediction, however, results from the fact that the tank peak pressure is reduced. This pressure reduction is an erroneous result generated by the frozen flow relief valve flow model.

3.4.2 Variations in Location of Test Section

This series of runs considered a tank-car with a fixed pitch angle of 30° from the horizontal. In the runs, the location of the test section was varied from the high end of the tank to 1/6 and 1/3 the way along the length of the tank from the high end. In other words, this series of runs when put together forms part of an approximate three-dimensional view of the pitched tank. It must be noted, however, that the three sections considered are not mathematically coupled, ie. axial gradients have not been

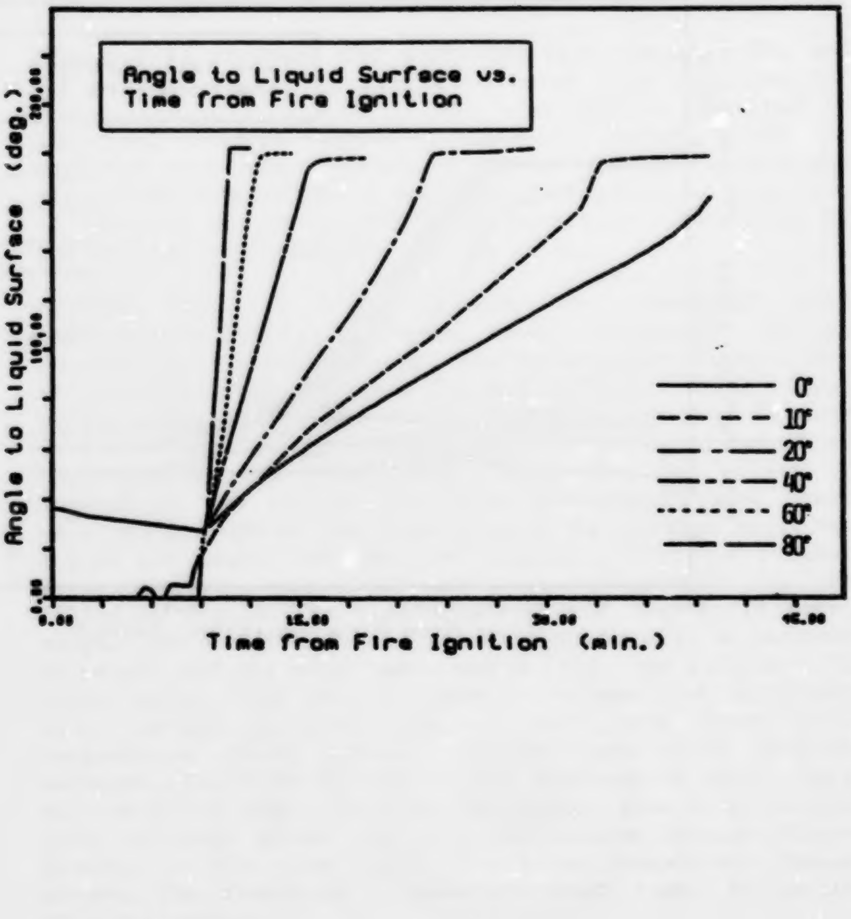

FIGURE 3-51 PREDICTED LIQUID LEVELS FOR UNPROTECTED TANKS WITH DIFFERENT PITCH ANGLES EXPOSED TO AN ENGULFING FIRE

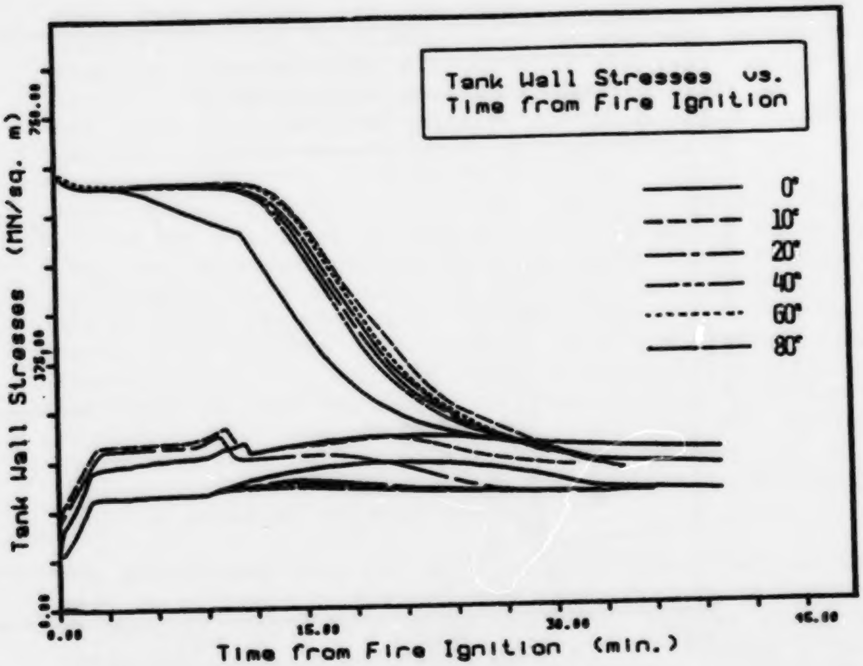

FIGURE 3-52 PREDICTED TANK WALL STRESSES AND TANK WALL MATERIAL STRENGTHS FOR UNPROTECTED TANKS WITH DIFFERENT PITCH ANGLES EXPOSED TO ENGULFING FIRES

accounted for. They are a series of two-dimensional models added together to give an approximate representation of a three-dimensional tank.

As with the other pitched tank simulations, the model predictions are partly erroneous because of the simplistic relief valve flow analysis used when the relief valve is submerged in liquid. As before, this "frozen flow" model results in an overestimate of the valve mass flow rate and therefore results in too short a time to empty condition.

Figure 3-53 presents the predicted tank pressure for the 30° pitched tank. It should be noted that the runs for the different locations of the test section resulted in identical pressure responses. This, of course, is what is expected since the location of the test section should not affect the prediction of the tank pressure rise, the rate of venting, or any of the other conditions determined by the average conditions within the tank.

Figures 3-54 to 3-56 present the predicted wall temperatures for the different cases considered. As can be seen from these figures, the temperature break times are significantly different for the different axial planes within the tank. This, of course, is as expected because of the way the liquid level progresses along the length of the tank in a pitched tank. When the test plane is located at the top of the tank, the temperatures break very early because the liquid level is located near the top of the tank. When the test section is located further down along the tank, initially that test section will be filled by liquid. As time progesses and the liquid level drops, eventually the test plane location will be exposed to vapour and the wall temperatures will rise rapidly. In other words, the only difference between the different test section is the time at which the first wall temperature break occurs. If the tank pitch remains constant, the distribution of wall temperature break times will stay the same. This can be clearly seen from Figures 3-54 to 3-56 where the only difference between these figures is the time where the first temperature break occurs, the remaining temperature break times follow in the same pattern.

Figure 3-57 presents the predicted liquid level in the different test sections considered. As can be seen from the figure, the case where the test section is at the top of the tank shows that initially the liquid level is at approximately 100° from top-dead-centre. In other words,

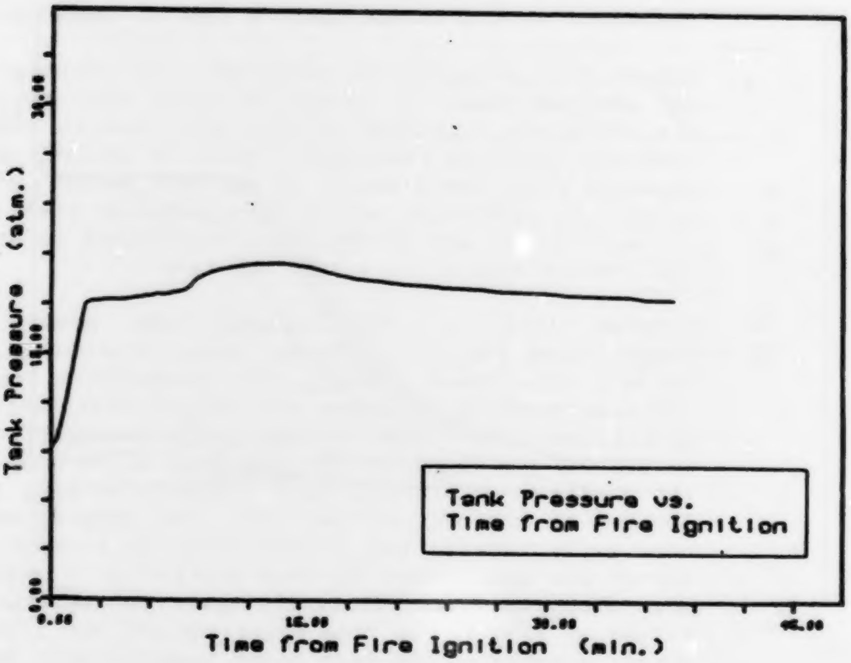

FIGURE 3-53 PREDICTED TANK PRESSURE FOR AN UNPROTECTED TANK PITCHED 30 DEGREES

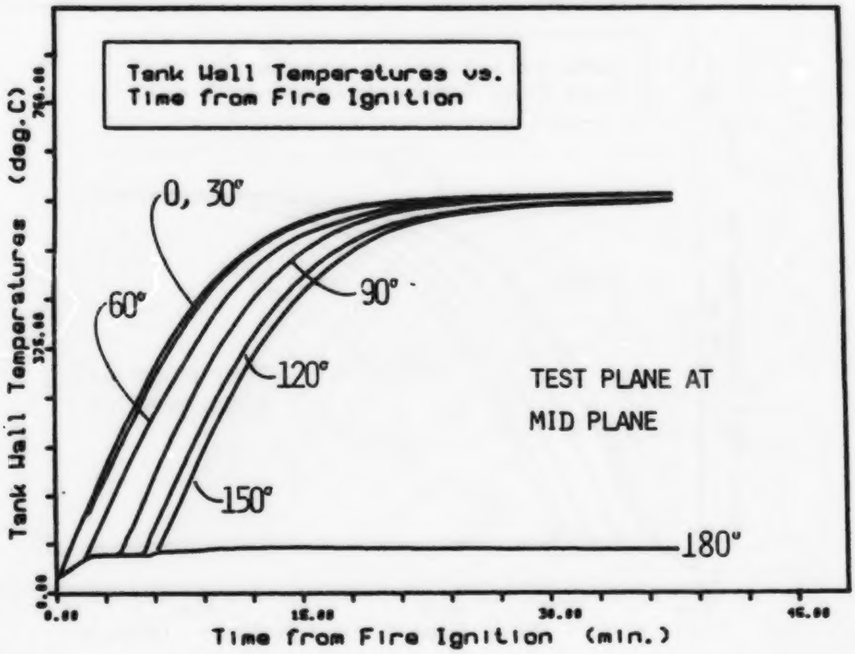

FIGURE 3-54 PREDICTED TANK WALL TEMPERATURES FOR A PITCHED, UNPROTECTED TANK EXPOSED TO AN ENGULFING FIRE (TEST SECTION AT MID PLANE, TANK PITCH = 30 DEGREES)

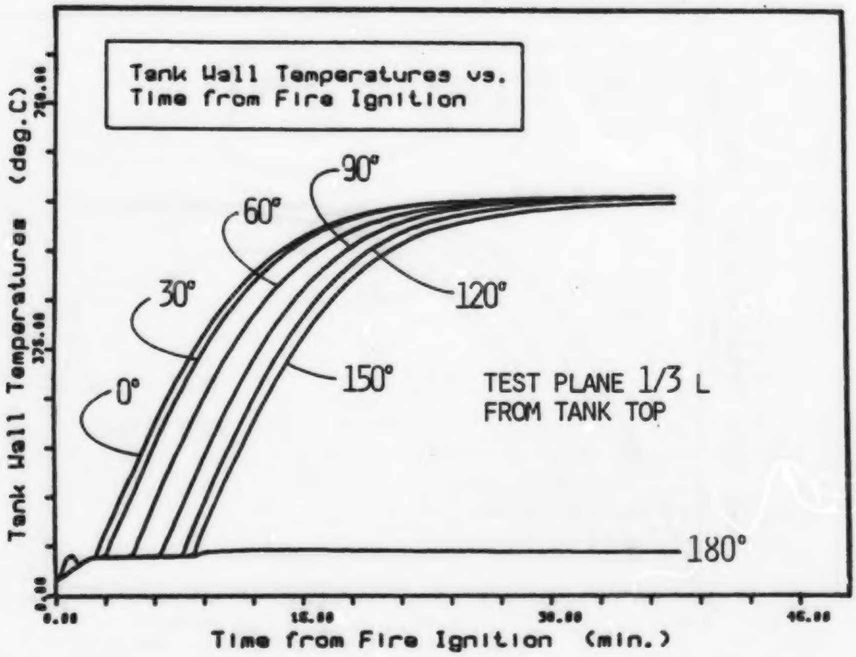

FIGURE 3-55 PREDICTED TANK WALL TEMPERATURES FOR A PITCHED, UNPROTECTED TANK EXPOSED TO AN ENGULFING FIRE (TEST SECTION AT 1/3 L FROM TANK TOP, TANK PITCH = 30 DEGREES)

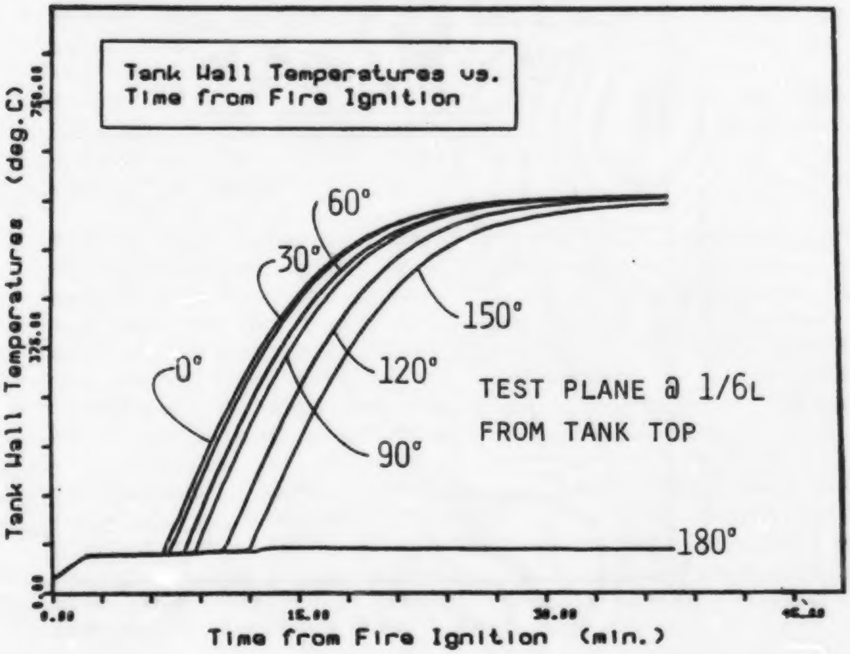

FIGURE 3-56 PREDICTED TANK WALL TEMPERATURES FOR A PITCHED, UNPROTECTED TANK EXPOSED TO AN ENGULFING FIRE (TEST SECTION AT 1/6 L FROM TANK TANK TOP, TANK PITCH = 30 DEGREES)

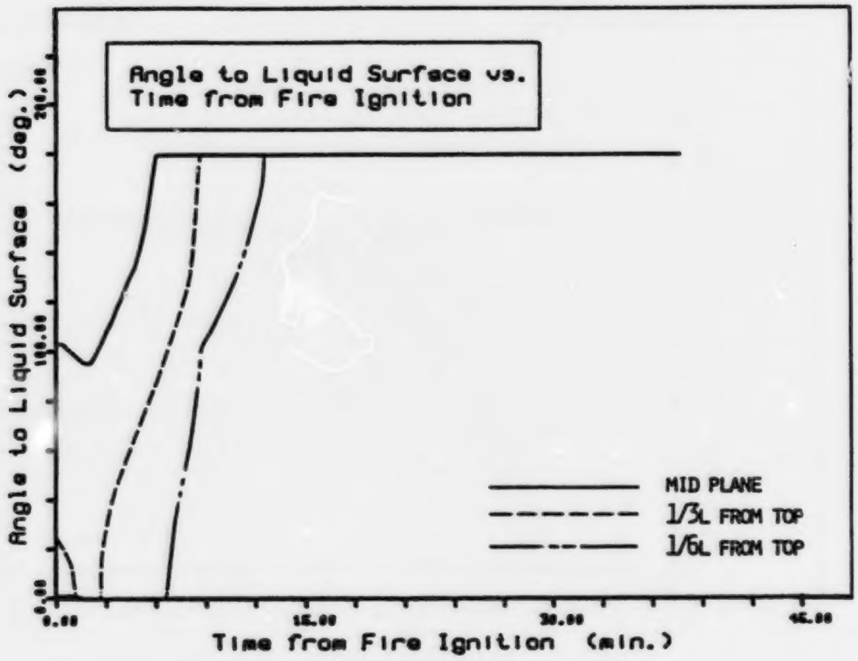

FIGURE 3-57 PREDICTED LIQUID LEVELS AT DIFFERENT AXIAL POSITIONS IN A PITCHED, UNPROTECTED TANK EXPOSED TO AN ENGULFING FIRE (PITCH = 30 DEGREES)

the vapour cap is located at the top end of the tank. For the case where the test section is located 1/6 of the way from the top end of the tank, initially the liquid level is at approximately 20° from top-dead-centre, but as the fire is started the liquid level expands to fill this test section and then once the relief valve comes into play, the liquid level drops below the location. For the case where the test section is located 1/3 of the way down from the top end of the tank, this test section is initially filled with liquid and as time progresses through the simulation, the liquid drops and eventually this test section is exposed to vapour. As the test sections are moved further and further from the top end of the tank, they are filled for longer periods of time with liquid and eventually the liquid level drops below and they are exposed to vapour.

Figure 3-58 presents the predicted wall stresses and material strengths at the different axial locations. As can be seen from the figure, the axial locations near the top end of the tank, where the vapour is, experience earlier reductions in the wall material strengths due to the earlier increases in the wall temperatures. This is, of course, as expected. One would expect that failure would initiate at the high end of a pitched tank.

In summary, these simulations show that the wall temperatures vary significantly along the length of a pitched tank. As expected, the top end of a pitched tank experiences rapid increases in wall temperatures earlier than lower sections of the tank because of the location of the liquid level.

3.5 LADING TYPE SENSITIVITY

This series of runs considered a full-scale unprotected tank (except for standard relief valve) filled with a number of different ladings. In all cases the tank was filled to 95% capacity and the ambient temperature was 25°C. In the simulations the tank was exposed to an engulfing pool fire.

Four different lading types were considered; propane, butane, pentane, and propylene. Therefore, the following simulations will show the difference in the thermal response of a tank-car due solely to differences in the thermal properties of the lading. All other conditions and parameters have been held fixed.

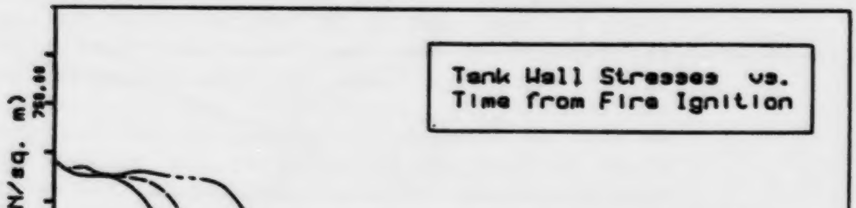

FIGURE 3-58 PREDICTED TANK WALL STRESSES AND TANK WALL MATERIAL STRENGTHS AT DIFFERENT AXIAL POSITIONS IN A PITCHED, UNPROTECTED TANK EXPOSED TO AN ENGULFING FIRE (PITCH = 30 DEGREES)

Figure 3-59 presents the predicted tank pressures for the different simulations. As can be seen from the plot the tank pressurization histories are significantly different for the different lading types. The tank initial pressures are dictated by the saturation pressures at the 25°C ambient conditions for the different ladings. The initial pressurization rates, that is, the slope of the pressure versus time curves initially are almost the same because the specific heats of the different ladings are quite similar. After the rapid initial pressurization the tank pressure reaches the valve set pressure and the valve cycling period begins. As can be seen from the plot, this level period is nearly the same for all the different ladings because the same pressure relief valve is assumed for all of these cases. What differs significantly between the ladings is the length of the cycling period. The most volatile of the ladings, that is propylene, has the shortest valve cycling period. The length of the valve cycling period for the remaining cases is again determined by the lading volatility. The ladings, in decreasing order of volatility are; propylene, propane, butane, and pentane.

The length of the valve cycling period is determined by the vapour generation rate within the tank. The valve will continue to cycle until the vapour generation rate within the tank is sufficient to maintain the pressure above the valve closing pressure. The vapour generation rate is dictated by the latent heat of vaporization of the lading and the heat transfer rate to the lading. For a given amount of heat added, a lading with a low latent heat of vaporization will have more vapour generated in a given length of time than a lading with a high latent heat of vaporization. The length of the valve cycling period is an important factor in the ultimate survival or failure of a tank. During the valve cycling period, the liquid level does not move significantly. When the valve leaves the cycling period and remains fully open, the liquid level drops rapidly. Therefore, the length of the valve cycling period has a significant affect on the rate in which the tank is emptied. This will be discussed further later.

Eventually the valve cycling period will end and the valve will remain fully open. During this time when the valve is fully opened, the pressure within the tank may rise above the valve set pressure, if the vapour generation rate within the tank is sufficient. The peak pressure reached during this continuous venting period is again tied to the lading volatility. The most volatile ladings

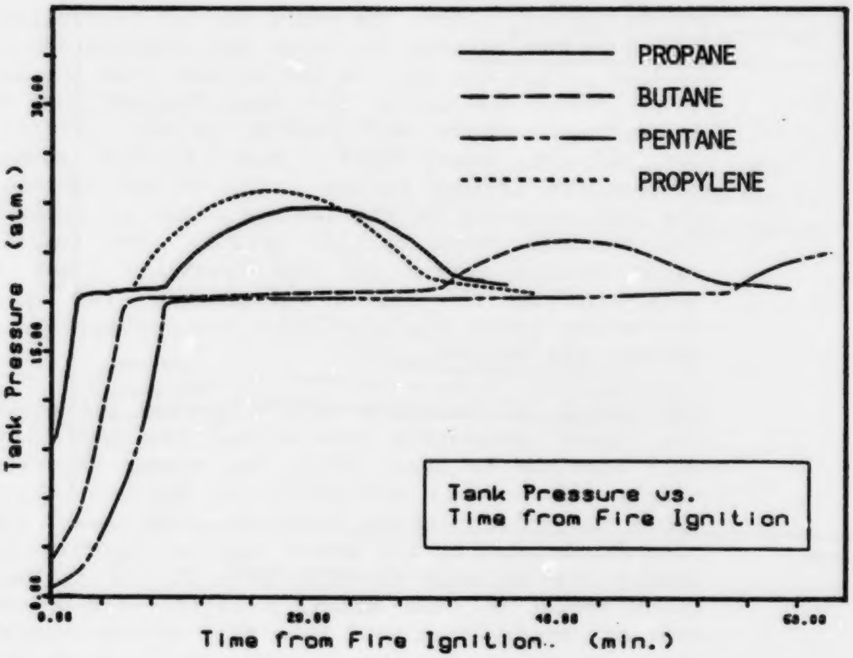

FIGURE 3-59 PREDICTED TANK PRESSURES FOR UNPROTECTED TANKS FILLED WITH DIFFERENT LADINGS, EXPOSED TO ENGULFING FIRES

will result in the highest tank peak pressures. The peak pressure, is of course a significant factor in the ultimate failure of the tank. Again, this will be discussed further later.

Figures 3-60 to 3-63 present the predicted tank wall temperatures for the different cases considered. As can be seen from these plots the wall temperatures are significantly affected by the thermal properties of the different ladings. The differences in the wall temperatures can be related directly to the length of the valve cycling period and the rate at which the tanks are emptied.

The wall temperatures are very sensitive to the liquid level within the tank. The liquid level, is of course dictated by the rate at which the lading is vented from the tank through the pressure relief valve. As mentioned before, when the valve is cycling the liquid level remains almost stationary. Whereas, when the valve is in the continuously venting mode, the liquid level drops rapidly. The location of the liquid level determines when a portion of the tank wall is exposed to vapour and when its temperature begins to rise rapidly. These temperature break times can be clearly seen on the figures.

The peak wall temperatures in the vapour wetted regions are not significantly affected by the different ladings. This is because the heat transfer from the vapour wetted walls is primarily due to radiant heat transfer, and this is not significantly affected by the lading type. The peak wall temperature in the liquid wetted wall region is, however, significantly affected by the different lading temperatures. The wall temperatures in the liquid wetted wall regions closely follow the temperature of the liquid lading. The temperature of the liquid lading, is itself controlled by the pressure relief valve. The temperature of the liquid lading will be the saturation temperature for the tank pressure. The tank pressure is of course controlled by the pressure relief valve. The most volatile ladings will have the lowest saturation temperature for a given pressure. This is seen in the plots because propylene has the lowest liquid wetted wall temperatures followed by propane, butane and pentane.

Based on these figures it can be concluded that the different ladings do not have a significant affect on the strength of the tank material. This is because the tank wall material strength is dependent upon the peak wall

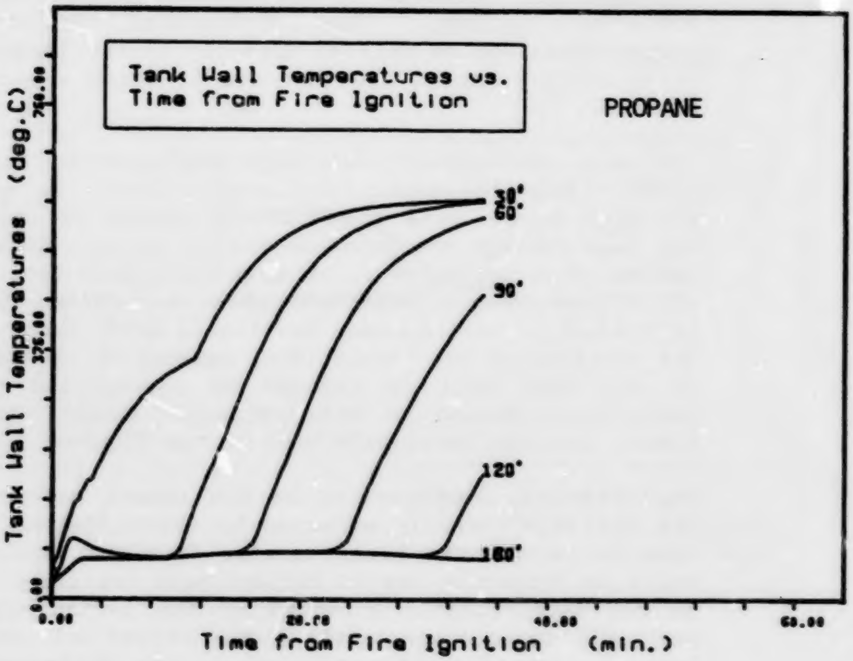

FIGURE 3-60 PREDICTED TANK WALL TEMPERATURES FOR AN UNPROTECTED TANK CONTAINING PROPANE, EXPOSED TO AN ENGULFING FIRE

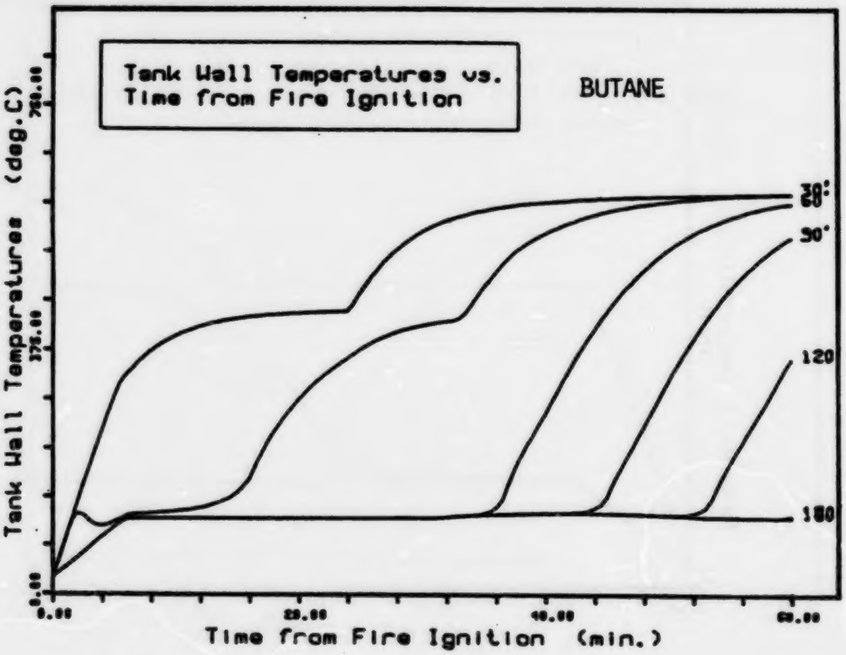

FIGURE 3-61 PREDICTED TANK WALL TEMPERATURES FOR AN UNPROTECTED TANK CONTAINING BUTANE, EXPOSED TO AN ENGULFING FIRE

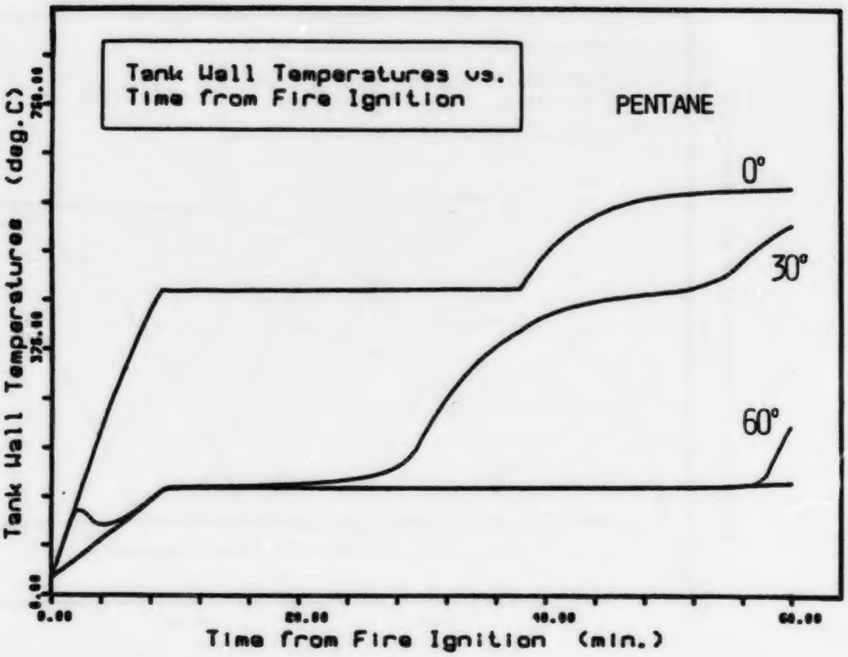

FIGURE 3-62 PREDICTED TANK WALL TEMPERATURES FOR AN UNPROTECTED TANK CONTAINING PENTANE, EXPOSED TO AN ENGULFING FIRE

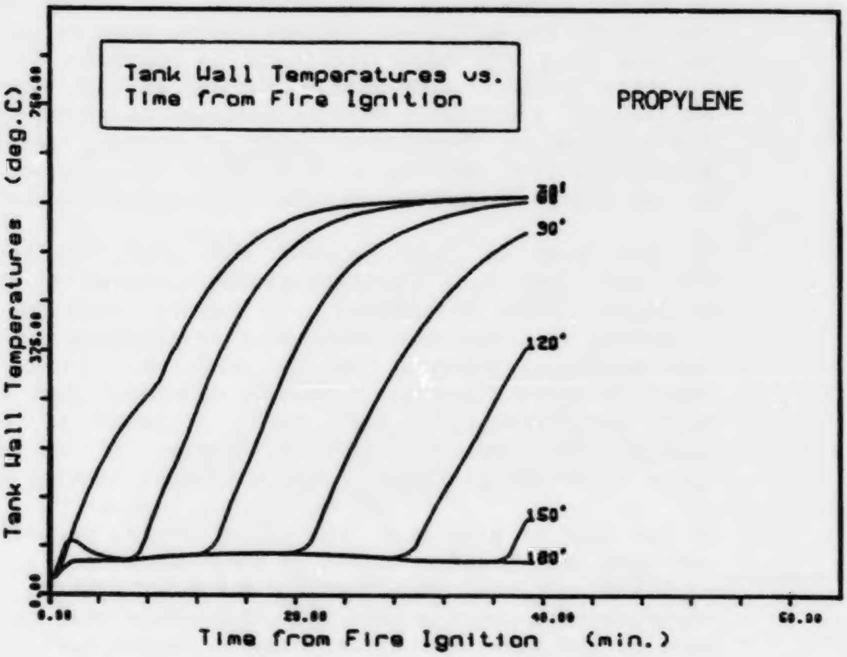

FIGURE 3-63 PREDICTED TANK WALL TEMPERATURES FOR AN UNPROTECTED TANK CONTAINING PROPYLENE, EXPOSED TO AN ENGULFING FIRE

temperatures experienced in the vapour space. As we have seen from the preceeding figures, the peak wall temperatures are quite similar. However, the time to reach these peak temperature are quite different for the different ladings. This of course is due to the different rates of venting for the different cases considered. This will be discussed further with the aid of the following plot.

Figure 3-64 presents the predicted liquid levels for the different cases under consideration. As can be seen from the figure the different ladings have a significant effect on the rate at which the tank is emptied. The most volatile lading, propylene, results in the most rapid emptying of the tank. This is followed by propane, butane and pentane in decreasing order of venting rates. The transition from cycling to continuous venting can be seen on the figure as sudden upturns in the four curves shown.

Figures 3-65 to 3-68 present the predicted tank wall stresses and tank wall material strengths for the different cases considered. As before, tank failure is indicated when the tank wall material strength drops below the predicted stresses in the tank wall inner fibres. Based on these figures, it can be concluded that the tank with propylene will fail first followed by propane, butane, and pentane. The differences in the time to failure are due entirely to the different venting rates.

In the case of propylene, the valve cycling period was the shortest and therefore onset of continuous venting occured earliest and the tank emptied quickest. With the tank emptying more rapidly than the other cases this means that more of the tank wall was exposed to vapour earlier in the event. With more wall area exposed to vapour, higher wall temperatures were experienced earlier on in the fire, and therefore material degradation due to high temperatures resulted. This is seen in the Figures as the rapid drop in the tank wall strength.

In summary, the different lading thermodynamic properties had a significant impact on the time to failure of the tank. However, it should be noted that it has been assumed that all of the tanks would be fitted with a pressure relief valve of the same size set to the same opening pressure. In reality, this may not be the case. In any event, the preceeding cases are good examples of how sensitive tank failure is to the rate at which the lading is vented from the tank. In an unprotected tank, the wall temperatures are very sensitive to the location

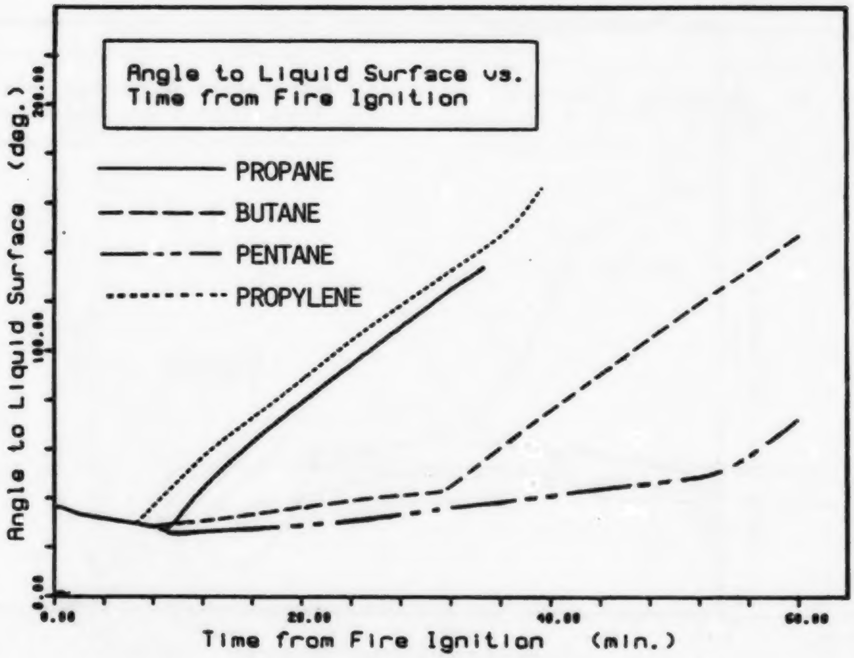

FIGURE 3-64 PREDICTED LIQUID LEVELS FOR UNPROTECTED TANKS CONTAINING DIFFERENT LADINGS, EXPOSED TO ENGULFING FIRES

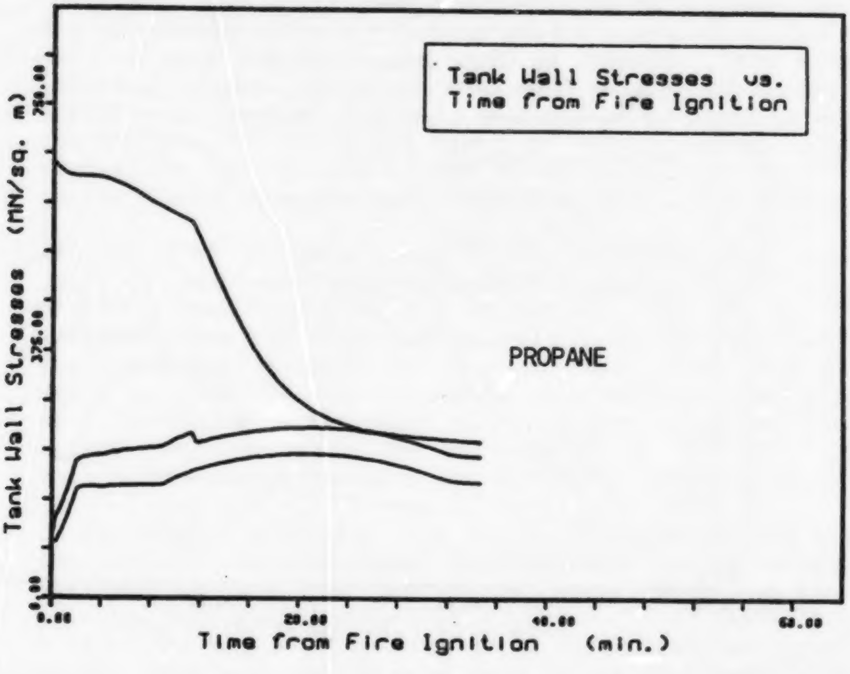

FIGURE 3-65 PREDICTED TANK WALL STRESSES AND TANK WALL MATERIAL STRENGTHS FOR AN UNPROTECTED TANK CONTAINING PROPANE, EXPOSED TO AN ENGULFING FIRE

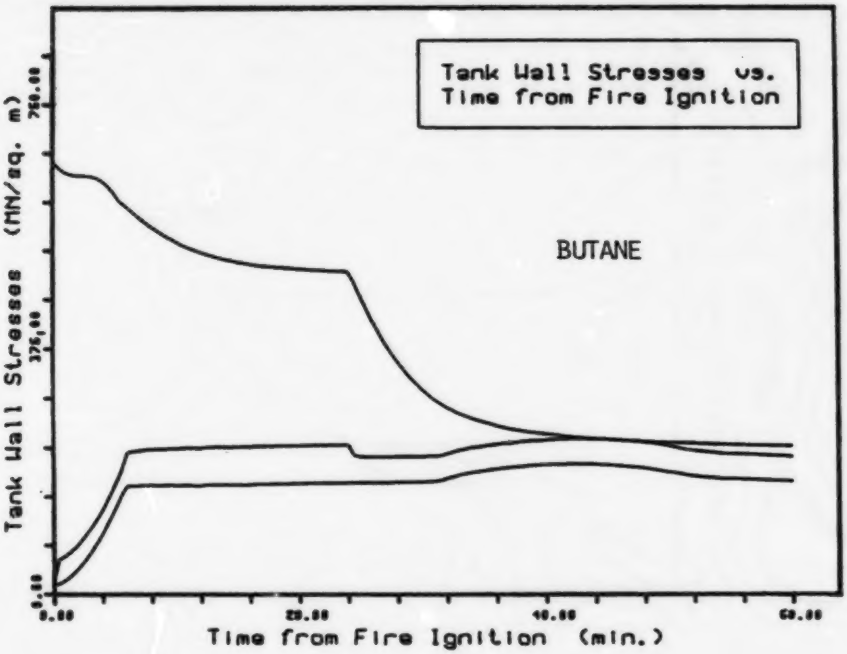

FIGURE 3-66 PREDICTED TANK WALL STRESSES AND TANK WALL MATERIAL STRENGTHS FOR AN UNPROTECTED TANK CONTAINING BUTANE, EXPOSED TO AN ENGULFING FIRE

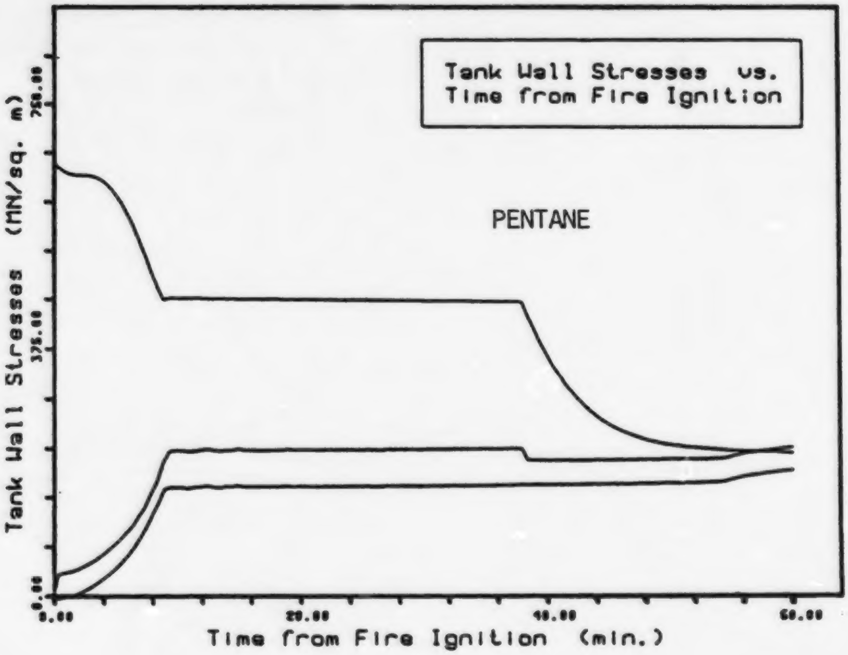

FIGURE 3-67 PREDICTED TANK WALL STRESSES AND TANK WALL MATERIAL STRENGTHS FOR AN UNPROTECTED TANK CONTAINING PENTANE, EXPOSED TO AN ENGULFING FIRE

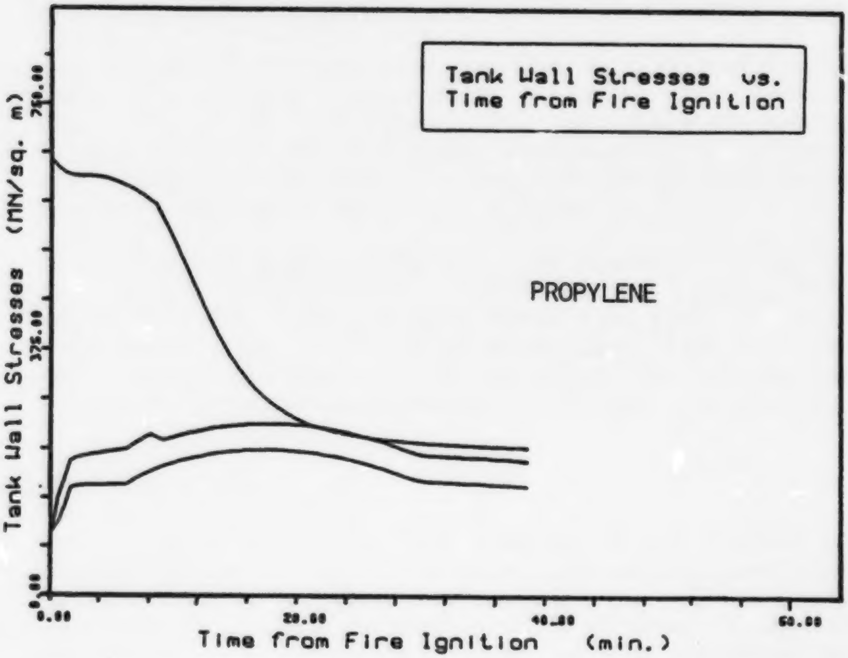

FIGURE 3-68 PREDICTED TANK WALL STRESSES AND TANK WALL MATERIAL STRENGTHS FOR AN UNPROTECTED TANK CONTAINING PROPYLENE, EXPOSED TO AN ENGULFING FIRE

of the liquid level. If the tank lading is vented very rapidly, one can expect that the wall temperatures near the top of the tank will also increase very rapidly and therefore time to failure will be very short.

4.0 EXAMPLES OF SIMULATIONS

This section presents the results of a number of model simulations of tanks with different thermal protection schemes. Three basic systems have been considered, insulated tanks, tank-cars with fusible plugs, and tank-cars equipped with Explosafe. A number of simulations were performed for each thermal protection system so that their performance could be predicted for different configurations of the thermal protection scheme.

Each simulation started with the same initial conditions, that is, initial temperature = 25°C, and initial fill = 95% of the tank capacity. In all cases the lading is pure propane, and the tank is assumed to be equipped with a standard size relief valve. All of the cases to be presented involved a tank fully engulfed in fire.

As before, the model predictions are presented using the four basic summary plots, pressure vs. time, wall temperature vs. time, liquid level vs. time and wall stresses vs. time. For reference purposes, each of these plots should be compared with the simulation results for an unprotected tank-car presented in the previous section.

4.1 INSULATED TANK

This section presents the results of a number of simulations involving a full-scale tank-car equipped with thermal insulation. Three simulations were performed with the tanks equipped with different thicknesses of thermal insulation with properties similar to that of asbestos. In all cases the insulation was assumed to be covered by a steel jacket.

The different simulations were performed to show the effects of thickening the thermal insulating layer on a tank-car. Figures 4-1 to 4-4 show the predicted response of the tank equipped with the different thicknesses of thermal insulation.

Figure 4-1 presents the predicted tank pressure for the different cases considered. As can be seen from the figure, the simulation for the tank with the thinnest insulating cover had the most rapid pressurization rate. This initial rapid pressurization rate was followed by a relatively short valve cycling period and then a rapid increase in the tank pressure during continuous venting.

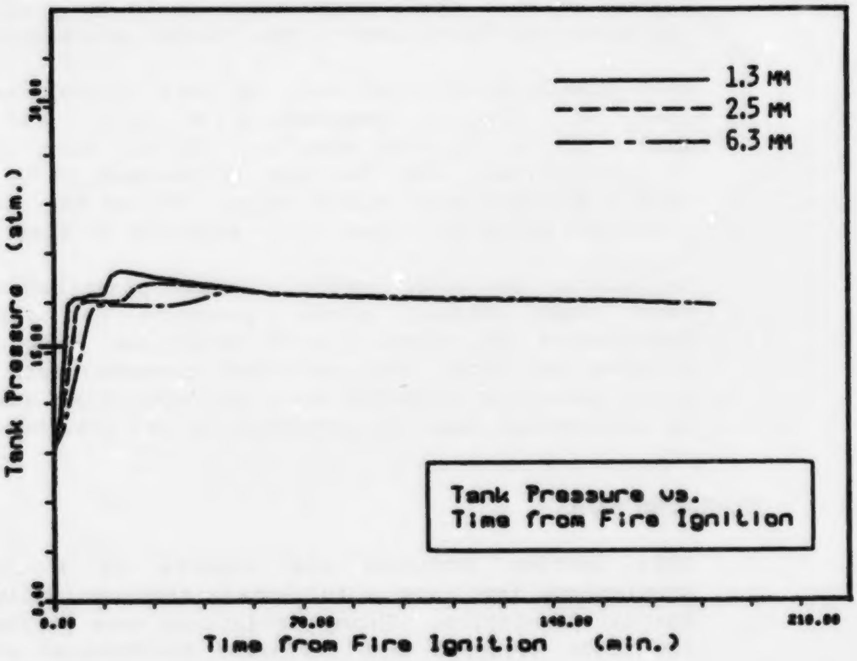

FIGURE 4-1 PREDICTED TANK PRESSURES FOR INSULATED TANKS WITH DIFFERENT THICKNESSES OF INSULATION, EXPOSED TO AN ENGULFING FIRE

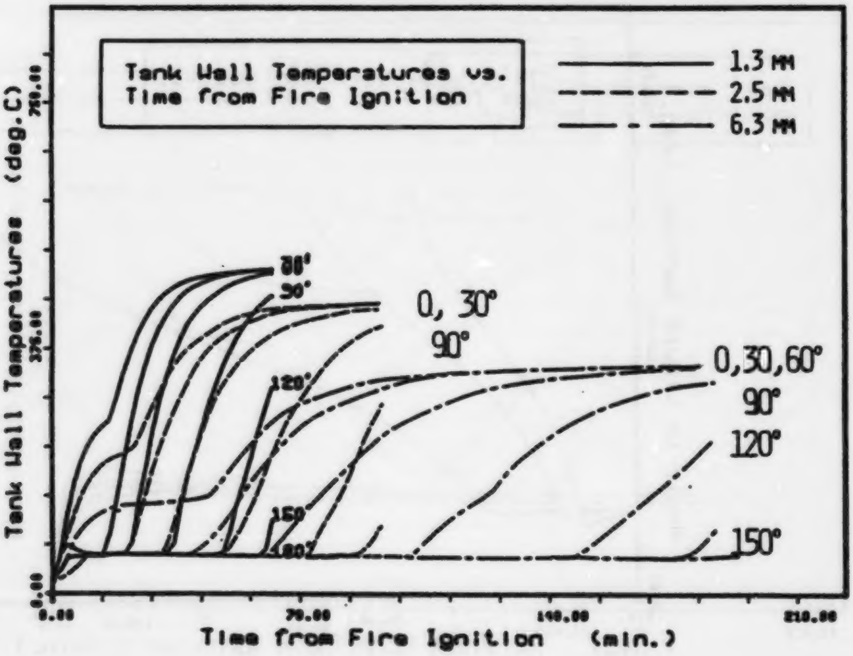

FIGURE 4-2 PREDICTED TANK WALL TEMPERATURES FOR INSULATED TANKS WITH DIFFERENT THICKNESSES OF INSULATION, EXPOSED TO AN ENGULFING FIRE

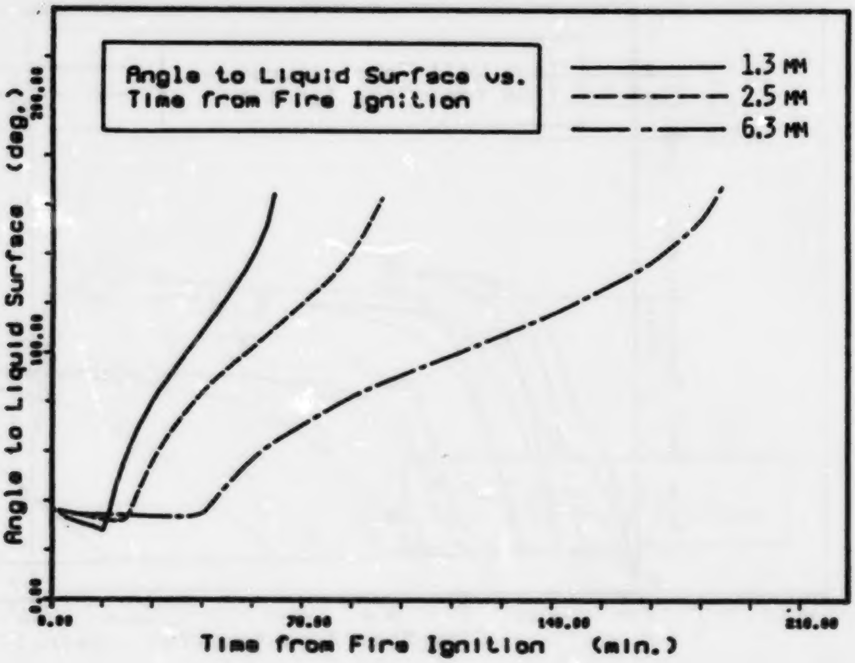

FIGURE 4-3 PREDICTED LIQUID LEVEL OF INSULATED TANKS WITH DIFFERENT THICKNESSES OF INSULATION, EXPOSED TO AN ENGULFING FIRE

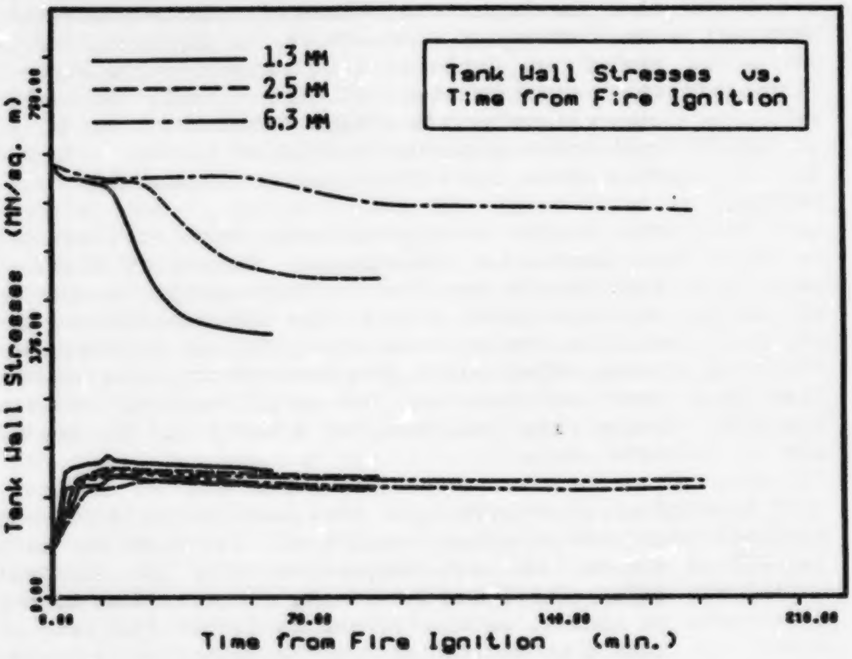

FIGURE 4-4 PREDICTED TANK WALL STRESSES AND TANK WALL MATERIAL STRENGTHS FOR INSULATED TANKS WITH DIFFERENT THICKNESSES OF INSULATION, EXPOSED TO AN ENGULFING FIRE

As can be seen from the figure, the valve cycling periods increase in duration as the thickness of the insulation is increased. The increased thickness of insulation also had the effect of reducing the tank peak pressure.

Figure 4-2 presents the predicted wall temperatures for the different cases considered. As can be seen from the figure, the thickness of the insulation layer has a significant effect on the predicted wall temperatures. As the insulation thickness is increased, the peak wall temperatures are decreased, as expected. It appears from the figure, that if the insulation thickness is doubled, the time scale of the simulation also doubles, approximately. In other words, the time during which the tank remains partially full of lading is increased as the insulation layer thickness is increased.

The results seem to indicate that, at least for the range of insulation thicknesses considered here, there is a significant benefit in increasing the insulation layer thickness. Of course, the fundamentals of heat transfer tell us and at some point the law of diminishing returns takes effect and a proportional increase in the insulation thickness does not give a proportional benefit. At this point, the economics of installing the insulation layer take over.

Figure 4-3 presents the predicted liquid level for the different cases considered. As can be seen from the figure, the simulation involving the thickest layer of insulation resulted in the longest time to empty. This, of course, is due to the fact that the rate at which the lading is vented through the relief valve is determined by the total heat input to the tank lading. By increasing the thickness of the insulating layer, the total heat input to the tank lading is reduced and this results in a lower venting rate.

Figure 4-4 presents the predicted wall stresses and tank material strengths for the different cases considered. As can be seen from the figure, none of the cases considered came close to rupturing. For the case with the thickest thermal insulation cover, there was very little loss of material strength due to high temperature degradation. However, the case with the thinnest insulation layer does show significant loss in material strength at the locations of the peak wall temperatures. The predicted wall stresses show that as the insulation layer is increased the difference between the stresses in the inner and outer fibres of the tank wall is decreased. This is, of course, due to the fact that the differences in the stresses of the inner and outer wall fibres is due to the thermal gradient through the wall, and this thermal gradient is of course reduced as the heat flux is reduced.

In summary, the simulations clearly that the thickness of the thermal insulation layer has a significant effect on the thermal response of the tank-car. Increasing the thickness of the thermal insulating layer does not have a significant effect on the tank pressure because the tank pressure is of course governed by the relief valve set pressure. The tank wall temperatures are significantly effected by the thickness of the insulating layer. The liquid level in the tank is also significantly effected by the thickness of the insulating layer. This is, of course, due to the fact that the liquid level is dictated by the rate of venting through the relief valve, and this venting process is controlled by the total heat input to the tank lading. As the thickness of the insulating layer is increased, the total heat flux to the lading is decreased. It was also shown in the simulations that the increase of the thermal insulating layer had a significant effect on the degree of reduction of the tank wall strength due to high temperature degradation. Although the tank pressure was not significantly effected by the changes in insulation thickness, the loss in material strength of the tank wall was. Therefore, it appears that the thickness of the insulating layer should be dictated by the peak wall temperature that will result in thermal degradation of the tank wall material. The insulating layer should be designed so that within a reasonable length of time the tank wall material will not reach temperatures where significant thermal degradation will occur. This, of course, is exactly how thermal insulating layers for tank-cars are evaluated.

4.2 TANK WITH FUSIBLE PLUGS

The simulations about to be presented involve full-scale tanks equipped with fusible plug devices. Fusible plugs are devices consisting of an orifice plugged by a low melting temperature material. If the temperature of the device exceeds some predetermined limit, the plug melts and is blown free thereby opening the orifice so that the tank lading can be vented. In other words, a fusible plug is a temperature sensitive relief valve. The disadvantage of such devices, is that they cannot be closed once they have been opened.

Two different sets of simulations were performed to show the sensitivity in the performance of fusible plugs to different plug numbers and melting temperatures. Figures 4-5 to 4-8 show the predicted response of a tank equipped with four, eight, or twelve two inch diameter plugs that melt out at 430°F. Figures 4-9 to 4-12 show predicted results for a full-scale tank equipped with four two inch diameter plugs that melt out at temperatures of 205, 315 and 430°C. In all the simulations, the plugs are located along the tank top-dead-centre. This, however, should not be regarded as a recommendation that fusible plugs be located only at the tank tdc. Fusible plug devices should be located strategically over the tank surface to ensure that at least some remain above the liquid surface for all possible tank orientations. This is necessary because the fusible plugs will not melt out as long as they remain liquid wetted. The optimum placement of fusible plug devices requires further study which is beyond the scope of the present project.

Case #1 Different Numbers of Fusible Plugs:

Figure 4-5 presents the predicted tank pressure for the different cases considered. As can be clearly seen from the figure, the tank response prior to the opening of the fusible plugs is identical to that of an unprotected tank-car. However, once the fusible plugs come into play, the tank pressure histories differ. As is indicated in the figure, increasing the number of fusible plugs increases the rate at which the tank pressure drops. The law of diminishing returns seems to apply with the number of fusible plugs. It seems that there is not a great advantage to increasing the number of fusible plugs above 8.

Figure 4-6 presents the predicted tank wall temperatures for the different cases considered. As can be seen from the figure, the presence of fusible plugs has no effect up until the point where the fusible plugs melt. This was also seen in the previous figure that showed the predicted tank pressure. Once the fusible plugs melt and material is vented through the devices, the wall temperatures are affected because the lading is vented more rapidly to the atmosphere. This results in earlier break times for the temperatures near the bottom of the tank.

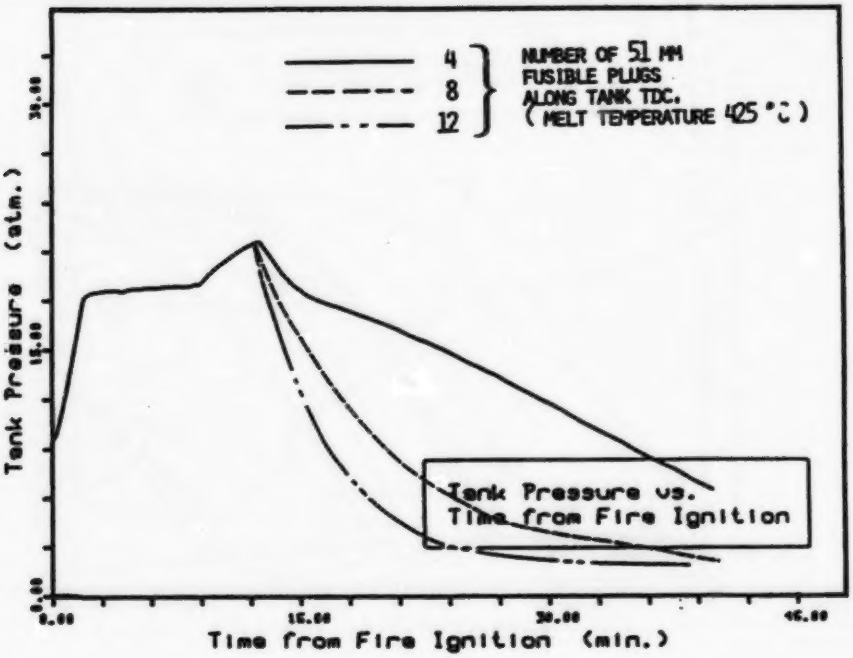

FIGURE 4-5 PREDICTED TANK PRESSURES FOR TANKS EQUIPPED WITH DIFFERENT NUMBERS OF FUSIBLE PLUGS, EXPOSED TO AN ENGULFING FIRE

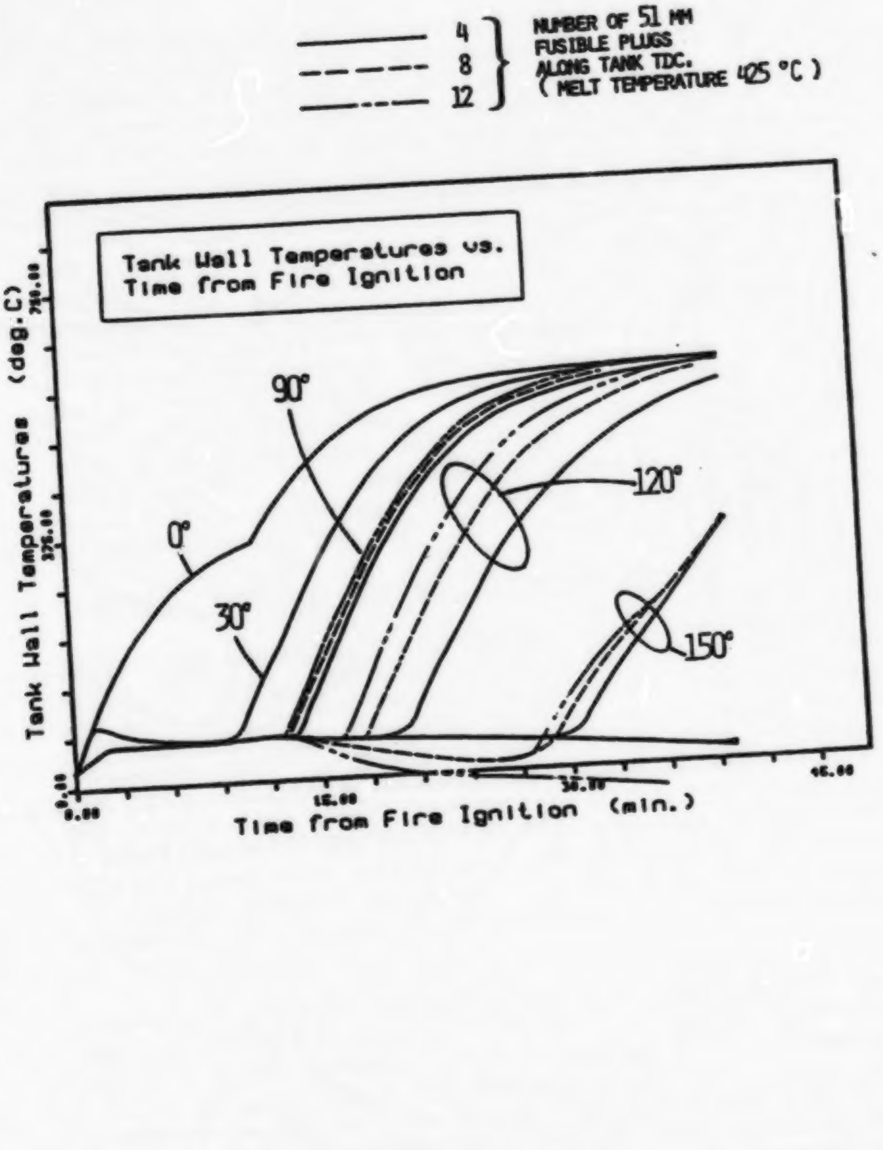

FIGURE 4-6 . PREDICTED TANK WALL TEMPERATURES FOR TANKS EQUIPPED WITH DIFFERENT NUMBERS OF FUSIBLE PLUGS, EXPOSED TO AN ENGULFING FIRE

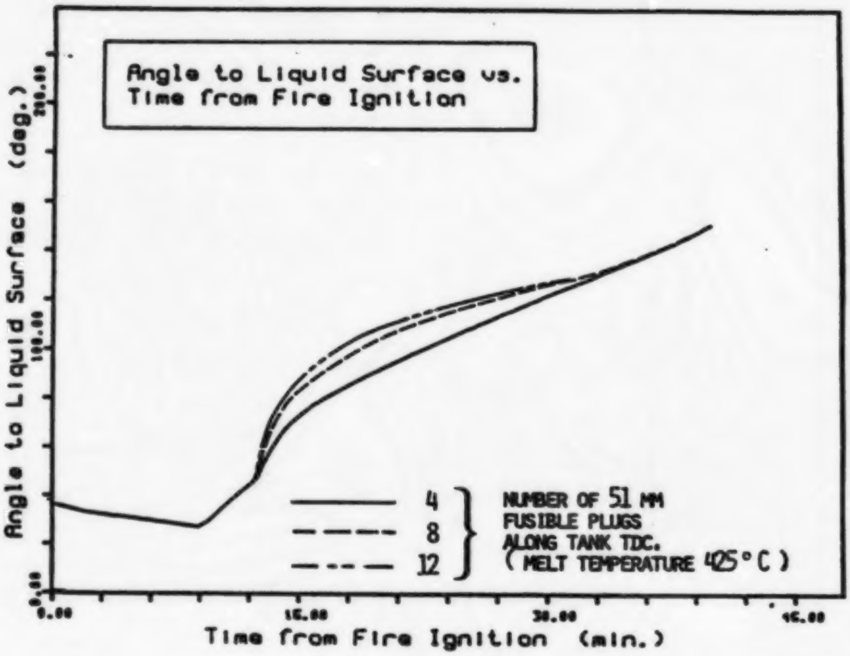

FIGURE 4-7 PREDICTED LIQUID LEVEL OF TANKS EQUIPPED WITH DIFFERENT NUMBERS OF FUSIBLE PLUGS, EXPOSED TO AN ENGULFING FIRE

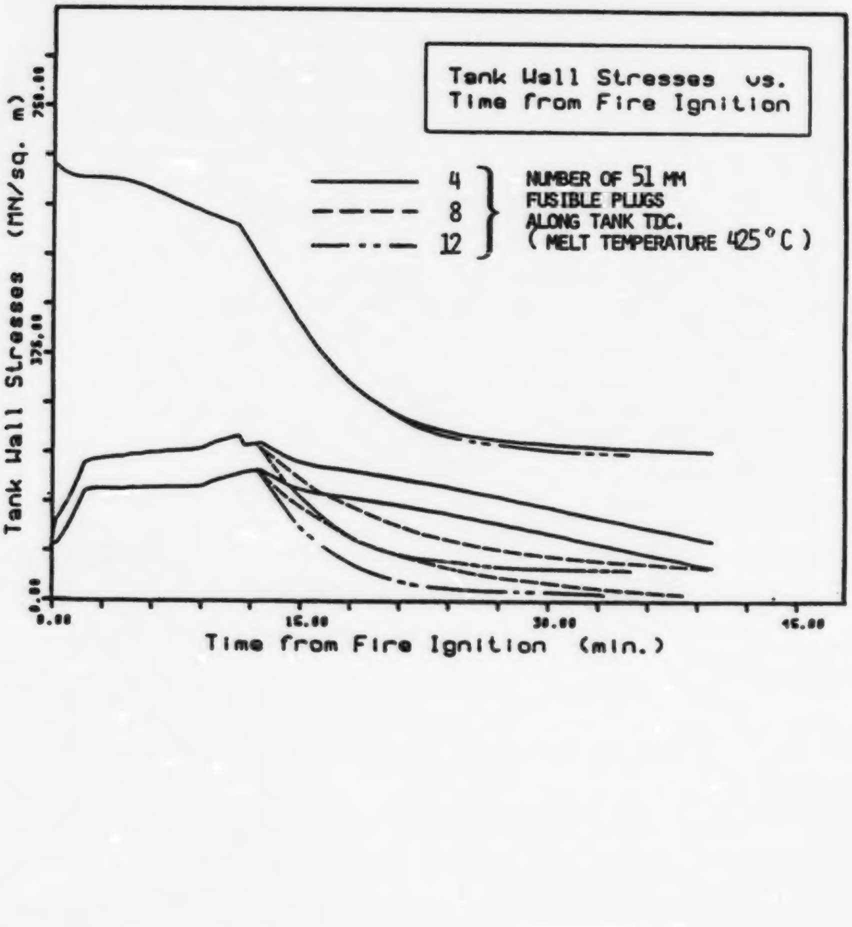

FIGURE 4-8 PREDICTED TANK WALL STRESSES AND TANK WALL MATERIAL STRENGTHS FOR TANKS EQUIPPED WITH DIFFERENT NUMBERS OF FUSIBLE PLUGS, EXPOSED TO AN ENGULFING FIRE

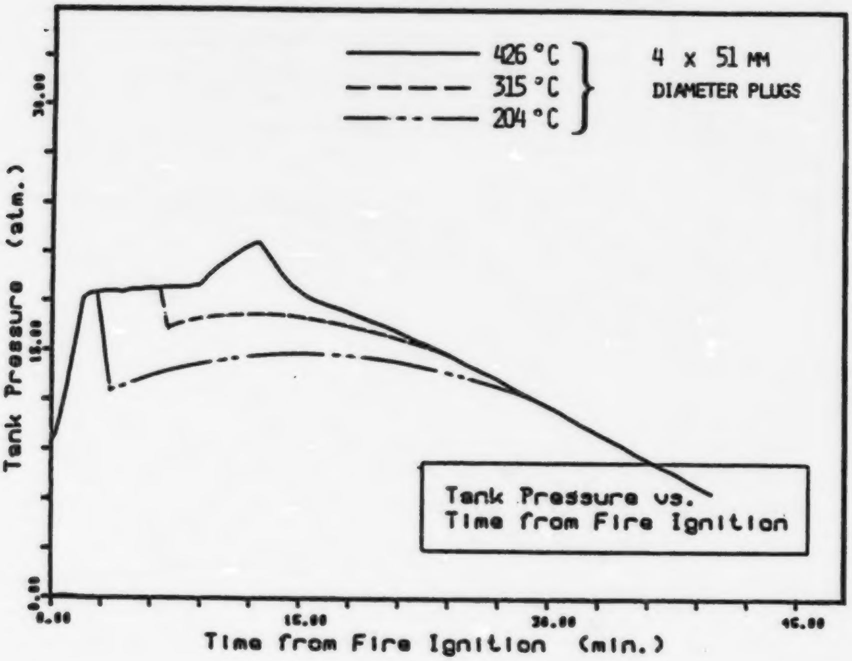

FIGURE 4-9 PREDICTED TANK PRESSURES FOR TANKS EQUIPPED WITH FUSIBLE PLUGS WITH DIFFERENT MELTING TEMPERATURES, EXPOSED TO AN ENGULFING FIRE

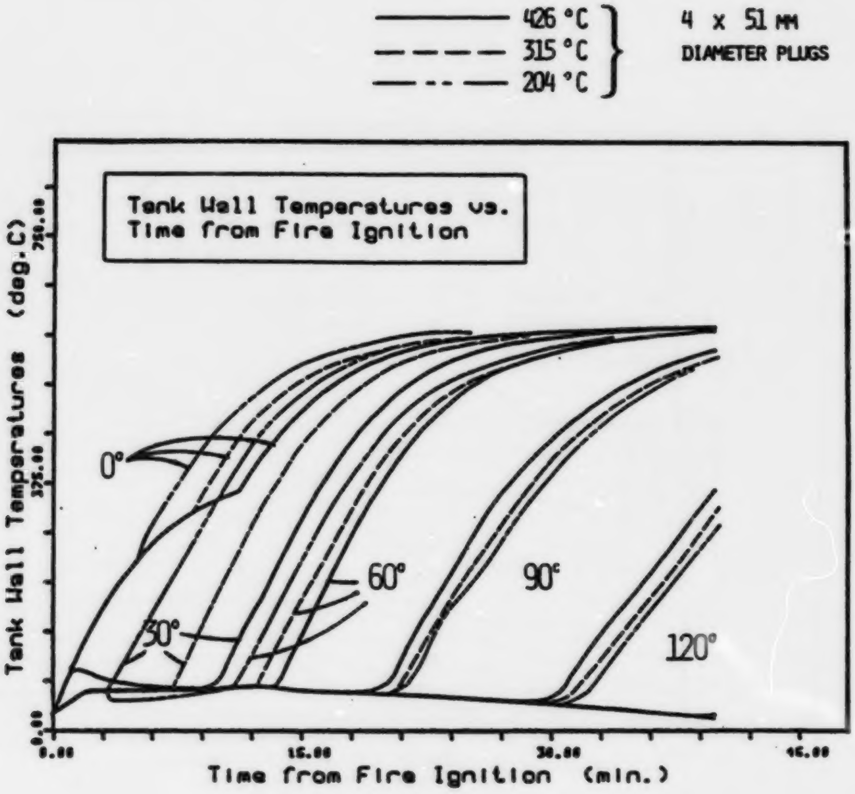

FIGURE 4-10 PREDICTED TANK WALL TEMPERATURES FOR TANKS EQUIPPED WITH FUSIBLE PLUGS WITH DIFFERENT MELTING TEMPERATURES, EXPOSED TO AN ENGULFING FIRE

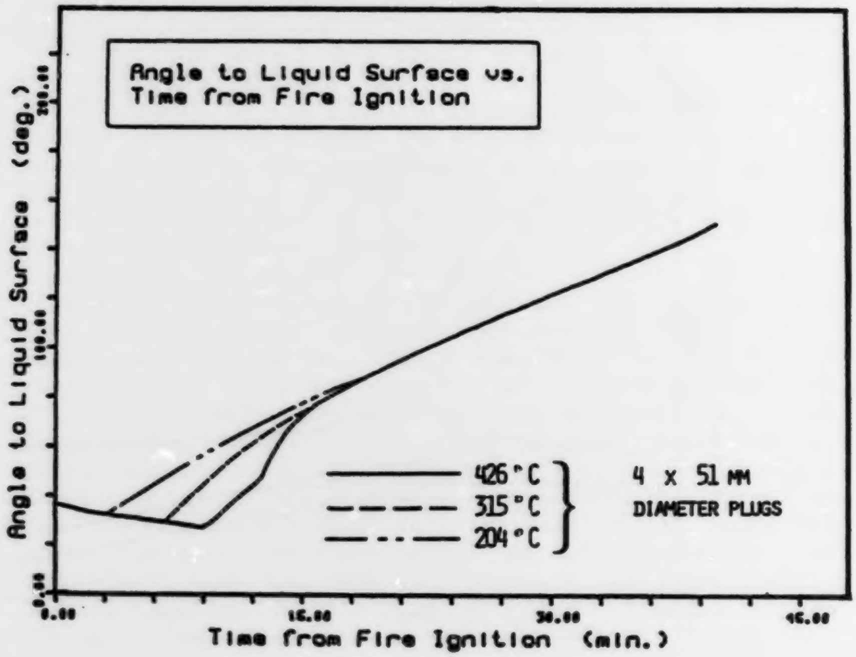

FIGURE 4-11 PREDICTED LIQUID LEVEL FOR TANKS EQUIPPED WITH FUSIBLE PLUGS WITH DIFFERENT MELTING TEMPERATURES, EXPOSED TO AN ENGULFING FIRE

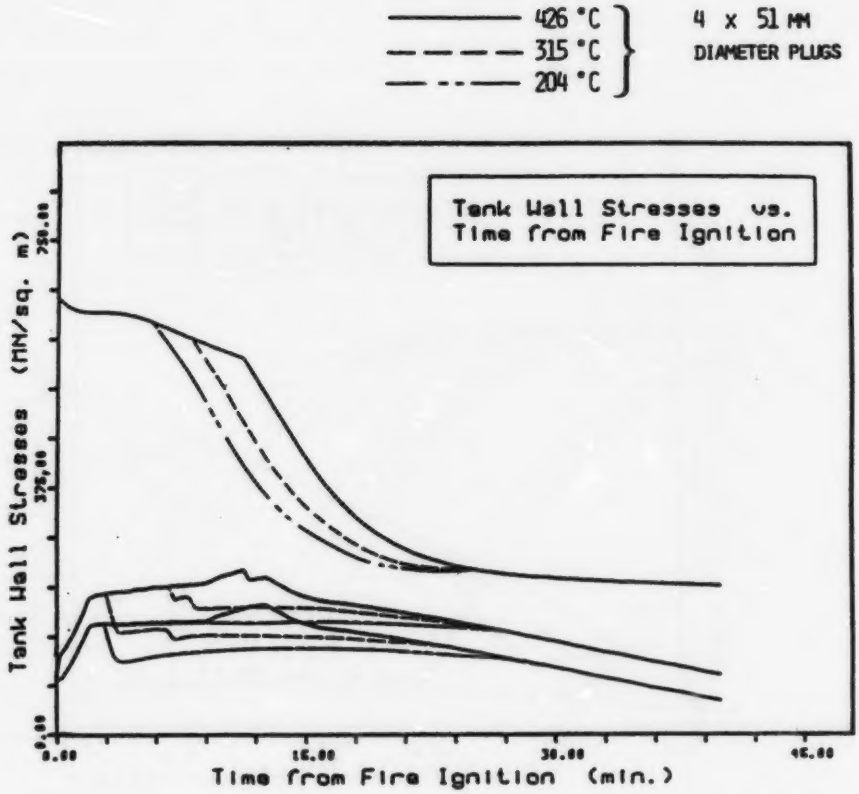

FIGURE 4-12 PREDICTED TANK WALL STRESSES AND TANK WALL MATERIAL STRENGTHS FOR TANKS EQUIPPED WITH DIFFERENT NUMBERS OF FUSIBLE PLUGS, EXPOSED TO AN ENGULFING FIRE

Figure 4-7 presents the predicted liquid level for the different cases considered. As can be seen from the figure, once the fusible plugs open there is a sudden increase in the rate at which the liquid level drops. However, the rate at which lading is vented from the tank eventually is reduced, and becomes almost identical to that for the case with the lowest number of fusible plugs. This can be explained as follows, as the tank pressure drops the rate at which lading is vented also drops. Therefore, by increasing the number of fusible plugs, one decreases the pressure at the same time one increases the total orifice area. The result of these two parameters being varied results in a cancelling out of the effectiveness of the fusible plugs. Therefore, this is another indication of the law of diminishing returns with regard to the number of fusible plugs used. It appears from the figure, that four fusible plugs are as good as twelve fusible plugs in terms of emptying the tank in a given period of time.

Figure 4-8 presents the predicted tank wall stresses and tank wall material strength for the different cases considered. As can be clearly seen from the figure, the fusible plugs have little effect on the material strength of the tank wall. This is because the peak tank wall temperatures are unaffected by the presence of the fusible plugs and it is these temperatures that determine the weakest point in the tank wall. The other two curves in the figure show the tank wall stresses at the inner and outer fibres of the tank wall. As can be clearly seen from the figure, the tank wall stresses are significantly reduced when the fusible plug is opened. This is because the tank pressure has been reduced and it is the tank pressure that is the determining factor in the tank wall stresses. Once again, the law of diminishing returns is clearly indicated in the predicted results. There seems to be little advantage in increasing the number of fusible plugs above 8.

In summary, it appears that there is an optimum number of fusible plugs to protect a tank-car. The optimum number of plugs will be determined by a balance of economic and thermal considerations. It appears that four fusible plugs, each of a diameter of 51 mm melting out at 220°C, is an effective means of protecting a tank-car from an engulfing fire environment. This assumes, however, the four plugs are all above the liquid surface (eg. at the tank top-dead-centre, and the tank is upright and horizontal) at the initiation of the fire. Therefore, plug placement has not been addressed here adequately for cases where the tank is rolled or pitched.

Case #2 Fusible Plugs of Different Melting Temperatures:

Figure 4-9 presents the predicted tank pressures for the different cases considered. As can be clearly seen from the figure, the tank response up until the point where the fusible plugs open is identical to that of an unprotected tank-car. The cases where the plugs melt out at lower temperatures show rapid drops in the tank pressure when the fusible plugs open. As expected, the fusible plugs with the lowest melting temperatures come into play earliest. Eventually, the tank pressures for the three different cases become equal as can be seen from the figure.

Figure 4-10 presents the predicted tank wall temperatures for the different cases considered. As can be seen from the figure, the tank wall temperatures are significantly affected by the different melting temperatures of the fusible plugs. However, the fusible plugs do not affect the peak wall temperatures which affect the strength of the tank. The only apparent affect is a shifting of the temperature break times along the time axis.

Figure 4-11 presents the predicted liquid level for the different cases considered. As can be seen from the figure, the case with the lowest melting temperature plugs shows an earlier break in the rate at which the liquid level drops. However, as time goes on, the rate at which the liquid levels drop all become equal for the different cases considered. The ultimate time to empty does not appear to be affected by the melting temperature of the plugs. Therefore, there does not appear to be any advantage in reducing the melting temperature of the plugs. In fact, lower melting temperature plugs increase the risk of accidental or unwanted plug openings.

Figure 4-12 presents the predicted tank wall stresses and tank wall material strength for the different cases considered. As can be seen from the figure, there is actually a larger drop in the material strengths of the tank wall, for the lower melting temperature plugs. This is an unwanted side effect of the earlier fusible plug opening times for the lower melting temperature plugs. Because the lower melting temperature plugs open earlier, the time at which wall areas are exposed to vapour is earlier. The lower melting temperature plugs also result in an earlier drop in the tank wall stresses due to the drop in the tank pressure. However, eventually, the tank wall stresses for all the cases become equal because of the law of diminishing returns with respect to the lower melting temperature of the plugs.

In summary, there appears to be little advantage in reducing the melting temperature of fusible plugs. As mentioned earlier, there is actually a detrimental effect caused by lower melting temperatures because the risk of accidental or unwanted plug melting is increased for the lower temperature plugs. It appears, that a reasonably high melting temperature plug, with temperature limits based on tank material strengths is acceptable.

4.3 EXPLOSAFE EQUIPPED TANK

This section presents the results of a number of simulations involving a full-scale tank protected with the thermal protection system known as Explosafe. Two series of simulations were performed to show the effects of varying the installation of the material.

The first series of simulations consider the case where the annular thickness of the Explosafe material is varied for a fixed orientation of the material. The second series considered a fixed thickness, but the material orientation was varied. The orientation of the Explosafe is important because its thermal properties are anisotropic (they vary with direction). The thickness of the Explosafe is important from the standpoint of the thermal effectiveness of the installation, and of course the economics of the installation (the thicker the annular layer; the higher the cost of the installation). The orientation of the Explosafe only effects the thermal effectiveness of the installation.

Case #1 The Effect of Varying the Annular Thickness

This series of simulations considered three different thicknesses of the Explosafe annulus - 51 mm, 102 mm, and 152 mm. The properties of the Explosafe were assumed to be identical to those used in the 1/5 scale tests conducted at Suffield. In all cases the Explosafe was oriented so that its highest thermal conductivity was parallel with the tank radius, and the second highest conductivity was oriented parallel with the circumference of the tank. This orientation is optimum if the Explosafe effect is caused by a fin effect, as it appears to be, based on simulations (see Case 2).

Figure 4-13 presents the predicted tank pressure for the different cases considered. As can be seen from the Figure, varying the annular thickness of the Explosafe material does not appear to effect the tank pressurization significantly. Increasing the thickness increases the peak tank pressure slightly because of the fact that the

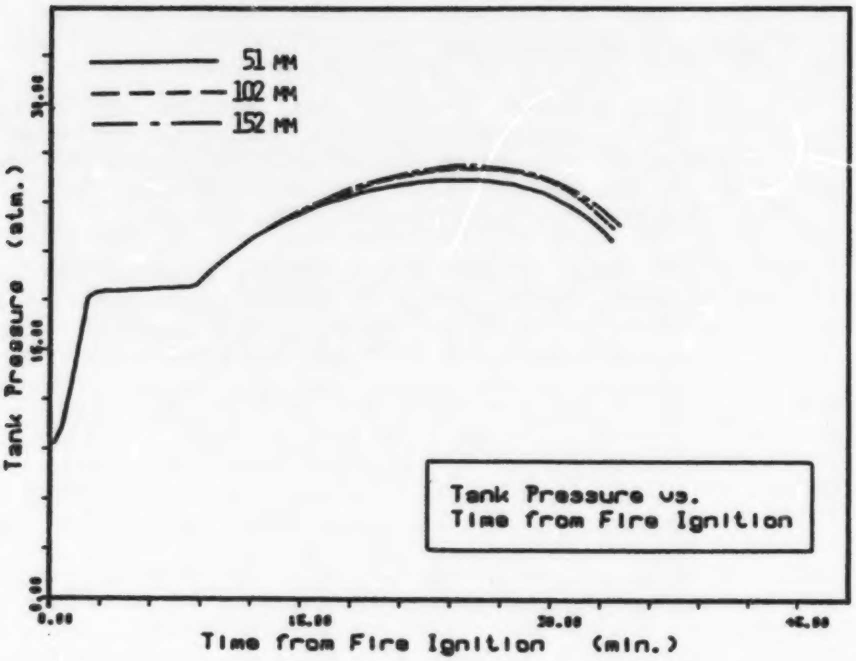

FIGURE 4-13 PREDICTED TANK PRESSURES FOR TANKS EQUIPPED WITH EXPLOSAFE OF DIFFERENT ANNULAR THICKNESSES, EXPOSED TO AN ENGULFING FIRE

Explosafe material will tend to increase the heat transfer from the inner surface of the tank wall. This, of course will increase the total heat flux to the lading, and hence the tank pressure increases.

Figure 4-14 presents the predicted tank wall temperatures for the different cases considered. As can be seen from the figure, the wall temperatures are affected by the variations in the annular thickness of the Explosafe. However, the effects on the wall temperatures are not large. As can be seen from the figure, there is little difference between the wall temperatures for the 102 mm and the 152 mm cases, and this indicates that there is little or no benefit to increase the thickness of the annulus above 102 mm.

Figure 4-15 presents the predicted liquid level for the different cases considered. Once again, it is clear from the figure that increasing the Explosafe thickness above 102 mm does not effect the response of the tank significantly.

Figure 4-16 presents the predicted tank wall stresses and material strengths for the different cases considered. In terms of tank wall stresses, the simulation results indicate that the wall stresses are actually increased by the thicker Explosafe because of the fact that the tank peak pressures are slightly higher for these cases. However, the tank wall material strengths (which are governed by the wall temperatures) are higher for the cases with the increased thickness of the Explosafe. The net result is that increasing the Explosafe thickness reduces the chance of thermally induced rupture of the tank wall. However, the benefits from increasing the Explosafe annulus from 102 mm to 152 mm are very small.

In summary, the simulation results indicate the increasing annular thickness of Explosafe above approximately 102 mm does not significantly increase the thermal effectiveness of the thermal protection system. From an economic standpoint, the optimum thickness of the Explosafe is the minimum thickness required for adequate thermal protection. Based on the simulations conducted, the practical limit in terms of effectiveness (the thickness beyond which incremental benefits are small) is approximately 102 mm. However, whether or not this thickness is actually adequate for the purposes of thermal protection is another question. The simulations indicate that the tank ruptures, or at least comes very close to rupture, for all the Explosafe thicknesses considered.

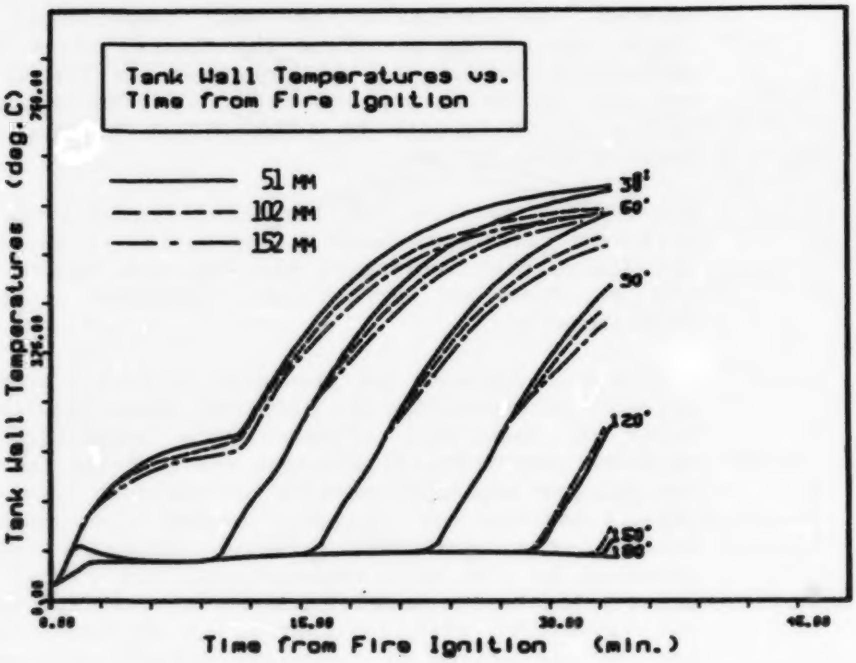

FIGURE 4-14 PREDICTED TANK WALL TEMPERATURES FOR TANKS EQUIPPED WITH EXPLOSAFE OF DIFFERENT ANNULAR THICKNESSES, EXPOSED TO AN ENGULFING FIRE

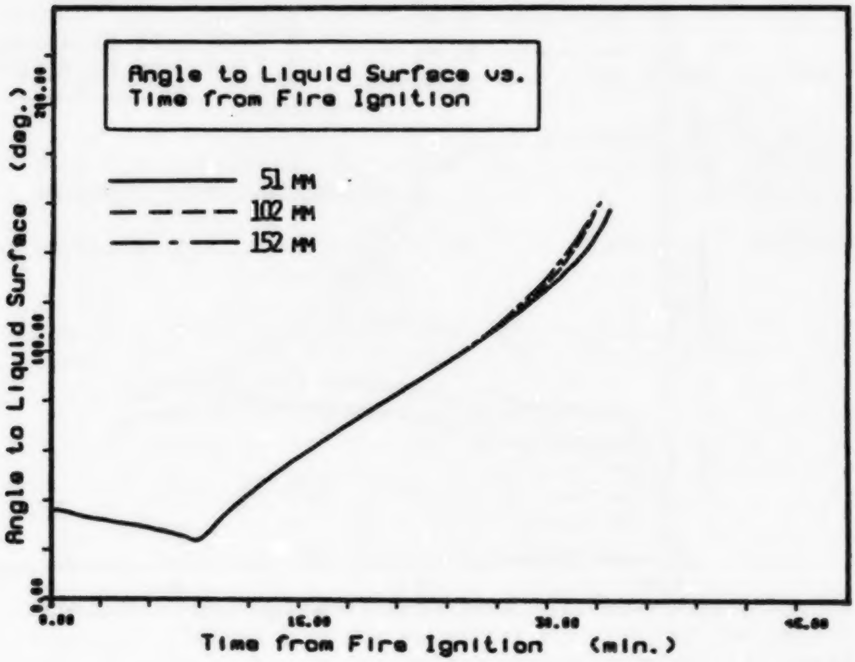

FIGURE 4-15 PREDICTED LIQUID LEVEL FOR TANKS EQUIPPED WITH EXPLOSAFE OF DIFFERENT ANNULAR THICKNESSES, EXPOSED TO AN ENGULFING FIRE

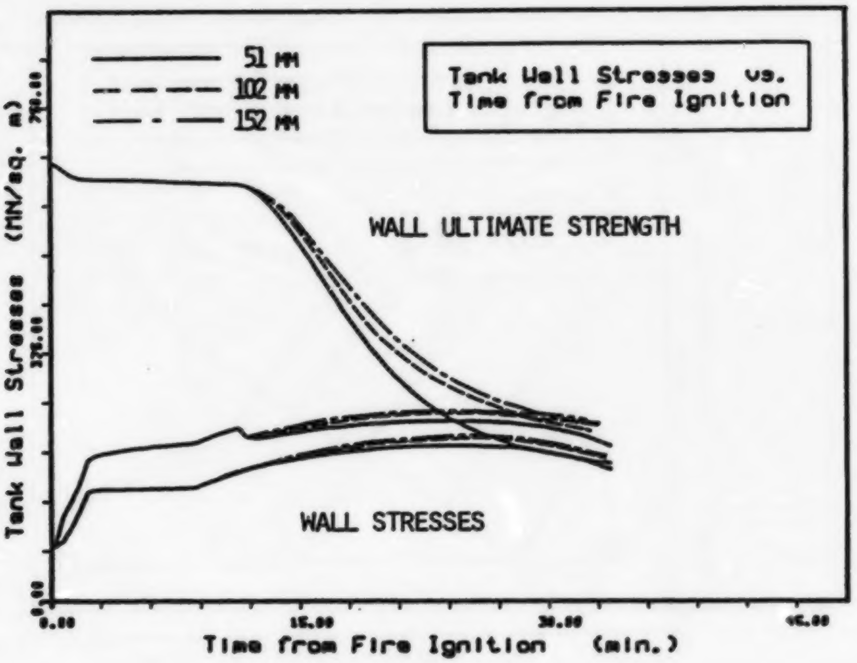

FIGURE 4-16 PREDICTED TANK WALL STRESSES AND TANK WALL MATERIAL STRENGTHS FOR TANKS EQUIPPED WITH EXPLOSAFE OF DIFFERENT ANNULAR THICKNESSES, EXPOSED TO AN ENGULFING FIRE

Case #2 The Effects of Varying the Orientation

This series of simulations were performed to investigate the effect of varying the orientation of the Explosafe material. As mentioned above, the orientation of the Explosafe is important because of its anisotropic thermal properties.

In total, six different cases were considered. The following definitions of the three principal axes of the Explosafe were used.

Direction 1: axial direction of maximum thermal conductivity.

Direction 2: axial direction of intermediate thermal conductivity.

Direction 3: axial direction of minimum thermal conductivity.

The six simulations conducted are described as follows based on the above definitions of the principal axes:

Run A : 1 radial, 2 circumferential
Run B : 1 radial, 3 circumferential
Run C : 2 radial, 1 circumferential
Run D : 2 radial, 3 circumferential
Run E : 3 radial, 2 circumferential
Run F : 3 radial, 1 circumferential

The radial direction refers to the direction parallel to the tank radius, and the circumferential direction refers to the direction parallel to the tank circumference. Only two tank reference axes are considered because the tank-car model is 2-dimensional (i.e., no axial gradients are accounted for, and therefore the Explosafe orientation relative to the tank axis is irrelevant). In all cases the Explosafe annular thickness was set at 102 mm.

Figure 4-17 presents the predicted tank pressures for the different cases considered. As can be seen from the figure, the runs where the Explosafe is oriented with its maximum thermal conductivity parallel with the tank radius resulted in the highest tank pressures. This indicates that the Explosafe is resulting in a higher heat transfer to the lading resulting in a higher tank pressure. All of the remaining cases resulted in lower tank pressures. It appears that there is very little difference between cases C, D, E and F.

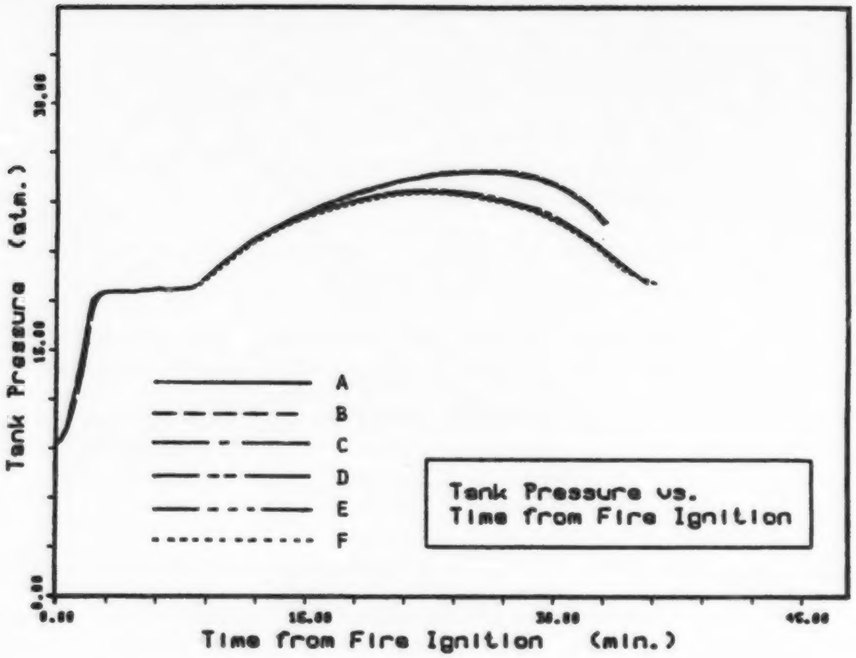

FIGURE 4-17 PREDICTED TANK PRESSURES FOR TANKS EQUIPPED WITH EXPLOSAFE OF DIFFERENT ORIENTATION, EXPOSED TO AN ENGULFING FIRE

Figure 4-18 presents the predicted tank wall temperatures for the different cases considered. As can be clearly seen from the Figure, cases A and B resulted in the lowest wall temperatures. Cases C, D, E and F resulted in significantly higher wall temperatures. Once again there appears to be very little difference between cases A and B and between cases C, D, E and F. The reason for the results as shown in Figure 4-18 are that the Explosafe is acting as a fin, i.e., the Explosafe is drawing the heat radially away from the wall into the lading. The Explosafe is not conducting the heat circumferentially away from the vapour wetted wall regions into the liquid lading.

Figure 4-19 presents the predicted liquid level for the different cases considered. As can be seen from the figure, the liquid dropped most rapidly for cases A and B because of the increased heat flux to the lading caused by the fin effect of the Explosafe.

Figure 4-20 presents the predicted tank wall stresses and material strengths for the different cases considered. As can be seen, the simulation results show that the Explosafe orientation has a significant effect on the predicted failure of the tank. For cases A and B the model predicts that the tank will narrowly escape failure, whereas the model predicts failure for the remaining cases. This clearly shows that the best orientation of the Explosafe is with the maximum thermal conductivity parallel to the tank radius.

In summary, the model simulations indicate that the best orientation for the Explosafe is with its maximum thermal conductivity parallel with the tank radius. It appears from the results that the orientations of the remaining axes are not significant. However, based on simple heat transfer considerations, it is believed that the minimum thermal conductivity axis should be parallel with the axis of the tank. When the maximum thermal conductivity is oriented in the radial direction, the tank experiences slightly higher peak pressures, and lower peak wall temperatures, with the net effect being a significant drop in the probability of tank rupture.

Based on the two cases considered, it appears that an efficient Explosafe design would involve a 102 mm thick annulus of Explosafe with the material oriented with the maximum thermal conductivity parallel to the tank radius and the minimum thermal conductivity parallel with the axis of the tank. However, even with this thickness and

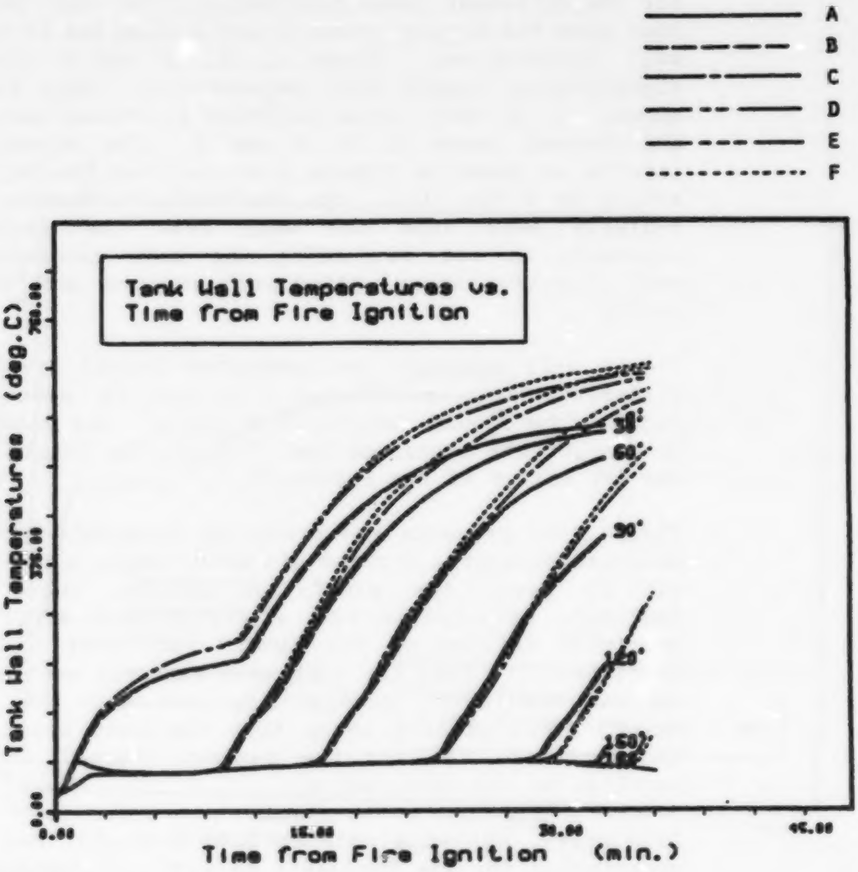

FIGURE 4-18 PREDICTED TANK WALL TEMPERATURES FOR TANKS EQUIPPED WITH EXPLOSAFE OF DIFFERENT ORIENTATIONS, EXPOSED TO AN ENGULFING FIRE

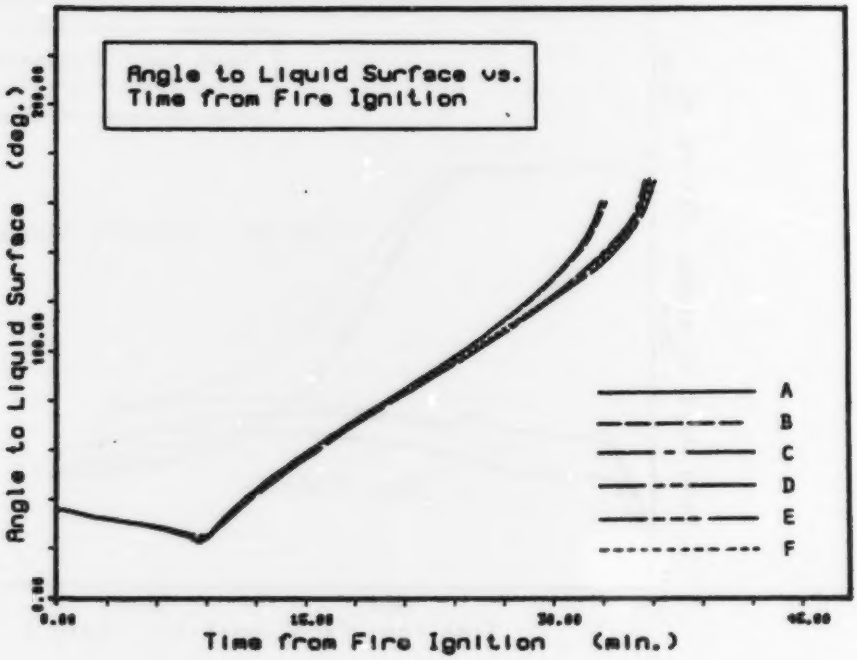

FIGURE 4-19 PREDICTED LIQUID LEVEL FOR TANKS EQUIPPED WITH EXPLOSAFE OF DIFFERENT ORIENTATIONS, EXPOSED TO AN ENGULFING FIRE

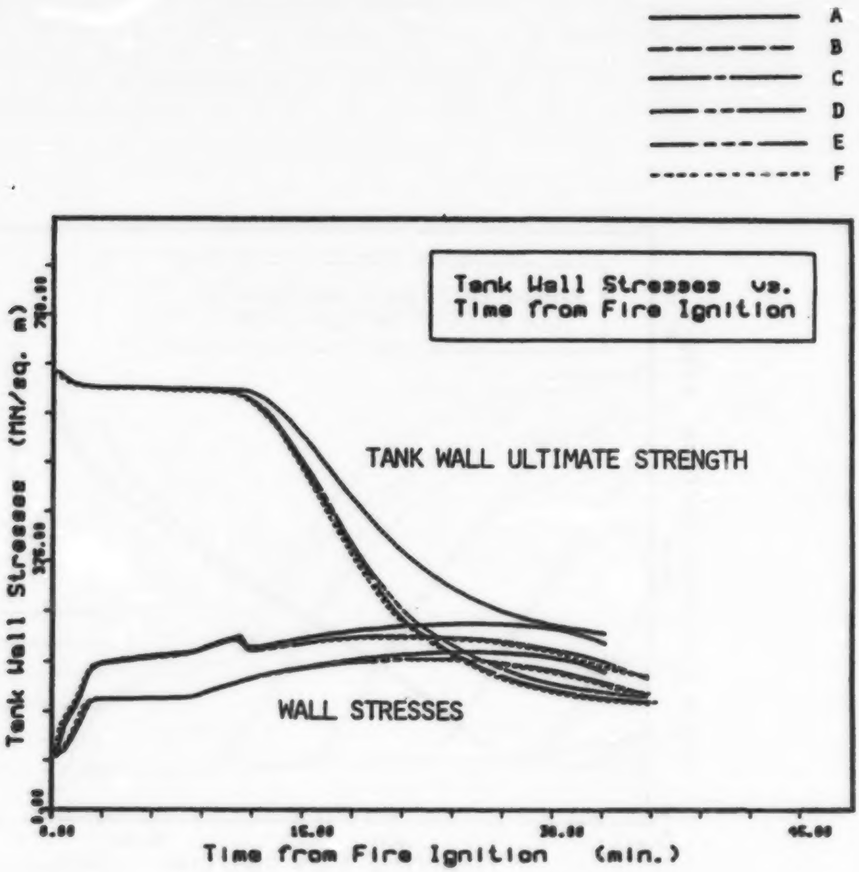

FIGURE 4-20 PREDICTED TANK WALL STRESSES AND TANK WALL MATERIAL STRENGTHS FOR TANKS EQUIPPED WITH EXPLOSAFE OF DIFFERENT ORIENTATIONS, EXPOSED TO AN ENGULFING FIRE

orientation, the tank will come dangerously close to failure when exposed to an engulfing fire. Therefore, based on the results of simulations, Explosafe does not appear to be a viable thermal protection system when used without thermal insulation.

5.0 FUTURE WORK

A great deal of effort has gone into the development of the tank-car thermal analysis computer program. However, the tank-car model should still be considered as being a research tool, and not a packaged piece of software ready for release to the general engineering community. The tank-car model requires further refinement, enhancement, and validation. Further validation can only take place when new data is made available from fire tests.

It is feasible that the ultimate version of the tank-car model will become a piece of software, or part of a computer aided design system, for designing and manufacturing all sorts of tanks to carry pressurized, hazardous commodities.

The following sections highlite some possible future work related to the development of the tank-car model. First, the major model weaknesses are identified and briefly discussed, and recommended model modifications are listed. In addition, areas that require further data are highlited.

5.1 OVERALL MODEL WEAKNESSES

As stated earlier, the tank-car model consists of a number of sub-models which represent the various processes taking place in and around the tank-car. Presently, there exists some weaknesses in the formulation of some of these submodels. The most important weaknesses in the overall tank-car model are associated with the following:

1. The thermodynamic process sub-model,
2. The inner surface heat transfer sub-model,
3. The relief valve flow sub-model, and
4. The thermal insulation degradation sub-model.

The thermodynamic process model is weak because it relies on two empirical constants. It has been assumed, that these constants remain the same for all different tank-car scales and configurations. However, there is no data to support this conclusion other than the results of the validation to-date. Ideally, the thermodynamic process sub-model should be based entirely on the fundamentals of thermodynamics, and no empirical constants should have to be set. For the tank-car model to become a versatile design tool, further work is necessary on the thermodynamic process sub-model.

Presently, the inner surface heat transfer sub-model is based on rather simplistic correlations from experimentally obtained heat transfer data. Ideally, the internal surface heat transfer coefficients should be calculated from the basic governing equations. Several such analyses are available in the open literature, and only minor modification is required before they could be implemented in the tank-car model.

Presently, the relief valve flow analysis can only account for choked vapour flow through the relief valve, and frozen liquid flow through the relief valve. It is a distinct weakness that the model cannot account for two-phase flow through the relief valve. However, there does not exist at present an adequate analysis to represent all possible flow conditions through the relief valve. In addition, the present relief valve model is a simplistic, steady state model. Therefore the dynamic action of the valve is not accounted for. Temperature effects on the action of the relief valve (changing set pressures, etc.) are also not accounted for. Therefore, further work, both experimental and theoretical is necessary before a comprehensive relief valve flow analysis can be performed.

Finally, the remaining weakness in the program is the lack of data on the thermal degradation of available thermal insulations. The present tank-car model can account for thermal degradation of thermal insulating materials, however, data is needed on how these thermal insulating layers degrade, and how this degradation affects the insulation thickness, and the insulation thermal conductivity. As well, many thermal insulating materials such as intumescent paints provide transpiration cooling effects. These transpiration cooling effects should also be accounted for in the tank-car thermal analysis program.

The above mentioned program weakness do not render the existing tank-car model useless. As can be seen from the model validation of a previous section, the tank-car model is still quite accurate in predicting the thermal response of a tank-car exposed to either engulfing or torch-type fire environments. However, if the tank-car model is eventually to become a design tool for the general engineering community, these weaknesses should be studied further.

5.2 RECOMMENDED MODEL MODIFICATIONS

Of the model weaknesses discussed in the previous section, the most important are the thermodynamic process sub-model, and the relief valve flow analysis sub-model.

It is recommended that the tank-car model be modified to include a more comprehensive thermodynamic process model. However, it is anticipated that such a model would require considerable computer effort. Therefore, it is also recommended that the present thermodynamic process model remain in the overall tank-car program. At run time, the user would specify which thermodynamic sub-model is to be used, and therefore if a quick calculation is required the user would specify the existing thermodynamic process model. However, if a run is to be performed on a tank-car scale and configuration where no present data exists for validation, then one would be well advised to use the comprehensive thermodynamic model.

It is recommended that the relief valve flow analysis in the overall tank-car model be modified so that it can account for two-phase flow through the relief valve. This is extremely important, because the accurate prediction of venting rates is important for determining the liquid level in the tank, and hence the tank wall temperatures. It is essential, that the tank wall temperatures and the liquid level be known accurately so that the ultimate tank failure or time to empty can be predicted.

6.0 CONCLUSIONS

Based on the results of the model validation process, the following conclusions have been made:

1) Results of the validation show that the model is quite accurate at predicting the response of unprotected and protected tank-cars exposed to engulfing, and torch fire environments. A high degree of confidence can be used when modelling the following situations:

   - unprotected horizontal tanks (full or fifth-scale)
   - unprotected horizontal rolled tanks (full or fifth-scale)
   - insulated tanks (full or fifth-scale, using simple insulations only)
   - Explosafe equipped (using angular configurations only, fifth-scale)

2) The tank-car model's two-dimensional torch analysis can be compared directly to the U.S. DOT Transportation Test Center Torch Fire Test Facility.

Based on the results of the program sensitivity analysis the following conclusions can be made:

1) The tank-car model can be very sensitive to the time step used depending on the type of protection being simulated. For unprotected tanks the time step should be kept below 30 seconds. For insulated tanks incorporating steel jacket, the time step should be below 5 seconds. For all other tank-car protection scenarios, the time step should be kept below 5 seconds.

2) The model predictions for a tank-car thermal response are extremely sensitive to the fire conditions. This includes both the fire temperatures (pool fire or torch fire) and the fire radiating characteristics (effective flame emissivity)

Based on the results on the example simulations, the following conclusions can be made:

1) Thermal insulation appears to be an excellent thermal protection against accidental impingement as long as the thermal insulating layer is not damaged.

2) Fusible plugs (or temperature sensitive valves) also appeared to be effective means of reducing the risk of accidental ruptures of tanks.

3) Based on the simulations performed, Explosafe does not appear to be an effective thermal protection for full-size tank-cars. The Explosafe provides a very limited amount of thermal protection in the form of slightly reduced wall temperatures.

The results of the model validation, sensitivity analysis, and example simulations, show that the tank-car model is a powerful tool for predicting the thermal response of tank-cars to accidental fire impingement. However, there are still weaknesses with the overall model and these weaknesses should be studied. Most important areas requiring further examination are:

- The thermodynamic process sub-model, which is the most important sub-model used to predict the thermal response of the tank,

- The pressure relief valve submodel which is extremely important in accurately predicting the rate at which the lading is vented, and

- The thermal insulation sub-model which represents the thermal degradation of the thermal insulating layers.

REFERENCES

1) Birk, A.M.; The Development and Validation of a Mathematical Model of a Rail Tank-Car Engulfed in Fire, Ph.D. Thesis, Queen's University, 1983.

2) Railroad Tank Car Safety Research and Test Project; Phase II Report on Full-Scale Fire Tests. AAR-RPI, RA-11-6-31, AAR-R-201, US6 AFI 17-75 ENG(BK).

3) Appleyard, R.D.; Testing and Evaluation of the Explosafe System as a Method of Controlling the Boiling Liquid Expanding Vapour Explosion, Transport Canada Report No. TP 2740, 1980.

4) Anderson, C. et al; Railroad Tank-Car Fire Test: Test #6, Ballistic Research Laboratories, US DOT FRA-OR&D 75-36, 1973.

5) Anderson, C. et al; Railroad Tank-Car Fire Test: Test #7, Ballistic Research Laboratories, US DOT FRA-OR&D 75-37, 1973.

6) Railroad Tank Car Safety Research and Test Project; Phase II Report on Analysis of 1/5 Scale Fire Tests, RPI-AAR, RA-11-5-26, US6 AFI 17-73 ENG(PF).

7) Railroad Tank Car Safety Research and Test Project; Phase II Report on Analysis of 1/5 Scale Fire Test Data, RPI-AAR, RA-11-2-14, US6 AFI 17-72 ENG(PF).

8) Anderson, C.E.; Rail Tank Car Safety by Fire Protection, 6th International Fire Protection Seminar, 1982.

9) Roberts, A.F., Cutler, D.P., Billinge, K.; Fire Engulfment Trials with LPG Tanks with a Range of Fire Protection Methods, Proc. 4th Int. Symposium on Loss Prevention and Safety Promotion in Process Industries, Vol. 3, Chem. Eng. Symposium Series, 1982.

CA1 MM
DTC845
85
V17
c.2.

10) Schulz-Forberg, B., Droste, B., Charlett, H.; Failure Mechanisms of Propane Tanks Under Thermal Stresses Including Fire Engulfment, Transport and Storage of LPG and LNG, pp. 295-305.

11) Jung, D.S.; Pool Boiling Heat Transfer: The Effects of Enhanced Surfaces, Masters Thesis, University of New Brunswick Fire Science Centre, May 1984.

12) Aydemir, N.U.; Transient Natural Convection in a Partially Filled Horizontal Cylinder, Masters Thesis, University of New Brunswick Fire Science Centre, May 1984.

13) Qureshi, G.; Experimental Determination of the Heat Transfer in the Vapour Space of a Partially Filled Horizontal Cylinder, Masters Thesis, University of New Brunswick Fire Science Centre, May 1984.

14) Szego, A., Premji, K., Appleyard, R.D.; Evaluation of Explosafe Explosion Suppression System for Aircraft Fuel Tank Protection, AFWAL-TR-80-2043, 1980.

15) Graves, K.W.; Development of a Computer Model for Modelling the Heat Effects on a Railroad Tank Car, FRA-OR&D 75-33, 1973.

16) User Documentation for the Rail Tank-Car Thermal Analysis Program (TNKCAR), Davis Engineering, C83-29, March 1985.

Library and Information Centre /
Centre de Documentation (GSLA)
RECEIVED – REÇU LE
JAN 9 1986
Transport Canada / Transports Canada